2009

An In Vivo Characterization of the Functional Role of Two Novel Genes: StARD5 and ADAM11

Marc Paul Waase

AN *IN VIVO* CHARACTERIZATION OF THE FUNCTIONAL ROLE OF TWO NOVEL GENES: StARD5 AND ADAM11

A Thesis Presented to the Faculty of

The Rockefeller University

in Partial Fulfillment of the Requirements for

the degree of Doctor of Philosophy

by

Marc Paul Waase

June 2009

AN *IN VIVO* CHARACTERIZATION OF THE FUNCTIONAL ROLE OF TWO NOVEL GENES: StARD5 AND ADAM11

Marc Paul Waase, Ph.D.
The Rockefeller University June 2009

Regulation of cholesterol levels within cells and organisms is crucial for their survival. Maintenance of cellular cholesterol homeostasis occurs mainly at the transcriptional level, via the Sterol Regulatory Element Binding Proteins (SREBP), the Liver X Receptors (LXR), and the Unfolded Protein Response (UPR)/ER Stress Response. This thesis attempts to characterize the *in vivo* physiological role of novel downstream target genes of these transcription factors: StARD5 and ADAM11.

This thesis outlines the development and characterization of a floxed mouse allele of the UPR-upregulated, reticuloendothelial gene StARD5, as well as two different transgenic mouse lines, one which expresses the human StARD5 gene in the liver and one which expresses the human StARD5 in the reticuloendothelial system. We show that StARD5 plays an indispensable role in early embryogenesis since homozygous knockouts are not viable. Haploinsufficiency in the adult mouse does not alter plasma cholesterol or triglyceride levels, liver cholesterol levels, gallbladder bile composition, glucose tolerance, cholesterol efflux from macrophages, or atherosclerosis susceptibility.

Two isoforms of the ADAM11 gene were identified, differing only in their cytoplasmic tails, with one highly expressed in the liver and the other highly expressed in the brain. The liver isoform of ADAM11 was induced by dietary cholesterol and the LXR transcription factor. In order to study the function of this gene, this thesis describes the development of a floxed mouse allele of ADAM11. Utilizing low and high cholesterol and cholic acid containing diets and the ADAM11 knockout, we did not find a phenotype for ADAM11 with respect to plasma cholesterol or triglyceride levels, liver lipid levels, gallbladder bile composition, glucose tolerance, or atherosclerosis susceptibility. We show that loss of ADAM11 in mice fed a high cholesterol diet lowers free plasma campesterol levels, without having an effect on total campesterol levels or other phytosterols. Using a yeast two-hybrid screen, we identified 3HAO as a putative ADAM11 cytoplasmic tail binding partner, which interacted non-specifically with the two cytoplasmic tail

forms. ADAM11 knockout mice were previously shown to have a neurological phenotype to which we now add absence-like epilepsy.

Finally, this thesis also outlines the development of a floxed mouse allele of the dietary cholesterol-downregulated, SREBP-upregulated liver gene StARD4; initial studies indicate that a full StARD4 knockout is viable.

Dedicated to my wife, Cecilia,

my mother, Danielle, and

my father, Paul,

for their unceasing and unconditional

love, guidance, and support.

Acknowledgments

I want to express my deep gratitude to the many people who have helped to get me where I am today. First and foremost, I would like to thank my advisor **Jan Breslow**. I am grateful for the time I have spent in his lab. Jan is one of the nicest people whom I have ever gotten to know. He was a great mentor, allowing me to freely explore without putting too much pressure on me, knowing full well that I do that enough by myself. Jan was always there for me to discuss science and always offered words of encouragement.

I am thankful for each and every member of the Breslow lab, past and present, for their help and friendship over the past four years. I want to thank **Kara Maxwell** for introducing me to the lab and getting me started. I want to thank particularly my campus-side bench-mates: **Josh Riegelhaupt** and **Ralph Burckhardt**, as well as my river-side lab-mates **Kristine Nowak**, **Changcheng Zhao**, and **Jose Rodriguez,** who over the past four years have been there to discuss ideas, scientific and not. I want to thank **Helen Yu** for all her work on sectioning my many mouse aortas. Our neighbors in the Stoffel and Strickland labs have also been extremely generous. I want to thank **Matt Poy** and **Jan Kreutzfeldt** in the Stoffel lab, who were more than willing to provide assistance and resources. I want to thank **Erin Norris** in the Strickland lab, who has also been extremely helpful. The Tri-Institutions have so many useful resources and so many kind people who have helped me, so I also want to thank **Suzana Couto** (SKI Pathology), **Chingwen Yang** (RU Gene Targeting), **Rada Norinsky** (RU Transgenics), and **Connie Zhao** (RU Genomics). I am also grateful for my classmates, the MD/PhD entering class of 2002, with whom I have been able to share the joys and the stresses of the past six years.

My graduate career would not have run as smoothly without the help of everyone behind the scenes at the Dean's office at the Rockefeller Graduate School and the Cornell MD/PhD office. **Marta, Kristen, Emily, Cristian, Sid, Renee, Elaine, Irma, Ruthie**, and especially **Olaf** made sure that I could focus my full attention on science and my work.

I thank my committee members: **Sandy Simon, James Darnell**, and **Carl Blobel** (HSS), for their advice and assistance over the past few years. I also thank a previous committee member **Markus Stoffel**, who got me started in science back when I was just a high school junior. I also want to thank my external committee

member, **Walter Miller** (UCSF). I want to thank **Eric Alani**, my undergraduate research adviser, for his kindness and constant support.

I never would have made it without the support and love from my family and friends. I want to thank my parents, **Paul** and **Danielle Waase** for their constant love, support and understanding. I want to thank my older sister **Carine**, who blazed a trail for me along this career path, always providing me with useful tips and ideas. I also want to thank my brother-in-law **Sebastian** and my new nephew/godson **Julien**, who has provided me with numerous fun breaks throughout my thesis writing.

Finally, I would like to thank my best friend and my wife, **Cecilia**. Your constant support and understanding has been amazing, and your refreshing sense of humor always keeps me with a smile on my face. I cannot express how thankful I am that I have you in my life.

Table of Contents

Chapter 3: Characterization of ADAM11

List of Figures:

List of Tables:

List of Abbreviations

25OH	25-hydroxycholesterol
ABC	ATP-binding bassette
ACAT	acyl-coenzyme A: cholesterol acyl transferase
ADAM	a disintegrin and metalloprotease
Apo	apolipoprotein
ARE	ACAT related enzyme
ARV	ARE2 required for viability
AUS	ATP-binding cassette family, involved in uptake of sterols
bHLH-Zip	basic helix-loop-helix-leucine zipper
CERT	ceramide transfer protein
CETP	cholesterol ester transfer protein
CoASH	coenzyme A-SH
Cyp	cytochrome P450
DGA	diacylglycerol acyltransferase
DLC	deleted in liver cancer
EGF	epidermal growth factor
ER	endoplasmic reticulum
ERAD	ER associated degradation
ERSE	ER stress response element
GFP	green fluourescence protein
GPBP	Goodpasture antigen-binding protein
GTT1	gestation trophoblastic tumor 1
HDL	high density lipoprotein
HMG CoA	hydroxymethylglutaryl coenzyme A
HMGR	HMG CoA reductase
HMGS	HMG CoA synthase
IGF	insulin-like growth factor
IMM	inner mitochondrial membrane
Insig	insulin-induced-gene
LDL	low density lipoprotein
LDLR	LDL receptor
LXR	liver X receptor
LXRE	LXR response element

MLN64	metastatic lymph node 64
MENTAL	MLN64 N-terminal domain
MENTHO	MLN64 N-terminal domain homologue
MMP	matrix metalloprotease
NPC	Niemann pick type c
OMM	outer mitochondrial membrane
ORF	open reading frame
ORP	OSBP related protein
OSBP	oxysterol binding protein
Osh	OSBP-homologoues
PC	phosphatidylcholine
PCR	polymerase chain reaction
PCTP	phosphatidylcholine transfer protein
PDR	pleiotropic drug resistance
PE	phosphatidylethanolamine
Pfu	particle forming units
PGP	phosphatidylglycerolphosphate
PH	pleckstrin homology domain
PM	plasma membrane
QTL	quantitative trait locus
RCT	reverse cholesterol transport
RhoGAP	rho GTPase activating protein
RNAi	RNA interference
RT	reverse transcriptase
S1P	site 1 protease
S2P	site 2 protease
SAA	serum amyloid A
SCAP	SREBP cleavage activating protein
SNP	single nucleotide polymorphism
SRE	sterol regulatory element
SREBP	sterol regulatory element binding protein
SSD	sterol sensing domain
StAR	steroidogenic acute regulatory protein
StARD	START domain containing
START	StAR-related lipid transfer

TACE	tumor necrosis factor-alpha converting enzyme
UPR	unfolded protein response
UPC	uptake control
Utr	untranslated region
VLDL	very low density lipoprotein

Chapter 1: Introduction

The Physiological and Pathophysiological Significance of Cholesterol

Cholesterol is a 27-carbon, four-ringed planar hydrophobic molecule that plays a vital physiological role in all mammalian cells. It is the most abundant sterol in the human body and is a fundamental component of cell membranes, enabling membrane permeability and providing rigidity to the phospholipid bilayer (Simons and Ikonen, 2000). Cholesterol is one of the major components of lipid rafts, membrane microdomains that serve as a platform for various cellular events, including signaling, cell-cell communication, and membrane trafficking (Tabas, 2002a). Cholesterol covalently modifies and activates proteins, e.g. sonic hedgehog, a protein essential for proper embryonic development. It serves as the building blocks for the calcium and phosphorus-regulating hormone vitamin D3 (cholecalciferol), and for the steroid hormones, including sex and stress hormones, specifically progesterone, estrogen, testosterone, cortisol, and aldosterone (Rose, 1998). Cholesterol is essential for the biosynthesis of bile acids, which aid in the digestion and absorption of lipids, fats, and fat-soluble vitamins and are a major mode for cholesterol excretion (Rose, 1998).

Cholesterol is thus critical for organismal homeostasis, and its levels must be carefully regulated, as cholesterol imbalance can lead to serious pathological consequences. Cholesterol synthesis, influx, and efflux must be tightly controlled not only to assure adequate supply and proper distribution of this essential lipid,

but also to avoid excess. Excess cellular free cholesterol is cytotoxic, and excess plasma cholesterol in the form of LDL is a major risk factor for atherosclerosis, a disease that kills nearly a million Americans each year (Anderson, 2001; Tabas, 2002b). In atherosclerosis, excess plasma cholesterol is deposited into the arterial subendothelial space, setting off a cascade of inflammatory responses including infiltration of monocytes, as well as proliferation and migration of smooth muscle cells, elaboration of extracellular matrix (ECM) in the arterial wall, and cellular apoptosis. Excess cholesterol in the biliary system can also result in disease, as elevated cholesterol is the major risk factor in the development of cholesterol gallstones, which account for nearly 80 percent of all gallstones. Every year, gallstones afflict over 20 million Americans and force almost half a million Americans to undergo cholecystectomy (surgical removal of their gallbladder) (Rose, 1998).

Sources of Cholesterol: *de novo* Synthesis and Dietary Uptake

Total body cholesterol originates from dietary intake as well as *de novo* synthesis. In the U.S., the typical daily internal production of cholesterol is about 1g and the typical daily dietary intake is 300–500 mg, while the total body content is approximately 35 g (Ikonen, 2006; Levy et al., 2007). The intestines are responsible for absorbing dietary cholesterol as well as reabsorbing biliary cholesterol (Rose, 1998). *De novo* synthesis of cholesterol occurs mainly in the liver, intestines, adrenal glands and reproductive organs, where it is synthesized through the HMG-CoA reductase pathway from acetyl CoA, a metabolic product of

glycolysis and fatty acid oxidation. The liver is the major site of synthesis, producing approximately 25% of *de novo* cholesterol

The liver exerts an extremely important role in maintaining organismal homeostasis; it synthesizes the majority of serum proteins, detoxifies hazardous materials, and controls metabolism. The liver carefully regulates the body's cholesterol balance by maintaining an equilibrium between cholesterol biosynthesis, degradation, utilization, uptake, transport, efflux, and storage (Rose, 1998). It receives cholesterol from the diet via chylomicron remnants and from extrahepatic synthesis via plasma lipoproteins. Cholesterol is utilized by liver cells (hepatocytes) either for incorporation into membranes, elimination into bile as free cholesterol or bile acids, or secreted as a component of plasma lipoproteins (Rose, 1998).

Mouse as a Model Organism for Studying Cholesterol and Atherosclerosis

Currently, the most popular *in vivo* model for the study of cholesterol transport and atherosclerosis is the mouse (mus musculus). Compared to humans, mice have high levels of HDL (high density lipoprotein) and low levels of VLDL (very low density lipoprotein) and LDL (low density lipoprotein). This anti-atherogenic profile makes mice relatively resistant to the development of atherosclerosis (Ikonen, 2006). Genetic and dietary manipulations have been developed to promote atherosclerosis in mice, usually involving increases in the levels of the apoB containing lipoproteins (LDL and VLDL). Among mouse strains, C57Bl6 mice

are one of the most sensitive to atherosclerosis.

Induced mutant mice deficient in apolipoprotein E (ApoE) or the LDL receptor (LDLR) are sensitized to developing atherosclerosis, and consequently are the two most popular murine models for studying this disease (Ikonen, 2006). Both apoE and the LDLR are involved in lipoprotein clearance. ApoE is the ligand for receptors that clear chylomicron and VLDL remnants. The LDLR is responsible for the clearance of LDL, which occurs mostly in the liver.

Using gene microarrays to identify novel dietary cholesterol-regulated genes in the mouse liver, Soccio and then Maxwell identified the novel cholesterol-regulated genes, ADAM11 and StARD4, respectively. Soccio found that StARD4 represented a subfamily of START domain containing genes, which also include StarD5 and StarD6. This thesis will employ dietary and genetic manipulations in mice to better understand the physiological functions of ADAM11 and StARD5.

Cholesterol Regulation of Gene Expression

Many of the genes important for regulating cholesterol homeostasis are regulated by cholesterol itself at the transcription level, more specifically by one of three major transcriptional pathways: the sterol regulatory element binding proteins (SREBPs), the liver X receptors (LXRs), and the Unfolded Protein Response (UPR)/Endoplasmic Reticulum (ER) Stress Response. These pathways will be described in detail in the following three sections.

The Sterol Regulatory Element-Binding Proteins (SREBP) Pathway

The sterol regulatory element-binding proteins (SREBPs) compose a family of transcription factors that regulate expression of genes involved in the synthesis and uptake of sterols, fatty acids, triglycerides, and phospholipids (Brown and Goldstein, 1999; Eberlé et al., 2004; Espenshade and Hughes, 2007; Horton et al., 2002). SREBP family members are initially synthesized on the ER membrane as inactive 1150 amino acid precursor proteins that contain the following domains: an N-terminal basic helix-loop-helix (bHLH) leucine zipper transcription factor domain that projects into the cytosol; two hydrophobic membrane spanning regions separated by a short hydrophilic loop that projects into the ER lumen; and a C-terminal regulatory domain that projects into the cystosol (Brown and Goldstein, 1999; Eberlé et al., 2004).

In mammalian cells, there are two SREBP genes (SREBP-1 and -2) encoding three distinct SREBP isoforms: 1a, 1c, and 2. Alternative promoters of SREBP-1 generate SREBP-1a and -1c, which differ only in the length of their N-terminal transcription factor domain (Eberlé et al., 2004; Espenshade and Hughes, 2007). Transgenic mice over-expressing the active domain (N-terminal) of either SREBP-1a, 1c, or 2 have been used to identify target genes (Horton et al., 1998; Shimano et al., 1996; Shimano et al., 1997a). These studies revealed SREBP-1c preferentially enhances transcription of genes involved in fatty acid synthesis (lipogenic genes), but not cholesterol synthesis (cholesterogenic genes), whereas

SREBP-2 preferentially enhances the expression of cholesterogenic genes, but not lipogenic genes. SREBP-1a is a potent activator of all SREBP-responsive genes, including those involved in both lipogenesis and cholesterologenesis. It is thought that SREBP-1a plays a limited role physiologically, because it is present in the liver at much lower concentrations than either SREBP-1c or SREBP-2. Knockout mice for each of the SREBPs have been made, but have been less

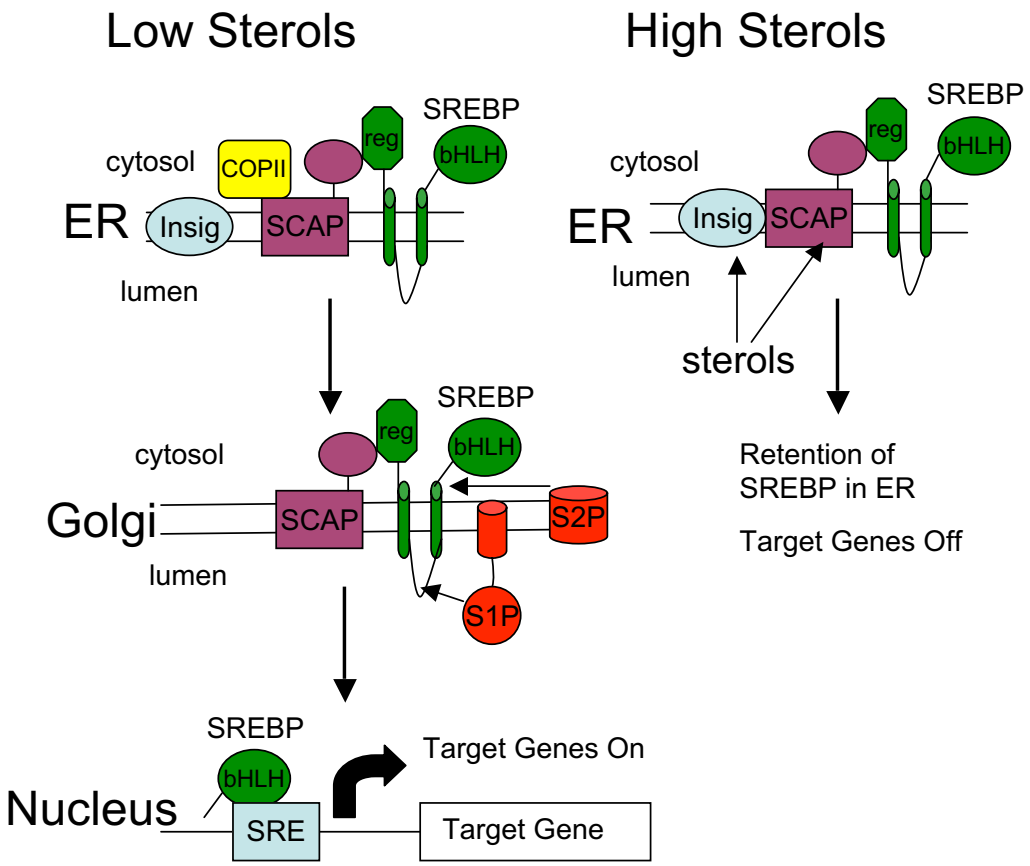

Figure 1.1. **Regulation of SREBP proteolytic activation by cellular sterol levels.** When sterols are abundant, SREBPs remain in the ER as inactive precursors associated with SCAP and Insig. When sterols are scarce, SCAP and Insig undergo conformational changes, which allow SCAP to interact with the COPII complex rather than Insig. This leads to the transport of the SCAP-SREBP complex from the ER to the Golgi apparatus, where the site 1 and site 2 protease (S1P and S2P) cleave SREBP, releasing the N-terminal bHLH transcriptional activation domain. The bHLH of SREBP is translocated to the nucleus and binds to target gene promoters via an SRE binding site. This leads to the activation of target genes involved in the synthesis and uptake of cholesterol and fatty acids.

revealing. Homozygosity for the SREBP-1a or SREBP-2 knockout traits results in embryonic lethality (Liang et al., 2002; Shimano et al., 1997b). However, homozygotes for the SREBP-1c knockout trait are viable and exhibit decreased lipogenesis, confirming the role for SREBP-1c suggested by the transgenic mouse studies (Shimano et al., 1997b).

The activity of SREBPs is regulated by several processes, including proteolysis within the secretory pathway, transcriptional control, post-translational modification, and interactions with coactivators (Bengoechea-Alonso and Ericsson, 2007). SREBPs are synthesized as inactive precursors tethered to the ER, with their carboxy(C)-terminal ends forming complexes with the membrane-bound, sterol-responsive chaperone SREBP-cleavage-activating-protein (SCAP) (Espenshade and Hughes, 2007). When cellular sterols are abundant, cholesterol-bound SCAP binds SREBP and forms a complex with the oxysterol-bound ER resident proteins insulin-induced-gene Insig1 and Insig2, promoting SREBP retention in the ER and thus blocking the transcription of SREBP-responsive genes (Yang et al., 2002). The importance of SCAP in regulating SREBP activity was demonstrated in transgenic mice carrying a SCAP mutant protein (D443N), which is unable to bind to Insig; this mutation resulted in constitutive nuclear localization of SREBP and up-regulation of SREBP target genes (Espenshade and Hughes, 2007; Korn et al., 1998). When cellular sterols are low, SCAP, which has a sterol sensing domain, undergoes a conformational change, releasing Insig (Brown et al.,

2002; Turtoi et al., 2008). This conformational change promotes the binding of the SCAP-SREBP complex to COPII vesicles via interactions with Sar1 and the Sec23/24 complex; this allows the SCAP-SREBP complex to translocate from the ER to the Golgi (Espenshade and Hughes, 2007). In the Golgi, the membrane-bound serine-protease site-1-protease (S1P) cleaves the luminal loop of SREBP, allowing the membrane-bound zinc-metalloprotease site-2-protease (S2P) to cleave SREBP, and thereby releasing the N-terminal domain of SREBP into the cytoplasm. This N-terminal domain, the active bHLH-Zip transcription factor, interacts with importin via its nuclear localization signal and is translocated into the nucleus, where it activates transcription by binding to sterol regulatory elements (SREs) and by interacting with other transcription factors (Espenshade and Hughes, 2007).

SREBPs are also regulated transcriptionally. Transcriptional coactivators, such as CBP/p300, Mediator, and PGC-1beta, play an important role in regulating SREBP activity (Bengoechea-Alonso and Ericsson, 2007). Transcription of SREBP-1c can also be regulated by insulin via a PI(3)-kinase dependent pathway, and by activation by the Liver X Receptor (LXR) alpha (Bengoechea-Alonso and Ericsson, 2007). SREBP-2 autoregulates its own expression through binding to the SRE located in its promoter. SREBP activity can also be regulated via post-translational modification in the nucleus, including phosphorylation, acetylation, sumoylation, and ubiquitination (Bengoechea-Alonso and Ericsson, 2007).

The LXR Pathway and the Process of Reverse Cholesterol Transport

The liver X receptor (LXR) transcription factors represent another family of transcription factors that regulates the expression of genes involved in reverse cholesterol transport, dietary cholesterol absorption, bile acid metabolism, glucose metabolism, and lipid biosynthesis (Repa and Mangelsdorf, 2002; Schoonjans et al., 2000). Liver X receptors (LXRalpha (NR1H3) and LXRbeta (NR1H2), are members of the nuclear hormone receptor superfamily of ligand-activated transcription factors that work in concert with co-activators and co-repressors to regulate gene expression. The LXRs are composed of the following domains: an N-terminal ligand-independent transcriptional activation domain (AF-1); a zinc finger DNA-binding domain (DBD), which binds to specific DNA sequences called hormone response elements (HREs); a flexible hinge region; a large ligand-binding domain (LBD), often with a lipophilic core and a dimerization interface; and a ligand-dependent transcriptional activation domain (AF-2) (Repa and Mangelsdorf, 2002). LXRalpha is expressed in the liver, spleen, adipose tissue, lung, and pituitary, while LXRbeta is expressed ubiquitously. Multiple studies have shown that LXR activation inhibits atherosclerosis, while LXR deficiency in macrophages increases lesion formation. Consequently, LXRs and their downstream genes have emerged as potential therapeutic targets for atherosclerosis (Repa and Mangelsdorf, 2002; Tontonoz and Mangelsdorf, 2003).

The LXRs function as obligate heterodimers with 9-cis retinoid X receptors

(RXR (NR2B1)) to activate gene transcription (Hu et al., 2003). These heterodimers bind to LXR-responsive elements (LXREs) that consist of direct repeats (DRs) of the core sequence AGGTCA separated by 4 nucleotides (DR-4) (Repa and Mangelsdorf, 2002; Tontonoz and Mangelsdorf, 2003; Yan and Olkkonen, 2008). LXRs are activated when sterols are abundant in the cell, and increase the expression of genes controlling sterol and fatty acid homeostasis. In the absence of ligand, the LXR/RXR heterodimer binds to co-repressors turning off expression of these target genes. In the presence of ligand, a conformational change in the heterodimer allows the release of co-repressors and the binding of co-activators, thereby activating transcription. Oxysterols, hydroxylated derivatives of cholesterol, as well as glucose and D-glucose-6-phosphate, act as specific agonists for LXRs (Repa and Mangelsdorf, 2002). Among the naturally occurring oxysterols, 22(R)-hydroxycholesterol, which is expressed in the gonads and the adrenals, 24(S)-hydroxycholesterol, which is expressed in the brain, and 24(S),25-epoxycholesterol, which is a byproduct of liver cholesterol biosynthesis and builds up in liver after cholesterol feeding, have been identified as high affinity ligands for LXR (Fu et al., 2001; Lala et al., 1997; Schoonjans et al., 2000). The most abundant oxysterol in plasma, 27-hydroxycholesterol, is only a weak LXR agonist. 27-hydroxycholesterol, because of its abundance in plasma and presence in macrophages, might be the most physiologically relevant LXR ligand. Moreover, several synthetic, nonsteroidal LXR-selective agonists (T0314407, T0901317,

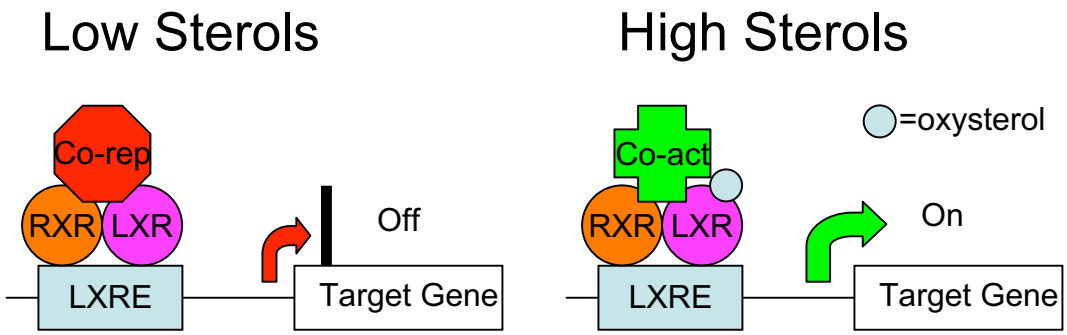

Figure 1.2. **Gene activation by LXRs in the presence of oxysterol ligands**. LXRs heterodimerize with RXR and bind to LXRE sites in the promoters of target genes. In the absence of ligand, the LXR-RXR heterodimer binds co-repressors and target genes are turned off. In the presence of ligand, such as oxysterols, the LXR-RXR heterodimer releases co-repressors, binds co-activators, and activates transcription. LXR target genes are generally involved in cholesterol efflux and reverse cholesterol transport.

GW3965) have also been identified (Collins et al., 2002; Schultz et al., 2000).

The use of natural and synthetic LXR ligands and LXR knockout mice have been useful in elucidating the functions and the target genes of the LXRs. Upon cholesterol feeding LXRalpha knockout mice fail to up-regulate transcription of the gene encoding cholesterol 7alpha-hydroxylase (Cyp7a), the rate-limiting enzyme in bile acid synthesis. This resulted in a rapid accumulation of large amounts of cholesterol in the liver and provides evidence that LXR-alpha can act as a sensor of dietary cholesterol (Peet et al., 1998). In contrast, cholesterol feeding of LXR-beta knockout mice did up-regulate Cyp7a in the liver and did not result in accumulation of cholesterol in the liver, indicating distinct metabolic roles for LXR-alpha and LXR-beta (Alberti et al., 2001).

When sterols are abundant in cells, LXRs bind their oxysterol ligands and activate transcription of downstream genes. Most known LXR target genes remove excess cholesterol through efflux, catabolism or decreased absorption. In other

words, they function in the process of reverse cholesterol transport (RCT), a process by which cholesterol is transported via HDL from peripheral cells to the liver, where it can be excreted into bile as free cholesterol or bile acids (Repa and Mangelsdorf, 2002). The importance of the LXR pathway in RCT has been demonstrated using LXR knockouts, transgenics, and agonists. In macrophages, LXRs activate members of the integral membrane ATP-binding cassette (ABC) transporter protein family, including ABCA1, which is critical for the efflux of excess cellular cholesterol to pre-betaHDL and to the apolipoprotein acceptor AI (ApoAI), and ABCG1 which plays a similar role in cholesterol efflux to HDL (Costet et al., 2000; Venkateswaran et al., 2000). LXRs stimulate macrophage and adipocyte transcription of the ApoE gene, which encodes a secreted protein that resides on the surface of chylomicron and VLDL remnants and serves as a ligand for hepatic receptor removal of these particles from plasma (Joseph et al., 2004). LXRs also up-regulate expression of genes that encode three lipoprotein remodeling enzymes: lipoprotein lipase (LPL), which catalyzes the hydrolysis of lipoprotein triglycerides and may promote the conversion of triglyceride-rich lipoproteins to cholesterol-rich remnants (Zhang et al., 2001); cholesterol ester transfer protein (CETP), which in humans mediates the transfer of HDL cholesterol esters to apoB containing particles (LDL) for return to the liver (Luo et al., 2001; Luo and Tall, 2000; Matsuura et al., 2006; Steffensen and Gustafsson, 2004); and phospholipid transfer protein (PTLP), which modulates HDL metabolism (Cao et al., 2002). In the liver, LXRs

up-regulate the expression of scavenger receptor B-1 (SRB-1), which mediates the liver uptake of cholesterol from HDL (Malerød et al., 2002; Silver and Tall, 2001). In the liver, LXRs also activate Cyp7a1, which converts cholesterol into bile acids, as well as the transporter proteins ABCG5 and ABCG8, which form a

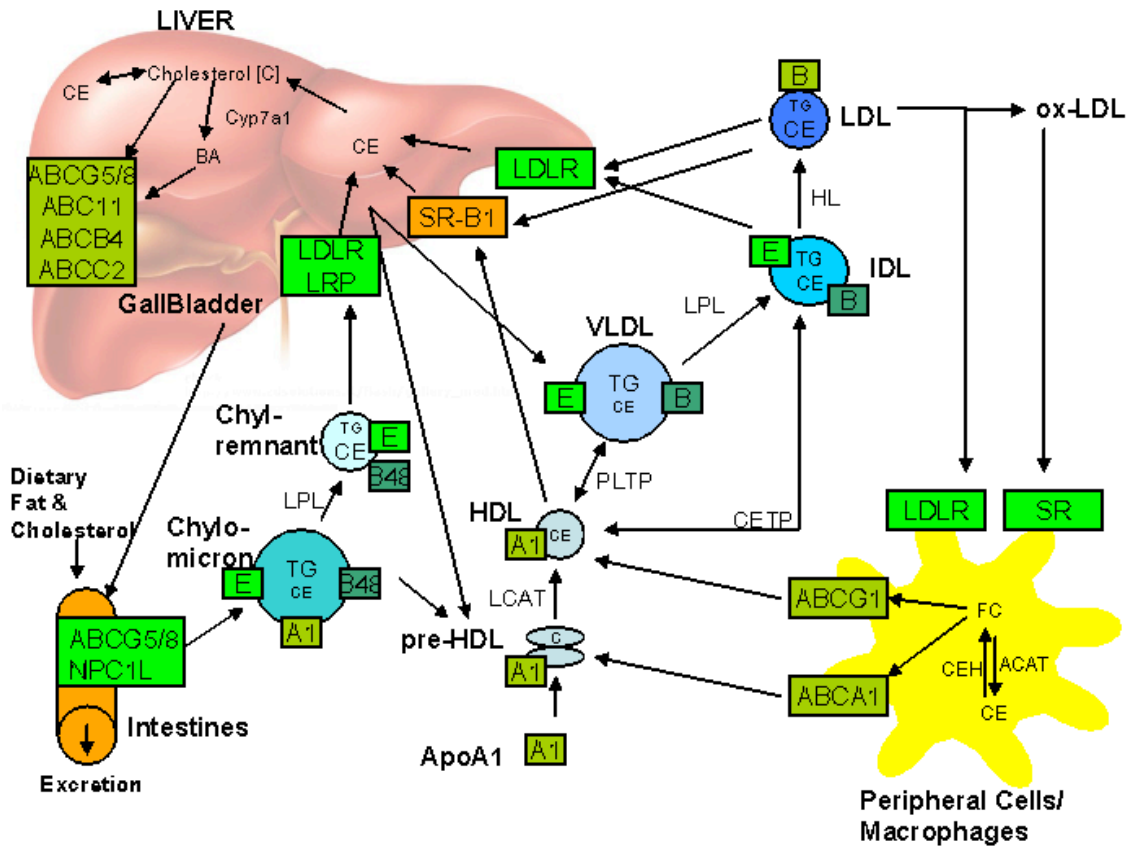

Figure 1.3. **Overview of lipoprotein metabolism along with the process of Reverse Cholesterol Transport.** Dietary cholesterol in the intestines are packaged into large ApoB-48 containing chylomicrons and secreted. In the plasma, chylomicrons acquire ApoE and ApoC; they are converted into chylomicron remnants via lipoprotein lipase (LPL) and are taken up by the liver. The liver produces apoB100 containing, triglyceride-rich VLDL. Through the action of LPL and hepatic lipase (HL), VLDL is converted into IDL, and LDL. LDL can be taken up into the liver and in in the periphery via the binding of apoB100 to the LDLR. Peripheral cells can efflux cholesterol to nascent ApoAI via ABCA1, creating pre-HDL particles, which are converted to HDL by LCAT. Peripheral cells can efflux cholesterol(C) to HDL via ABCG1. Cholesterol ester transfer protein (CETP) transfers cholesterol ester(CE) and phospholipid transfer protein (PLTP) transfers phospholipids between HDL and ApoB containing lipoproteins. HDL can be taken up by the liver via SR-B1. Cholesterol in the liver may be converted to bile acids via Cyp7a1 or effluxed directly into the bile via ABCG5/8 or other ABC transporters.

heterodimer in the apical (canalicular) membrane of the hepatocyte and pump cholesterol out of the liver into bile (Yu et al., 2003). In the intestine, LXRs activate ABCA1, ABCG5, and ABCG8 to decrease absorption of dietary cholesterol (Repa et al., 2002). All of these processes seem to have the net effect of removing excess cholesterol from the periphery to the liver and then out into bile.

In addition to their ability to modulate cholesterol metabolism, LXRs are also key regulators of hepatic lipogenesis and glucose metabolism. LXRs can transcriptionally activate SREBP-1c expression enhancing lipogenesis and leading to hypertriglyceridemia (Repa et al., 2000; Schultz et al., 2000). Treatment of mice with synthetic LXR ligands can cause hepatic steatosis (Schultz et al., 2000). LXRs can increase hepatic glucose utilization and decrease hepatic glucose output by induction of glucokinase and decreasing hepatic gluconeogenic genes such as phosphoenolpyruvate carboxykinase and glucose-6-phosphatase; thereby improving glucose tolerance (Wójcicka et al., 2007). Recent studies have shown that LXRs also possess anti-inflammatory activity, repressing several inflammatory genes (iNOS, COX2, IL-6 IL-1βMCP-1, MCP-3, and MMP9) after bacterial, LPS, TNF-α, or IL-1βstimulation (Yan and Olkkonen, 2008).

In summary, LXR has the ability to promote reverse cholesterol transport, improve glucose tolerance, and limit inflammation. All of which make LXRs attractive targets for pharmacological intervention for the treatment of cardiovascular, metabolic, and/or inflammatory diseases.

The Endoplasmic Reticulum Stress Response / The Unfolded Protein Response

The ER accounts for nearly 50% of the cellular membranes and is a major site of cellular calcium storage, sterol and lipid synthesis, and protein synthesis, folding, and modification (Maxfield and Menon, 2006). The ER also plays a major role in sensing cellular homeostasis. Only properly folded and modified proteins in the ER are exported to the Golgi, while mis-folded or mis-modified proteins are degraded. Disruption of this process via generation of reactive oxygen species (ROS), excessive secretory protein synthesis, or cholesterol overload results in "ER stress" and causes activation of three trans-membrane proteins (PERK, IRE-1, and ATF6), which bring about the Unfolded Protein Response (UPR), also called the ER Stress Response (Kaufman et al., 2002; Schroder and Kaufman, 2005; Shen et al., 2004).

The ER proteins ATF6, IRE-1, and PERK are normally bound and sequestered by BiP (GRP78), an ER chaperone. BiP preferentially binds to mis-folded proteins, and in their presence, ATF6, IRE-1, and PERK become untethered and initiate the UPR (Kaufman et al., 2002). ATF6, the ER-membrane bound activating-transcription-factor-6, translocates to the Golgi, where it is cleaved by S1P and S2P, releasing its N-terminal domain, an active basic leucine zipper (bZIP) transcription factor, which translocates to the nucleus (Haze et al., 1999). IRE1, the ER type I trans-membrane kinase/endoribonuclease, homodimerizes and

undergoes trans-autophosphorylation, which then allows it to mediate splicing of XBP1 mRNA resulting in the synthesis of the active bZIP transcription factor XBP1 (Back et al., 2005). PERK, another type I transmembrane kinase, phosphorylates eIF2alpha, which attenuates translation of most mRNAs, while also selectively enhancing the translation of another bZIP transcription factor ATF4 (Brewer and Diehl, 2000).

The three transcription factors, ATF6, XBP1, and ATF4, up-regulate expression of target genes by interacting with the ERSE (ER Stress Response Element) in their promoters. The induced target genes increase the folding capacity of the ER by increasing the capacity of the ER to synthesize phospholipids, to re-esterify sterols, and to process proteins by promoting proper folding, i.e., chaperones and folding enzymes (Back et al., 2005; Kaufman et al., 2002; Schroder and Kaufman, 2005; Sriburi et al., 2004). They also down-regulate the ER load by decreasing transcription and translation of most other genes. By up-regulating ER associated degradation (ERAD), they also increase the clearance of unfolded/misfolded proteins from the ER. If, however, these processes fail to remedy the stress, the UPR can ultimately signal apoptosis and eliminate the unhealthy cell via activation of the C/EBP homologous protein transcription factor (CHOP), as well as c-Jun NH2-terminal kinase (JNK) and caspases. It is now known that this apoptotic pathway plays a fundamental role in the pathogenesis of multiple human diseases including diabetes, atherosclerosis and

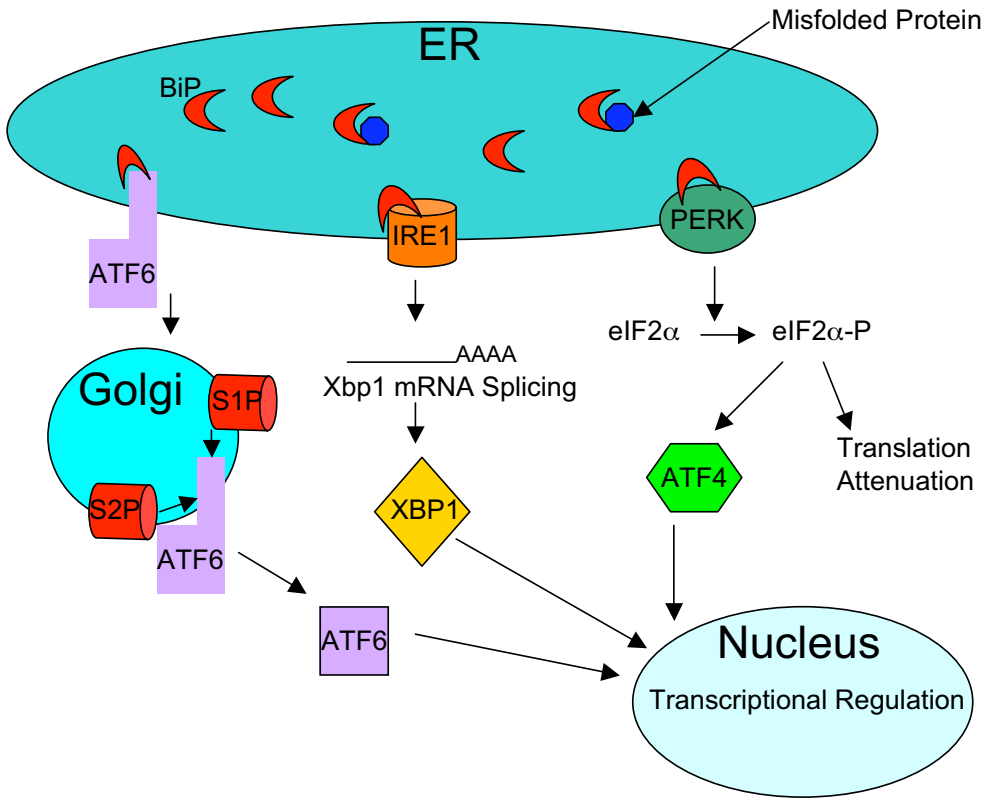

Figure 1.4. **Signaling the Unfolded Protein Response (UPR) / ER Stress Response Pathway.** Three proximal sensors IRE1, PERK and ATF6 regulate the UPR through their respective signaling cascades. Under non-stressed conditions, BiP binds to the lumenal domains of IRE1, ATF6, and PERK. Upon accumulation of unfolded proteins in the ER lumen, BiP is sequestered, releasing IRE1, PERK, and ATF6. IRE1 mediates non-traditional splicing of Xbp1 mRNA. ATF6 is activated by proteolysis in the Golgi similar to SREBP processing. The PERK pathway phosphorylates eIF2α, which leads to transient attenuation of global translation, but activation of ATF4 translation. The ER stress signals are then transduced via these three parallel transcription factors: ATF4, XBP1, and ATF6.

neurodegenerative diseases (Malhotra and Kaufman, 2007; Zhang and Kaufman, 2006).

Accumulation of free cholesterol (FC) in the ER has been shown to trigger the UPR (Tabas, 2002b). Normally, the ER cholesterol concentration is quite low and maintained that way by the combined efforts of cholesterol efflux/transporters and ER cholesterol esterification via ACAT. The latter converts ER free cholesterol

to cholesterol esters, which are relatively inert and can be stored in cytoplasmic droplets (Feng et al., 2003a). However, when these mechanisms fail or are overwhelmed, cholesterol accumulates in the ER, which perturbs the normally cholesterol-low ER membrane. Utilizing an *in vitro* cell culture model, the Tabas laboratory has clearly shown that loading macrophages with free cholesterol by incubation with acetylated LDL in the presence of an ACAT inhibitor causes depletion of ER calcium stores, activation of the UPR and ultimately apoptosis (Feng et al., 2003a; Tabas, 2002b).

UPR activation occurs at all stages of atherosclerotic lesion development (Zhou et al., 2005). During atherosclerogenesis, macrophages take up cholesterol/lipoproteins via scavenger receptors, the expression of which on cells is independent of cellular cholesterol status. This leads to excess cellular FC provoking the UPR, which early on enhances cell survival, but prolonged ER stress, at least in part due to FC accumulation, leads to apoptosis. This is evidenced by the correlation of FC accumulation with the expression of CHOP and apoptosis in advanced atherosclerotic lesions in ApoE knockout mice (Zhou et al., 2005).

Intracellular Cholesterol Transport

In mammalian cells, there are marked asymmetries in free cholesterol concentration and distribution between cellular organelles. Approximately, 65% to 80% of free cholesterol, resides in the plasma membrane (PM); in contrast, only 0.1% to 2% of free cholesterol resides in the ER, despite the fact that the surface

areas of these two membranes in a cell are approximately equal (Liscum and Munn, 1999; Maxfield and Menon, 2006; Maxfield and Wustner, 2002; Prinz, 2002; Prinz, 2007). In the PM, free cholesterol comprises approximately 30% to 45% of total lipid, whereas in the ER and mitochondria cholesterol comprises less than 10% of total lipid. The free cholesterol concentration in the Golgi is intermediate between the PM and the ER (Repa and Mangelsdorf, 2002; Liscum and Munn, 1999; Maxfield and Wustner, 2002; Prinz, 2002). Moderate changes in total cellular cholesterol have drastic effects on cholesterol levels within the ER, stimulating the signaling mechanisms involved in maintaining homeostasis. The exact mechanisms for forming and maintaining this large gradient across organelles need to be elucidated; a sorting mechanism must exist to include or exclude cholesterol at various membranes. Understanding the process of cellular cholesterol transport, either via vesicular or non-vesicular pathways, could clarify the mechanism(s) behind this gradient (Ikonen, 2006, 2008; Prinz, 2007).

In eukaryotic cells most organelles, with the exception of mitochondria, transport cargo in small, membrane-enclosed vesicles that move along the cytoskeleton by an ATP dependent process. Evidence for this mechanism derives from the observations that treating cells with Brefeldin A, which disrupts the cytoskeleton, inhibits delivery of newly synthesized cholesterol from the ER to the PM, and ATP depletion by metabolic poisons also disrupts intracellular sterol transport (Prinz, 2007). In addition, it is known that Rab GTPases are key

regulators of vesicular trafficking and disrupting them with Rab-GDI (GDP dissociation inhibitors) impairs cholesterol movement, while over-expression of Rab GTPases alter cellular cholesterol distribution between membranes. The latter suggests that cholesterol transport by vesicles is necessary for the proper distribution of cholesterol between membranes (Ikonen, 2008). There is some evidence that cholesterol is sorted into vesicles headed toward the PM and excluded from vesicles headed to the ER. For example, cholesterol and sphingomyelin are both excluded from CopI-vesicles, which move from the Golgi back to the ER (Brügger et al., 2000; Prinz, 2007). Sorting cholesterol between vesicles and membranes could also be driven by membrane curvature and microdomain formation within membranes (Prinz, 2007; Roux et al., 2005). Thus vesicles can move sterols within cells, but much remains to be learned about the mechanisms involved and their importance in cellular cholesterol homeostasis.

It is clear that non-vesicular cholesterol transport plays a large role in cellular cholesterol homeostasis. For example, blocking the vesicular pathway does not significantly alter the cholesterol gradient across organelles, suggesting that the bulk of intracellular sterol trafficking occurs via a non-vesicular pathway (Prinz, 2007; Soccio and Breslow, 2004). Moreover, treating cells with enough Brefeldin A to block over 90% of protein secretion only decreases newly synthesized cholesterol transport to the PM by 20% (Prinz, 2007; Soccio and Breslow, 2004). Non-vesicular trafficking is mediated by various diffusible carrier proteins that

contain a hydrophobic region allowing hydrophobic cholesterol molecules to be transported across the aqueous cytosol. The next sections will review some of the putative intracellular cholesterol transport proteins, including the Nieman Pick C proteins, the oxysterol binding protein-related proteins, the sterol carrier protein-2, the caveolins, and the steroidogenic acute regulatory–related lipid transfer domain proteins.

The Role of Niemann Pick C Proteins

Niemann Pick Type C (NPC) disease is a rare autosomal recessive, lipid storage disorder that manifests as a progressive neurodegenerative disease (Ikonen, 2006; Liscum and Sturley, 2004; Prinz, 2007). It is caused by mutations in either the NPC1 or NPC2 genes and is characterized by the intracellular accumulation of cholesterol and other lipids, particularly sphingolipids, in the late endosomal/lysosomal compartment. NPC1 is a late endosomal membrane protein that contains a sterol sensing domain (SSD) capable of binding cholesterol, and is essential for the transfer of cholesterol out of endosomes and lysosomes. NPC2, also known as HE-1, is a small, soluble cholesterol-binding glycoprotein that resides in the lumen of late endosomes and lysosomes (Cheruku et al., 2006; Friedland et al., 2003; Ko et al., 2003; Patel et al., 1999; Sleat et al., 2004; Watari et al., 1999). The crystal structure of NPC2 reveals a hydrophobic tunnel too small to contain a cholesterol molecule; so the protein is thought to undergo a conformational change to accommodate cholesterol (Friedland et al., 2003).

The loss of NPC1 or NPC2 in mouse models leads to intracellular sterol accumulations, similar to the phenotype seen in NPC disease. ApoE knockout mice whose macrophages are heterozygous for NPC1 deficiency have diminished lesional necrosis and macrophages that resist apoptosis (Feng et al., 2003b). ApoE knockout mice whose macrophages are homozygous for NPC1 deficiency have larger lesions with evidence of atherothrombosis, and arterial medial degradation (Feng and Tabas, 2002; Welch et al., 2007). LDLR knockout mice whose macrophages are homozygous for NPC1 deficiency have larger lesions and macrophages with impaired cholesterol efflux and increased ROS (Zhang et al., 2008).

The Role of Oxysterol Binding Protein (OSBP) - Related Proteins (ORPs)

A family of oxysterol binding protein (OSBP)-related proteins (ORP) has been described containing 12 members in humans and mice, and seven members in budding yeast (OSPB-homologoues (Osh) (Fairn and McMaster, 2008; Yan and Olkkonen, 2008). ORPs are thought to play roles in lipid distribution and metabolism, cell signaling, and vesicular transport (Beh and Rine, 2004; Fairn and McMaster, 2008; Prinz, 2007; Yan and Olkkonen, 2008). The C-terminus of all ORPs contain the lipid binding OSBP-related protein domain (ORD) with the signature OSBP motif (EQVSHHPP). ORPs appear to bind 25-hydroxycholesterol (25OH) and other oxysterols via this domain; sterol binding assays have shown that 25OH can bind to OSBP, ORP1, ORP2, ORP3, ORP4, ORP5, ORP6, ORP7,

ORP8, ORP10 and ORP11. ORP 5 and 8 also contain a putative trans-membrane domain at their C-termini. The N-termini of ORPs are variable and can contain FFAT motifs, pleckstrin homology domains (PH), and ankyrin repeats. The N-terminal domains may mediate interactions with other proteins or subcellular localization, but their exact roles are still unknown. Alternative splicing is common in ORPs and results in long (denoted by –L) and short (denoted by –S) forms of these proteins; the short forms lacks the N-terminal region present in the long forms. The subcellular localization of ORPs can vary. For example, OSBP changes its intracellular location in the presence of oxysterols.

Much of our understanding of the functions of ORPs has come from work in the yeast S. cerevisiae (Beh and Rine, 2004; Fairn and McMaster, 2008; Prinz, 2007; Yan and Olkkonen, 2008). In this model organism ORPs are referred to as Oshs. *In vitro* it was shown that Osh 4 (Kes1) can extract cholesterol from liposomes and transfer it to acceptor membranes, suggesting that ORPs may function as soluble sterol transporters. Deleting any one of the seven Osh proteins has little effect on sterol transfer, suggesting redundant functionality. However, conditional deletion of all seven Osh proteins (osh-del, osh4-1) alters intracellular sterol distribution, causes vacuolar fragmentation, causes accumulation of lipid droplets in the cytoplasm and within vacuolar fragments, and eventually leads to cell death (Beh and Rine, 2004; Fairn and McMaster, 2008; Prinz, 2007; Yan and Olkkonen, 2008).

The exact role of mammalian ORPs is unknown, and there is no direct evidence that mammalian ORPs function as sterol transfer proteins. In mammalian cells, ORPs can be subdivided into six subfamilies based on sequence homology (OSBP and ORP4; ORP1 and 2; ORP5 and 8; ORP3, 6, and 7; ORP9; and ORP10 and 11).

OSBP is normally localized in the cytoplasm, but relocates to the Golgi when cells are treated with 25-hydroxycholesterol (Fairn and McMaster, 2008). Over-expression of OSBP in CHO cells increases cholesterol and sphingomyelin synthesis, possibly due to sequestration of endogenous sterols. Knocking down OSBP via RNAi causes no significant change in cholesterol or fatty acid synthesis (Fairn and McMaster, 2008). OSBP appears to be involved in regulating sphingomyelin production by recruiting the CERT-dependent ceramide transporter StARD11 (more on this gene in the START section) from the ER to the Golgi (Perry and Ridgway, 2005, 2006). Adenoviral over-expression of OSBP in mouse liver leads to an increase in plasma VLDL and triglycerides (TG), due in part to up-regulation of hepatic SREBP-1c, causing increased hepatic triglyceride synthesis (Yan et al., 2007b). The close OSBP homologue, ORP4 has two splice variants: ORP4L and ORP4S, both of which co-localize with the intermediate filament vimentin. Over-expression of ORP4S causes a collapse of the vimentin network, suggesting a role for ORP4S in the regulation of microtuble formation (Wang et al., 2002). Cells over-expressing ORP4S also display reduced esterification of low-

density-lipoprotein(LDL)-derived cholesterol, suggesting ORP4 modulates the transfer of LDL derived free cholesterol from the lysosome to the ER where it undergoes esterification by ACAT, perhaps by a vesicular pathway along a microtubular network involving vimentin (Wang et al., 2002).

The ORP1 and ORP2 subfamily may also play a role in intracellular lipid metabolism. ORP1 has two splice variants and the expression of ORP1S predominates in heart and skeletal muscle, whereas ORP1L expression predominates in brain, lung, and macrophages (Johansson et al., 2003). ORP1L localizes to the late endosomal compartment and via its ankyrin repeat region interacts with and stabilizes the late endosomal GTPase Rab7. In cell culture over-expression of ORP1L enhances LXRalpha-mediated transactivation of a reporter gene, suggesting a role for ORP1L in transport of LXRalpha-ligands such as oxysterols (Johansson et al., 2003). *In vivo* macrophage over-expression of ORP1L driven by the scavenger receptor A promoter increases atherosclerotic lesions in LDLR knockout mice, also suggesting it may play a role in macrophage sterol metabolism (Yan et al., 2007a).

ORP2 has only one known form (Laitinen et al., 2002), and over-expression in CHO or HeLa cells causes up-regulation of cellular cholesterol efflux, reducing cellular free cholesterol. Cells over-expressing ORP2 also decreased cholesterol esterification, reduced triglycerides, and caused a shift of polyunsaturated fatty acids from neutral lipids to phospholipids (Hynynen et al., 2005; Käkelä et al., 2005).

ORP8, which localizes to the ER via its C-terminal trans-membrane domain, may also play a role in cellular lipid metabolism. Immunohistochemical analysis has revealed that ORP8 is highly expressed in macrophages in human atherosclerotic lesions (Yan et al., 2008). RNAi knock down of ORP8 expression in THP-1 macrophages results in increased in ABCA1 expression and concomitantly an increase in cholesterol efflux to ApoA1 (Johansson et al., 2003).

ORP9 can negatively regulate Akt phosphorylation and in this manner influence Akt signaling pathways that control cell cycle, survival, and glucose metabolism (Lessmann et al., 2007; Wyles and Ridgway, 2004). There is some evidence that ORP3 might interact with the actin cytoskeleton, and in this manner influence cell polarity and cell adhesion (Collier et al., 2003; Lehto et al., 2005; Lehto et al., 2008). The roles of ORP5, 6, 7, 10, and 11 have not been explored.

The Role of Sterol Carrier Protein-2 (SCP-2)

Sterol carrier protein-2 was discovered as a soluble protein that binds and transfers cholesterol as well as phospholipids (Gallegos et al., 2001). The SCP-2 gene has two initiation sites that produce distinct proteins, the 58-kDA sterol carrier protein-x (SCP-x) and the 15-kDA pro-SCP-2 protein, which share the same C-terminus (Gallegos et al., 2001). Both can be post-translationally cleaved to produce the same active 13-kDa protein SCP-2. In addition to a fully functional 13-kDa SCP-2 protein, the cleavage of the 58-kDA SCP-x also produces a 46-kDa protein. SCP-x and SCP-2 are highly expressed in tissues involved in cholesterol

trafficking and oxidation, notably the liver, intestine, adrenal glands, testis, and ovary. While SCP-x is almost exclusively localized to peroxisomes, SCP-2 is also found in cytoplasm, ER, mitochondria, and lysosomes (Gallegos et al., 2001). The 58 kDa SCP-x and its 46 kDa cleavage product are 3-ketoacyl-CoA thiolases that oxidize straight and branched-chain lipids, and play an essential role in detoxification and bile acid synthesis (Gallegos et al., 2001; Seedorf et al., 2000). Mice lacking SCP-x have defects in branched chain fatty acid catabolism, due to the lack of peroxisomal thiolase activity (Seedorf et al., 1998). Furthermore, SCP-2 knockout mice have impairments in biliary lipid and hepatic cholesterol metabolism (Fuchs et al., 2001).

SCP-2 has also been called the non-specific lipid transfer protein (nsLTP), because it binds many lipids, including cholesterol, phospholipids, fatty acids, fatty acyl CoAs, lysophosphatidic acid, phosphatidylinositol, and sphingolipids, and *in vitro* has been shown capable of transferring these lipids between membranes (Gallegos et al., 2001; Prinz, 2007). There is no definitive proof that SCP-2 functions in this manner *in vivo*. However, over-expression in cell culture suggests SCP-2 may facilitate non-vesicular sterol trafficking. In McA-RH7777 rat hepatoma cells, over-expression of SCP-2 increases the rate of newly synthesized cholesterol transfer to the plasma membrane, alters cholesterol uptake and efflux to HDL, inhibits cholesterol ester synthesis and high density lipoprotein cholesterol secretion, and alters plasma membrane lipid distribution (Atshaves et al., 2007a;

Atshaves et al., 2007b; Atshaves et al., 2007c; Baum et al., 1997; Gallegos et al., 2001; Moncecchi et al., 1996; Ren et al., 2004a; Schroeder et al., 2007; Schroeder et al., 2001).

The Role of Caveolins

The precise function of caveolins in non-vesicular/vesicular cholesterol transport is still being debated (Prinz, 2007). Caveolins are abundant integral membrane proteins that are essential for the formation of caveolae, a subset of lipid rafts with a flask-shaped plasma membrane invagination. There are three caveolins 1, 2, and 3; caveolin-1 and caveolin-2 have multiple isoforms. Caveolins are located on the cytoplasmic face of caveolae. They serve as structural components of caveolae and scaffolding proteins capable of recruiting and regulating various signaling molecules (Cohen et al., 2004).

Caveolin-1 is a 22 kDa protein that is highly expressed in adipocytes, endothelial cells, fibroblasts, and type I pneumocytes. In non-muscle cells caveolin-1 is necessary and sufficient to drive caveolae formation; wheras in muscle cells caveolin-3, which is muscle specific, performs the same function (Cohen et al., 2004).

In cell culture studies caveolin-1 has been shown to affect cholesterol trafficking and two mechanisms have been proposed whereby caveolin-1 either regulates the formation of plasma membrane caveolae or caveolin-1 acts in a chaperone complex (Cohen et al., 2004; Prinz, 2007). Smart has proposed that

caveolins form a cytosolic cholesterol-caveolin-chaperone macromolecular complex, representing a novel intracellular lipid-protein particle analogous in character to plasma lipoproteins (Li et al., 2005; Liu et al., 2002; Smart et al., 1996; Uittenbogaard and Smart, 2000; Uittenbogaard et al., 1998). In addition to its plasma membrane localization, in some cell types caveolin-1 is also found as a soluble cytosolic protein, in secretory vesicles, and/or in mitochondria.

Caveolin-1 knockout mice have been used to infer the function of caveolin-1 *in vivo*. Given the requirement of caveolin-1 for the formation of caveolae in all non-muscle cells, surprisingly caveolin-1 knockout mice are viable (Razani et al., 2002) with normal plasma cholesterol levels and intestinal cholesterol absorption. The caveolin-1 knockout trait has been bred on to the atherosclerosis prone ApoE knockout background, and the ApoE-Caveolin-1 double knockout mice have less atherosclerosis than the ApoE single knockouts, despite higher levels of plasma non-HDL cholesterol and triglycerides. By way of explanation, Frank has suggested that caveolins play a role in cholesterol uptake by macrophages, and this important process may be blunted in the absence of Caveolin-1 (Frank et al., 2004). Treating mice with an caveolin-1 expressing adenovirus was shown to cause a two-fold elevation in plasma HDL-cholesterol levels, possibly due to disruption of SR-B1 mediated hepatic HDL uptake. If this is not an artifact of non-physiological Caveolin-1 over-expression, it suggest a role for Caveolin-1 in the regulation of HDL metabolism (Frank et al., 2001).

The Role of the Steroidogenic Acute Regulatory–Related Lipid Transfer Domain Protein Family

The StAR-related lipid transfer (START) domain is a highly conserved ~210 amino acid lipid binding domain (Ponting and Aravind, 1999). The human and mouse genomes each have 15 genes encoding START domains, and phylogenetic analysis divides the family into six subfamilies (STAR, PCTP, acyl CoA thioesterase, RhoGAP, StARD9, and StARD4) (Alpy and Tomasetto, 2005; Soccio and Breslow, 2003; Thompson et al., 1994). The X-ray crystal structure of the START domain encoded by several of these genes (StARD 2, 3, 4, and 11) shows a highly conserved helix-grip fold forming a hydrophobic pocket large enough to accommodate a cholesterol or similarly sized molecule plus a C-terminal alpha-helical lid structure (Kudo et al., 2008; Roderick et al., 2002; Romanowski et al., 2002; Tsujishita and Hurley, 2000). The START domain of each gene varies slightly in the number of amino acids as well as in lipid binding specificity. The next six sub-sections present an in-depth discussion of the six START subfamilies. In part this thesis attempts to understand the physiological role of one of the genes in the StARD4 subfamily, StARD5.

The StAR Subfamily

StARD1/StAR

StARD1, also known as the steroidogenic acute regulatory protein (StAR), regulates the limiting step in steroidogenesis in the adrenal cortex and gonads, by

promoting the translocation of cholesterol from the outer mitochondrial membrane (OMM) to the inner mitochondrial membrane (IMM), where the first step in steroid biosynthesis is catalyzed (Clark et al., 1995; Clark and Stocco, 1995; Clark et al., 1994; Miller, 2007b; Miller and Strauss, 1999; Stocco, 2001; Sugawara et al., 1995). StAR delivers cholesterol to the cytochrome P450 side chain cleavage (P450scc) enzyme on the matrix side of the IMM, allowing for the conversion of cholesterol to pregnenolone (Alpy and Tomasetto, 2005; Miller, 2007a). Normally, pituitary trophic hormones can induce steroidogenesis acutely by activating pre-existing StAR through phosphorylation, and by inducing the rapid synthesis of new StAR (Miller and Strauss, 1999). The functional role of StAR in promoting steroidogenesis was identified through transfection and mutational studies. When StAR is transfected in Leydig MA-10 and Cos-1 cells, steroidogenesis increases, and when StAR is mutated, steroidogenesis is severely impaired (Lin et al., 1995; Stocco, 2002; Sugawara et al., 1995).

In humans, mutations in StAR cause congenital lipoid adrenal hyperplasia (lipoid CAH), a rare autosomal recessive disease that results in almost complete inability to synthesize steroids, leading to deficiencies in mineralocorticoids, glucocorticoids, and sex steroids (Lin et al., 1995). The condition is also accompanied by pathological accumulation of cholesterol and cholesterol esters in the gonads and adrenal glands. Knocking out StAR in mice causes a similar disorder to that in humans; mice die prematurely from either respiratory distress or

volume depletion (Caron et al., 1998; Caron et al., 1997). Due to the hormone synthesis deficiency, these knockout mice all have female external genitalia, as well as lipid deposits in the adrenal cortex. Alternatively, mice in which StAR was over-expressed in liver via adenovirus had an elevated rate of bile acid synthesis (BAS) due to increased delivery of cholesterol to mitochondria. (Ren et al., 2004a; Ren et al., 2004b).

StAR contains an N-terminal mitochondrial targeting sequence along with its C-terminal START domain. Deletion mutagenesis studies have shown that StAR lacking its mitochondrial targeting sequence (62 N-terminal amino acid residues) (N-62 StAR) is still functional in cells, suggesting that the protein acts on the cytosolic face of the OMM (Arakane et al., 1998a; Arakane et al., 1998b). The N-terminus appears to simply confine StARs action to the mitochondria and keep the protein away from other organelles (Miller, 2007a). Consistent with this hypothesis, StAR remains functionally active when fused to the C-terminus of the mitochondrial proteins Tom20, Tim9, or Tim40 *in vitro* and then added to steroidogenic mitochondria. In cell culture, StAR also remains active when fused to the C-terminus of Tom20, a mitochondrial pore protein found on the OMM. However, *in vivo* StAR becomes inactive when fused to the C-terminus of Tim9, a protein found in the mitochondrial intramembranous space, or Tim40, a protein localized to the mitochondrial matrix, thereby indicating that it was the localization of the fusion protein, not the structure, that rendered them inactive in cell culture (Bose et al.,

2002; Miller, 2007b).

Exactly how StAR assists in transferring cholesterol from the OMM to the IMM and in stimulating steroidogenesis remains unclear (Prinz, 2007). Mutation studies suggest these two functions may be separable. For example, the StAR mutant R182L can bind and transfer cholesterol, but cannot stimulate steroidogenesis (Miller, 2007a; Tuckey et al., 2002). Recent studies suggest that StAR stimulation of steroidogenesis requires interaction with the peripheral benzodiazepine receptor (PBR), a small OMM protein with a cytoplasmic "cholesterol recognition amino acid consensus" (CRAC) domain (Hauet et al., 2005; Miller, 2007b; West et al., 2001).

StARD3/MLN64

StARD3, also known as MLN64 (metastatic lymph node 64), is an integral membrane protein expressed in all tissues and localizes within cells to late endosomes. The C-terminal START domain is oriented towards the cytosol and consistent with its X-ray crystal structure is capable of binding cholesterol in a 1:1 manner (Tsujishita, 2003; Tsujishita and Hurley, 2000). The N-terminal region consists of four transmembrane domains, has been termed the MENTAL domain. The MENTAL domain is also capable of binding cholesterol, and may play a role in targeting the protein to the late endosome (Alpy et al., 2002). The MENTAL domain can mediate homodimerization of StARD3 as well as heterodimerization with MENTHO (MLN64 N-terminal domain homologue). MENTHO is a product of a

different gene, but encodes a region highly homologous to the MENTAL domain of StARD3, but lacks a START domain (Alpy et al., 2002). MENTHO is ubiquitously expressed and is located in the membrane of late endosomes, with both its N- and C-termini projecting into the cytoplasm. Alpy has speculated there is a sequential transfer of cholesterol from the MENTAL domain of MENTHO to the MENTAL domain of StARD3, to the START domain of StARD3, and finally to an acceptor membrane or protein (Alpy and Tomasetto, 2006).

The function of StARD3 *in vivo* is not yet fully understood. StARD3 was originally identified as a gene over-expressed in breast cancer (Tomasetto et al., 1995), and was also recently found to be over-expressed in gastric, prostate, and esophageal cancers. One theory posits that it might play a role in tumorogenesis by increasing intra-tumoral steroidogenesis. Alternatively, over-expression of StARD3 in tumors might be attributable to tumoral amplification of a neighboring oncogene c-erb-B2 (her-2/neu) (Bièche et al., 1996; Dressman et al., 2003; Hyman et al., 2002; Kauraniemi et al., 2001; Pollack et al., 2002; Tomasetto et al., 1995)

In vitro, the isolated StARD3 START domain is capable of binding and transferring cholesterol to liposomes and mitochondria. It has been suggested that in tissues not expressing StAR, such as placenta and brain, StARD3 might play a role in steroid hormone synthesis (Tuckey et al., 2002; Watari et al., 1997). However, the mechanism is not straight forward, since as shown for placenta full length StARD3 is localized to late endosomes, presumably tethered by its N-

terminal membrane spanning domains. Moreover, in cell culture full length StARD3 is not capable of increasing steroidogenic activity (Watari et al., 1997). However, in placenta antibodies to the StARD3 START domain detect not only the full length protein, but smaller bands. These are presumably proteolysis products that contain the START domain but have lost some or all of the N-terminal region membrane spanning domains. Thus it is possible that in late endosomes cholesterol is transferred to intact StARD3, followed by proteolytic separation of the START domain allowing cholesterol transfer to mitochondria for steroidogenesis. In cell culture, while the full length StARD3 has no steroidogenic activity, mutant StARD3 containing only the START domain promotes steroidogenesis (Watari et al., 1997).

A competing theory posits that physiologically StARD3 may be involved in the movement of cholesterol from late endosomes to lysosomes and then to the plasma membrane, rather than to mitochondria or the ER. Evidence for this comes from studies in primary rat hepatocytes, where over-expression of StARD3 causes only a modest increase in the rate of bile acid synthesis, in contrast to the large increase in bile acid synthesis observed when over-expressing the mitochondrial sterol transporter StAR or the enzyme that catalyzes the rate-limiting step in the conversion of cholesterol to bile acids, CYP7A1 (Ren et al., 2004a). The over-expression of StARD3 along with either StAR or CYP7A1 actually inhibits StAR or CYP7A1 up-regulation of bile acid synthesis, suggesting that StARD3 actually sequesters cholesterol, rather than transports cholesterol to the mitochondria or

the ER, where the bile acid synthetic enzymes CYP27A1 and CYP7A1, respectively, reside(Ren et al., 2004a).

In vivo adenoviral mediated over-expression of StARD3 in mice, which occurs mainly in liver, was hepatotoxic. Moreover, StARD3 over-expression both in mouse liver and in CHO cells was shown to cause apoptosis (Tichauer et al., 2007). The adenoviral studies also showed over-expression of StARD3 leads to increased biliary bile acid concentration and increased liver cholesterol, mainly free cholesterol (Tichauer et al., 2007).

Since in late endosomes StARD3 co-localizes with NPC1; Strauss has hypothesized that NPC2, NPC1, and StARD3 act sequentially to sense cholesterol and move it to an acceptor protein or membrane (Strauss et al., 2002). Consistent with this hypothesis, studies tracking GFP-tagged StARD3 and StARD3 mutants reveal that the N-terminal domain mediates endocytosis of StARD3 from the plasma membrane to the late endosomes and that StARD3 colocalizes and traffics in the same dynamic late endosomal tubules as NPC1 (Zhang et al., 2002). Further research has demonstrated that that the START domain of StARD3 participates in intracellular sterol transport, moving lysosomal cholesterol; a truncated StARD3 without the START domain acts as a dominant negative mutant, causing extensive cholesterol accumulation in the lysosomes of CHO cells and COS-7 cells, inhibition of late endosomal tubular trafficking, and the failure of the use of lysosomal cholesterol in mitochondria steroidogenesis, similar to the NPC phenotype (Zhang

et al., 2002). However, to date, no StARD3 mutations have been reported in Nieman Pick C disease. Furthermore, mice lacking the StARD3 START domain were normal and did not suffer from an NPC-like disorder (Kishida, 2004). These knockout mice were viable, neurologically intact, and fertile; they had no significant changes in plasma lipid levels or liver lipid content and distribution, and showed only moderate changes in cellular sterol metabolism. These results imply that StARD3 in mice is dispensable for sterol metabolism and steroidogenesis, thereby calling into question the importance of StARD3 in whole body cholesterol homeostasis (Kishida, 2004).

Recent research has indicated that the main function of StARD3 may be in modulating the interaction of late endosomes and actin, rather than functioning in cellular sterol balance (Hölttä-Vuori et al., 2005). StARD3 depletion in cell culture causes a similar phenotype to actin disruption, impairing clustering and fusion of late endocytic organelles, scattering late endocytic organelles, and delaying cargo degradation (Hölttä-Vuori et al., 2005). Meanwhile, over-expression of StARD3 leads to an enhanced formation of actin patches on the organelles harboring StARD3 (Hölttä-Vuori et al., 2005).

The PCTP Subfamily

The genes in this subfamily are not as closely related as the genes in the other subfamilies, since they do not share the same common exonic organization or homology outside their START domain and also appear to bind different lipids.

StARD2/PCTP

StARD2, also known as phosphatidylcholine transfer protein (PCTP) is a highly specific intracellular lipid binding protein which, through its START domain, binds exclusively to phosphatidylcholine in a 1:1 stoichiometric manner (Kanno et al., 2007b; Roderick et al., 2002). The crystal structure of StARD2 in complex with a phoshatidylcholine (PC) reveals a unique hydrophobic lipid-binding tunnel, consistent with a START domain able to accommodate a single molecule of PC (Roderick et al., 2002). However, it appears that a major conformational change in StARD2 is needed to allow PC to enter and exit the lipid tunnel of StARD2. *In vivo* and *in vitro* results differ on the exact type of phosphatidylcholine bound to StARD2, with *in vitro* studies pointing to specific binding to an sn-1 palmitoyl and an sn-2 unsaturated acyl chain, and *in vivo* studies pointing to specific binding to an sn-1 stearoyl and sn-2 polyunsaturated chain (Kanno et al., 2007a; Wirtz, 1991). StARD2 is thought to promote the transfer of phosphatidylcholine from its site of synthesis in the ER to the plasma membrane and the mitochondria.

StARD2 is highly expressed in liver, placenta, testis, kidney, and macrophages. Radioimmunoassay and photo-bleaching studies indicate that PCTP is highly mobile in the cytoplasm, but is also present in the nucleus and associates with the mitochondria (de Brouwer et al., 2002). In mice StARD2 expression is increased by fibrates through activation of the trancription factor PPARalpha and by adenoviral over-expression of the transcription factor

PPARgamma. Since the nuclear hormone receptor PPAR transcription factors play a role in controlling lipid and glucose metabolism, these experiments suggest that StARD2 might also be involved in these processes (de Brouwer et al., 2002).

The precise physiological role of StARD2 is still under investigation. Many of the proposed functions of StARD2 were found to be normal in StARD2 knockout mice, including hepatocellular selection and secretion of biliary phospholipids, production of lung surfactant (the major lipid being PC), and leukotriene biosynthesis (van Helvoort et al., 1999). Cohen and colleagues have extensively studied StARD2 knockout mice fed either a chow or a lithogenic diet, (Baez et al., 2005; Scapa et al., 2008; Wang et al., 2006; Wu and Cohen, 2005a, b; Wu et al., 2005). On a chow diet, the knockouts had normal biliary phospholipids secretion and composition. However, on a lithogenic diet, which increases biliary secretion rates of bile salts, phospholipids, and cholesterol, the knockouts had impaired biliary secretion of all three, yet maintained normal hepatocellular selection and secretion of phosphatidylcholine (Wu et al., 2005). The livers of StARD2 knockouts fed a chow diet exhibited increased esterified cholesterol and ACAT activity, and decreased free cholesterol and phospholipids. However, the livers of these mice on a lithogenic diet failed to show up-regulation of ACAT, resulting in an increased free cholesterol-to-phospholipid ratio (Wu and Cohen, 2005a; Wu et al., 2005). The knockouts on a chow diet showed accumulation of small alpha-migrating HDL particles in plasma, whereas those on a lithogenic diet had increased plasma

cholesterol and phospholipid levels (Wu and Cohen, 2005b). Cholesterol ester loaded macrophages from these knockouts exhibited decreased ABCA1 expression and decreased efflux of phospholipids and cholesterol to apoA-I (Baez et al., 2005). Compatible with this observation, over-expression of StARD2 in cell culture accelerates apolipoprotein A-I-mediated efflux of phospholipid and cholesterol as pre-beta-HDL particles (Baez et al., 2002). Thus StARD2 appears to play a role *in vivo* in biliary lipid secretion, hepatic cholesterol metabolism in response to a lithogenic diet, as well as HDL metabolism.

StARD2 was hypothesized to serve an atheroprotective function. StARD2's role in atherosclerosis was studied by breeding the StARD2 knockout trait on to the ApoE knockout background. Compared to ApoE knockouts, the double knockout male mice had a slight increase in atherosclerosis at 4 months of age accompanied by increased cholesterol levels; however, at 6 months of age both male and female mice had a slight reduction in atherosclerosis, which in the male mice was accompanied by a decrease in plasma cholesterol levels (Wang et al., 2006). Compared to wild-type mice, free cholesterol loading of macrophages from StARD2 knockout mice causes markedly increased apoptotic cell death (Baez et al., 2005).

Recent studies from Cohen and colleagues also indicate that StARD2 knockout mice show increased hepatic insulin sensitivity and reduced hepatic glucose production, suggesting a role for StARD2 in regulating energy metabolism

(Scapa et al., 2008). In a quantitative trait locus (QTL) study from the Quebec Family Study (QFS), StARD2 gene variants were found to be associated with LDL peak particle size (LDL-PPD), a trait often associated with the Metabolic Syndrome (Dolley et al., 2007).

StARD7/GTT1

StARD7 (gestation trophoblastic tumor 1 (GTT1), was identified by its over-expression in choriocarcinoma cell lines compared to cell lines derived from normal trophoblastic tissue and nonmalignant hydatidiform moles (Durand et al., 2004). Computer mediated homology search of the primary amino acid sequence of StARD7 revealed homology to StARD2 in its conserved START domain. However, the precise lipid binding specificity of StARD7 is unknown. Expression patterns of StARD7 in normal tissues is unknown. StARD7 is expressed in several cancer-derived cell lines, and it was suggested it might play a role in phospholipid-mediated signaling in tumors (Durand et al., 2004). No functional studies of StARD7.have appeared in the literature.

StARD10/PCTP-like

StARD10 (PCTP-like) was also identified as a protein over-expressed in breast cancers, and appears to cooperate with ErbB, a member of the epidermal growth factor (EGF) receptor family and of the receptor tyrosine kinase family (Alpy and Tomasetto, 2005; Olayioye et al., 2004; Olayioye et al., 2005). Through electron spin resonance measurement, StARD10 was shown to interact with

phosphatidylcholine (PC) and phosphatidylethanolamine (PE); mass spectrometry revealed a preferential selection for lipids containing a palmitoyl or stearoyl chain in the sn-1 position and an unsaturated fatty acyl chain (18:1 or 18:2) in the sn-2 position (Olayioye et al., 2005). *In vitro* studies suggest that StARD10 is capable of transferring PC and PE between membranes.

The StARD10 gene is expressed in several tissues and the regulation of its expression as well as the cellular location of the protein suggests it participates in many physiological processes relating to phospholipid metabolism. In germ cells of the testis the StARD10 protein is found in the sperm flagellum, implying a role in sperm energy metabolism (Olayioye et al., 2004; Olayioye et al., 2005). In mammary glands, StARD10 expression increased in late pregnancy and lactation, implying a role in phospholipid enrichment of milk. Expression in the liver implies a role in delivery of phospholipids to the canalicular membrane for biliary excretion. StARD10 is also expressed in the kidney and intestine, as well as many tumor cell lines. Olayioye hypothesizes that StARD10 over-expression in tumors may by replenishing membrane PC and PE activating specific phospholipases, thereby contributing to aberrant lipid signaling and cellular transformation (Olayioye et al., 2005).

StARD11/CERT

There are two StARD11 transcripts: one encodes a long isoform, the Goodpasture antigen-binding protein (GPBP) also known as the CERTL, and the

other a more abundant short isoform, the ceramide transfer protein (CERT) (Hanada et al., 2003; Raya et al., 2000). Both isoforms are expressed in striated muscle and brain, but poorly expressed in placenta, lung and liver. The CERT form is also highly expressed in kidney, pancreas, and a number of cancer cell lines.

StARD11 was originally described as a protein that binds and phosphorylates serine residues in the non-collagenous C-terminal region of the a3 chain of collagen IV (Good-pasture antigen), which is involved in the dermatologic autoimmune disease Goodpasture's Syndrome (Raya et al., 1999; Raya et al., 2000). However, StARD11 lacks a protein kinase motif suggesting this may be an indirect effect due to an associated kinase.

Both isoforms of StARD11 have ceramide transport activity *in vitro* and *in vivo*, thereby leading to the hypothesis that StARD11 is responsible for the delivery of ceramide from the ER where it is synthesized to the Golgi where conversion to sphingomyelin (SM), a major plasma membrane component, takes place (Hanada et al., 2007; Hanada et al., 2003). Studies of GFP-tagged StARD11 indicate both cytosolic localization as well as enrichment in the Golgi. The N-terminus of StARD11 contains a phosphoinositide binding pleckstrin homology (PH) domain that recognizes the Golgi-associated phosphatidylinositol 4-phosphate (PtdIns 4-phosphate), and this interaction may be responsible for Golgi targeting. The N-terminus also contains an FFAT motif that recognizes and binds the ER integral membrane protein VAMP-associated protein (VAP), and this may be responsible

for ER targeting (Levine and Munro, 2002; Loewen et al., 2003). Mutations in either the PH domain of the FFAT motif impair ER-to-Golgi ceramide transport. RNAi knockdown of VAP decreases SM synthesis, presumably by preventing the proper loading of ceramides onto StARD11 (Perry and Ridgway, 2006). The N-terminus also contains a serine-rich motif and a coiled-coil region (Hanada et al., 2007). The C-terminus of StARD11 contains a ceramide binding START domain. StARD11 binds ceramides in a 1:1 molar ratio and efficiently transfers various types of naturally occurring ceramides with C(14), C(16), C(18), and C(20) chains, but not longer acyl chains (Kumagai et al., 2005). StARD11 also mediates efficient transfer of C(16)-dihydroceramide and C(16)-phyto-ceramide. The crystal structure confirms that StARD11 can distinguish ceramide from other lipid types, yet still can recognize multiple species of ceramides (Kudo et al., 2008).

In cell culture, deletion mutants reveal that only the START domain of StARD11 mediates the specific exchange of ceramide from donor to acceptor membranes. Knocking down StARD11 via RNAi in C6 glioma cells showed a significant but not complete reduction of SM synthesis (Giussani et al., 2008). Furthermore, in a CHO-K1 cell line where StARD11 is mutated, there is diminished ABCG-1 mediated cholesterol and SM efflux, and in CHO-K1 cells over-expressing StARD11, there is enhanced ABCG1 mediated cholesterol and SM efflux (Nagao et al., 2007; Sano et al., 2007).

Loss of StARD11 appears to be lethal to cells and organisms. UVB

irradiation of keratinocytes induces the rapid formation of a stable, but inactive StARD11 homotrimer complex, leading to accumulation of cellular ceramides and a reduction in sphingomyelin synthesis. This increase in cellular ceramide causes what is known as UVB irradiation-induced apoptosis in cultured human keratinocytes (Charruyer et al., 2008). Inactivation of StARD11 in keratinocytes by chemical means also increases apoptosis. Knocking out the StARD11 homologue in Drosophila melanogaster causes premature death, reduced thermal tolerance, reduced ATP, increased glucose levels, and a reduction in the sphingomyelin analog, ceramide phosphoethanolamine, which leads to increased plasma membrane fluidity and heightened susceptibility to damage by ROS (Rao et al., 2007).

StARD11 activity can be regulated in several ways. Phosphorylation of the serine-repeat motif of StARD11 down-regulates the ER-to-Golgi transport of ceramides, by inducing an inhibitory interaction between the PH and START domains. This inactivates both ceramide transfer activity and the ability of StARD11 to bind phosphoinositides. The ensuing decrease in cellular sphingomyelin and accompanying cholesterol are hypothesized to cause changes in SM/cholesterol rafts, which then leads to the dephosphorylation of the serine-repeat motif of StARD11, thereby resulting in reactivation of StARD11 (Kumagai et al., 2007). StARD11 can also be dephosphorylated by protein phosphatase 2Cepsilon (PP2Cepsilon), which negatively regulates the stress-activated protein kinase

pathways (Saito et al., 2008). PP2Cepsilon dephosphorylation of StARD11 allows it carry out ceramide transport to the Golgi. Over-expression of PP2Cepsilon enhances the association between StARD11 and VAP, while RNAi knock down of PP2Cepsilon attenuates this interaction and decreases sphingomyelin synthesis (Saito et al., 2008). Another enzyme that can regulate StARD11 is PI 4-kinase beta. RNAi knock down of this enzyme decreases StARD11 mediated ceramide transport to the Golgi (Tóth et al., 2006). Finally, RNAi knock-down of OSBP decreases StARD11 activity and SM synthesis, suggesting that OSBP might interact directly or indirectly with shared binding partners of StARD11 at the Golgi and/or the ER (Perry and Ridgway, 2005, 2006).

The RhoGap Subfamily

Each member of this subfamily contains a Rho GTPase activating protein (RhoGAP) domain, which appear to act as tumor suppressors. RhoGAPs are negative regulators of members of the Ras super-family, by stimulating the intrinsic GTPase activity of the Rho family of small GTPases. The Rho family of small GTPases control cell growth, morphogenesis, cell motility, cytokinesis, trafficking, and organization of the cellular cytoskeleton, as well as are involved in malignant transformation and metastasis of tumors (Moon and Zheng, 2003). In addition to the RhoGAP and START domains, each family member also contains an N-terminal sterile alpha motif (SAM), a putative protein interaction domain that can also interact with RNA and lipids (Kim and Bowie, 2003). To date, studies of these genes have

mainly focused on their RhoGAP domains.

StARD12/DLC-1

StARD12, also known as the deleted in liver cancer 1 (DLC-1) or the p122-RhoGAP gene, was identified as tumor suppressor gene, that is decreased in expression, and often entirely deleted, in liver, breast, colon, and prostate cancers (Kim et al., 2003b; Ng et al., 2000; Plaumann et al., 2003; Teramoto et al., 2004; Wong et al., 2003; Yuan et al., 2003a; Yuan et al., 2004; Yuan et al., 1998; Yuan et al., 2003b; Zheng et al., 2003; Zhou et al., 2004b). Further evidence of StARD12's role as a tumor suppressor comes from a study in which adenoviral expression of StARD12 inhibited the proliferation, invasiveness, and anchorage-independent growth of PC-3 and C4-2-B2 cells *in vitro* by inducing cell-cycle arrest. StARD12 has also been shown to inhibit tumorogenicity of PC-3 cells in nude mice (Guan et al., 2008).

StARD12 appears to have a dual function. First, StARD12 interacts with the enzyme phospholipase C delta1 (PLC-delta1) activating phosphatidylinositol 4,5-bisphosphate (PIP2) hydrolyzing activity, which causes a rapid elevation of intracellular Ca2+ levels (Homma and Emori, 1995). Second, StARD12 possesses RhoGAP activity specific for RhoA, enhancing the conversion of RhoA from its GTP-bound active state to GDP-bound inactive state (Homma and Emori, 1995).

Over-expression of StARD12 induces the disassembly of stress fibers and reorganization of the actin cytoskeleton and focal adhesions, causing the

morphological rounding of various adherent cells (Sekimata et al., 1999). Meanwhile, cells mutant in the GAP domain of StARD12 fail to undergo these morphological changes. Studies of GFP-tagged StARD12 localize the protein to punctate structures at the plasma membrane, in particular to caveolae, where StARD12 interacts with caveolin-1 (Yamaga et al., 2007; Yamaga et al., 2004). The GAP domain of StARD12 is sufficient for this localization; cholesterol content of the membranes also affects this protein's localization (Kawai et al., 2004; Yamaga et al., 2007; Yamaga et al., 2004).

Mice homozygous for the StARD12 knockout trait undergo embryonic lethality after embryonic day 10.5, with defects in neural tube, brain, heart, and placenta (Durkin et al., 2005). Mice heterozygous for the StARD12 knockout are phenotypically normal. Consistent with a putative role for StARD12 in the cytoskeleton, cultured embryonic fibroblasts from the homozygous knockout embryos display alterations in the organization of actin filaments and focal adhesions (Durkin et al., 2005).

StARD13/DLC-2

StARD13, also known as the deleted in liver cancer 2 (DLC-2) gene, was identified as a tumor suppressor gene that is decreased in expression and often absent or deleted in hepatocellular carcinomas (Ching et al., 2003; Leung et al., 2005). Recent studies have shown a decrease in StARD13 expression in other solid tumors, including lung, ovarian, renal, breast, uterine, gastric, colon and rectal

tumors. StARD13 encodes a RhoGAP specific for RhoA and Cdc42 and to some extent Rac1 (Ching et al., 2003; Nagaraja and Kandpal, 2004). StARD13 exists in four isoforms. Initial studies localized StARD13 to the cytoplasm; however, recent studies indicate that it also localizes to mitochondria and lipid droplets (Ng et al., 2006).

In mouse fibroblast cell culture, over-expression of StARD13 causes a marked suppression in cell proliferation, motility, and transformation, as well as in RhoA activity (Leung et al., 2005). Over-expression changes the morphology of the cells and inhibits Rho-mediated formation of actin stress fibers and suppresses lysophosphatidic acid-induced stress fiber formation (Leung et al., 2005). Over-expression also inhibits Ras signaling and Ras-induced cellular transformation. RNAi knock down of StARD13 results in cells with increased levels of active GTP-bound RhoA and reduced C(2)-ceramide induction of mitochondrial phosphatidylglycerolphosphate (PGP) synthase activity (Hatch et al., 2008).

StARD8/DLC-3

StARD8, also known as the deleted in liver cancer 3 (DLC-3) gene, was identified as tumor suppressor gene (Durkin et al., 2007a; Durkin et al., 2007b; Katoh and Katoh, 2004). It is widely expressed in normal tissues, and there is a decrease or total loss of expression of StARD8 in various cancer cell lines as well as in kidney, lung, ovarian, uterine, prostate, and breast cancers. Immunohistochemistry studies reveal that StARD8 localizes intra-cellularly to focal

adhesions (Kawai et al., 2007). StARD8 has two isoforms, alpha, which is highly similar in structure to STARD12 and 13, and beta, which lacks the N-terminal SAM domain. As with other members of this subfamily, StARD8 stimulates PLCdelta1 and has RhoGAP activity for RhoA and Cdc42 (Durkin et al., 2007a). Consistent with a role as a tumor suppressor, transfection of breast and prostate cancer cells with StARD8alpha inhibits cell proliferation, colony formation and growth in soft agar (Durkin et al., 2007a; Kawai et al., 2007).

The Acyl-CoA Thioesterase Subfamily

Both genes in this subfamily contain two N-terminal acyl hydrolase domains as well as a C-terminal START domain (Alpy and Tomasetto, 2005).

StARD14/BFIT

StARD14, also known as brown fat-inducible thioesterase (BFIT), acyl-coA thioester hydrolase 11 (ACOT11), or thioesterase adipose-associated (THEA), appears to play a role in energy metabolism and obesity (Adams et al., 2001). Humans have two splice variants, which differ in their C-terminus and therefore have slightly different START domains. However, mice only have one isoform. Consistent with its thioesterase domain structure, recombinant StARD14 protein displays hydrolytic acyl-CoA thioester cleavage activity towards medium- (C12) and long-chain (C14) fatty acyl substrates, and may play a role in altering intracellular fatty acyl-CoA concentrations (Adams et al., 2001).

The StARD14 gene localizes to a QTL region for the dietary-obese 1(Do1)

trait; causing Adams and colleagues to speculate this might be the culprit gene at this locus responsible for body weight regulation in response to a high fat diet (Adams et al., 2001). Consistent with this hypothesis is the observation that expression of StARD14 is induced in brown adipose tissue (BAT) in cold challenged mice, but repressed in BAT of mice at warm temperatures. Also consistent are the observations that StARD14 is more highly expressed in BAT of obesity-resistant compared to obesity-prone mice fed high fat diets, and StARD14 expression is increased in the BAT of control lean mice compared to obese ob/ob mice (Adams et al., 2001).

StARD15/CACH

StARD15, also known as cytosolic acetyl CoA hydrolase (CACH) or acyl-CoA thioesterase 12 (ACOT12), has a hydrolase activity for acetyl-CoA and short chain (C4 and C6) acyl-CoAs, and therefore, may act to maintain the equilibrium between concentrations of cytosolic acetyl-CoA and the coenzyme A-SH (CoASH). Through maintaining this equilibrium, StARD15 may therefore function in fatty acid and cholesterol metabolism (Suematsu and Isohashi, 2006; Suematsu et al., 2001). StARD15 is enzymatically active only when the protein homodimerizes or tetramerizes and binds ATP, whereas when bound to ADP activity is inhibited (Isohashi et al., 1983a, b). StARD15 mRNA is found in liver, spleen, muscle, and testes, but its enzymatic activity has been only detected in liver and kidney. The activity of StARD15 appears to be regulated in several metabolic states. Activity

of the enzyme increases in rats that were starved, fed a fat-free high carbohydrate diet, fed a high cholesterol diet (reducing *de novo* hepatic cholesterol synthesis), treated with cholesterol synthesis inhibitors, treated with PPARalpha agonists, fed a diet with thyroid powder, containing T3 to stimulate hyperthyroidism, or treated with streptozotocin to induce insulin deficient diabetes (Ebisuno et al., 1988; Matsunaga et al., 1985; Nakanishi et al., 1985).

The StARD9 Protein

Very little is known about StARD9, except that the gene contains 11 exons and encodes an 1820 amino acid protein with a C-terminal START domain but no other recognizable domains (Halama et al., 2006). StARD9 exists in a full-length form and an exon 8 deleted form. It is highly expressed in muscle and nervous tissues. StARD9 maps to a region of the genome linked to limb-girdle muscular dystrophy type 2A (LGMD2A), an autosomal recessive form of limb-girdle muscular dystrophy, and StARD9 has been speculated to play a role in this disease (Halama et al., 2006).

The StARD4 Subfamily

Members of this subfamily contain only a START domain and share approximately 30% homology (Soccio et al., 2002; Soccio and Breslow, 2003).

StARD4

StARD4 was originally identified in a microarray study as a gene down-regulated in the liver by feeding mice a high cholesterol diet (Soccio et al., 2002;

Soccio and Breslow, 2003). StARD4 was shown to be transcriptionally up-regulated by SREBP2 and to have an active sterol response element (SREs) in its promoter. StARD4 can also be up-regulated by ER stress through the transcription factor ATF6 (Yamada et al., 2006). StARD4 also has an ERSE-like element in its promoter (Soccio et al., 2005; Soccio et al., 2002; Yamada et al., 2006).

StARD4 may play an important role as a cholesterol transporter in maintaining cellular cholesterol homeostasis. StARD4 was shown to bind cholesterol, and increased expression of StARD4 in primary mouse hepatocytes leads to a marked increase in intracellular cholesterol esters and in the rate of bile acid synthesis (Rodriguez-Agudo et al., 2008; Romanowski et al., 2002). Forced expression of StARD4 in cell culture stimulates steroidogenesis by P450scc and liver X receptor reporter gene activity (Soccio et al., 2005; Soccio et al., 2002). Miller speculated that StARD4 might aid in transferring cholesterol to the OMM, where StAR can then transfer cholesterol to the IMM for steroid biosynthesis (Miller, 2007c). To understand the physiological role of StARD4, knockout mice were developed, and this thesis will describe the design and development of a StARD4 knockout mouse.

StARD5

StarD5 was shown to selectively bind cholesterol and the potent regulatory oxysterol, 25-hydroxycholesterol (Rodriguez-Agudo et al., 2006; Rodriguez-Agudo et al., 2005). In human liver initial studies found StARD5 to be in the cytosolic

fraction. Further studies indicated StARD5 co-localized with CD68 in Kupffer cells, but not in parenchymal cells (Rodriguez-Agudo et al., 2006). StARD5 was also shown to be expressed in monocytes, macrophages, mast cells, basophils, and pro-myelocytic cells, but not in human hepatocytes, endothelial cells, fibroblasts, osteocytes, astrocytes, or brain tissue. Cell fractionation and immunocytochemical studies with THP-1 macrophages localized StARD5 to the cytosol and supported an association with the Golgi (Rodriguez-Agudo et al., 2006).

StARD5 expression is not down-regulated by cholesterol via SREBPs, nor is it up-regulated by oxy-cholesterol derivatives via liver X receptors (LXRs). Instead, StARD5 expression is increased by the ER stress response. This has been observed in free cholesterol-loaded macrophages, or in NIH-3T3 cells treated with ER stressors (Soccio et al., 2005). Co-transfection of StARD5 and P450scc expression vectors into Cos-1 cells stimulated steroidogenesis, and co-transfection of a StARD5 expression vector along with an LXR promoter-reporter vector into Cos-1 cells augmented reporter expression (Soccio et al., 2005). Furthermore, transfection of a StARD5 expression vector in primary hepatocytes caused a marked increase in microsomal free cholesterol (Rodriguez-Agudo et al., 2006; Rodriguez-Agudo et al., 2005). These experiments suggest StARD5 can move cholesterol within cells, but do not reveal its specific physiological function. This thesis will undertake to understand the physiological role of StARD5 by several methods, including the development and characterization of StARD5 transgenic

and knockout mice.

StARD6

Initial studies found StARD6 expressed only in male germ cells as they matured during spermatogenesis. It was speculated that StARD6 regulated sterol movement within sperm as they matured (Gomes et al., 2005; Soccio and Breslow, 2003). However, recent studies have found StARD6 expression in the rat nervous system in cerebral cortex (layers V and VI), hippocampus, substantia gelatinosa of the spinal cord, suggesting a possible role for StARD6 in sterol transport or sensing in the nervous system (Chang et al., 2007).

Table 1.1 **START Domain Proteins**

Gene Name	Common Alternative Name	Mouse Knockout Phenotype	Lipid Specificity	Possible/Suggested Function
STAR Subfamily				
StARD1	STAR	congenital lipoid adrenal hyperplasia (lipoid CAH)	Cholesterol	transport cholesterol from the OMM to the IMM; rate-limiting step in steroidogenesis; aids cholesterol to pregnenolone
StARD3	MLN64	Normal viability and fertility No obvious phenotype	Cholesterol	mobilize cholesterol from endosomes/lysosomes; modulate actin-endosome interaction
RhoGAP Subfamily				
StARD12	DLC-1	embryonic lethal after e10.5 day with defects in the neural tube, brain, heart, and placenta	Unknown	tumor suppressor posseses GAP activity modifies PLC-delta1 activity reorganize actin cytoskeleton and focal adhesions
StARD13	DLC-2	None Available	Unknown	tumor suppressor posseses GAP activity modifies PLC-delta1 activity mediates ceramide activation of phosphatidylglycerolphosphate synthase
StARD8	DLC-3	None Available	Unknown	tumor suppressor posseses GAP activity modifies PLC-delta1 activity

Table 1.1 **START Domain Proteins** *(continued)*

Gene Name	Common Alternative Name	Mouse Knockout Phenotype	Lipid Specificity	Possible/Suggested Function
PCTP Subfamily				
StARD2	PCTP	Decrease efflux to ApoAI Increase macrophage apoptosis Modulate atherosclerosis Increase hepatic insulin sensitivity, Increase hepatic cholesterol ester, Alter hepatic FC-phospolipid ratio Impaired biliary lipid secretion	PC	promote the intermembrane transfer of phosphatidylcholine (PC) from the site of synthesis (ER) to the PM and mitochondria
StARD7	GTT1	None available	Unknown	role in the phospholipid-mediated signalling; mediates transplacental lipid transport; role in syncytialization
StARD10	PCTP-2	None Available	PC, PE	transfers phosphatidyl-choline(PC) and ethanolamine (PE) between membranes; cooperates with the ErbB family of receptor tyrosine kinases
StARD11	CERT GPBP	None Available	Ceramides	associated with Goodpasture's non-vesicular ceramide-carrier protein aiding sphingomyelin synthesis
acyl CoA Thioesterase Subfamily				
StARD14	ACOT11 THEA BFIT	None Available	Unknown	energy metabolism and obesity, alter intracellular fatty acyl-CoA concentration
StARD15	ACOT12 CACH	None Available	Unknown	maintain equilibrium between concentrationsof cytosolic acetyl-CoA and the coenzyme A-SH
StARD9 Subfamily				
StARD9		None Available	Unknown	role in modifying LGMD2A
StARD4 Subfamily				
StARD4		preliminary: viable	Cholesterol	SREBP and ER Stress target gene stimulates steroidogenesis directional cholesterol transporter
StARD5		embryonic lethal before e9.5	Cholesterol 25OH-cholesterol	ER Stress target gene stimulates steroidogenesis directional cholesterol transporter role in embryogenesis
StARD6		None Available	Unknown	lipid sensing in germ cells lipid sensing of the nervous sytsem

A Disintegrin and Metalloprotease (ADAM) Family

Amongst the dietary cholesterol responsive genes in the liver was ADAM11. This gene was up-regulated by dietary cholesterol, and encodes a trans-membrane protein that bears no relationship to the START-domain family of proteins. This thesis also includes experiments to determine the physiological function(s) of ADAM11. This section will review the background information on ADAM11 and the ADAM gene family.

ADAM Family

A disintegrin and metalloproteinase (ADAM) proteins are multi-domain, type I transmembrane proteins. They possess an N-terminal pro-peptide domain, a metalloprotease domain, a disintegrin domain, a cysteine-rich region, an epidermal growth factor (EGF)-like sequence, a trans-membrane domain, and a C-terminal cytoplasmic tail (Seals and Courtneidge, 2003). Previous literature referred to this family as the MDC family, indicating the presence of Metalloprotease, Disintegrin, and Cysteine-rich domains. The ADAMs belong to the metzincin super-family, which also includes ADAMs with Thrombospondin motifs (ADAM-TS), Matrix Metalloproteinases (MMP), Serralysins, Leishmanolysins, and Snapalysin. In this super-family only the ADAMs and ADAM-TSs contain an integrin-binding (disintegrin) domain. Individual ADAM family members are regulators of cell-cell and cell-matrix interactions, as well as processors of growth factors, cytokines, and receptors (Seals and Courtneidge, 2003).

To date, approximately 40 members of the ADAM family have been reported. ADAMs have been identified in *Schizosaccharomyces pombe*, *Caenorhabditis elegans*, Drosophila, Xenopus, and in vertebrates, but not in *Escherichia coli, Saccharomyces cerevisiae* or plants (Seals and Courtneidge, 2003). It was recently shown that ADAM18 and ADAM27 are the same gene and likewise for ADAM21 and ADAM31, leaving 38 novel ADAM family members. Of these ADAMs 13, 14, 16, and 35 are not expressed in mammals. The remaining 34 ADAMs are expressed, but only 25 are expressed in humans.

Although all ADAMs contain a metalloprotease domain, only two-thirds of these have an active or predicted active catalytic domain, represented by the conserved sequence HEXGHXXGXXHD; (ADAMs 1, 8, 9, 10, 12, 13, 15, 16, 17, 19, 20, 21, 24, 25, 26, 28, 30, 33-40). The remaining ADAMs have one or more residues in this sequence incompatible with protease activity. The 34 mammalian ADAMs can be divided into four groups based on their expression patterns and whether or not they have or are predicted to have catalytic activity. Nineteen ADAMs are exclusively or predominantly expressed in the testis; of these 11 are catalytically active ADAMs 20, 24, 25, 26, 30, 34, 36-40, and 8 catalytically inactive ADAMs 2, 3, 4, 5, 6, 18, 29, 32. The remaining 15 ADAMs have somatic expression; of these 11 are catalytically active ADAMs 1, 8, 9, 10, 12, 15, 17, 19, 21, 28, 33, and 4 catalytically inactive ADAMs 7, 11, 22, 23. Although this review categorizes ADAMs 2, 3, 4, 5, 21 as exclusively or predominantly expressed in the

testis, these ADAMs are also expressed in the nervous system (Yang, 2006). Humans and mice express 25 and 34 ADAMs, respectively, and the difference is in the number of testis-specific catalytically active ADAMs expressed in mice and not in humans, including ADAMs 24, 25, 26, 34, 36-40).

A web site maintained by Judith White at the University of Virginia contains the up-to-date list of all ADAMs:

(http://www.people.virginia.edu/~jw7g/Table_of_the_ADAMs.html

The Roles of the Multi-Domains of the ADAMs

The N-terminal region of ADAMs contains a pro-domain that acts as a chaperone, directing ADAMs into the secretory pathway. This serves to allow proper ADAM folding and maintains the protease domain in an inactive state. The pro-domain of most ADAMs are thought to be cleaved by a furin-type pro-protein convertase, although some like ADAM8 and ADAM28 may undergo autocatalytic cleavage (Seals and Courtneidge, 2003; Blobel, 2005).

Twenty-two of 24 ADAMs possess a metalloprotease catalytic site in an active configuration. The active metalloprotease sites contain zinc and water molecules, which are necessary for the hydrolytic processing of protein substrates. Some substrates for the catalytically active ADAMS are known. Tissue inhibitors of metalloproteases (TIMPs) are endogenous regulators of MMPs, and these can inhibit the metalloprotease catalytic activity of ADAMs as well (Seals and Courtneidge, 2003; Blobel, 2005).

The disintegrin domain is named due to its homology to short soluble proteins in snake venom that bind and inhibit platelet integrins. Many of these snake venom proteins contain an RGD consensus motif that form the disintegrin loop and which bind integrins. Although only human ADAM15 has an RGD sequence, the other ADAMs appear to have a generalized disintegrin loop (CRX5CDX2EXC) or an ECD motif, which are also capable of binding integrins (Seals and Courtneidge, 2003; Blobel, 2005).

The cysteine-rich domain and the EGF-like domains are poorly understood. The cysteine-rich domain appears to play a role in assisting or determining specificity of binding by the disintegrin domain. The EGF-like domain may mediate signaling (Seals and Courtneidge, 2003; Blobel, 2005).

The trans-membrane domain anchors the protein to the cell, and most ADAMs are found at the plasma membrane. The cytoplasmic tails of ADAMs are highly variable both in length and sequence, often containing proline-rich SH3-binding sites, and serine-threonine and tyrosine kinase phosphorylation sites. Alternative splicing of ADAMs is common and as a result an ADAM can have alternative cytoplasmic tails. These cytoplasmic tails might be involved in inside-out regulation of metalloprotease activity, outside-in regulation of cell signaling, regulation of ADAM expression and localization, and mediating protein-protein interactions (Seals and Courtneidge, 2003; Blobel, 2005).

The Functional Role of ADAMs:

Somatically Expressed, Catalytically Active ADAMs

To date, most studies have focused on the somatically expressed, catalytically active ADAMs 1, 8, 9, 10, 12, 15, 17, 19, 21, 28, 33.

ADAM1, also known as fertilin alpha, is found in male germ cells as well as in somatic tissues, such as the hippocampus (Evans et al., 1997; Kim et al., 2003a; Nishimura et al., 2002). In mice there are two different isoforms, ADAM1a localizes to the endoplasmic reticulum of testicular germ cells, and ADAM1b localizes to the plasma membrane of epididymal sperm. Knockout of ADAM1a results in male infertility due to severely impaired sperm migration from the uterus through the uterotubal junction into the oviduct (Nishimura et al., 2004). *In vitro*, epididymal sperm of ADAM1a-deficient mice are capable of fertilizing cumulus-intact, zona pellucida-intact eggs. ADAM1a knockout mice appear normal in other respects, suggesting ADAM1a does not play a significant somatic functional role. Knockout of ADAM1b results in fertile mice with no significant defect in sperm migration or egg penetration (Kim et al., 2006). Of unknown significance, sperm from ADAM1b knockout mice show a severe reduction of ADAM2 on the epididymal sperm cell surface, despite the normal presence of ADAM2 in testicular germ cells (Kim et al., 2006).

ADAM8 is expressed in immune, neuronal, and bone progenitor cells and has been implicated in a variety of processes, including tissue-remodeling (Ainola

et al., 2008; Amour et al., 2002; Fourie et al., 2003; King et al., 2004; Matsuno et al., 2006; Mochizuki and Okada, 2007; Sriraman et al., 2008; Valkovskaya et al., 2007). ADAM8 is hormonally regulated by progesterone. The ADAM8 knockout has normal viability and fertility with no obvious pathology (Kelly et al., 2005).

ADAM9, also known as meltrin gamma, is ubiquitously expressed and has been implicated in cleaving the ecto-domain of heparin-binding epidermal growth factor-like growth factor (HB-EGF) and cleaving by alpha secretase activity the amyloid precursor protein (Seals and Courtneidge, 2003). The ADAM9 knockout appears to be fertile, develop normally, and have no major pathological phenotype. In the knockouts there is normal ectodomain shedding of HB-EGF implying another protein performs this function *in vivo* either primarily or as a back-up to ADAM9 (Weskamp et al., 2002). Over-expression of ADAM9 in HT29 human colon cancer cells results in growth factor-induced endocytosis, dynamic recycling of E-cadherin, and prevention of E-cadherin degradation (Hirao et al., 2006).

ADAM10, also known as kuzbanian, can act on many type I and type II single membrane-spanning proteins causing shedding of their ectodomians (Blobel, 2005). Such proteins include Notch, EGF receptor ligands, Ephrins, and amyloid precursor protein. The ADAM10 knockout mice die in utero at embryonic day 9.5 as a result of multiple major defects in development of the central nervous system and the cardiovascular system. The ADAM10 knockouts also have cadherin processing defects and aberrant expression of Notch target genes (Hartmann et

al., 2002).

ADAM12, also known as meltrin alpha, has been implicated in multiple cellular processes, including cell differentiation, proliferation, migration, and invasion. ADAM12 may act by cleaving IGF-binding proteins and in this manner trigger insulin-like growth factor (IGF) receptor signaling. ADAM12 can also cleaving the ectodomain of the epidermal growth factor receptor (EGFR) causing shedding of membrane-tethered EGFR ligands and EGFR activation. Due to its expression pattern during development, ADAM12 was thought to play a role in myogenesis, adipogenesis, and organ development; however, ADAM12 knockout mice have no recognizable muscle pathology (Kurisaki et al., 2003; Masaki et al., 2005). ADAM12 knockout mice exhibit low penetrance perinatal lethality, brown adipose tissue loss, and neck and inter-scapular muscle defects. ADAM12 knockouts mice are resistant to high-fat feeding induced weight gain perhaps because they fail to increase the number of adipocytes (Kurisaki et al., 2003; Masaki et al., 2005). Over-expression of ADAM12 increases muscle regeneration and significantly reduces muscle loss in mdx, dystrophin deficient mice (Guo et al., 2005).

ADAM15, also known as metargidin, is the only ADAM that possesses an RGD integrin-binding sequence in the disintegrin loop and may play a role in mediating inflammation and neovascularization (Seals and Courtneidge, 2003). ADAM15 knockout mice have no major developmental defects or pathological

phenotypes. However, they do exhibit a reduction in ischemia-induced retinal neovascularization, choroidal neovascularization at rupture sites in Bruch's membrane, and VEGF-induced subretinal neovascularization (Horiuchi et al., 2003).

ADAM17, also known as tumor necrosis factor-alpha converting enzyme (TACE), cleaves and mobilizes receptor-ligands that are initially synthesized as membrane-tethered precursors, including TNFalpha, heparin-binding EGF, TGFalpha, amyloid precursor protein, and many others (Blobel, 2005; Seals and Courtneidge, 2003). ADAM17 knockout mice have a neonatal lethal phenotype with multiple defects in heart, lung, and skin (Peschon et al., 1998). This is similar to the phenotype of EGF receptor and TGFalpha knockouts, consistent with ADAM17's role in cleavage-dependent activation EGF receptor and TGFalpha.

ADAM19, also known as meltrin beta, is necessary for the proper morphogenesis of the conotruncus and the endocardial cushion, structures that give rise to the heart valves and the membranous ventricular septum. ADAM19 knockout mice have a neonatal lethal phenotype with severe defects in cardiac morphogenesis, including ventricular septal defect (VSD), abnormal formation of the aortic and pulmonary valves leading to valvular stenosis, and abnormal cardiac vasculature (Zhou et al., 2004a). ADAM19 is highly expressed in the osteoblast-like cells of the bone, but does not appear to be essential for bone growth and skeletal development. Mouse embryonic fibroblasts from ADAM19 knockout mice

exhibit decreased ectodomain shedding of type I Neuregulin, one of the ErbB ligands expressed in endocardial cells. This suggests ADAM19-mediated proteolytic cleavage of ErbB ligands is required for proper heart development (Kurohara et al., 2004; Yokozeki et al., 2007; Zhou et al., 2004a).

The location of ADAM21 expression is disputed with some studies suggesting testis specificity, whereas others indicating expression in the nervous system. The function of ADAM21 is not yet determined, but Yang has speculated that ADAM21 may regulate neurogenesis through guiding neuroblast migration through cleavage-dependent protein activation and/or integrin binding (Yang et al., 2005, 2006).

ADAM28, also known as MDC-L, has its highest expression in epididymis, suggesting a role in sperm maturation. ADAM28 is also present at lower levels in lungs and leukocytes (Howard et al., 2000; Mochizuki et al., 2004; Oh et al., 2005; Shimoda et al., 2007). ADAM28 knockout mice have not yet been reported and ADAM28 function *in vivo* is still unclear.

ADAM33 is expressed in lung, heart, testis, and brain, and was identified in linkage studies as a putative asthma and bronchial hyper-responsiveness gene (Del Mastro et al., 2007; Holgate et al., 2006; Van Eerdewegh et al., 2002). ADAM33 knockout mice are viable and fertile, develop normally, and have no morphological abnormalities (Chen et al., 2006). These mice have normal allergen-induced airway hyper-reactivity, immunoglobulin E production, mucus metaplasia,

and airway inflammation. Therefore, ADAM33 is not essential for growth or reproduction, nor does it modulate baseline or allergen-induced airway responsiveness. The precise physiological role of ADAM33 is unknown, and the link of ADAM33 to asthma needs further elucidation.

Somatically Expressed, Catalytically Inactive ADAMs

ADAM7 is found solely in epididymis and in anterior pituitary gonadotropes and its expression requires androgens and testicular factors (Cornwall and Hsia, 1997). ADAM7 is transferred from the epididymis to the sperm surface and redistributed on the sperm head during the acrosome reaction, indicating it may play a role in fertilization (Oh et al., 2005). ADAM7 knockout mice have not been reported.

The other three somatically expressed, catalytically inactive ADAMs (ADAM11, 22, 23) belong to an ADAM subfamily that is highly expressed in the nervous system. These proteins share ~50% identity and have been previously described by Sagane as predominantly “CNS-expressed brain” ADAMs (Sagane et al., 1998; Sagane et al., 1999). Uniquely amongst the ADAMs, ADAM22 and ADAM23 are expressed predominantly in the nervous system, whereas ADAM11 is expressed in the brain and other tissues.

ADAM22 is expressed throughout the brain, but most strongly in neurons of the basal ganglia and cerebellum. ADAM22 is localized to the plasma membrane of post-synaptic neurons where it interacts with LGI1 secreted by pre-synaptic

neurons. LGI1 binds to the extra-cellular disintegrin domain of ADAM22 enhancing AMPA receptor-mediated synaptic transmission (Fukata et al., 2006). A single amino acid substitution in the ADAM22 disintegrin domain can prevent this interaction. In the postsynaptic density the intra-cellular cytoplasmic tail of ADAM22 interacts with PSD95 and in this manner anchors ADAM22 to the cytoskeletal scaffold, which contains stargazin (Fukata et al., 2006). ADAM22 knockout mice are normal at birth, however, by postnatal day 10 they display progressive weight loss and severe ataxia and die by 25 days of age (Sagane et al., 2005). At autopsy ADAM22 knockout mice have marked hypomyelination of peripheral nerves, but no major structural abnormalities in the cerebral cortex or cerebellum (Sagane et al., 2005). The cytoplasmic tail of ADAM22 also interact with 14-3-3zeta and may in this manner regulate cell adhesion and spreading, which suggests a potential role in neural development (Zhu et al., 2005).

The pattern of ADAM23 expression is similar to that of ADAM22. As with ADAM22 knockouts, ADAM23 knockout mice are normal at birth, however, soon afterwards exhibit tremors, and ataxia and die by 14 days of age (Mitchell et al., 2001). No detailed analysis of the nervous system in the ADAM23 knockout mouse has been reported. It was speculated that through its disintegrin-like domain ADAM23 might function as an adhesion molecule involved in alphavbeta3-mediated cell interactions, including progression of malignant tumors of neural origin (Cal et al., 2000).

Table 1.2 **ADAM Family Proteins**

Gene Name	Common Alternative Name	Mouse Knockout Phenotype	Possible/Suggested Function
somatically expressed, catalytically active (HEXGHXXGXXHD)			
ADAM1	fertilin alpha	1a-expressed in testicular germ cells, infertile males due to sperm immotility 1b-expressed in epididymal sperm, fertile	Role in fertility Role in fertility
ADAM8		Normal viability and fertility No obvious phenotype	Role in tissue-remodeling
ADAM9	meltrin gamma	Normal viability and fertility No obvious phenotype	mediates growth factor-induced endocytosis and dynamic recycling of E-cadherin
ADAM10	kuzbanian	embryonic lethal at e9.5 days Multiple defects in nervous and cardiovascular system	embryonic development involved in Notch pathway, alpha-secretases for amyloid precursor protein and ErbB ligands, involved in the shedding of many type I and type II single membrane-spanning proteins
ADAM12	meltrin alpha	low penetrance perinatal lethality brown adispose defect, resistance to high-fat induced obesity	cleaves IGF-binding proteins, trigger IGF receptor signaling cleaves ectodomain of EGFR ligands trigger EGFR pathways
ADAM15	metargidin	Normal viability Reduced neovascularization	homeostatic role in neovascularization and cartilage remodeling
ADAM17	TACE	Neonatal lethal Multiuple defects in lung and cardiac development	processes TNFalpha, heparin-binding TGFalpha, amyloid precursor protein, among many others
ADAM19	meltrin beta	Neonatal lethal Cardiac septal and valve defects	proteolytic regulation of ErbB ligands cardiovascular development
ADAM21	ADAM31	None available	guide neuroblast migration, neurogenesis and axonal growth in CNS
ADAM28	MDC-L	None available	role in sperm maturation
ADAM33		Normal viability and fertility No obvious phenotype Normal allergen-induced airway responsiveness	role in asthma and bronchial hyperresponsiveness
somatically expressed, catalytically inactive			
ADAM7		None available	role in fertility
ADAM11	MDC	Normal viability and fertility, Defects in spatial learning Defects in motor coordination Absence-like epilepsy Normal cholesterol homeostasis	role in Nervous System role in Reverse Cholesterol Transport
ADAM22	MDC2	postnatal lethality ataxia and tremors	role in Nervous system; binds LGI1, stabilizes PSD95 and AMPA receptors in neurons
ADAM23	MDC3	postnatal lethality, ataxia and tremors	role in Nervous system;

This thesis will undertake several different methods to understand the physiological role of ADAM11, including the development and characterization of a knockout mouse. A thorough review of the literature pertaining to ADAM11 will be included in Chapter 3.

Primarily Testis Specific ADAMs, Catalytically Active and Inactive

Very little is known about these ADAMs. As mentioned earlier, of the 19 testis specific ADAMs, eleven are catalytically active (ADAM20, 24, 25, 26, 30, 34, 36, 37, 38, 39, 40), while the other eight are catalytically inactive (ADAM2, 3, 4, 5, 6, 18, 29, 32). These catalytically active and inactive ADAMs are thought to play roles in fertility due to their testes-specific expression, but specific studies are only available for ADAM2 and ADAM3.

ADAM2, also known as fertilin beta, plays a role in sperm function, as ADAM2 knockout male mice are infertile. Sperm from these mice are present in normal numbers, with normal motility, and undergo the normal acrosome reaction and activation, however, they are deficient in migration from the uterus to the oviduct, and adhesion to and fusion with the egg membrane (Cho et al., 1998). ADAM2 knockout mouse sperm also lack ADAM1 and ADAM3, indicating ADAM2 may play a role in stabilizing these other ADAMs (Nishimura et al., 2007; Stein et al., 2005). It is possible that the infertility-related phenotypes might in part be due to the loss of these proteins. A recent finding suggests ADAM2 might also play a role in promoting rostral migration of neuroblasts to the olfactory bulb (Murase et

Table 1.2 **ADAM Family Proteins** (continued)

Gene Name	Common Alternative Name	Mouse Knockout Phenotype	Possible/Suggested Function
testis specific (primarily), catalytically inactive			
ADAM2	fertilin beta	Normal viability, male infertility	stabilizes Adam1 and Adam3 on sperm crucial in the fertilization process sperm-zona pellucida interaction
ADAM3	cyritestin	Normal viability, male infertility	
ADAM4		None available	
ADAM5		None available	
ADAM6		None available	
ADAM18	ADAM27	None available	
ADAM29		None available	
ADAM32		None available	
testis specific (primarily), catalytically active (HEXGHXXGXXHD)			
ADAM20		None available	
ADAM24	testase1	None available	
ADAM25	testase2	None available	
ADAM26	testase3	None available	
ADAM30		None available	
ADAM34	testase4	None available	
ADAM36	testase 6	None available	
ADAM37	testase7	None available	
ADAM38	testase8	None available	
ADAM39	testase9	None available	
ADAM40	testase10	None available	
not expressed in mammallian cells			
ADAM13			
ADAM14			
ADAM16			
ADAM35			

al., 2008).

Reminiscent of ADAM2, ADAM3, also known as cyritestin, plays a role in sperm function, as ADAM3 knockout male mice are infertile. Sperm from these mice are present in normal numbers with normal motility, and undergo the normal acrosome reaction and activation. However, unlike the ADAM2 knockouts, sperm from these mice migrate normally from the to the oviduct (Shamsadin et al., 1999). The sperm defect in these mice appears due to an inability to bind to the zona pellucida. If the zona pellucida is removed, sperm from ADAM3 knockout mice can

fertilize eggs (Shamsadin et al., 1999).

The Role of ADAM Family Members in Atherosclerosis

Three ADAMs (ADAM9, ADAM15 and ADAM17) have been shown to modulate atherosclerosis. ADAM17 is present in atherosclerotic lesions of ApoE knockout mice. ADAM17 was implicated as the culprit gene at the proximal chromosome 12 atherosclerosis susceptibility locus identified by quantitative trait locus (QTL) mapping in an intercross between C57BL/6J and FVB/N mice on the LDL receptor knockout background (Canault et al., 2006; Canault et al., 2008; Holdt et al., 2008). ADAM17 presumably acts by cleaving and mobilizing receptor-ligands that play a role in atherogenesis, which are initially synthesized as membrane-tethered precursors, including TNFalpha, heparin-binding EGF, TGFalpha, amyloid precursor protein, and many others (Holdt et al., 2008). Consistent with the finding that increased ADAM17 expression is associated with atherosclerotic resistance, knocking out genes that are targets for the ADAM17 metalloprotease, such as intercellular adhesion molecule-1 (ICAM- 1), VCAM-1, interleukin (IL)-1 receptor, CX3CL1 (fractalkine), is also associated with decreased atherosclerosis (Holdt et al., 2008). HDL is protective against atherosclerosis and it is perhaps relevant that HDL can alter the lipid raft structure of cells in a manner that activates ADAM17-dependent processing of trans-membrane substrates (Tellier et al., 2008).

ADAM15 and ADAM9 have been detected in atherosclerotic lesions, but not in normal aorta (Al-Fakhri et al., 2003; Charrier-Hisamuddin et al., 2008; Herren et

al., 1997). ADAM15 was detected in foam cells of smooth muscle cell (SMC) origin and in SMCs surrounding the necrotic lipid core. The integrin binding partners of ADAM15 and ADAM9, alpha5beta1 and alphavbeta3, respectively, are also found in atherosclerotic lesions (Al-Fakhri et al., 2003). It is possible that ADAM15 and ADAM9 expression and interactions with their integrin-binding partners might modulate SMC-matrix interactions in a manner that alters SMC migration within the atherosclerotic plaque. Other studies have suggested that ADAM15 might play a role in atherosclerosis by activating platelets and in this manner augment inflammation (Charrier-Hisamuddin et al., 2008).

This thesis investigates a possible role for the novel cholesterol up-regulated gene ADAM11 in cholesterol homeostasis and atherosclerosis susceptibility through creation and study of ADAM11 knockout mice.

Chapter 2: Characterization of StARD5

Background

In order to better understand responsiveness to dietary cholesterol, Soccio and colleagues fed 6-week-old C57Bl/6 mice a semi-synthetic modified AIN76A diet containing 4.5% fat and either 0.02% or 0.5% cholesterol for three weeks (Soccio et al., 2002). RNA was isolated from the livers of these mice, and gene expression on low and high cholesterol diets compared using a cDNA microarray representing several thousand genes. Dietary cholesterol down-regulated six genes on the microarray; one of these was novel and subsequently named StARD4 (Soccio et al., 2002). Homology searching led to the discovery of StARD5 and StARD6. These genes were shown to comprise a novel START-domain containing subfamily, likely cholesterol binders consisting solely of the ~210 amino acid START-domain itself. As mentioned earlier, StARD5 expression was not affected by cholesterol feeding, over expression of truncated nuclear SREBP, LXR agonists, oxysterols, or statins. However, StARD5 was shown to be up-regulated in macrophages by free-cholesterol loading and in NIH-3T3 cells by drugs known to induce ER stress (UPR) (Soccio et al., 2005; Soccio et al., 2002). Rodriguez and colleagues showed that in liver StARD5 is localized to Kuppfer rather than parenchymal cells where StARD4 is expressed. They also showed StARD5 expression in monocytes and macrophages (Rodriguez-Agudo et al., 2006). StARD5 selectively binds cholesterol and the potent regulatory oxysterol, 25-

hydroxycholesterol (Rodriguez-Agudo et al., 2005). These findings suggest StARD5 is an intra-cellular sterol transporter that might be involved in removing excess free-cholesterol from the ER; possible destinations include transporting free-cholesterol from the ER to other cellular compartments or to the PM for excretion. It is also possible that StARD5 facilitates the conversion of free-cholesterol to cholesterol-ester by the ER enzyme ACAT. However, the precise *in vivo* role of StARD5 is unknown, and this thesis attempts to understand StARD5 function by generating and studying StARD5 knockout as well as StARD5 transgenic mice.

The Targeted Disruption of StARD5

In order to allow the gene to be inactivated in a tissue- or temporal-specific fashion, a strategy was undertaken to create a StARD5 conditional knockout mouse (cKO mouse). Traditionally through homologous recombination loxP sites are inserted into two introns of a gene bracketing one or more exons with subsequent expression of Cre recombinase catalyzing recombination between the loxP sites eliminating the sandwiched exons and inactivating the gene. Cre recombinase expression using a tissue-specific promoter can inactive the gene in a cell-type-specific fashion, whereas using an inducible Cre expression systems or a viral delivery systems (such as adenovirus or lentivirus) can inactivate the gene in a temporal-specific fashion.

StARD5 is a 213 amino acid protein encoded by 6 exons on mouse chromosome 7. Based on databases from the Sanger Institute and Ensembl, no

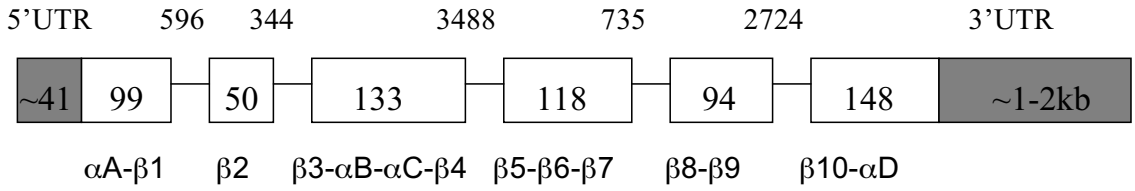

Figure 2.1. **Exonic structure of mStARD5 and secondary structure of protein encoded by each exon.** StARD5 is a 213 amino acid protein encoded by 6 exons. Exons are represented as boxes with lengths in nucleotides, as determined by alignment of cDNA with genomic DNA. Coding sequences are white and untranslated regions (UTR) are gray. Lines connecting the boxes represent introns, with lengths in nucleotides indicated just above. Below the exon structure are the secondary structural elements aligned to each exon.

other genes or miRNA are known to overlap the region encompassing the StARD5 gene (location: 90,780,510-90,789,625). Directly 5'upstream of the StARD5 gene in the mouse is the Tmc3 gene, whose 3'UTR ends approximataly 6kb before the 5UTR of StARD5. Directly 3'downstream of the StARD5 gene in the mouse is the IL16 gene, whose 5'UTR begins approximately 2kb after the 3' UTRof StARD5.

A BAC clone encompassing the StARD5 locus was obtained from a C57BL/6 genomic library (BacPac Resources, RP24-252B21). A strategy was devised to flank the 133bp long exon 3 with loxP sites and then to knock it out using Cre-recombinase, thereby removing 44 amino acids that includes critical regions that form the StARD5 hydrophobic pocket (beta-pleated sheets 3, 4, and 5, and alpha-helices B and C) (Figure 2.1). Alternative splicing from exon 2 to exon 4 would be also out-of-frame and would create several termination codons. Using the recombineering techniques described by Copeland and colleagues (Liu et al., 2003), a targeting vector was constructed in the MC1-TK-containing plasmid that introduced a loxP site into StARD5 intron 2 and an Frt-Pgk-em7-Neo-Frt-loxP cassette into StARD5 intron 3 (Figure 2.2). The loxP site was placed 152bp after

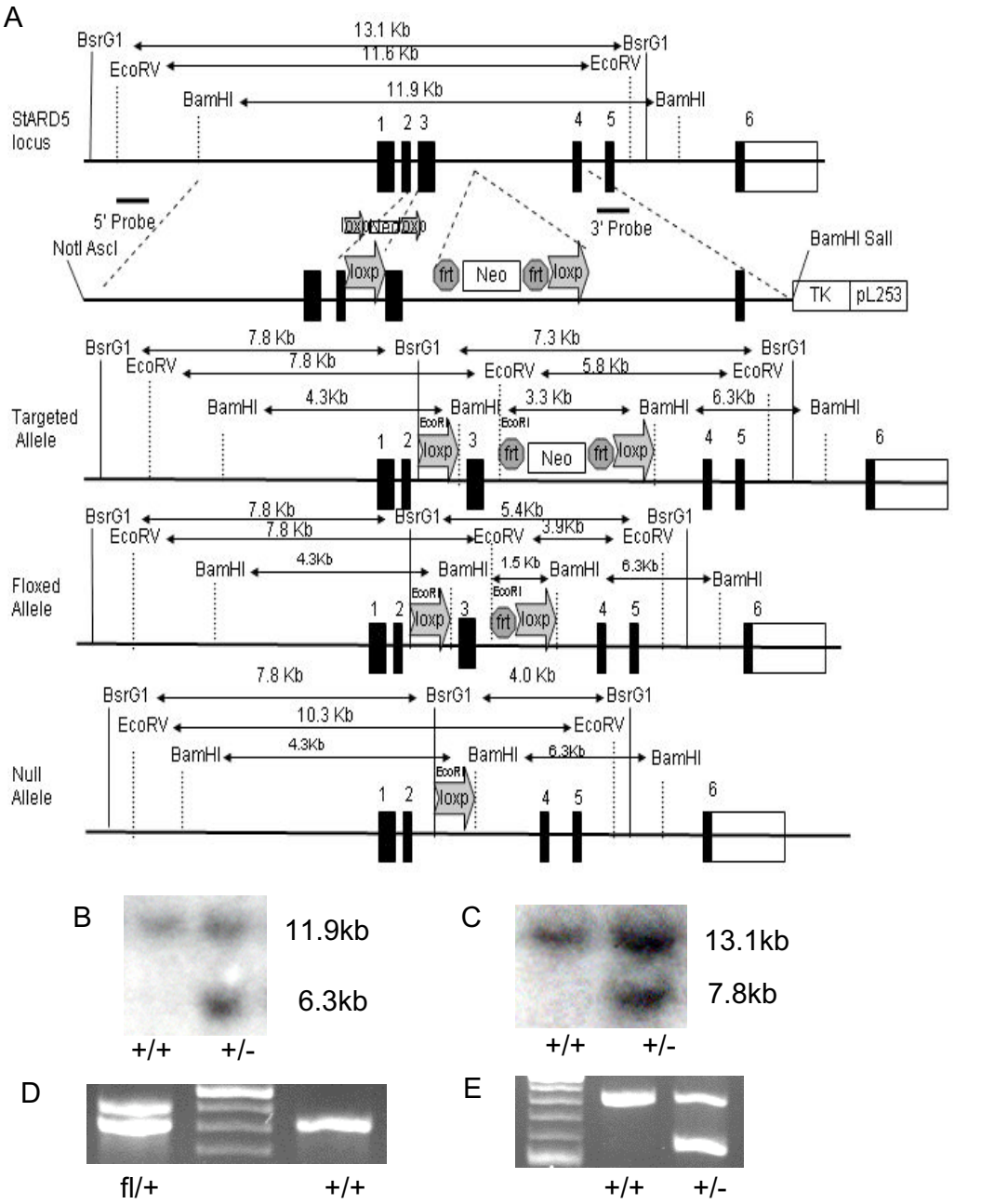

Figure 2.2. **Gene targeting and generation of a conditional knockout (floxed) allele of the StARD5 gene**. A) Targeting strategy to flank exon 3 of StARD5 with loxP sites. The targeting vector was constructed by placing a Neo selectable marker flanked by Frt sites with a loxP site in intron 3. A second loxP site was introduced in intron 2. B) A southern blot (BamHI) using the external 3' probe was used to monitor homologous recombination. C) A southern blot (BsrGI) using the external 5'probe was used to monitor homologous recombination D) PCR analysis in order to determine the presence of the wildtype (bottom band) and/or floxed (top band) alleles in heterozygous (fl/+) as well as wildtype (+/+) controls D) PCR analysis in order to determine the presence of the wildtype(top band) and/or null allele (bottom band) in heterozygous (+/-) as well as wildtype (+/+) controls.

exon 2 within the 344bp intron 2, and the cassette placed 1606bp after exon 3 within the 3488bp intron 3. The MC1-TK cassette was used for negative selection against random integration events, while the Neo cassette allowed for positive selection. The Neo floxed allele of the StARD5 gene was generated through homologous recombination in isogenic mouse embryonic stem (ES) cells. Thirteen correctly targeted ES clones were identified by Southern blotting using BamHI or EcoRV restriction digests of genomic DNA, and external 5' or 3' probes, respectively, that were not part of the targeting vector. Five ES cell clones were expanded and injected into blastocysts to produce chimeras, but only one (#118) led to germ-line transmission.

Viability, Fertility, and Fecundity in the StARD5 Mice

After detection of germ-line transmission of the targeted allele, an attempt was made to breed the Neo floxed gene to homozygosity. Brother-sister mating of Neo floxed heterozygous mice failed to yield homozygous offspring. This failure to achieve the expected Mendelian ratios indicated the genetically altered StARD5 allele was not able to encode functional StARD5, perhaps by interfering with splicing. It also suggested that the loss of StARD5 might cause embryonic lethality.

Since it was possible that the large Neo cassette in intron 3 might have interfered with proper splicing of StARD5, an attempt was made to remove it by breeding StARD5 Neo floxed heterozygous mice to C57BL/6 ACT-FLPe transgenic mice. The latter express FLP1 recombinase, an enzyme derived from

Saccharomyces cerevisiae that recognizes a 34bp FLP1 recombinase target (FRT) sequence. This enzyme efficiently excises DNA located between similarly oriented FRT sites and recombines the DNA ends. This leaves a single FRT site in place of the intervening sequence. The promoter of the FLPe transgene drives expression in germ-line cells and many other tissues, essentially completely removing the Neo cassette from the StARD5 gene of targeted mice. After the loss of the Neo cassette, the result was a targeted allele with 2 loxP sites flanking StARD5 exon 3, which is referred to as the floxed allele. Brother-sister mating of floxed heterozygous mice again failed to yield homozygous offspring (33% wild-type, 67% heterozygotes) (Figure 2.2). This strongly suggests that the loxP sites in introns 2 and 3 themselves interfere with proper splicing of the StARD5 mRNA and in this manner prevent StARD5 protein expression. In other experiments, bone marrow macrophages from these StARD5 heterozygous floxed mice expressed only ~50% of normal StARD5 protein, supporting the hypothesis that the placement of the loxP sites in the targeted allele interferes with proper protein expression.

The floxed allele was converted to a null allele by crossing StARD5 floxed

Table 2.1. **Fertility and Fecundity of StARD5cKO Mice**

Deleted	**wt:het:homo**	**litter size (mean +/- SD)**
Male +/- x Female +/-	29:56:0	5.9 +/- 2.3
Floxed		
Male +/fl x Female +/fl	36:73:0	6.6 +/- 2.5

Deleted	**# pregnancies**	**litter size (mean +/- SD)**
Male +/+ x Female +/-	15	6.0 +/- 1.5
Male +/- x Female +/+	5	6.6 +/- 1.5

heterozygous mice with C57BL/6 CMV-Cre transgenic mice. Cre-recombinase, an enzyme derived from the bacteriophage P1, recognizes adjacent loxP sites and efficiently mediates the excision of DNA located between them. This enzyme also recombines the DNA ends, leaving a single loxP site in place of the intervening sequence. The promoter of the Cre transgene drives expression in germ-line cells and many other tissues, essentially completely removing exon 3 from the StARD5 gene of targeted mice (Figure 2.2). Again, brother-sister mating of StARD5 null heterozygous mice failed to yield homozygous offspring (34% wild-type, 66% heterozygotes) (Table 2.1). As with the floxed allele, bone marrow macrophages from StARD5 heterozygous null mice expressed only ~50% of normal StARD5 protein (Figure 2.3). Together with the breeding experiments, these results indicate that the loss of StARD5 is embryonic lethal in C57BL/6 mice (Figure 2.4).

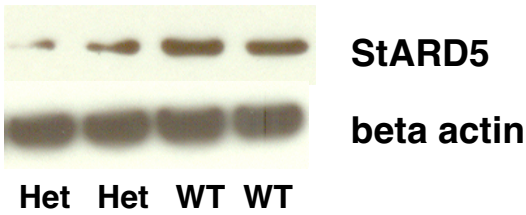

Figure 2.3. **Expression of StARD5 in bone marrow macrophages of StARD5 heterozygous mice.** Bone marrow macrophages from StARD5 heterozygous mice and wild-type mice were extracted and grown in culture. Protein lysates were collected and Western blot performed for StARD5. Het: Heterozygote, WT: Wild-type.

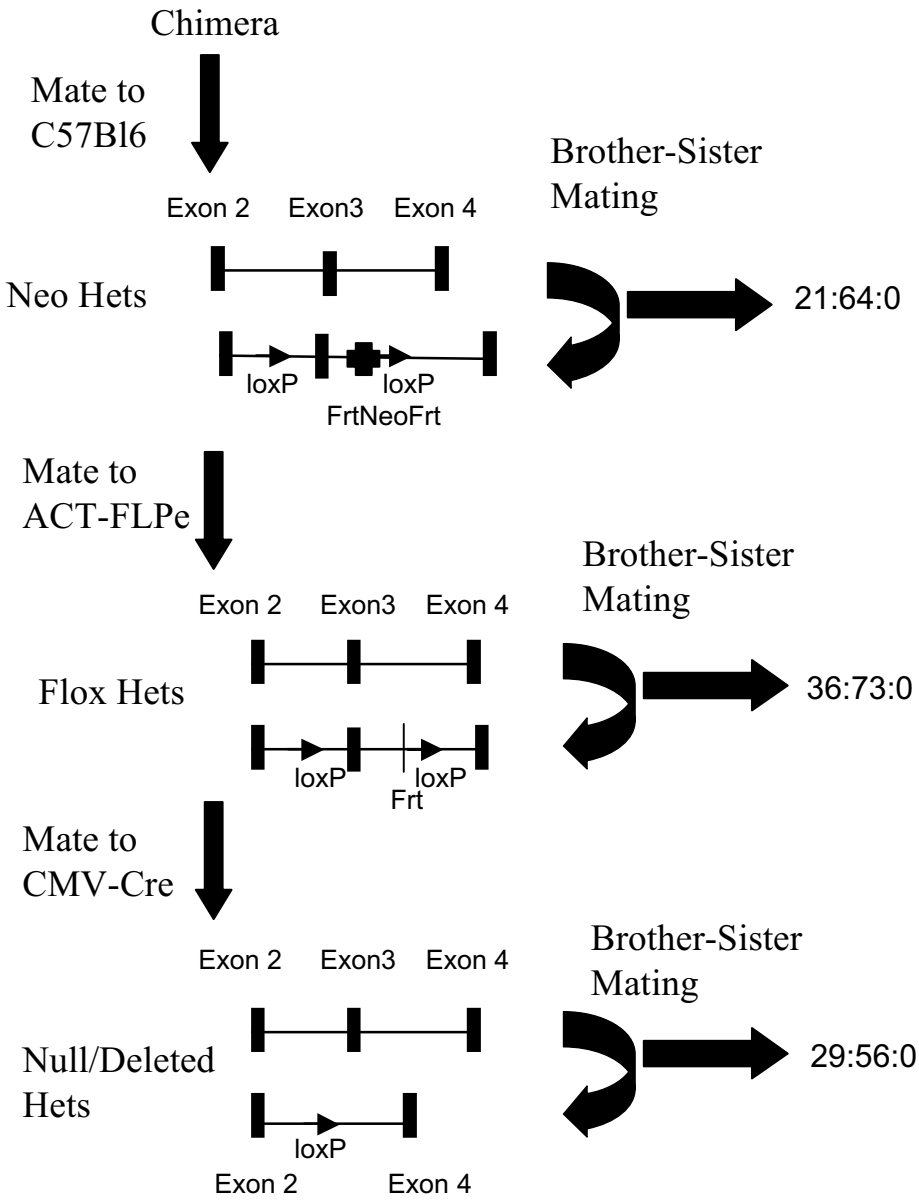

Figure 2.4. **Mating strategy in generation of the StARD5 knockout.**
Chimera mice were mated to C57Bl6 to generate Neo heterozygotes. These Neo heterozygotes were brother-sister mated in an attempt to generate Neo homozygotes. The Neo heterozygotes were also mated to the ACT-FLPe transgenic mice to remove the FrtNeoFrt cassette and to generate Flox heterozygotes. These Flox heterozygotes were brother-sister mated in an attempt to generate Flox homozgotes. The Flox heterozygotes were mated to CMV-Cre transgenic mice to remove exon 3 and to generate Null/Deleted heterozygotes. These Null heterozygotes were brother-sister mated in an attempt to generate Null homozygotes. Results of the brother-sister matings are indicated on the right; the order is wildtype:heterozygotes:homozygotes. No homozygote Neo, floxed, or null mice have been identified. Rectangles represent exons, triangles represents loxP sites, cross represents the FrtNeoFrt cassette, line vertical line represents Frt site after Flp recombinase, thick arrows represent matings.

Embryonic Lethality of StARD5 Homozygous Knockouts

Both males and female heterozygous null mice were capable of breeding the null trait when crossed to wild-type mice, indicating that sperm and oocyte carrying the StARD5 knockout trait are viable and capable of fertilization and that lethality of the homozygosity must occur between fertilization and birth. Timed matings of StARD5 heterozygous intercrosses were performed to determine at what stage of gestation embryonic lethality occurs. Embryos were collected on days E16.5, E15.5, E14.5, E13.5, E12.5, E11.5, E10.5 and E9.5, and genotyping revealed that none were homozygous null mutants (Table 2.2). Thus it appears that the lack of StARD5 leads to embryonic lethality before the E9.5 stage of development. Potential causes for the lethality of the StARD5 homozygous embryo at this early stage include a failure of cleavage, compaction, hatching, implantation, gastrulation, hematopoeisis, or cardiovascular development.

Table 2.2. **Genotypes of Embryos from Intercross of StARD5+/- Mice**

Age	WT	Het	KO	Undetermined
E16.5	3	4	0	
E14.5	3	11	0	1
E13.5	3	13	0	2
E11.5	2	6	0	
E10.5	1	4	0	
E9.5	12	14	0	5

Pathology of StARD5 Heterozygous Knockouts

A small significant decrease (approximately 6%) in weight was observed between wild-type and StARD5 heterozygous floxed mice at 12 weeks of age, in both males and females on a chow diet (Table 2.3), as was a corresponding decrease in liver weight. This was also found between female wild-type and StARD5 heterozygous null mice, however, not between male wild-type and StARD5 heterozygous null mice (Table 2.3). In the experiment with the wild-type and StARD5 heterozygous null mice weights were measured from weaning at 4 weeks until sacrifice at 12 weeks of age and the difference between the genotypes did not become significant until week 12 (Figure 2.5). Upon sacrifice at 12 weeks of age a complete pathological examination was performed on StARD5 heterozygous null

Table 2.3. **Body composition of StARD5 mice at 12 weeks old**

		Male		Female	
Null Mice		**Wt**	**Het**	**Wt**	**Het**
Mouse Weight (g)		24.3 +/- 0.6	24.8 +/- 0.4	21.2 +/- 0.6	19.3 +/- 0.3*
	***n*=**	*6*	*12*	*6*	*15*
Liver Weight (g)		1.04 +/- 0.02	1.00 +/- 0.03	0.98 +/- 0.04	0.85 +/- 0.02*
	***n*=**	*6*	*12*	*6*	*15*
Floxed Mice					
Mouse Weight (g)		25.7 +/- 0.3	24.3 +/- 0.4*	19.6 +/- 0.6	18.3 +/- 0.2*
	***n*=**	*10*	*14*	*8*	*16*
Liver Weight (g)		1.12 +/- 0.04	1.06 +/- 0.05	0.88 +/- 0.03	0.79 +/- 0.03*
	***n*=**	*6*	*7*	*3*	*7*

All values are means +/- SEM, number of mice (N) is given for each value,

* indicates p values < 0.05

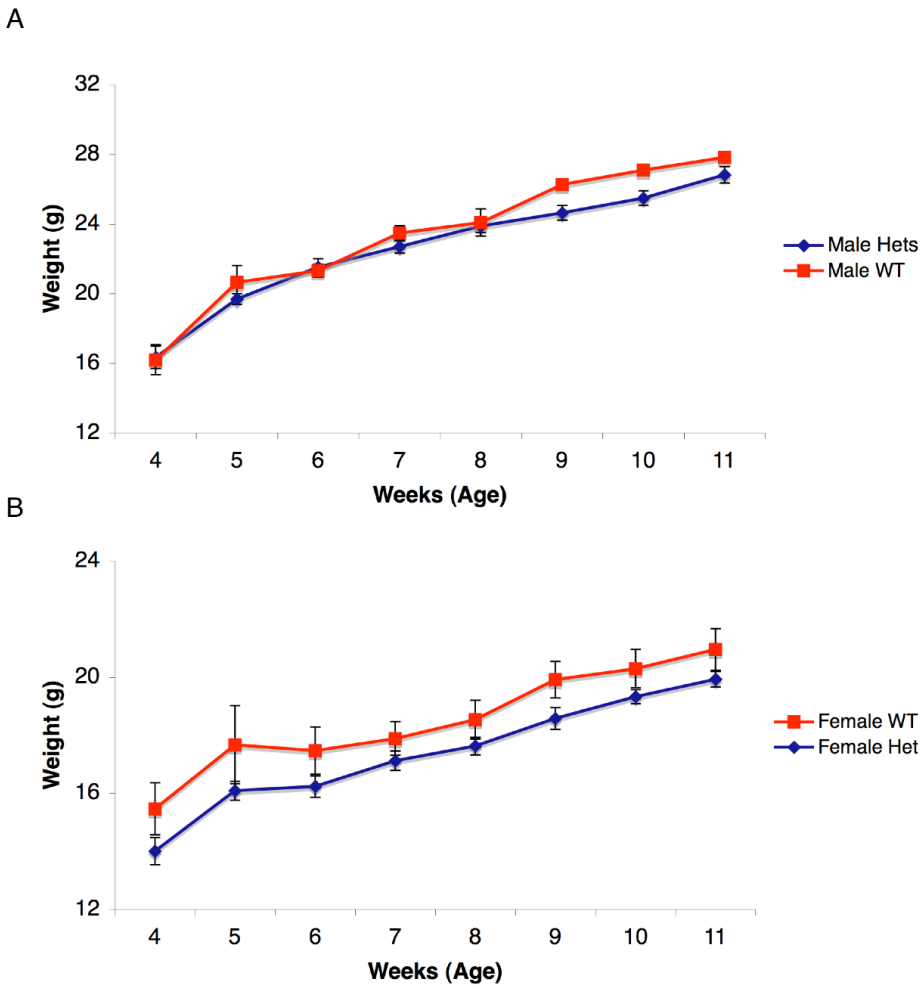

Figure 2.5. **Growth curve of StARD5 mice**.
A) Males B) Females. The cross of StARD5 heterozygous null mice were weaned at 4 weeks and fed a chow diet until sacrfice at 12 weeks. Weight of mice were taken each week. Blue points represent values for StARD5 heterozygous null mice; red points represent wild-type siblings. Mean weight (g) plus or minus SEM at each time point are indicated in graph Each data point represents 5-15 mice.

mice and their wild-type litter-mates by the Tri-Institutional Core Facility located in the MSKCC Pathology Department. No apparent anatomical-histological differences were observed in heart, lungs, esophagus, thymus, tongue, kidneys, pancreas, renal lymph nodes, spleen, salivary glands, stomach, duodenum, jejunum, ileum, colon, cecum, pancreas, brown fat, urinary bladder, thyroid glands, trachea, adrenal glands, liver, sciatic nerve, spinal cord, gallbladder, or brain.

Plasma Cholesterol, Triglycerides, and Glucose levels

Comparison of wild-type and StARD5 heterozygous null or floxed mice at 12 weeks of age on a chow diet revealed no significant differences in plasma total and free cholesterol, HDL, and LDL cholesterol, triglycerides, and glucose levels (Table 2.4).

Table 2.4. **Plasma levels of StARD5 mice at 12 weeks old**

		Male		Female	
Null Mice		**Wt**	**Het**	**Wt**	**Het**
Triglycerides		31 +/- 3	31 +/- 2	37 +/- 5	30 +/- 7
(mg/dL)	***n*=**	*6*	*12*	*4*	*14*
Total Cholesterol		71 +/- 3	69 +/- 2	67 +/- 4	63 +/- 4
(mg/dL)	***n*=**	*6*	*12*	*4*	*14*
HDL (mg/dL)		51 +/- 2	49 +/- 1	41 +/- 3	40 +/- 1
	***n*=**	*6*	*12*	*4*	*14*
LDL (mg/dL)		21 +/- 1	22 +/- 3	24 +/- 3	24 +/- 2
	***n*=**	*6*	*12*	*4*	*14*
non-HDL		20 +/- 2	20 +/- 2	26 +/- 4	23 +/- 3
(calculated)	***n*=**	*6*	*12*	*4*	*14*
Free Cholesterol		6 +/- 1	10 +/- 1	9 +/- 1	9 +/- 1
(mg/dL)	***n*=**	*6*	*12*	*4*	*14*
Glucose		116 +/- 9	126 +/- 8	109 +/- 7	122 +/- 11
(mg/dL)	***n*=**	*5*	*10*	*3*	*7*
Floxed Mice					
Triglycerides		31 +/- 2	30 +/- 2	25 +/- 2	28 +/- 2
(mg/dL)	***n*=**	*6*	*9*	*7*	*14*
Total Cholesterol		92 +/- 4	89 +/- 5	73 +/- 3	80 +/- 4
(mg/dL)	***n*=**	*7*	*12*	*7*	*14*
HDL (mg/dL)		64 +/- 6	62 +/- 3	48 +/- 2	50 +/- 2
	***n*=**	*5*	*10*	*7*	*14*
LDL (mg/dL)		24 +/- 3	21 +/- 2	23 +/- 2	23 +/- 2
	***n*=**	*5*	*10*	*7*	*14*
non-HDL		27 +/- 1	29 +/- 3	24 +/- 3	31 +/- 3
(calculated)	***n*=**	*5*	*10*	*7*	*14*

All values are means +/- SEM, number of mice (N) is given for each value

Hepatic Cholesterol Levels

Similarly, there were no significant differences between wild-type and StARD5 heterozygous null or floxed mice at 12 weeks of age on a chow diet in hepatic total cholesterol (Table 2.5).

Table 2.5. **Hepatic levels of StARD5 male mice at 12 weeks old**

Null Mice		**Wt**	**Het**
Total Cholesterol		2.4 +/- 0.4	2.4 +/- 0.1
	***n*=**	*3*	*3*
Floxed Mice			
Total Cholesterol		2.5 +/- 0.3	2.7 +/- 0.2
	***n*=**	*3*	*3*

Values are in mg/g liver, all values are means +/- SEM,
number of mice (N) is given for each value

Gallbladder Bile Composition

There were no significant differences between wild-type and StARD5 heterozygous null or floxed mice at 12 weeks of age on a chow diet in gallbladder bile concentrations of cholesterol, bile acids, or phospholipids (Table 2.6).

Table 2.6. **Gallbladder bile levels of StARD5 mice at 12 weeks old**

		Male		**Female**	
Null Mice		**Wt**	**Het**	**Wt**	**Het**
Cholesterol		133 +/- 17	155 +/- 20	182 +/- 23	231 +/- 17
(mg/dL)	***n*=**	*5*	*9*	*3*	*12*
Phospholipids		1304 +/- 313	1504 +/- 145	1946 +/- 177	1907 +/- 208
(mg/dL)	***n*=**	*3*	*7*	*3*	*10*
Bile Acids		71 +/- 11	75 +/- 6	100 +/- 10	89 +/- 6
(mM)	***n*=**	*5*	*9*	*3*	*12*
Floxed Mice					
Cholesterol		160 +/- 13	157 +/- 11	200 +/- 22	237 +/- 12
(mg/dL)	***n*=**	*6*	*6*	*7*	*10*
Phospholipids		2045 +/- 118	1902 +/- 141	1928 +/- 195	2105 +/- 106
(mg/dL)	***n*=**	*6*	*6*	*7*	*10*

All values are means +/- SEM, number of mice (N) is given for each value

Glucose Tolerance

The same mice were subjected to an intra-peritoneal glucose tolerance test (IPGTT) a few days before sacrifice, with glucose measurements made 0, 15, 30, 60, and 120 minutes after injecting a glucose bolus of 2g/kg. Again, there was no significant differences between wild-type and StARD5 heterozygous null mice (Figure 2.6).

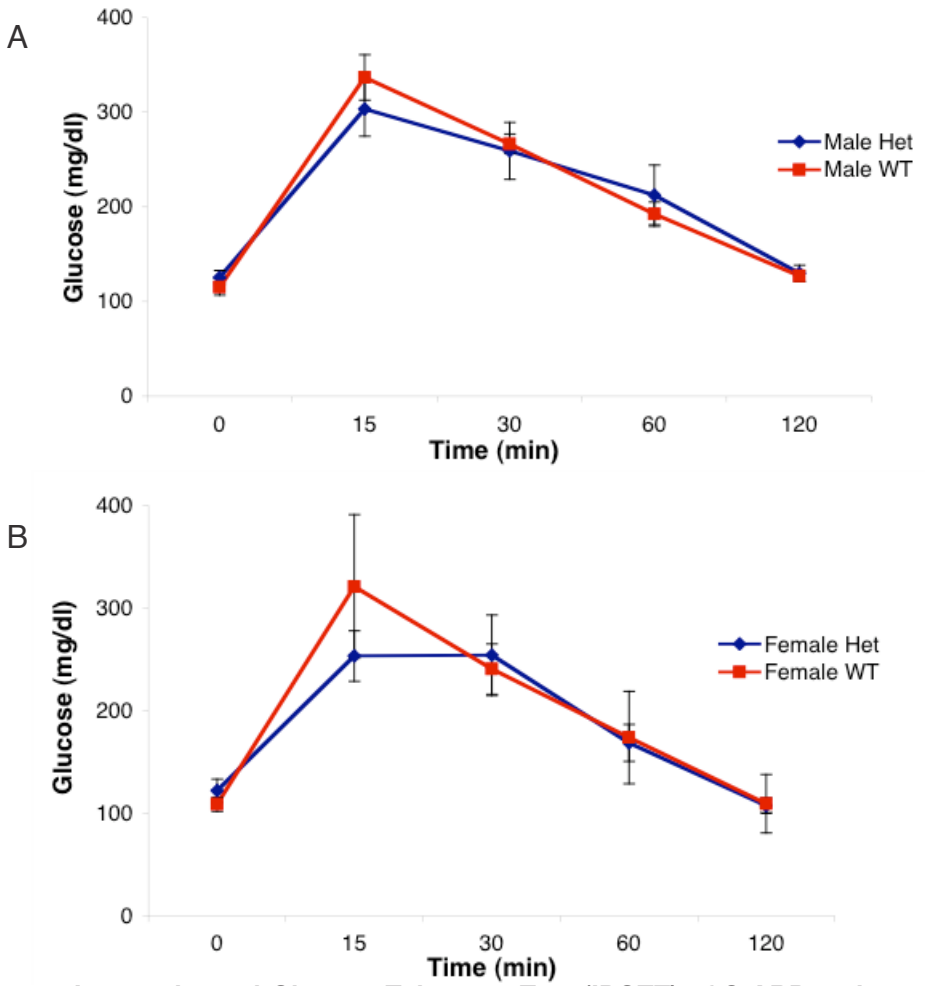

Figure 2.6. **Intraperitoneal Glucose Tolerance Test (IPGTT) of StARD5 mice.** 11.5 week old StARD5 heterozygous null mice were tested by injecting a bolus of 2g glucose/kg body weight; mean blood glucose values are indicated with SEM for error bars.
AUC, area under curve, for IPGTT is also provided.
A) Male (n=5 WT, 10 Het); AUC: wt: 24,408 +/- 1074; het: 24,808 +/- 2495
B) Female (n=3 WT, 7 Het) AUC: wt: 22,159 +/- 4534; het: 21,243 +/- 2059

Macrophage Cholesterol Efflux

Bone marrow macrophages from wild-type and StARD5 heterozygous null male mice were isolated and then loaded with 3H-cholesterol. Measuring efflux of radiolabeled cholesterol to ApoAI or HDL, testing the ABCA1 and ABCG1 pathways, respectively, over 4 and 8 hours showed no differences between genotypes (Figure 2.7).

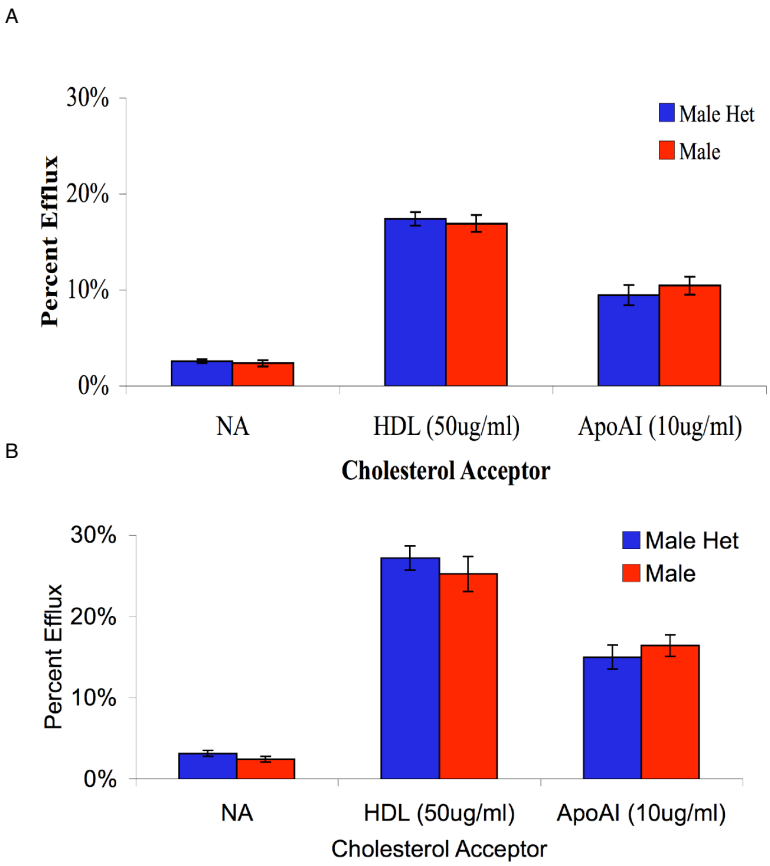

Figure 2.7. **Bone marrow macrophage cholesterol efflux of StARD5 male mice.** Bone marrow macrophages fromStARD5 heterozygous null mice were extracted and grown in culture. ^{3}H-cholesterol was added to the medium for 24 hours; acLDL and 3H Cholesterol was added for an additional 24 hours. Media was removed. Cells were washed and placed with media containing No Acceptor (NA), HDL (50ug/ml) or ApoAI (10ug/ml) as the cholesterol acceptor. Cells and media were counted (cpm) after (A) 4 or (B) 8 hours, and percent efflux was calculated as counts in media divided by the total counts in the media and cells. (n=3 for each genotype, efflux from each mouse is measured for each acceptor and time point in triplicate). Mean values plus or minus SEM are indicated.

Crossing the StARD5 Knockout Trait onto the LDLR Knockout Background

To identify a possible effect of StARD5 on atherosclerosis susceptibility, StARD5 heterozygous null mice were crossed onto the atherosclerosis-susceptible B6.LDLR KO background. After weaning at 4 weeks, mice were fed a low-fat low-cholesterol semi-synthetic diet for 16 weeks. The animals were sacrificed at 20 weeks of age and aortic root cross sectional lesion area compared between wild-type and heterozygous StARD5 null mice. No significant differences were observed for either gender between the genotypes (Figure 2.8). Comparison of

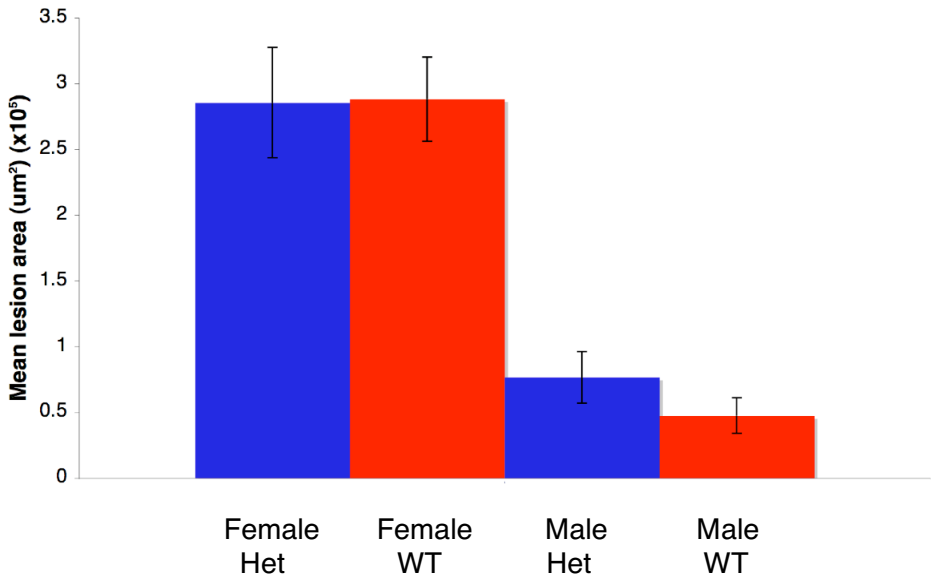

Figure 2.8. **Atherosclerotic lesion size at the aortic root of StARD5 mice on LDLR KO background.** Average lesion size (um^2) at the aortic root was measured in each StARD5 null heterozygous and wild-type mouse after 16 weeks on semi-synthetic AIN76a diet (n= 6 heterozygote females, 10 wildtype females, 9 heterozygote males, 6 wildtype males). Mean values ($x10^5$) plus or minus SEM for lesion area are indicated.

wild-type and StARD5 heterozygous null mice on the LDLR KO background did not show any differences in body weight or liver weight (Table 2.7), total, HDL, LDL and VLDL cholesterol, triglycerides, glucose or free cholesterol (Table 2.8), gallbladder bile cholesterol, bile acids and phospholipid concentrations (Table 2.9), and glucose tolerance as measured by the IPGTT (Figure 2.9).

Table 2.7. **Body composition of StARD5 mice on LDLR KO background**

		Male		Female	
Null Mice		**Wt**	**Het**	**Wt**	**Het**
Mouse Weight (g)		27.9 +/- 0.8	28.3 +/- 0.5	21.8 +/- 0.6	21.4 +/- 0.9
	***n*=**	*6*	*9*	*10*	*6*
Liver Weight (g)		1.09 +/- 0.07	1.05 +/- 0.04	0.97 +/- 0.04	0.93 +/- 0.03
	***n*=**	*6*	*8*	*10*	*6*

All values are means +/- SEM, number of mice (N) is given for each value

Table 2.8. **Plasma levels of StARD5 mice on LDLR KO background**

		Male		Female	
Null Mice		**Wt**	**Het**	**Wt**	**Het**
Triglycerides		148 +/- 27	98 +/- 10	99 +/- 15	113 +/- 21
(mg/dL)	***n*=**	*6*	*9*	*10*	*6*
Total Cholesterol		521 +/- 41	556 +/- 35	617 +/- 42	671 +/- 83
(mg/dL)	***n*=**	*6*	*9*	*10*	*6*
Free Cholesterol		147 +/- 18	125 +/- 26	136 +/- 11	155 +/- 18
(mg/dL)	***n*=**	*6*	*9*	*10*	*6*
HDL		76 +/- 2	73 +/- 3	55 +/- 4	46 +/- 5
(mg/dL)	***n*=**	*6*	*9*	*10*	*6*
LDL		379 +/- 47	409 +/- 36	410 +/- 33	407 +/- 51
(mg/dL)	***n*=**	*6*	*9*	*10*	*6*
VLDL		45 +/- 15	49 +/- 10	97 +/- 14	117 +/- 29
(mg/dL)	***n*=**	*6*	*9*	*10*	*6*
Glucose		146 +/- 11	160 +/- 11	131 +/- 8	119 +/- 10
(mg/dL)	***n*=**	*6*	*7*	*9*	*4*

All values are means +/- SEM, number of mice (N) is given for each value

Table 2.9. **Gallbladder bile levels of StARD5cko on LDLR KO background**

Null Mice		Male		Female	
		Wt	Het	Wt	Het
Cholesterol (mg/dL)		175 +/- 23	166 +/- 29	186 +/- 36	163 +/- 39
	***n*=**	*4*	*6*	*6*	*4*
Phospholipids (mg/dL)		1471 +/- 351	1684 +/- 161	2352 +/- 379	1355 +/- 194
	***n*=**	*3*	*4*	*4*	*3*
Bile Acids (mM)		127 +/- 19	85 +/- 13	55 +/- 14	70 +/- 21
	***n*=**	*3*	*6*	*3*	*3*

All values are means +/- SEM, number of mice (N) is given for each value

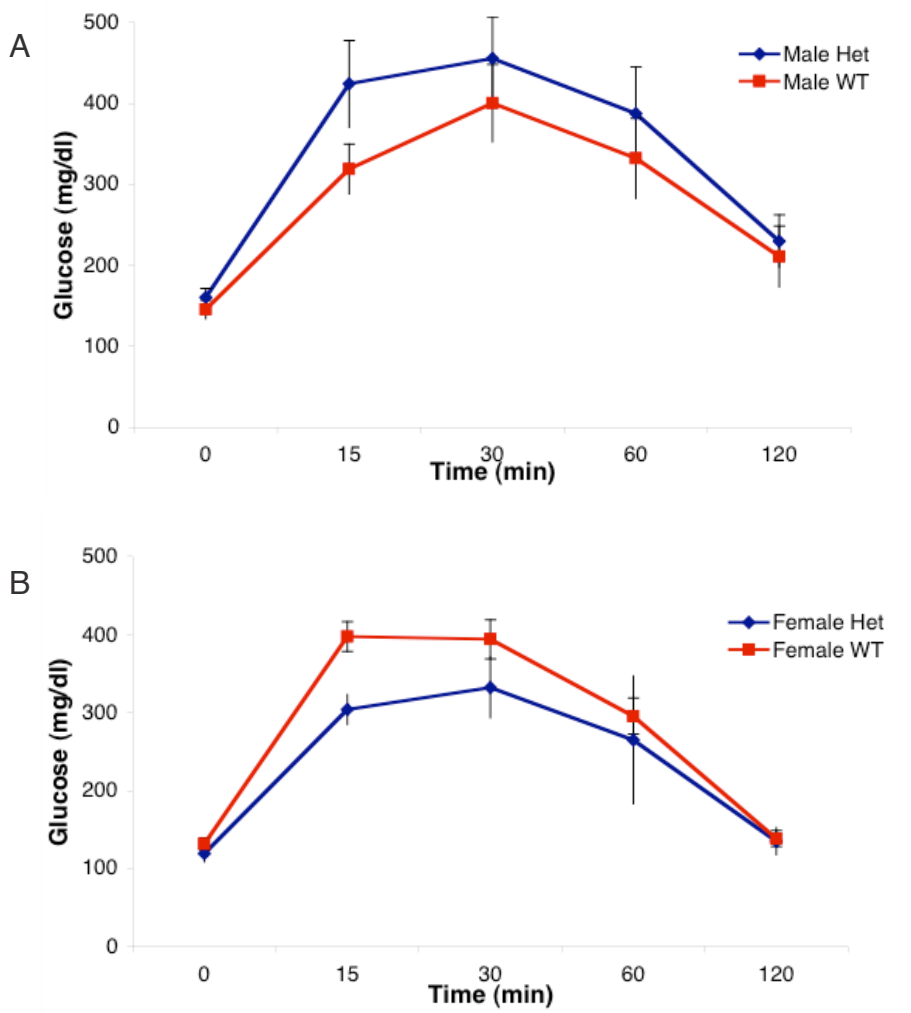

Figure 2.9. **Intraperitoneal Glucose Tolerance Test (IPGTT) of StARD5 mice on the LDLR KO background.** 19.5 week old mice were tested after 15.5 weeks on diet, by injecting a bolus of 2g glucose/kg body weight; mean blood glucose values plus or minus SEM are indicated.
AUC, area under curve, for IPGTT is also provided.
A) Male (n=6 WT, 7 Het); AUC: wt: 36,160 +/- 4227; het: 42,147 +/- 5149
B) Female (n=9 WT, 4 Het); AUC: wt: 33,262 +/- 1745; het: 28,909 +/- 4843

Development of Transgenic Mice Over-Expressing Human StARD5 in Macrophages Using the Scavenger Receptor A Enhancer and Promoter

In another attempt to probe the function of the StARD5, transgenic mice were created expressing human StARD5 only in macrophages. This also involved utilizing the Copeland's recombineering techniques. Human genomic StARD5 DNA was obtained from a BAC clone (BacPac Resources RP11-770M20), placed under control of the promoter and enhancer regions of Scavenger Receptor A (SR-A) (a gift from D'Armiento and Glass) (Liu et al., 2003), and injected into C57BL/6 ES cells. Using human StARD5 sequences allowed transgene expression to be easily distinguished from endogenous StARD5 expression. Transgenic mice were identified by PCR and 2 founder lines were obtained. In both cases, bone marrow macrophages expressed StARD5 mRNA at low levels; approximately half the levels of mouse StARD5 mRNA in the same cells (Figure 2.10). To help assess the

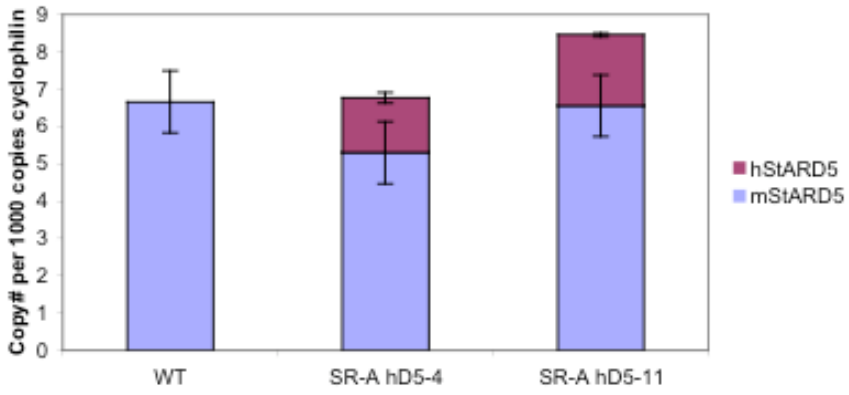

Figure 2.10. **Expression of hStARD5 in bone marrow macrophages of SR-A-hStARD5 transgenics**. Bone marrow macrophages were extracted and grown in culture. Blue bars represent expression levels of mStARD5, while red bars represent expression levels of hStARD5. Values are in copy number of transcript per 1000 copies of cyclophilin A transcript. Expression levels of hStARD5 in both transgenic lines are approximately one-third the expression levels of mStARD5. All values are means +/- SEM.

possible physiological significance of this relatively small amount of human StARD5 expression, wild-type and hStARD5 transgenic mice at 6 weeks of age were placed on the AIN76a diet free of cholesterol for one week. After this the mice were switched to the AIN76a diet containing 0.5% cholesterol for one week and then sacrificed at 8 weeks of age. Comparison of wild-type and both hStARD5 transgenic mouse lines failed to reveal significant differences in body weight or liver weight (Table 2.10), total, HDL, LDL and VLDL cholesterol and triglycerides (Table

Table 2.10. **Body composition, plasma, liver and gallbladder bile levels of SR-A-hStARD5 transgenic mice on high 0.5% cholesterol diet**

Male		Wt	Transgenic-11	Transgenic-4
Body Weight		22.8 +/- 0.5	23.1 +/- 0.4	21.8 +/- 0.9
(g)	***n*=**	*14*	*14*	*11*
Liver Weight		1.10 +/- 0.04	1.25 +/- 0.06	1.07 +/- 0.07
(g)	***n*=**	*13*	*14*	*11*
Plasma		91 +/- 5	96 +/- 5	106 +/- 10
Cholesterol (mg/dl)	***n*=**	*15*	*14*	*11*
HDL (mg/dL)		54 +/- 4	60 +/- 2	61 +/- 5
	***n*=**	*15*	*14*	*11*
LDL (mg/dL)		32 +/- 2	36 +/- 2	42 +/- 3
	***n*=**	*15*	*14*	*11*
VLDL (mg/dL)		7 +/- 1	7 +/- 1	7 +/- 1
	***n*=**	*15*	*14*	*11*
Triglycerides (mg/dL)		37 +/- 2	37 +/- 3	36 +/- 3
	***n*=**	*15*	*14*	*11*
Liver Total		14.0 +/- 0.8	15.2 +/- 0.8	13.8 +/- 1.1
Cholesterol (mg/g)	***n*=**	*15*	*14*	*11*
Bile		365 +/- 36	298 +/- 25	341 +/- 27
Cholesterol (mg/dL)	***n*=**	*12*	*12*	*8*
Phospholipids(mg/dL)		1653 +/- 107	1769 +/- 141	1708 +/- 139
	***n*=**	*12*	*12*	*8*

All values are means +/- SEM, number of mice (N) is given for each value; Liver cholesterol values are in mg/g liver

Table 2.10. *Continued.* **Body composition, plasma, liver and gallbladder bile levels of SR-A-hStARD5 transgenic Mice on high 0.5% cholesterol diet**

Female		Wt	Transgenic-11	Transgenic-4
Body Weight		18.2 +/- 0.3	18.7 +/- 1.0	17.4 +/- 0.3
(g)	***n*=**	*16*	*8*	*11*
Liver Weight		0.94 +/- 0.02	0.94 +/- 0.06	0.90 +/- 0.03
(g)	***n*=**	*16*	*9*	*11*
Plasma		82 +/- 5	73 +/- 11	92 +/- 9
Cholesterol (mg/dl)	***n*=**	*16*	*8*	*11*
HDL (mg/dL)		41 +/- 2	35 +/- 2	41 +/- 3
	***n*=**	*16*	*8*	*11*
LDL (mg/dL)		36 +/- 2	36 +/- 3	45 +/- 7
	***n*=**	*16*	*8*	*11*
VLDL (mg/dL)		7 +/- 1	7 +/- 3	9 +/- 1
	***n*=**	*16*	*8*	*11*
Triglycerides (mg/dL)		27 +/- 2	26 +/- 4	29 +/- 3
	***n*=**	*16*	*8*	*11*
Liver Total		21.6 +/- 1	22.8 +/- 1.5	25.8 +/- 4.5
Cholesterol (mg/g)	***n*=**	*16*	*8*	*11*
Bile		288 +/- 25	328 +/- 25	360 +/- 60
Cholesterol (mg/dL)	***n*=**	*12*	*6*	*9*
Phospholipids(mg/dL)		1950 +/- 197	2121 +/- 158	*1910 +/- 294*
	***n*=**	*12*	*6*	*9*

All values are means +/- SEM, number of mice (N) is given for each value; Liver cholesterol values are in mg/g liver

2.10), hepatic cholesterol content (Table 2.10), and gallbladder bile cholesterol and phospholipid concentrations (Table 2.10).

Crossing the hStARD5 Macrophage-Specific Transgenic Lines onto the LDLR Knockout Background

To identify a possible effect of StARD5 over-expression (albeit low level) on atherosclerosis susceptibility, the hStARD5 macrophage-specific transgenic trait was crossed onto the atherosclerosis-susceptible B6.LDLR KO background. After weaning at 4 weeks, mice were fed a low-fat low-cholesterol semi-synthetic diet

for 16 weeks. The animals were sacrificed at 20 weeks of age and aortic root cross sectional lesion area compared between wild-type and hStARD5 macrophage-specific transgenic lines. No significant differences were observed in for either gender between the genotypes (Figure 2.11). Comparison of wild-type and

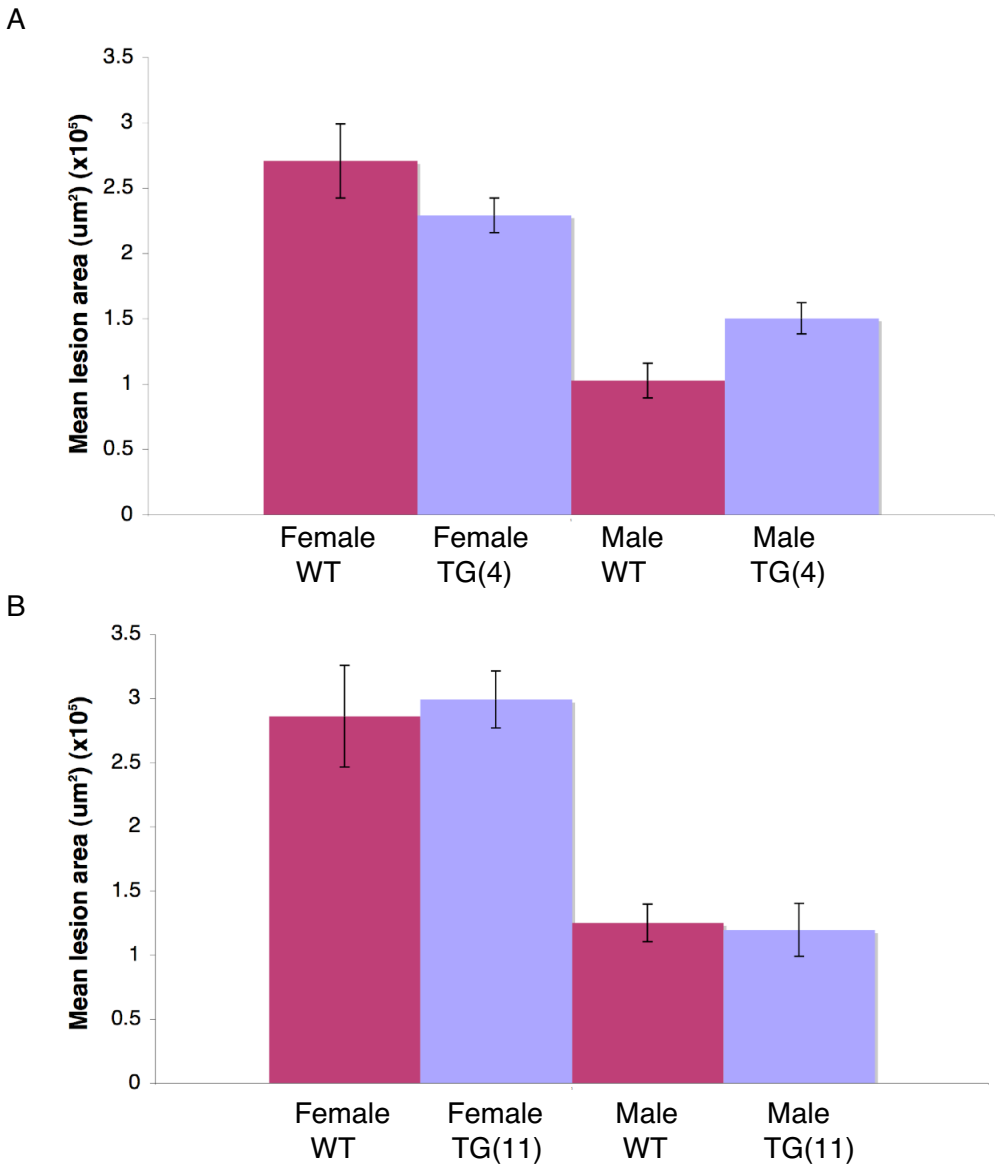

Figure 2.11. **Atherosclerotic lesion size at the aortic root of SR-A-hStARD5 transgenic mice on LDLR KO background**. A) Trangenic-4; B) Transgenic-11
Average lesion size (um^2) at the aortic root was measured in each transgenic and wild-type mouse after 16 weeks on semi-synthetic AIN76a diet (8-12 per gender and genotype). Mean values (x10^5) plus or minus SEM for lesion area are indicated.

hStARD5 macrophage-specific transgenic lines on the LDLR KO background did not show any differences in body weight, liver weight, total, HDL, LDL and VLDL cholesterol, or triglyceride levels (Table 2.11); nor was there a difference in the ability of bone marrow macrophages from wild-type and hStARD5 transgenic mice on the LDLR knockout background loaded with 3H-cholesterol to efflux radiolabeled cholesterol to ApoAI or HDL (Figure 2.12).

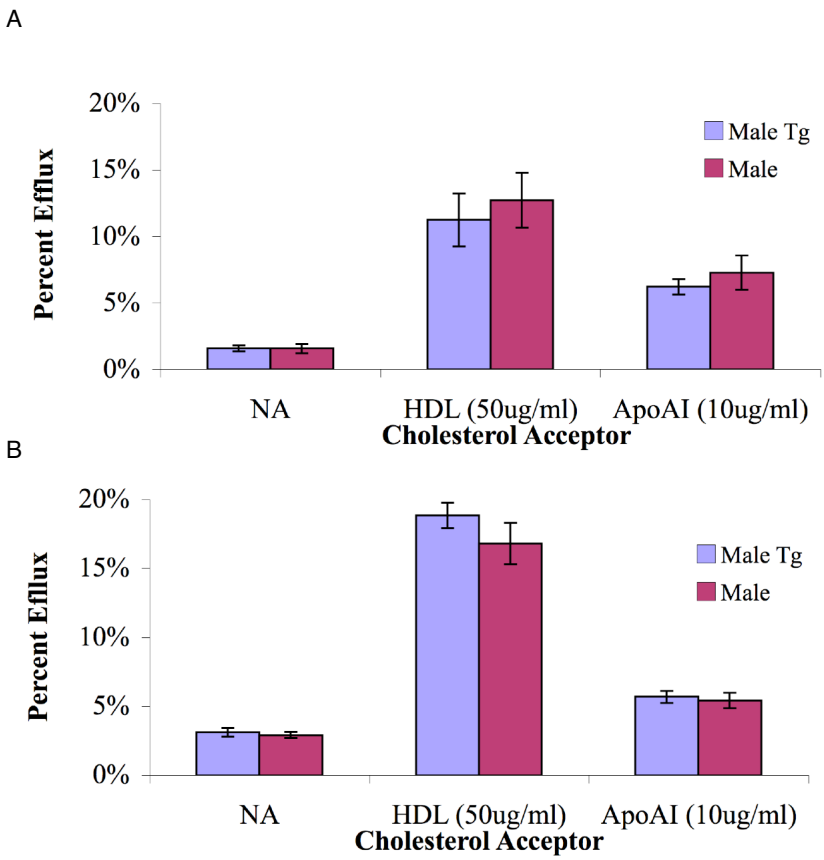

Figure 2.12. **Bone marrow macrophage cholesterol efflux of SR-A-hStARD5 transgenic male mice on LDLR KO background.** (n=3 for each genotype, efflux from each mouse is measured for each acceptor and time point in triplicate) ^{3}H Cholesterol was added to the medium for 24 hours, acLDL and ^{3}H Cholesterol was added for an additional 24 hours. Media was removed. Cells were washed and placed with media containing No Acceptor (NA), HDL (50ug/ml) or ApoAI (10ug/ml) as the cholesterol acceptor. Cells and media were counted (cpm) after 4 hours, and percent efflux was calculated as counts in media divided by the total counts in the media and cells. A) Transgenic-4, B) Transgenic-11. Mean values plus or minus SEM are indicated.

Table 2.11. **Body composition and plasma levels of SR-A StARD5 transgenic mice on LDLR KO background**

		Male		Female	
Transgenic 11		**Wt**	**TG**	**Wt**	**TG**
Body Weight		26.1 +/- 0.5	26.1 +/- 1.1	20.9 +/- 0.3	20.6 +/- 0.5
(g)	***n*=**	*21*	*13*	*11*	*11*
Liver Weight		1.01 +/- 0.04	1.08 +/- 0.05	0.96 +/- 0.03	0.90 +/- 0.02
(g)	***n*=**	*21*	*13*	*11*	*11*
Plasma		593 +/- 42	487 +/- 56	801 +/- 50	688 +/- 51
Cholesterol (mg/dl)	***n*=**	*21*	*13*	*11*	*11*
HDL (mg/dL)		63 +/- 4	65 +/- 3	40 +/- 5	47 +/- 6
	***n*=**	*15*	*11*	*8*	*6*
LDL (mg/dL)		413 +/- 32	378 +/- 32	508 +/- 28	440 +/- 28
	***n*=**	*15*	*11*	*8*	*6*
VLDL (mg/dL)		74 +/- 7	69 +/- 13	226 +/- 31	164 +/- 28
	***n*=**	*15*	*11*	*8*	*6*
Triglycerides		136 +/- 18	94 +/- 14	99 +/- 17	91 +/- 14
(mg/dL)	***n*=**	*12*	*8*	*6*	*9*
Glucose (mg/dL)		148 +/- 12	121 +/- 12	107 +/- 7	116 +/- 8
	***n*=**	*7*	*7*	*4*	*5*

		Male		Female	
Transgenic 4		**Wt**	**TG**	**Wt**	**TG**
Body Weight		25.3 +/- 0.8	23.5 +/- 1.0	19.2 +/- 0.4	19.5 +/- 0.3
(g)	***n*=**	*9*	*8*	*11*	*8*
Liver Weight		1.01 +/- 0.05	0.98 +/- 0.06	0.81 +/- 0.04	0.87 +/- 0.04
(g)	***n*=**	*9*	*8*	*11*	*8*
Plasma		631 +/- 28	677 +/- 52	641 +/- 32	733 +/- 52
Cholesterol (mg/dl)	***n*=**	*8*	*8*	*11*	*8*
HDL (mg/dL)		64 +/- 8	55 +/- 4	43 +/- 4	49 +/- 4
	***n*=**	*5*	*7*	*11*	*7*
LDL (mg/dL)		438 +/- 27	449 +/- 36	392 +/- 22	467 +/- 25
	***n*=**	*5*	*7*	*11*	*7*
VLDL (mg/dL)		62 +/- 10	124 +/- 10	134 +/- 10	159 +/- 25
	***n*=**	*5*	*7*	*11*	*7*
Triglycerides		66 +/- 21	110 +/- 7	116 +/- 20	110 +/- 21
(mg/dL)	***n*=**	*8*	*8*	*11*	*8*
Glucose (mg/dL)		132 +/- 9	125 +/- 7	111 +/- 4	119 +/- 11
	***n*=**	*4*	*7*	*11*	*8*

All values are means +/- SEM, number of mice (N) is given for each value

Development of Transgenic Mice Over-Expressing Human StARD5 in Liver Using the ApoE Promoter

StARD5 was originally described as a liver expressed gene and it was assumed this meant parenchymal cell expression. Therefore, early in my thesis work I cloned the human StARD5 gene into the pLIV.7 vector so that expression was driven by the human ApoE enhancer/promoter which was known to produce high levels of transgene expression in liver parenchymal cells. I used this construction to create 4 transgenic founder lines. After I had begun to characterize them, Rodriguez and colleagues published convincing evidence for liver StARD5 expression in Kuppfer cells and not in parenchymal cells. Since I wanted to characterize the physiological functions of StARD5, I decided that the transgenic lines with liver parenchymal cell expression were not germane, so I abandoned these studies.

Preliminary work had been done on one of these transgenic lines (ApoEhStARD5-1). Quantitative PCR was used to show liver expression of human StARD5 (data not shown). The effect of the transgene was assessed on 3 different diets, the AIN76a diet containing 0.0% or 0.5% cholesterol and a chow diet. The protocol used was similar to the one described for the hStARD5 macrophage-specific transgenic mice. Wild-type and hStARD5 liver-parenchymal-cell-expressing transgenic mice at 6 weeks of age were placed on the AIN76a 0.0% cholesterol diet for one week. After this mice were either kept on the AIN76a 0.0%

cholesterol diet or switched to the AIN76a diet containing 0.5% cholesterol for one week and then sacrificed at 8 weeks of age. The chow diet group was kept on chow from weaning to 8 weeks of age. Comparison of wild-type and hStARD5 liver-parenchymal-cell-expressing transgenic mice showed little effect of the transgene on plasma cholesterol levels (Table 2.12). In males the transgene lowered triglyceride levels by 30% and 40% on the 0.0% and 0.5% cholesterol diets, respectively, without change on the chow diet. In females the transgene had no effect on triglyceride levels on any of the diets (Table 2.12). In addition, there were no changes in liver total, free or esterified cholesterol levels on the AIN76a 0.5% cholesterol and the chow diets of males (the livers of mice on the AIN76a 0.0% cholesterol diet were not analyzed). In males the transgene decreased gallbladder bile cholesterol concentration 43% on the AIN76a 0.5% cholesterol diet, with no change on the AIN76a 0.0% cholesterol diet and a 48% reduction on the chow diet (Table 2.12). In females the transgene decreased gallbladder bile cholesterol concentration 30% on the AIN76a 0.5% cholesterol diet, with no change on the AIN76a 0.0% cholesterol diet and a 38% reduction on the chow diet. Both males and females had a 31% reduction in gallbladder bile phospholipid concentrations on the AIN76a 0.5% cholesterol diet, but no change on the chow diet (the phospholipids levels of mice on the AIN76a 0.0% cholesterol diet were not analyzed) (Table 2.12). On a chow diet, the transgene decreased gallbladder bile acid concentration 28% in males, but had no change in females (the bile acid

concentrations of mice on the AIN76a 0.0% or 0.5% cholesterol diet were not analyzed). In view of the findings of Rodriguez and colleagues (Rodriguez-Agudo et al., 2006), the findings in this one founder family were not followed up in the other founder families. Therefore, we do not know if they are gene-specific or due to off-target transgene insertional effects. With this caveat, the data suggest ectopic StARD5 expression in parenchymal cells is capable of sequestering cholesterol and preventing its movement into the bile.

Table 2.12. **Plasma, hepatic, and gallbladder bile levels of ApoEhStARD5-1 transgenic mice fed the indicated diets**

		Male		Female	
ApoEhD5-1		**Wt**	**TG**	**Wt**	**TG**
Plasma	0.5% Cholesterol	84 +/- 8	85 +/- 9	66 +/- 4	65 +/- 2
	n=	*7*	*7*	*8*	*7*
Cholesterol	0.0% Cholesterol	74 +/- 5	83 +/- 7	68 +/- 4	59 +/- 4
	n=	*5*	*6*	*3*	*3*
	Chow	78 +/- 4	89 +/- 7	63 +/- 5	65 +/- 4
(mg/dl)	*n*=	*9*	*7*	*6*	*13*
	0.5% Cholesterol	41 +/- 4	40 +/- 4	28 +/- 1	25 +/- 1
	n=	*7*	*7*	*8*	*7*
HDL (mg/dL)	0.0% Cholesterol	47 +/- 5	51 +/- 4	38 +/- 1	32 +/- 4
	n=	*5*	*6*	*3*	*3*
	Chow	36 +/- 2	37 +/- 2	25 +/- 2	25 +/- 2
	n=	*9*	*7*	*6*	*12*
Triglycerides	0.5% Cholesterol	45 +/- 5	27 +/- 1*	28 +/- 2	26 +/- 2
	n=	*7*	*7*	*8*	*7*
	0.0% Cholesterol	55 +/- 2	38 +/- 4*	23 +/- 3	25 +/- 3
	n=	*5*	*6*	*3*	*3*
	Chow	51 +/- 5	44 +/- 5	45 +/- 6	36 +/- 3
(mg/dL)	*n*=	*9*	*7*	*6*	*13*

All values are means +/- SEM, number of mice (N) is given for each
* indicates p values < 0.05, ND indicates values not determined

Table 2.12. **Plasma, hepatic, and gallbladder bile levels of ApoEhStARD5-1 transgenic mice fed the indicated diets**

		Male		Female	
ApoEhD5-1		**Wt**	**TG**	**Wt**	**TG**
Liver Total Cholesterol (mg/g)	0.5% Cholesterol *n*=	10.3 +/- 0.4 *3*	10.3 +/- 0.4 *3*	ND	ND
	Chow *n*=	3.7 +/- 0.2 *3*	3.8 +/- 0.5 *3*	ND	ND
Liver Free Cholesterol (mg/g)	0.5% Cholesterol *n*=	6.9+/-0.5 *3*	8.1 +/- 0.6 *3*	ND	ND
	Chow *n*=	3.2 +/- 0.3 *3*	3.1 +/- 0.4 *3*	ND	ND
Liver Cholesterol Ester (mg/g)	0.5% Cholesterol *n*=	3.5 +/- 0.2 *3*	2.3 +/- 0.7 *3*	ND	ND
	Chow *n*=	0.6 +/- 0.3 *3*	0.7 +/- 0.3 *3*	ND	ND
Liver Triglycerides (mg/g)	0.5% Cholesterol *n*=	42 +/- 5 *3*	55 +/- 6 *3*	ND	ND
	Chow *n*=	130 +/- 9 *3*	113 +/- 4 *3*	ND	ND
Bile Cholesterol (mg/dL)	0.5% Cholesterol *n*=	320 +/- 35 *6*	181 +/- 19* *7*	271 +/- 20 *7*	189 +/- 14* *6*
	0.0% Cholesterol *n*=	66 +/- 11 *5*	80 +/- 18 *4*	110 +/- 13 *3*	77 +/- 18 *3*
	Chow *n*=	129 +/- 14 *8*	68 +/- 7* *7*	156 +/- 15 *6*	98 +/- 4* *13*
Bile Phospholipid (mg/dL)	0.5% Cholesterol *n*=	2048 +/- 170 *6*	1396 +/- 189* *7*	2692 +/- 142 *7*	1856 +/- 258* *6*
	0.0% Cholesterol *n*=	ND	ND	ND	ND
	Chow *n*=	1933+/- 203 *8*	1403 +/- 124 *7*	1988 +/-241 *6*	1704 +/- 134 *13*
Bile Acids (mM)	Chow *n*=	75 +/- 8 *8*	54 +/- 6* *7*	67 +/- 7 *6*	68 +/- 4 *13*

All values are means +/- SEM, number of mice (N) is given for each
liver values are in mg/g liver
* indicates p values < 0.05, ND indicates values not determined

Expression of StARD5 in *Saccharomyces cerevisiae*

and Complementation Assays

The yeast is an excellent model organism for studying cell autonomous functions like intra-cellular lipid transport. Although the yeast genome does not encode START-domain containing proteins, yeast have been used to discover and characterize many genes for other types of lipid transporters. Yeast mutants deficient in many of these have been established, and we endeavored to determine if any of those deficient in sterol transport might be complemented by StARD5. If successful this would have been a powerful way to gain insight into StARD5 function. This work was done in collaboration with Steve Sturley's laboratory at Columbia University. A plasmid was constructed containing human StARD5 cDNA with an N-terminal GFP under the control of an inducible galactose promoter (pRS426) (gift from Sturley). This StARD5 expression vector was transfected into wild-type yeast grown in galactose and inducible expression of StARD5 was confirmed both by GFP levels in a fluorescence assay and StARD5 amount by Western-blotting analysis (Figure 2.13).

This StARD5 expression vector was transfected into the upc2.1 strain, which is a gain of function mutant for the transcription factor regulating the ATP-binding cassette transporters AUS1 and PDR11. The expression of these transporters allows sterol influx to occur under aerobic conditions. If StARD5 was capable of promoting cholesterol efflux from yeast, we were hoping its expression might

diminish yeast sterols and alter the lipid profile, but this did not occur. Similarly the arv1 yeast strain contains a temperature sensitive mutation in a putative sterol transporter that moves sterols from the ER to the Golgi. At the inactivation (restrictive) temperature the ER accumulates excess free sterols and the ER stress response is triggered. If StARD5 was able to move cholesterol from the ER to the Golgi we might have expected the arv1 strain to be rescued from the ER stress response. However, transfection of the StARD5 expression plasmid had no effect as evidenced by continued expression of Hac1, the yeast ATF homolog.

	1	2	3	4	5	6	7	8
Galactose	-	-	+	+	-	-	+	+
Glucose	+	+	-	-	+	+	-	-

Figure 2.13. **Expression of hStARD5-GFP in wildtype yeast**. Western blot of yeast showing galactose-inducible expression of GFP-hStARD5 (anti-GFP antibody). 10ug protein used. Protein bands are approximately 52kDa, which is the expected size of the fusion of StARD5 and GFP. Lane 1-4 Control Plasmid; Lane 5-8 hStARD5-GFP transformed cells. Lane1-2, 5-6 cells grown in glucose; Lane 3-4, 7-8 cells grown in galactose.

We were about to test other yeast mutants for complementation with StARD5 when Rodriguez and colleagues published a paper showing that StARD5 bound cholesterol and 25-hydroxycholesterol, but not 27-hydoxycholesterol, 24-hydroxycholesterol, 24,25-hydroxycholesterol, 7alpha-hydroxycholesterol, beta-sitosterol, or cholic acid. The unexpected (at least to us) specificity with which StARD5 bound sterols made us reconsider our work in yeast, which has ergosterol as its major sterol. Although ergosterol is synthesized, regulated, and esterified

in yeast in a manner similar to the way cholesterol is metabolized in mammals, ergosterol is structurally different from cholesterol in that it has two additional double bonds at C7 and C22, plus an additional methyl group at C24 (Figure 2.14). These differences would most likely prevent StARD5 from binding ergosterol. This would explain our negative complementation results with the upc2.1 and arv1 yeast strains, and strongly suggest that any similar effort to complement other yeast mutants with defective ergosterol transport would also be fruitless. This realization caused us to abandon our efforts to determine StARD5 function by yeast complementation studies.

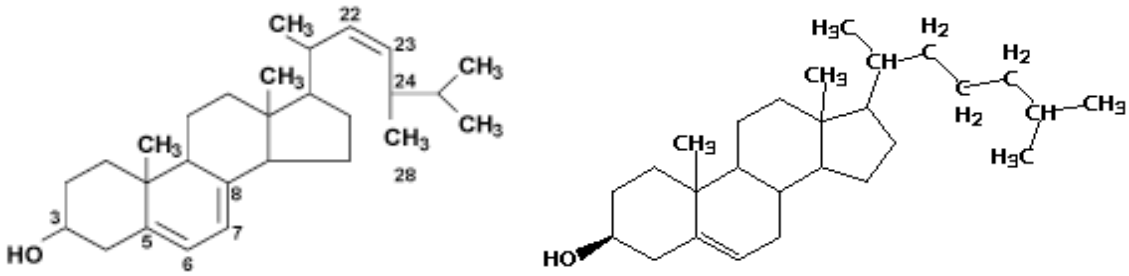

Figure 2.14 **Structure of ergosterol and cholesterol**.
Ergosterol (left) differs structurally from cholesterol (right) with two additional double bonds at C7 and C22, along with an additional methyl group at C24.

Summary

This chapter describes our studies attempting to determine the physiological functions of StARD5 *in vivo* through the creation and study of a knockout mouse and two different transgenic mice. With the knockout, we demonstrated that StARD5 is essential for the early development of mouse embryos, but that haploinsufficiency does not alter plasma cholesterol or triglyceride levels, liver cholesterol levels, gallbladder bile composition, glucose tolerance, cholesterol efflux from macrophages or atherosclerosis susceptibility. In addition, tissue-specific transgenic over-expression of human StARD5 in macrophages had no effect on plasma cholesterol or triglyceride levels, liver cholesterol levels, gallbladder bile composition, cholesterol efflux from macrophages or atherosclerosis susceptibility. Moreover, although StARD5 is normally expressed in liver Kuppfer cells, inappropriate transgenic over expression in liver parenchymal cells lowered plasma triglyceride levels and decreased gallbladder bile cholesterol, phospholipids, and bile acids concentration. Finally, in yeast complementation assays human StARD5 failed to complement two mutant yeast strains with defects in sterol transport, probably because StARD5 fails to transport ergosterol.

Chapter 3: Characterization of ADAM11

Background

One of the goals of our laboratory is to understand diet responsiveness. In this regard, Soccio and colleagues undertook an experiment to feed low and high cholesterol diets to C57BL/6J mice to determine which genes were regulated by dietary cholesterol. At the time of his experiments the only gene expression array available to our laboratory was a cDNA array displaying a few thousand genes. Several years later with availability of commercial oligonucleotide microarrays displaying sequences corresponding to most genes, this experiment was repeated with minor modifications by Maxwell and colleagues (Maxwell et al., 2003). C57BL/6 mice at 6 weeks of age were placed on the AIN76a 0.0% cholesterol diet for one week. After this, mice were either kept on the AIN76a 0.0% cholesterol diet or switched to the AIN76a diet containing 0.5% cholesterol for one week and then all of the mice were sacrificed at 8 weeks of age. Under these conditions compared to the AIN76a 0.0% cholesterol diet the AIN76a 0.5% cholesterol diet increased liver total, free and esterified cholesterol. Liver RNA was isolated and gene expression assessed by Affymetrix microarrays MGU74v2. There were 69 dietary cholesterol regulated gens, 39 down-regulated (including StARD4 as seen in the earlier study by Soccio) and 32 up-regulated. One of the relatively novel up-regulated genes was ADAM11, and this is the second gene studied in depth as part of this thesis.

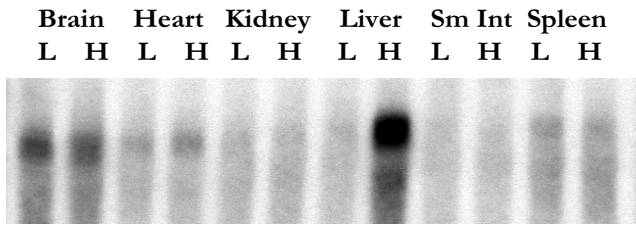

Figure 3.1. **ADAM11 mRNA is regulated by sterol levels**. (From K.Maxwell) Northen blot of RNA from multiple tissues pooled from male C57Bl6 mice fed a Low Cholesterol (L) (0.0%) diet or a high cholesterol (H) (0.5%) cholesterol diet. Blots were probed with ADAM11A 3ütr.

In previous work Maxwell had shown that ADAM11 up-regulation by dietary cholesterol was only in liver and not in other tissues (Figure 3.1). In vivo she showed that injection into mice of the LXR agonist T0901317 increased ADAM11 mRNA, confirming ADAM11 as an LXR target gene. Rybnikova and colleagues had previously shown ADAM11 expression in liver parenchymal cells of mice (Rybnikova et al., 2002). The role of ADAM11 in the liver is unknown, although it is tempting to speculate it might be involved in reverse cholesterol transport, since it is up-regulated by cholesterol feeding and is an LXR target gene as are many others in this pathway. This thesis attempts to understand ADAM11 function by generating an ADAM11 conditional knockout (cKO) mouse and characterizing it metabolically, as well as creating an ADAM11 adenovirus to study the consequences of over-expression of ADAM11 in the liver in vivo.

The Targeted Disruption of ADAM11

In order to allow the gene to be inactivated in a tissue- or temporal-specific fashion, a strategy was undertaken to create an ADAM11 cKO mouse. The ADAM11 gene contains 26 or 27 exons (see next paragraph) and is located on

mouse chromosome 11. A BAC clone encompassing the ADAM11 locus was obtained from a C57BL/6 genomic library (BacPac Resources, RP24-166M9). Utilizing the recombineering techniques described by Copeland and colleagues (Liu et al., 2003), a targeting vector was constructed in the MC1-TK-containing plasmid with a loxP site in ADAM11 intron 11 and an Frt-Pgk-em7-Neo-Frt-loxP cassette in ADAM11 intron 18 (Figure 3.2). The MC1-TK cassette was used for negative selection against random integration events, while the Neo cassette allowed for positive selection. The Neo floxed allele of the ADAM11 gene was generated through homologous recombination in isogenic mouse ES cells. Twelve correctly targeted ES clones were identified by Southern blotting using BamHI or EcoRV restriction digest of genomic DNA and external 5'or 3'probes, respectively, that were not part of the targeting vector. Five ES cell clones were expanded and injected into blastocysts to produce chimeras, but only one (#138) led to germ-line transmission.

Like other members of the ADAM family, ADAM11 is a multi-domain protein (see Chapter 1)(Figure 3.3). Two alternatively spliced isoforms of ADAMm11 mRNA exist: one expressed primarily in brain, and the other predominantly in liver. These isoforms share the first 25 exons and differ only in their C-terminal cytoplasmic tails. The liver form of ADAM11, ADAM11a, is a 778 amino acid protein encoded by 26 exons, whereas the brain form of ADAM11, ADAM11b, is a 773 amino acid protein encoded by 27 exons. ADAM11 exons 1-7 encode the prodomain, exons 8-15

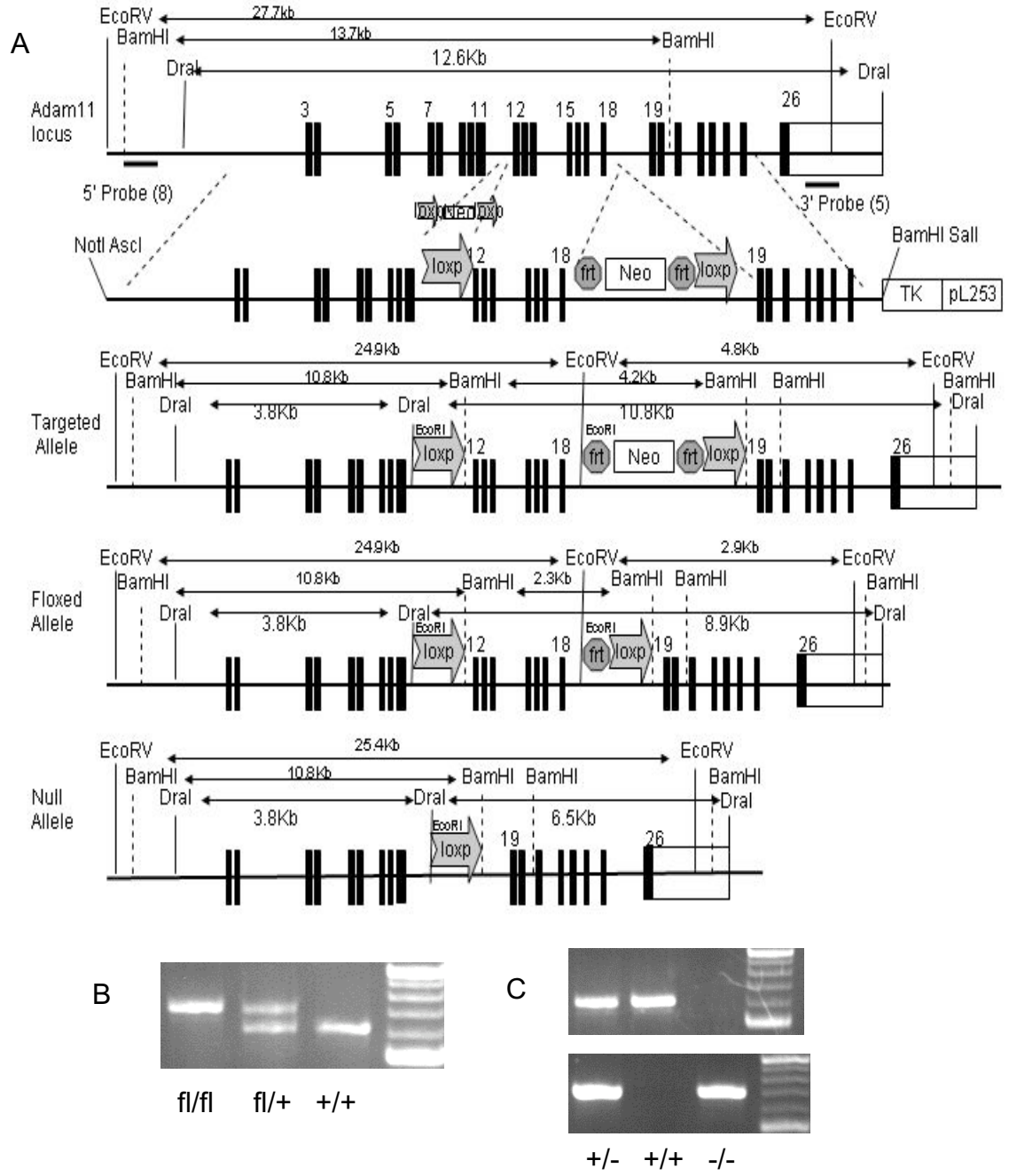

Figure 3.2. **Gene targeting and generation of a conditional knockout (floxed) allele of the ADAM11 gene**. A) Targeting strategy to flank exon 12 through exon 18 of ADAM11 with loxP sites. The targeting vector was constructed by placing a Neo selectable marker flanked by Frt sites with a loxP site. A second loxP site was introduced in intron 11. B) PCR analysis in order to determine the presence of the wildtype and/or floxed alleles in heterozygous (fl/+), homozygous mutants (fl/fl) as well as wildtype controls. C) PCR analysis in order to determine the presence of the wildtype (top) and/or null allele(bottom) in in heterozygous (+/-), homozygous mutants (-/-) as well as wildtype (+/+) controls.

encode the inactive metalloprotease domain, exons 15-18 encode the disintegrin domain, exons 18-23 encode the cysteine-rich domain, exons 23-24 encode the EGF-like domain, exons 24-25 encode the transmembrane domain, and exons 25-26 (ADAM11a) or exons 25-27 (ADAM11b) encode the cytoplasmic tail. We undertook to knockout exons 12 to 18 by flanking these exons with loxP sites and using Cre-recombinase to remove them, thus deleting coding sequences for much of the metalloprotease domain and the entire disintegrin domain. In addition, splicing of exon 11 to either exons 19, 20 or 21 would be out of frame and result in

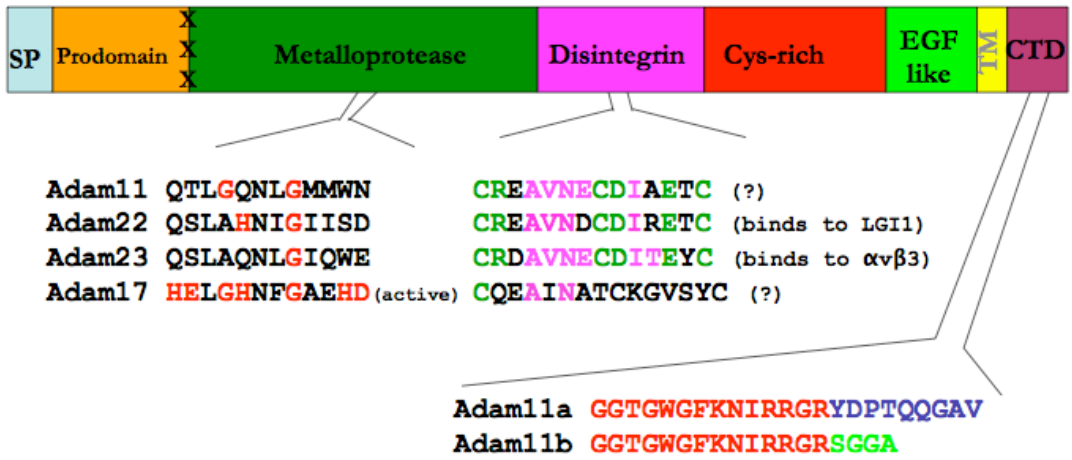

Figure 3.3. **Domain structure of ADAM11**. Mouse ADAM11 protein is made up of a signal peptide (SP), a pro-domain, a metalloprotease domain, a disintegrin domain, a cysteine-rich domain, an EGF-like domain, a single transmembrane domain, and a cytoplasmic C-terminal domain (CTD). ADAM11 (along with its subfamily members ADAM22 and ADAM23) does not contain the conserved histine residues (H) within the metalloprotease domain that are necessary for protease activity. ADAM11 contains a similar potential integrin binding loop as ADAM22 and ADAM23. There are two transcripts of ADAM11: A and B, which differ at their C-terminal ends. Exons 1-7 encode the signal peptide and pro-domain; exons 8-15 encode the metalloprotease domain; exons 15-18 encode the disintegrin domain; exons 18-23 encode the cysteine-rich domain, exons 23-24 encode the EGF-like domain, exons 24-25 encode the transmembrane domain, and exons 25-26(A) or 25-27(B) encode the cytoplasmic domain.

termination codons. The possible splicing of exon 11 to either exons 22 or 23 would be in frame, however, the proteins encoded would also be missing the cysteine-rich domain, which is thought to provide protein stability.

Viability, Fertility, and Fecundity in the ADAM11 cKO Mice

After detection of germ-line transmission of the targeted allele, brother-sister mating of ADAM11 heterozygous cKOs with the Neo floxed allele was carried out and yielded offspring with genotypes compatible with the expected Mendelian pattern of inheritance. The ADAM11 homozygous Neo floxed cKO mice produced were viable, grew normally. Next, the ADAM11 cKO mice heterozygous for the Neo floxed allele were bred to C57BL/6 ACT-FLPe transgenic mice, which efficiently removed the Neo cassette from the ADAM11 gene (Figure 3.2). Again, brother-sister mating of ADAM11 heterozygous cKOs with the floxed allele was carried out and yielded offspring with genotypes compatible with the expected Mendelian pattern of inheritance. The ADAM11 homozygous floxed cKO mice produced were viable, grew normally, and were fertile. Finally, the ADAM11 cKO mice heterozygous for the floxed allele were bred to C57BL/6 CMV-Cre transgenic mice, which efficiently removed exons 12-18 from the ADAM11 gene leaving in their place a single loxP site (Figure 3.2). Again, brother-sister mating of ADAM11 heterozygous cKOs with the null allele was carried out and yielded offspring with genotypes compatible with the expected Mendelian pattern of inheritance (Table 3.1). The ADAM11 homozygous null cKO mice produced were viable, grew

Table 3.1. **Fertility and Fecundity of ADAM11cKO Mice**

Floxed	**wt:het:homo**	**litter size (mean +/- SD)**
Male +/fl x Female +/fl	14:23:14	6.4 +/- 2.0
Deleted		
Male +/- x Female +/-	17:28:15	6.6 +/- 1.5

normally, and were fertile, indicating that the ADAM11 gene is not essential for survival or normal development.

ADAM11 protein levels were examined by Western-blotting in the brain of ADAM11 heterozygous and homozygous cKO null mice and compared to wild-type mice found to be about half normal in the former and absent in the latter. A similar analysis of ADAM11 heterozygous and homozygous cKO floxed mice showed normal levels of ADAM11 protein; the latter indicating that the loxP sites in introns 11 and 18 do not interfere with proper splicing and protein synthesis (Figure 3.4) (Figure 3.5).

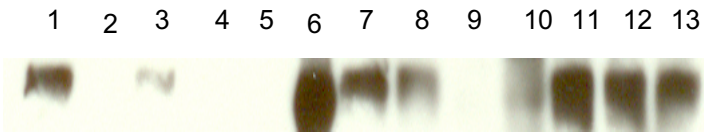

Figure 3.4. **Western blot of brains of ADAM11 mice.**
Absence of ADAM11 protein in the knockout brain was shown using anti-ADAM11 monoclonal antibody. Comparison of the Takahashi null mutant and the full knockout developed in our lab. Expression is detected in our homozygous floxed allele, but not in the full knockout or in the Takahashi null mutant. Expression of ADAM11 in the heterozygote KO is approximately half the levels of wildtype mice,
Lane 1) Homozygous Floxed, 2) Takahashi null mutant, 3) Takahashi heterozygote mutant,
4) Takahashi null mutant, 5) Empty, 6) ADAM11 recombinant protein,
7) Wildtype, 8) Heterozygote KO, 9) Homozygote KO, 10) Heterozygote KO, 11) Wildtype,
12) Heterozygote Floxed, 13) Homozygote Floxed.
Brain homogenate was processed via ConA Sepharose 4B treatment. 25ug of protein from brain was was added in each lane, equal and proper transfer was confirmed by Ponceau staining.

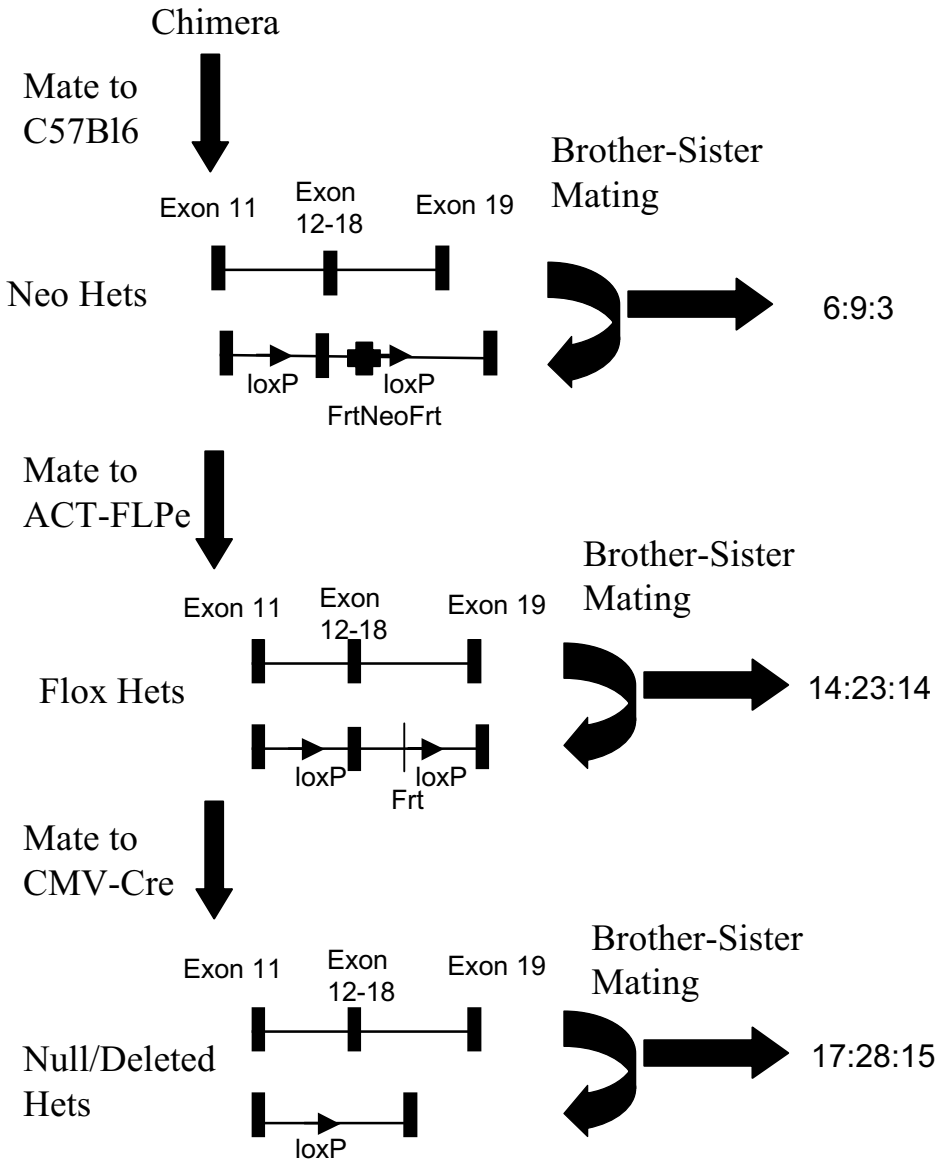

Figure 3.5. **Mating strategy in generation of the ADAM11 knockout**.
Chimera mice were mated to C57Bl6 to generate Neo heterozygotes. These Neo heterozygotes were brother-sister mated in an attempt to generate Neo homozygotes. The Neo heterozygotes were also mated to the ACT-FLPe transgenic mice to remove the FrtNeoFrt cassette and to generate Flox heterozygotes. These Flox heterozygotes were brother-sister mated in an attempt to generate Flox homozgotes. The Flox heterozygotes were mated to CMV-Cre transgenic mice to remove exon 12-18 and to generate Null/Deleted heterozygotes. These Null heterozygotes were brother-sister mated in an attempt to generate Null homozygotes. Results of the brother-sister matings are indicated on the right; the order is wildtype:heterozygotes:homozygotes. Results of the matings followed Mendellian laws. Rectangles represent exons, triangles represents loxP sites, cross represents the FrtNeoFrt cassette, line vertical line represents Frt site, arrows represent matings.

Full Knockout of ADAM11 has a Neurologic Phenotype

ADAM11 was originally identified as a gene highly expressed in the CNS of the adult mouse by Sagane and colleagues (Sagane et al., 1998; Sagane et al., 1999). Rybnikova and colleagues further showed the spatiotemporal expression pattern of the ADAM11 gene in adult mice and during development, and identified the cells expressing the gene (Rybnikova et al., 2002). In the adult CNS, ADAM11 mRNA was present throughout the forebrain, including different cortical fields and diencephalic nuclei (Rybnikova et al., 2002). In brainstem, low to moderate expression was detected in certain midbrain nuclei, while several pontine and medullary nuclei showed a very strong signal (Rybnikova et al., 2002). High expression was observed in the cerebellar cortex and spinal cord. In addition, ADAM11 was expressed in ganglia of the peripheral nervous system (PNS), retina, testes, liver, and at lower levels in epidermal and mucosal epithelia, kidney, and salivary gland (Rybnikova et al., 2002). Expression occurred only in neurons in all examined CNS and PNS subfields.

In parallel with our work, Takahashi and colleagues also developed an ADAM11 knockout mouse. Their main objective was to understand the physiological role of ADAM11 in the brain. Their knockout strategy consisted of introducing a stop codon in exon 5 and replacing exon 6 with a Neo cassette by homologous recombination, thereby creating a null gene (Takahashi et al., 2006a; Takahashi et al., 2006b). In agreement with our findings, they found ADAM11

homozygous knockout mice to be viable, grow normally, and be fertile. They also showed that at autopsy ADAM11 homozygous knockout mice had no anatomical or histological abnormalities (Takahashi et al., 2006a; Takahashi et al., 2006b). Because ADAM11 is highly expressed in the hippocampus and cerebellum, Takahashi and colleagues examined ADAM11 homozygous knockout mice for learning using visual and hidden water maze tasks, and motor coordination using a rotating rod task (Takahashi et al., 2006a; Takahashi et al., 2006b). They showed that while the mice performed normally in the visual water maze task, they had deficits in the hidden water maze, suggesting a deficit in spatial learning (Takahashi et al., 2006a; Takahashi et al., 2006b). The mice also had impairments in the rotating rod task, while exhibiting normal grip strength, suspension from a wire, and walking, suggesting ADAM11 knockout mice have a CNS deficit in motor coordination, but not muscle weakness or other PNS deficits. Further testing showed these mice to have normal responses to stimuli in the von Frey and hot plate tests, but reduced responses to the formalin paw test and acetic acid writhing test, suggesting ADAM11 may also play a role in pain transmission and perception (Takahashi et al., 2006a; Takahashi et al., 2006b).

The mice created by Takahashi and colleagues were available for study prior to our ADAM11 cKO mice, and they generously provided them to us. It is their mice that were used for the functional studies presented in this thesis. When we received them, their mice, originally created using strain 129 ES cells, had undergone 14

generations of backcrossing to the C57BL/6 background. However, to ensure a pure C57BL/6 background, especially necessary for atherosclerosis studies, the mice were backcrossed to C57BL/6 another 4 times, and then genotyped by microsatellite and SNP analysis and confirmed to be (over 99.5% C57BL/6).

ADAM11 Knockout has Absence-like Seizures

As described in Chapter 1, ADAM11 is the closest paralog of ADAM22 and ADAM23. Deletion of either ADAM22 or ADAM23 results in severe seizures and peri-natal death, but ADAM11 null mice appear to develop normally and do not exhibit an overt seizure phenotype. However, because of structural similarity between these genes a more careful examination for seizure activity was performed by doing an electroencephalograph (EEG) on ADAM11 knockout mice. In collaboration with Dr. Noebels at Baylor University, 3 ADAM11 knockout males and 2 wild-type male siblings at approximately 20 weeks of age were examined. The EEG results showed a major change in background rhythms of the knockout mice, with most of the power in the 5-6Hz or theta range, while no faster activity (beta or alpha) was detected. This could explain the impairments in memory and exploration-related behaviors. ADAM11 knockout mice also exhibited constant cortical discharges and frequent (approximately 1/hour) non-convulsive seizures, indicative of absence-like epilepsy (Figure 3.6).

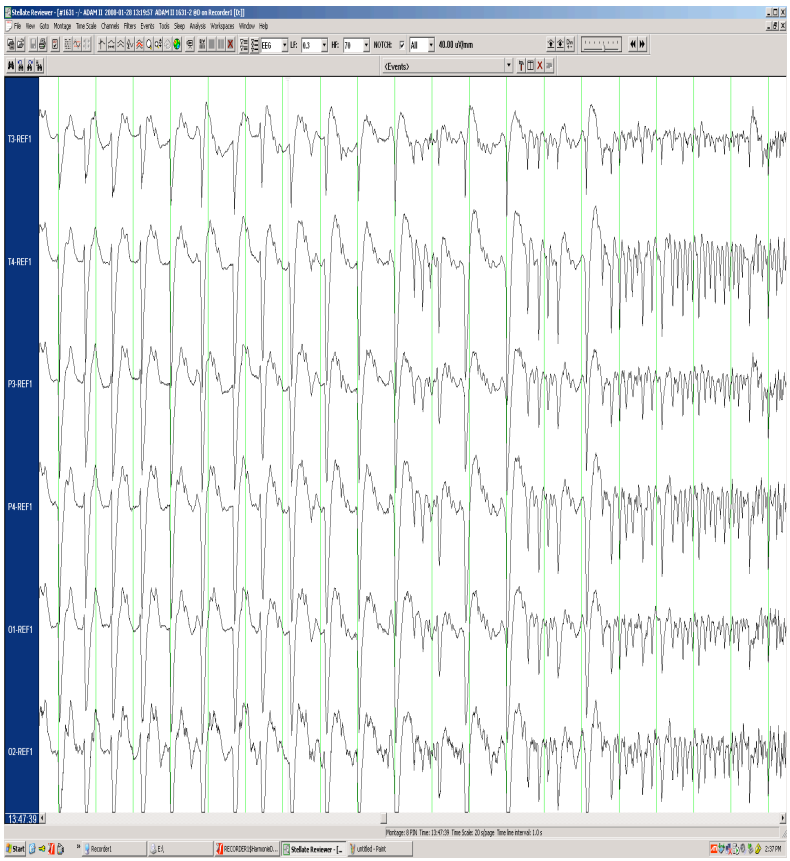

Figure 3.6. **EEG Analysis of ADAM11 mice**.
ADAM11 mutant mice display absence-like epilepsy and altered brain wave activity. Power is in the 5-6Hz or theta range, with no fasterr activity (alpha or beta waves). Mice also exhibited constant cotical discharges and frequent (1/hour) non-convulsive seizures.
(J.Noebels, Baylor, Texas).

Fear Conditioning Testing

The hippocampus and amygdala are responsible for regulating the body's responses to stress. Contextual fear depends on hippocampus and amygdale, whereas cued fear depends on the amygdala. ADAM11 knockout and wild-type mice (eight to twelve mice of each gender and each genotype) were tested in a fear conditioning assay. As measured by the time the mouse spends frozen after a given stimulus, ADAM11 mice showed normal baseline fear, learned fear, contextual fear, and cued fear (Figure 3.7).

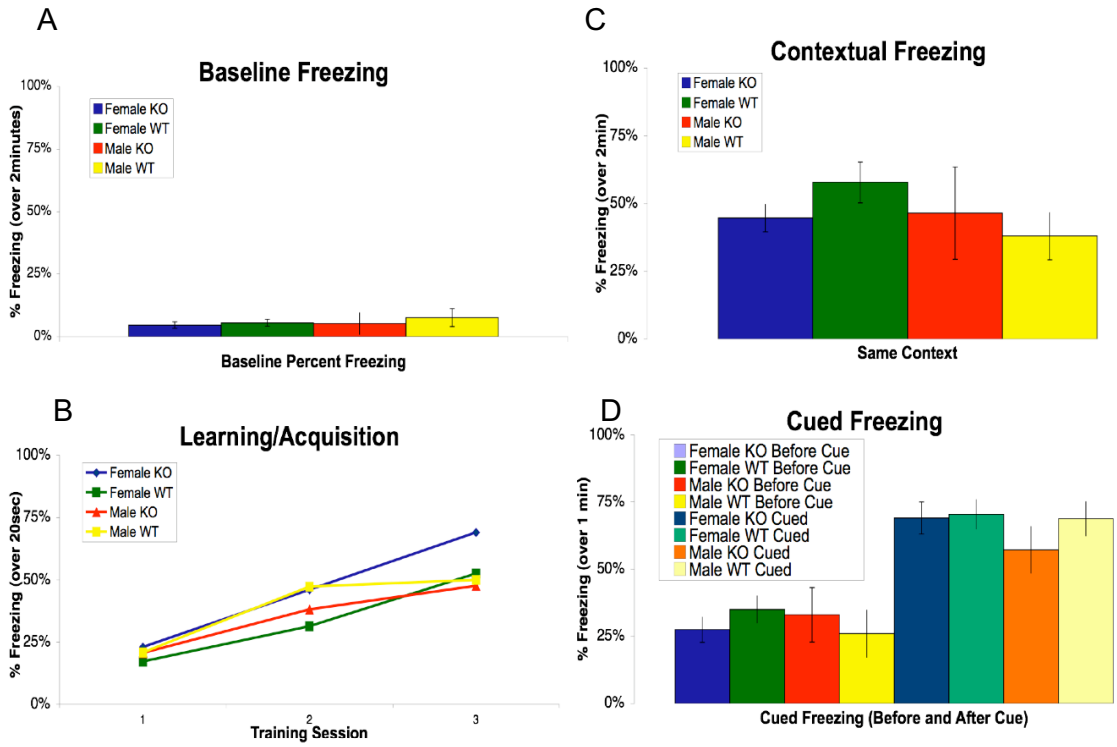

Figure 3.7. **Fear Conditioning of ADAM11 Mice.** (n=8-12 mice per gender and genotype). A) Initial baseline percent freezing over 2-minute interval, B) Learning Phase, percent freezing over 30-second interval after initial tone and before shock, C) Contextual Freezing, percent freezing over 2-minute interval after placement of mice in same context (same cage, same scent), D) Cued Freezing, percent baseline freezing (Before Cue) in new context (new cage, new scent) over 1-minute interval, and then percent freezing after cue (Cued) (same tone) over 1-minute interval. Values are means of percent freezing plus or minus SEM.

The Dietary Feeding Paradigms of ADAM11 Knockout Mice

Experiments were undertaken to determine the effect of ADAM11 deficiency on lipid and glucose homeostasis. Wild-type and ADAM11 heterozygous and ADAM11 homozygous knockout mice at 6 weeks of age were placed on the AIN76a 0.0% cholesterol diet for one week. These mice were then either kept on the AIN76a 0.0% cholesterol diet or switched to either the AIN76a diet containing 0.5% cholesterol or the AIN76a diet containing 0.5% cholic acid for one week. At 8 weeks of age measurements were made and the mice sacrificed. In confirmation of the previous study by Maxwell, wild-type mice did respond to one week of high cholesterol feeding by increasing liver levels of ADAM11 mRNA.

Pathology of ADAM11 Knockout Mice on the High Cholesterol Diet

There was no difference in body or liver weight between wild-type and ADAM11 heterozygous and homozygous knockout mice fed the three diets at 8 weeks of age (Table 3.2). The ADAM11 knockout mice on the AIN76a 0.5% cholesterol diet were autopsied by the Tri-Institutional Core Facility located at the MSKCC Pathology Department. Compared to wild-type litter-mates there were no apparent anatomical-histological differences observed in heart, lungs, esophagus, thymus, tongue, kidneys, pancreas, renal lymph nodes, spleen, salivary glands, stomach, duodenum, jejunum, ileum, colon, cecum, pancreas, brown fat, urinary bladder, thyroid glands, trachea, adrenal glands, liver, sciatic nerve, spinal cord, gallbladder, or brain.

Table 3.2. **Body composition of ADAM11 mice fed the indicated diets**

Male		**Wt**	**Het**	**Ko**
Mouse Weight (g)	**0.0% Cholesterol**	21.6 +/- 0.6	21.1 +/- 0.3	21.5 +/- 0.3
	***n*=**	*18*	*36*	*10*
	0.5% Cholesterol	22.4 +/- 0.3	22.7 +/- 0.2	21.8 +/- 0.5
	***n*=**	*38*	*61*	*28*
	0.5% Cholic Acid	20.6 +/- 0.4	21.7 +/- 0.4	20.4 +/- 0.4
	***n*=**	*10*	*17*	*14*
Liver Weight (g)	**0.0% Cholesterol**	1.07 +/- 0.04	1.02 +/- 0.02	1.10 +/- 0.04
	***n*=**	*18*	*36*	*10*
	0.5% Cholesterol	1.15 +/- 0.02	1.19 +/- 0.02	1.17 +/- 0.03
	***n*=**	*38*	*61*	*28*
	0.5% Cholic Acid	1.08 +/- 0.04	1.09 +/- 0.02	1.02 +/- 0.03
	***n*=**	*10*	*17*	*14*
Female		**Wt**	**Het**	**Ko**
Mouse Weight (g)	**0.0% Cholesterol**	16.7 +/- 0/4	16.7 +/- 0.3	17.7 +/- 0.6
	***n*=**	*16*	*22*	*6*
	0.5% Cholesterol	17.2 +/- 0.2	17.4 +/- 0.2	17.6 +/- 0.3
	***n*=**	*25*	*75*	*25*
	0.5% Cholic Acid	17.7 +/- 0.3	16.7 +/- 0.4	16.9 +/-0.5
	***n*=**	*8*	*21*	*6*
Liver Weight (g)	**0.0% Cholesterol**	0.83 +/- 0.03	0.83 +/- 0.03	0.85 +/- 0.06
	***n*=**	*16*	*22*	*6*
	0.5% Cholesterol	0.94 +/- 0.02	0.94 +/- 0.01	0.98 +/- 0.02
	***n*=**	*25*	*75*	*25*
	0.5% Cholic Acid	0.92 +/- 0.04	0.87 +/- 0.03	0.90 +/- 0.05
	***n*=**	*8*	*21*	*6*

All values are means +/- SEM, number of mice (N) is given for each value

Effect of ADAM11 Deficiency on Plasma Total, HDL and LDL Cholesterol, Free Cholesterol, Triglycerides, Glucose, ALT and Plant Sterol Levels

There were no differences between wild-type, ADAM11 heterozygous knockout, and ADAM11 homozygous knockout mice of each gender fed the three diets in plasma total, HDL and LDL cholesterol, free cholesterol, triglycerides, glucose, and ALT levels (Table 3.3).

Levels of plant sterols were compared in wild-type and ADAM11 homozygous knockout mice fed the AIN76a 0.5% cholesterol diet. ADAM11 deficiency in mice of each gender had no effect on plasma levels of total, free or esterified brassicasterol, campesterol, or sitosterol, with the exception in male mice of a 20% decrease in free campesterol. ADAM11 deficiency had no effect on total lathosterol levels (Table 3.4).

Mice fed the AIN76a 0.5% cholic acid diet had a modest increase in plasma levels of ALT, but this was independent of genotype (data not shown).

Blood Amino Acid Levels

Blood levels of the amino acids alanine, arginine, asparagine, aspartic acid, glutamic acid, glutamine, histidine, isoleucine, leucine, methionine, phenylalanine, proline, serine, threonine, tryptophan, tyrosine, valine, as well as ornithine and citrulline did not differ between wild-type and ADAM11 homozygous knockout mice fed the AIN76a 0.5% cholesterol diet (data not shown).

Table 3.3. **Plasma levels of ADAM11 mice fed the indicated diets**

Male		Wt	Het	Ko
Triglycerides	**0.0% Cholesterol**	42 +/- 3	29 +/- 3	45 +/- 3
	***n*=**	*16*	*31*	*8*
	0.5% Cholesterol	33 +/- 2	32 +/- 1	34 +/- 2
	***n*=**	*27*	*50*	*21*
	0.5% Cholic Acid	31 +/- 9	38 +/- 12	29 +/- 5
(mg/dL)	***n*=**	*3*	*3*	*5*
Total Cholesterol	**0.0% Cholesterol**	84 +/- 4	85 +/- 3	79 +/- 8
	***n*=**	*18*	*36*	*9*
	0.5% Cholesterol	89 +/- 3	87 +/- 2	91 +/- 4
	***n*=**	*27*	*50*	*21*
	0.5% Cholic Acid	73 +/- 6	88 +/- 8	77 +/- 4
(mg/dL)	***n*=**	*5*	*7*	*9*
	0.0% Cholesterol	54 +/- 3	55 +/- 2	55 +/- 6
	***n*=**	*18*	*36*	*9*
HDL (mg/dL)	**0.5% Cholesterol**	47 +/- 2	48 +/- 1	48 +/- 2
	***n*=**	*27*	*50*	*21*
	0.5% Cholic Acid	28 +/- 4	34 +/- 2	28 +/- 2
	***n*=**	*5*	*7*	*9*
	0.0% Cholesterol	23 +/- 1	23 +/- 1	20 +/- 2
	***n*=**	*18*	*36*	*9*
LDL (mg/dL)	**0.5% Cholesterol**	30 +/- 2	30 +/- 2	30 +/- 2
	***n*=**	*27*	*49*	*21*
	0.5% Cholic Acid	36 +/- 1	42 +/- 6	36 +/- 3
	***n*=**	*5*	*7*	*9*
	0.0% Cholesterol	2 +/- 1	3 +/- 1	3 +/- 1
	***n*=**	*12*	*19*	*6*
VLDL (mg/dL)	**0.5% Cholesterol**	7 +/-2	6 +/- 1	7 +/- 1
	***n*=**	*9*	*14*	*5*
	0.5% Cholic Acid	8 +/- 1	7 +/- 1	7 +/- 1
	***n*=**	*5*	*7*	*9*
non-HDL	**0.0% Cholesterol**	30 +/- 2	30 +/- 2	25 +/- 2
	***n*=**	*18*	*36*	*9*
(calculated)	**0.5% Cholesterol**	45 +/- 3	39 +/- 2	43 +/- 3
	***n*=**	*27*	*50*	*21*
	0.5% Cholic Acid	43 +/- 3	53 +/- 7	48 +/- 5
(mg/dL)	***n*=**	*5*	*7*	*9*
Free Cholesterol	**0.5% Cholesterol**	14.9 +/- 0.5	ND	15.0 +/- 0.7
(mg/dL)	***n*=**	*16*		*16*
Glucose	**0.5% Cholesterol**	177 +/- 16	ND	182 +/- 11
mg/dL	***n*=**	*4*		*5*

All values are means +/- SEM, number of mice (N) is given for each value
ND indicates not determined

Table 3.3. *(cont.)* **Plasma levels of ADAM11 mice fed the indicated diets**

Female		Wt	Het	Ko
Triglycerides	**0.0% Cholesterol**	32 +/- 2	32 +/- 3	33 +/- 3
	***n*=**	*13*	*18*	*4*
	0.5% Cholesterol	25 +/- 2	26 +/- 1	26 +/- 2
	***n*=**	*14*	*44*	*15*
	0.5% Cholic Acid	35 +/- 6	30 +/- 4	30 +/- 5
(mg/dL)	***n*=**	*4*	*6*	*3*
Total Cholesterol	**0.0% Cholesterol**	67 +/-3	68 +/- 3	70 +/- 6
	***n*=**	*16*	*22*	*6*
	0.5% Cholesterol	69 +/- 3	76 +/- 3	79 +/- 4
	***n*=**	*14*	*46*	*15*
	0.5% Cholic Acid	57 +/- 6	72 +/- 11	52 +/- 4
(mg/dL)	***n*=**	*5*	*10*	*3*
HDL (mg/dL)	**0.0% Cholesterol**	43 +/- 2	43 +/- 2	45 +/- 3
	***n*=**	*15*	*22*	*6*
	0.5% Cholesterol	33 +/- 2	34 +/- 1	33 +/-2
	***n*=**	*14*	*46*	*14*
	0.5% Cholic Acid	25 +/- 2	23 +/- 2	23 +/- 2
	***n*=**	*5*	*10*	*3*
LDL (mg/dL)	**0.0% Cholesterol**	19 +/- 2	22 +/- 2	21 +/- 2
	***n*=**	*15*	*22*	*6*
	0.5% Cholesterol	24 +/- 3	29 +/- 2	26 +/- 4
	***n*=**	*14*	*45*	*14*
	0.5% Cholic Acid	25 +/- 2	33 +/- 6	22 +/- 4
	***n*=**	*5*	*10*	*3*
VLDL (mg/dL)	**0.0% Cholesterol**	2 +/- 1	2 +/- 1	2 +/- 1
	***n*=**	*7*	*10*	*3*
	0.5% Cholesterol	13 +/- 2	16 +/- 3	14 +/- 3
	***n*=**	*5*	*11*	*7*
	0.5% Cholic Acid	6 +/- 1	10 +/-4	6 +/- 1
	***n*=**	*5*	*10*	*3*
non-HDL	**0.0% Cholesterol**	26 +/- 2	24 +/- 2	24 +/- 3
	***n*=**	*15*	*22*	*6*
(calculated)	**0.5% Cholesterol**	37 +/- 3	42 +/- 3	45 +/- 4
	***n*=**	*14*	*46*	*14*
	0.5% Cholic Acid	32 +/- 3	34 +/- 10	28 +/- 3
(mg/dL)	***n*=**	*5*	*10*	*3*
Free Cholesterol	**0.5% Cholesterol**	10.4 +/- 0.5	ND	11.9 +/- 1.3
(mg/dL)	***n*=**	*16*		*16*
Glucose	**0.5% Cholesterol**	131 +/- 7	ND	130 +/- 10
mg/dL	***n*=**	*4*		*4*

All values are means +/- SEM, number of mice (N) is given for each value
ND indicates not determined

Table 3.4. **Plasma phytosterol levels of ADAM11 mice on 0.5% cholesterol diet**

Male	Wt	Ko
Total Brassicasterol/cholesterol	1.18 +/- 0.14	1.15 +/- 0/17
Free Brassicasterol/cholesterol	0.23 +/- 0.05	0.21 +/- 0.05
Ester Brassicasterol/cholesterol	0.95 +/- 0.10	0.95 +/- 0.13
Total Campesterol/cholesterol	17.43 +/- 1.16	15.91 +/- 1.10
Free Campesterol/cholesterol	5.03 +/- 0.30	3.98 +/- 0.27*
Ester Campesterol/cholesterol	12.41 +/- 0.88	11.93 +/- 0.85
Total Sitosterol/cholesterol	0.80 +/- 0.14	0.55 +/- 0.11
Free Sitosterol/cholesterol	0.63 +/- 0.08	0.52 +/- 0.10
Ester Sitosterol/cholesterol	0.16 +/- 0.08	0.04 +/- 0.03
Total Lathosterol/cholesterol	0.17 +/- 0.02	0.19 +/- 0.02
Female	**Wt**	**Ko**
Total Brassicasterol/cholesterol	1.95 +/- 0.17	1.77+/- 0.11
Free Brassicasterol/cholesterol	0.28 +/- 0.03	0.32 +/- 0.05
Ester Brassicasterol/cholesterol	1.67 +/- 0.15	1.45 +/- 0.09
Total Campesterol/cholesterol	22.99 +/- 1.07	21.07 +/- 0.89
Free Campesterol/cholesterol	5.14 +/- 0.35	4.13 +/- 0.45
Ester Campesterol/cholesterol	17.85 +/- 0.76	16.94 +/- 0.86
Total Sitosterol/cholesterol	0.68 +/- 0.17	1.33 +/- 0.31
Free Sitosterol/cholesterol	0.58 +/- 0.13	0.81 +/- 0.21
Ester Sitosterol/cholesterol	0.10 +/- 0.07	0.52 +/- 0.23
Total Lathosterol/cholesterol	0.22 +/- 0.03	0.23 +/- 0.03

(n= 16 for each gender and genotype); All values are means +/- SEM
All values are multiplied by a factor of 10,000.
(* is for values $p<0.05$)

Hepatic Cholesterol and Triglyceride Levels on the High Cholesterol Diet

There were no differences between wild-type and ADAM11 homozygous knockout mice of each gender fed the AIN76a 0.5% cholesterol diet in hepatic free and esterified cholesterol as well as triglyceride levels (Table 3.5).

Table 3.5. **Hepatic levels of ADAM11 mice on 0.5% cholesterol diet**

	Male		Female	
	Wt	**Ko**	**Wt**	**Ko**
Total Cholesterol	10.6 +/- 0.8	10.5 +/- 0.7	14.7 +/- 1.2	14.8 +/- 0.7
***n*=**	*14*	*11*	*8*	*5*
Free Cholesterol	4.0 +/- 0.2	3.7 +/- 0.2	4.1 +/- 0.3	4.3 +/- 0.4
***n*=**	*14*	*11*	*8*	*5*
Triglycerides	36.5 +/- 3.6	35.6 +/- 2.5	47.2 +/- 3.6	53.3 +/- 6.0
***n*=**	*14*	*11*	*8*	*5*

All values are in mg/g liver, all values are means +/- SEM,
number of mice (N) is given for each value

Gallbladder Bile Composition

There were no differences between wild-type, ADAM11 heterozygous knockout, and ADAM11 homozygous knockout mice of each gender fed the three diets in gallbladder bile concentrations of cholesterol, phospholipids, and bile acids (Table 3.6).

Table 3.6. **Gallbladder bile levels of ADAM11 mice fed the indicated diets**

Male		**Wt**	**Het**	**Ko**
Cholesterol	**0.0% Cholesterol**	120 +/- 11	108 +/- 9	126 +/- 13
	***n*=**	*12*	*8*	*4*
	0.5% Cholesterol	253 +/- 17	310 +/- 20	287 +/- 21
	***n*=**	*24*	*27*	*16*
	0.5% Cholic Acid	184 +/- 20	231 +/- 55	225 +/- 14
(mg/dL)	***n*=**	*10*	*3*	*13*
Phospholipids	**0.0% Cholesterol**	1532 +/- 113	1521 +/- 125	1406 +/- 250
	***n*=**	*12*	*8*	*4*
	0.5% Cholesterol	1370 +/- 75	1480 +/- 92	1539 +/- 82
	***n*=**	*24*	*27*	*16*
	0.5% Cholic Acid	1342 +/- 90	1345 +/- 152	1529 +/- 90
(mg/dL)	***n*=**	*10*	*3*	*13*
Bile Acids (mM)	**0.5% Cholesterol**	56 +/- 5	57 +/- 3	65 +/- 7
	***n*=**	*11*	*22*	*6*
Female		**Wt**	**Het**	**Ko**
Cholesterol	**0.0% Cholesterol**	117 +/- 4	126 +/- 7	115 +/- 10
	***n*=**	*10*	*9*	*4*
	0.5% Cholesterol	272 +/- 21	307 +/- 15	296 +/- 21
	***n*=**	*11*	*28*	*17*
	0.5% Cholic Acid	223 +/- 11	ND	206 +/- 24
(mg/dL)	***n*=**	*6*		*5*
Phospholipids	**0.0% Cholesterol**	2013 +/- 78	2198 +/- 101	1936 +/- 214
	***n*=**	*10*	*9*	*4*
	0.5% Cholesterol	2173 +/- 97	2356 +/- 82	2180 +/- 102
	***n*=**	*11*	*28*	*17*
	0.5% Cholic Acid	1755 +/- 132	ND	1742 +/- 154
(mg/dL)	***n*=**	*6*		*5*
Bile Acids (mM)	**0.5% Cholesterol**	78 +/- 13	80 +/- 4	85 +/- 13
	***n*=**	*4*	*24*	*4*

All values are means +/- SEM, number of mice (N) is given for each value,
ND indicates not determined

Glucose Tolerance

Wild-type, ADAM11 heterozygous knockout, and ADAM11 homozygous knockout mice of each gender fed the AIN76a 0.5% cholesterol diet were subjected to an IPGTT. The mice were given a bolus of glucose (2g/kg) intraperitoneally and glucose measurements made at 0, 15, 30, 60, and 120 minutes. No differences were observed in glucose tolerance between the genotypes (Figure 3.8).

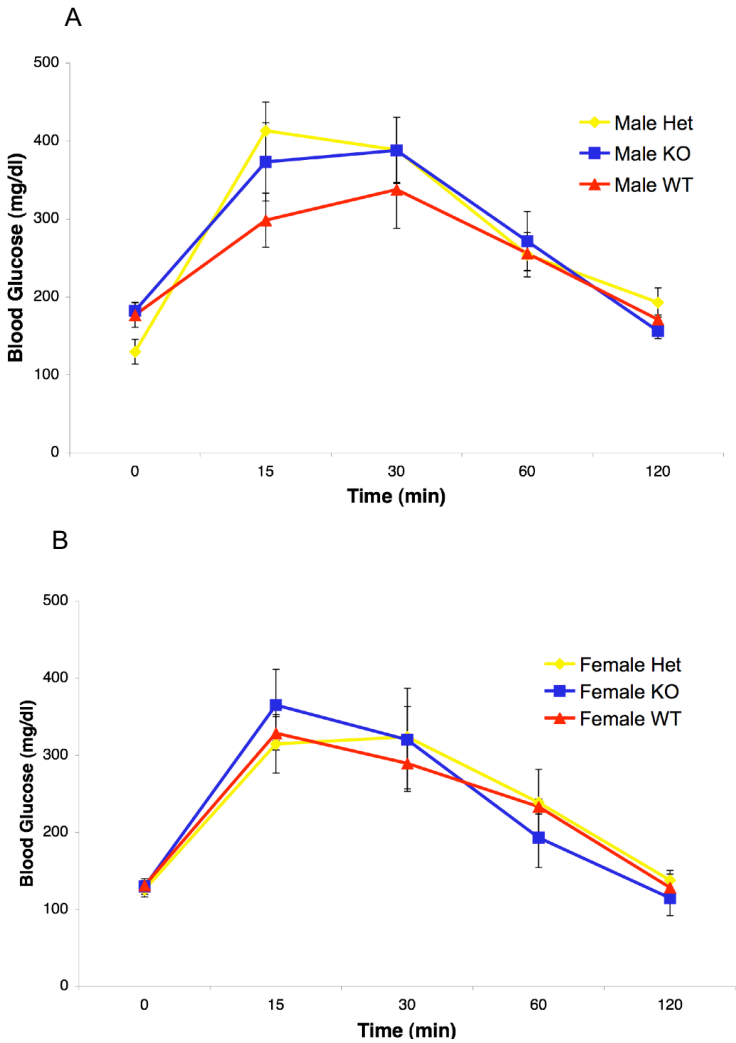

Figure 3.8. **Intraperitoneal Glucose Tolerance Test (IPGTT) of ADAM11 mice on 0.5% cholesterol diet.** 7.5 week old mice were tested after 4 days on high cholesterol diet, by injecting a bolus of 2 mg glucose/g body weight; mean blood glucose values are indicated plus or minus SEM. AUC, area under curve, for IPGTT is also provided.
A) Male (n=4wt, 9 het, 5 ko); AUC: wt: 30,038 +/- 1630, het: 32,159 +/- 2417, ko: 32,590 +/- 3669
B) Female (n=5wt, 7 het, 4 ko); AUC: wt: 26,759 +/- 1652, het: 27,819 +/- 3078, ko: 23,966 +/- 3661

Global Transcript Profiling of Liver

In view of dietary cholesterol up-regulation of liver ADAM11 mRNA levels, the lack of a phenotype related to plasma and liver lipids, gallbladder bile composition, and glucose tolerance was puzzling. Therefore, we undertook assessment of global liver gene expression analysis with hope that it might lead us to the true function of ADAM11 in the liver. Utilizing the feeding paradigm outlined previously, wild-type and ADAM11 homozygous knockout mice were fed AIN76a 0.0% or 0.5% cholesterol diets. As controls quantitative PCR was used to show that wild-type mice on the AIN76a 0.5% cholesterol diet had higher levels of liver ADAM11 mRNA than on the AIN76a 0.0% cholesterol diet, and in the ADAM11 homozygous knockout mice liver ADAM11 mRNA levels were undetectable on both diets. Affymetrix gene expression arrays (MOE 430) were probed with liver RNA as follows: three different pools of five male wild-type mice and three different pools of five male ADAM11 homozygous knockout mice fed the AIN76a 0.5% cholesterol diet, and two different pools of five male wild-type mice and two different pools of five male ADAM11 homozygous knockout mice fed the AIN76a 0% cholesterol diet. On the AIN76a 0.5% cholesterol diet compared to wild-type, in liver from ADAM11 homozygous knockouts only 8 genes were down-regulated and 10 up-regulated by a 2-fold change. Not surprisingly, ADAM11 was the most highly down-regulated gene (Table 3.7). All 17 of the other regulated genes were expressed at low or marginal levels, and none had a known function related to sterol metabolism.

Therefore, we have elected not to further investigate these genes. A third array with pools of male mice (knockout and wild-type) fed the AIN76a 0% cholesterol diet was not peformed, because none of the genes regulated by a 2-fold change detected in the two prior arrays intersected with the 17 regulated genes on the AIN76a 0.5% cholesterol diet, and again none of these genes had a known function related to sterol metabolism either; statistics were not performed on this data set.

Table 3.7. **Affymetrix list of genes regulated two-fold in the liver of ADAM11 mice fed the 0.5% cholesterol diet**

Affy Extension	Mean Fold Change	Gene Name	Fold Change in 3 arrays 1	2	3
1443610_at	7.6	5' of steroid 5 {alpha} -reductase 2-like	2.34	17.47	10.54
1446596_at	7.4	Protein kinase C mu	21.56	3.61	5.27
1440771_at	4.2	Zinc finger with KRAB and SCAN domains 1	1.93	2.35	16.42
1440729_at	3.5	epidermal growth factor receptor pathway substrate 15	1.88	2.16	10.27
1433277_at	3.1	gephyrin	1.74	6.55	2.54
1440565_at	2.5	zinc finger and BTB domain containin 20	2.33	2.31	2.88
1459984_at	2.4	melanoma inhibitory activity 3	2.46	2.2	2.48
1423597_at	2.2	ATPase, aminophospholipid transporter (APLT), class I, type 8A, member 1	2.91	1.86	1.99
1442540_at	2.1	Transcribed sequences	1.95	2.53	1.98
1425686_at	2.0	caspase 8 and FADD-like apoptosis regulator	1.81	1.74	2.54

Affy Extension	Mean Fold Change	Gene Name	Fold Change in 3 arrays 1	2	3
1450248_at	-3.0	a disintegrin and metalloprotease domain 11	-2.96	-2.4	-3.68
1444240_at	-2.9	Shank1 (SH3 ankyrin domain gene 1)	-2.43	-1.83	-5.38
1455298_at	-2.7	inhibitor of DNA binding 4	-1.9	-2.13	-4.72
1442808_at	-2.6	Transcribed sequences	-1.87	-3.52	-2.75
1451095_at	-2.6	asparagine synthetase	-3.38	-3	-1.76
1437389_x_at	-2.4	Sam68/Khdrbs1	-1.81	-2.26	-3.44
1451771_at	-2.1	two pore channel 1	-1.9	-2.54	-1.95
1436213_a_at	-2.0	ribulose-5-phosphate-3-epimerase	-1.71	-1.81	-2.61

Experiments 1-3 each compared liver gene expression of pools of five mice that were either ADAM11 KO or their wildtype siblings; each mouse was fed a one week high 0.5% cholesterol diet.

Crossing the ADAM11 Knockout Trait onto the LDLR Knockout Background

To identify a possible effect of ADAM11 on atherosclerosis susceptibility, the ADAM11 knockout trait was crossed on to the atherosclerosis-susceptible B6.LDLR KO background. Brother-sister mating of LDLR KO ADAM11 heterozygous knockout mice was carried out to produce wild-type and ADAM11 homozygous knockout mice on the LDLR KO background for atherosclerosis studies. After weaning at 4 weeks, these mice were fed the AIN76a 0.02% cholesterol diet for 16 weeks. The mice were sacrificed at 20 weeks of age and aortic root cross sectional lesion areas measured. No significant differences were observed for either gender between the genotypes (Figure 3.9). Comparisons of wild-type, ADAM11 heterozygous knockout, and ADAM11 homozygous knockout mice on the LDLR KO background did not show any differences in body weight or liver weight (Table 3.8), total, HDL, LDL and VLDL cholesterol, triglycerides, glucose or free cholesterol (Table 3.9), gallbladder bile cholesterol and phospholipid concentrations (Table 3.10), and glucose tolerance as measured by the IPGTT (Figure 3.10).

Table 3.8**. Body composition of ADAM11 mice on LDLR KO background**

Male		**Wt**	**Het**	**Ko**
Mouse Weight (g)		30.3 +/- 0.7	29.6 +/- 0.5	29.2 +/- 0.5
	***n*=**	*23*	*32*	*19*
Liver Weight (g)		1.18 +/- 0.25	1.24 +/- 0.12	1.18 +/- 0.10
	***n*=**	*3*	*3*	*6*
Female		**Wt**	**Het**	**Ko**
Mouse Weight (g)		22.8 +/- 0.8	21.2 +/- 0.4	20.5 +/- 0.6
	***n*=**	*16*	*26*	*19*
Liver Weight (g)		1.05 +/- 0.05	0.92 +/- 0.07	1.09 +/- 0.07
	***n*=**	*4*	*3*	*3*

All values are means +/- SEM, number of mice (N) is given for each value

Table 3.9. **Plasma levels of ADAM11 mice on LDLR KO background**

Male		**Wt**	**Het**	**Ko**
Triglycerides		155 +/- 14	175 +/- 20	162 +/- 17
mg/dL	***n*=**	*13*	*19*	*10*
Total Cholesterol		417 +/- 29	515 +/- 37	474 +/- 42
mg/dL	***n*=**	*22*	*28*	*17*
HDL		57 +/- 3	62 +/- 3	58 +/- 3
mg/dL	***n*=**	*21*	*23*	*17*
LDL		260 +/- 19	303 +/- 21	282 +/- 27
mg/dL	***n*=**	*21*	*23*	*16*
VLDL		59 +/- 8	54 +/- 7	63 +/- 9
mg/dL	***n*=**	*21*	*23*	*17*
Glucose		142 +/- 7	152 +/- 6	135 +/- 11
mg/dL	***n*=**	*21*	*29*	*15*
Female		**Wt**	**Het**	**Ko**
Triglycerides		177 +/- 27	189 +/- 20	167 +/- 22
mg/dL	***n*=**	*10*	*29*	*15*
Total Cholesterol		671 +/- 51	695 +/- 34	731 +/- 63
mg/dL	***n*=**	*16*	*36*	*17*
HDL		38 +/- 3	48 +/- 8	38 +/- 2
mg/dL	***n*=**	*16*	*31*	*17*
LDL		374 +/- 28	364 +/- 17	385 +/- 22
mg/dL	***n*=**	*16*	*31*	*17*
VLDL		177 +/- 23	157 +/- 15	177 +/- 17
mg/dL	***n*=**	*16*	*31*	*17*
Glucose		131 +/- 11	124 +/- 5	117 +/- 10
mg/dL	***n*=**	*12*	*35*	*17*

All values are means +/- SEM, number of mice (N) is given for each value

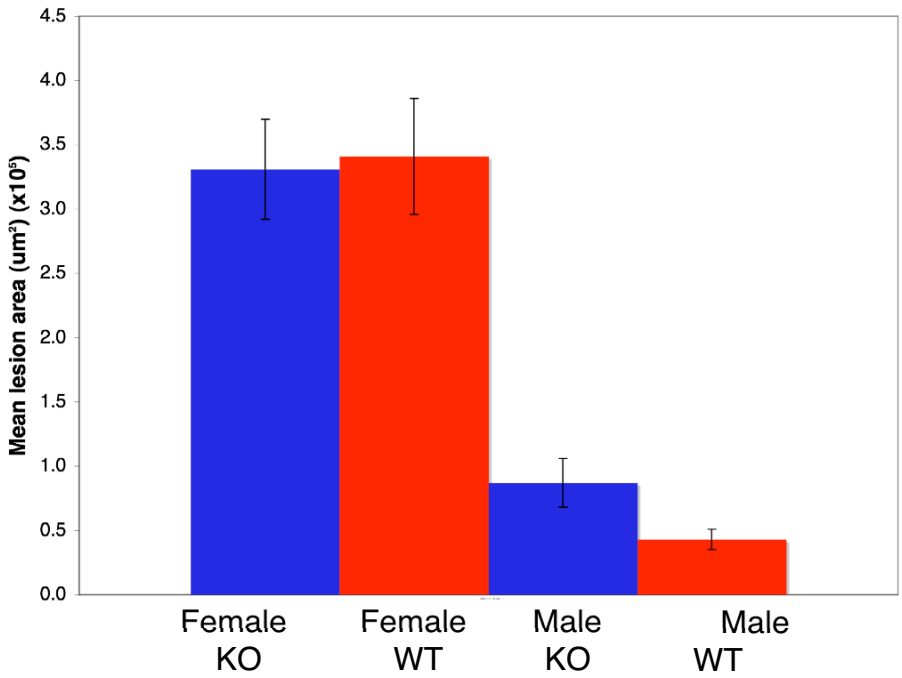

Figure 3.9. **Atherosclerotic lesion size at the aortic root of ADAM11 mice on LDLR KO background.** Average lesion size (um^2) at the aortic root was measured in each ADAM11 knockout and wild-type mouse after 16 weeks on semi-synthetic AIN76a diet (18-22 per gender and genotype). Mean values ($x10^5$) plus or minus SEM for lesion area are indicated.

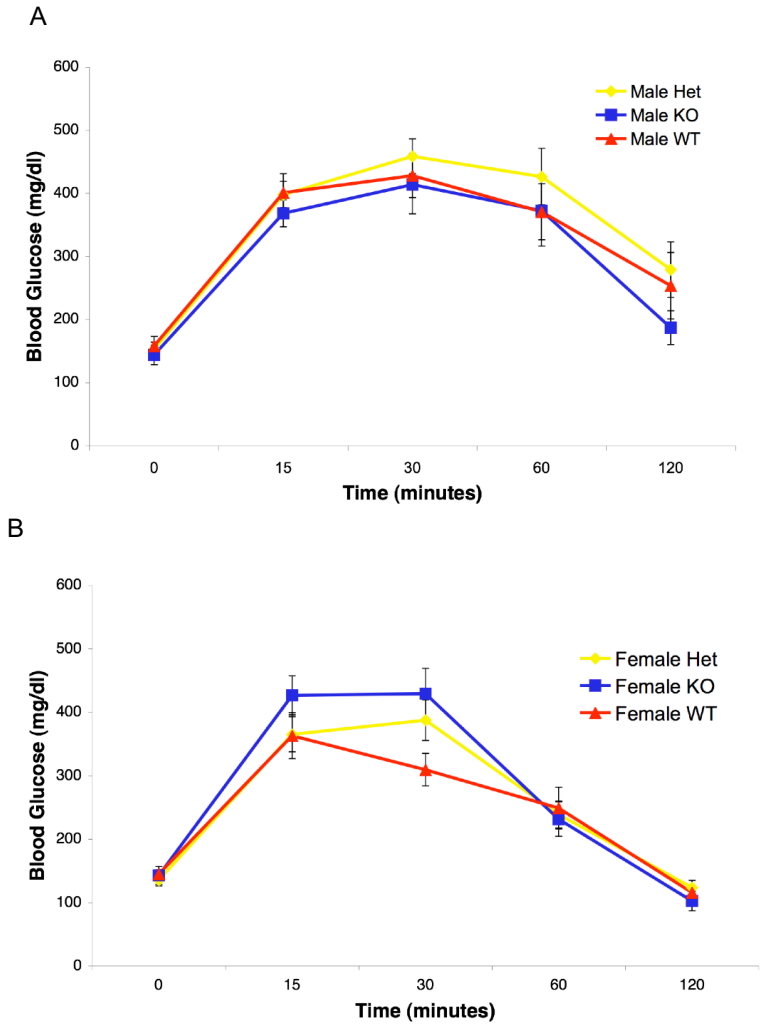

Figure 3.10. **Intraperitoneal Glucose Tolerance Test (IPGTT) of ADAM11 mice on LDLR KO background.** 19.5 week old mice were tested after 15.5 weeks on diet, by injecting a bolus of 2 mg glucose/g body weight; mean blood glucose values are indicated plus or minus SEM. AUC, area under curve, for IPGTT is also provided..
A) Male (n= 9wt, 12 het, 7 ko); AUC: wt: 41,105 +/- 4410, het: 44,998 +/- 3561, ko: 38,285 +/- 4551
B) Female (n= 7wt, 10 het, 5 ko); AUC: wt: 28,179 +/- 2657, het: 29,679 +/- 2004, ko: 30,624 +/- 2210

Over-Expression of ADAM11 in Liver by Injection of ADAM11-Adenovirus

An adenovirus capable of expressing the liver isoform of ADAM11 (Ad-ADAM11a) designed by Maxwell (Maxwell Thesis 2006) and produced by Viraquest at a dose of 1e9 pfu was injected retro-orbitally into chow fed 8-week old male C57Bl/6 mice. High levels of ADAM11 expression was detected as early as 17 hours post-infection and through 101 hours when the experiment was terminated at both the mRNA level by qPCR and the protein level by Western-blotting. At 101 hours post-infection, there were no differences between mice infected with Ad-ADAM11a or an empty control adenovirus (AD-Empty) in plasma total, HDL, and non-HDL cholesterol levels, or gallbladder bile concentrations of cholesterol, phospholipids, and bile acids.

The high levels of liver ADAM11 expression achieved without effects on plasma or gallbladder lipid levels caused us to search deeper for a phenotype. Therefore, we again undertook assessment of global liver gene expression analysis with hope that it might lead us to the true function of ADAM11 in the liver. Affymetrix gene expression arrays (MOE set 430A&B) were probed with pools of liver RNA from 5 chow fed mice at various times post-infection (5, 17, 29, 53, and 101 hours) with either Ad-ADAM11a or AD-Empty. Compared to infection with AD-Empty, infection with Ad-ADAM11a up-regulated several genes involved in liver regeneration, but did not change expression of genes involved in lipid metabolism. Since liver enzymes were elevated only in plasma from the Ad-ADAM11a infected

mice, increased liver regeneration genes may have been a manifestation of a toxic affect from the extremely high levels of ADAM11 expression and not a clue to the physiologic function of liver expressed ADAM11. Therefore, this observation was not pursued further.

A Yeast Two Hybrid Screen for Proteins Interacting with ADAM11 Cytoplasmic Tails

In a collaboration with the Duke Yeast Model Systems Genomics Group, we made a fusion construct of the Gal4 DNA-binding domain with the liver form of the cytoplasmic tail of mouse ADAM11. This construct was used as bait for the screening of a mouse liver yeast two-hybrid cDNA library. One strongly positive clone was identified that interacted with the cytoplasmic tail of ADAM11a. This clone encoded 3-hydroxyanthranilic acid oxygenase (3HAO), the most active enzyme in the kynurenine pathway of tryptophan metabolism. We also made a similar construction, but with the brain form of the cytoplasmic tail of mouse ADAM11, and this was also shown to strongly interact with 3HAO (Figure 3.11). Livers from wild-type and ADAM11 homozygous knockout mice did not differ in 3HAO mRNA levels or in the levels of mRNA of other members of the kynurenic pathway. Antibodies to mouse 3HAO are not available precluding measurement of protein levels. Levels of blood tryptophan were also unaltered between ADAM11 homozygous knockout and wild-type mice fed the high cholesterol (AIN76a 0.5% cholesterol) diet. Whole liver 3HAO functional activity assays did not reveal

different activity levels between ADAM11 homozygous knockout and wild-type mice fed the high cholesterol diet (Table 3.11).

A)
ADAM11a: N-terminal- GGTGWGFKNIRRGRYDPTQQGAV (23aa)
ADAM11b: N-terminal- GGTGWGFKNIRRGRSGGA (18aa)

B)

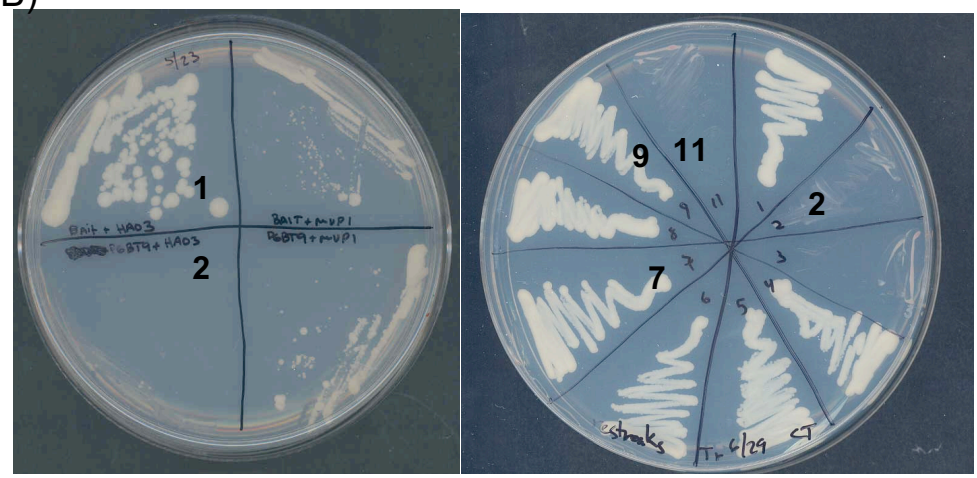

Figure 3.11. **Yeast two hybrid of the cytoplasmic tails of ADAM11**. A) amino acid sequence of ADAM11 cytoplasmic tail cloned into DBD of yeast two hybrid screen, ADAM11a is predominantly the liver splice form, and ADAM11b is predominantly the brain splice form. B) Left Panel: 1) Bait: ADAM11a, Prey: 3HAO; 2) Bait: Control, Prey: 3HAO; Right Panel: 2) Bait: ADAM11a , Prey: Neg Control (negative control); 7) Bait: Pos Control, Prey: Pos Control (positive control); 9) Bait: ADAM11b, Prey: 3HAO; 11) Bait: ADAM11b, Prey: Neg Control (negative control)

Summary

This chapter describes the development of a conditional knockout of the ADAM11 gene. ADAM11 knockout mice were previously shown to have a neurological phenotype to which we now add absence-like epilepsy. This chapter also evaluates the role of ADAM11 in cholesterol metabolism. Utilizing low and high cholesterol and cholic acid containing diets in wild-type and ADAM11 heterozygous and homozygous knockout mice, we failed to find a phenotype for ADAM11 with respect to plasma cholesterol or triglyceride levels, liver lipid levels, gallbladder bile lipid concentrations, glucose tolerance, or atherosclerosis susceptibility. Finally, a previously unsuspected binding partner, 3HAO, for the cytoplasmic tails of both the liver and brain forms of ADAM11 has been identified.

Chapter 4: Discussion and Future Directions

Discussion of StARD5

StARD5 is a member of the Steroidogenic Acute Regulatory–Related Lipid Transfer (START) domain protein family, more specifically the StARD4 subfamily. *In vivo* StARD5 expression is restricted to reticuloendothelial (RE) cells, and *in vitro* StARD5 was shown capable of binding cholesterol and 25-hydroxycholesterol (Rodriguez-Agudo et al., 2006; Rodriguez-Agudo et al., 2005). In a variety of cell types ER stress induces the expression of StARD5; and in macrophages free cholesterol loading was shown to induce ER stress and StARD5 expression (Rodriguez-Agudo et al., 2006; Soccio and Breslow, 2003). It is hypothesized that excess ER free cholesterol triggers the ER stress response in part to increase StARD5, which then transports excess free cholesterol away from the ER to other cellular membranes or to facilitate excretion (Soccio and Breslow, 2003). In this manner StARD5 might allow the cell to restore homeostasis rather than undergo apoptosis. This thesis describes the first studies to directly examine the role of StARD5 *in vivo*. To aid our attempts at elucidating the physiological function(s) of StARD5, we created StARD5 conditional knockout mice. We also made a transgenic line expressing StARD5 in RE cells using the scavenger receptor A promoter/enhancer, and another expressing StARD5 in liver parenchymal cells using the apoE promoter.

Brother-sister mating of StARD5 heterozygous knockout mice did not

produce homozygous offspring. Timed matings and genotyping embryos at various stages of development indicated lethality prior to day E9.5; suggesting StARD5 is essential for early embryonic development. It is probable the mechanism involves some aspect of intracellular cholesterol transport necessary for normal embryonic development. For example, hedgehog is a PM signaling protein required for embryo survival. Hedgehog is covalently bound to cholesterol, which anchors it to the PM. It is possible that intracellular cholesterol transport by StARD5 might facilitate its covalent attachment to hedgehog; and the lack of StARD5 render hedgehog functionally defective.

Our planning strategy involved creation of a conditional knockout in anticipation of the possibility that the total knockout might be an embryonic lethal. The hope was that tissue-specific knockout mice might be viable under conditions in which total knockout mice are not. The general method involves flanking one or more exons with loxP sites and exposure to cre-recombinase driven by a tissue specific promoter. This then causes elimination of these exons in only that tissue, resulting in production of mRNA that is either unstable or codes for a non-functional transcript. We chose to flank StARD5 exon 3 with loxP sites (floxed allele) to eliminate this exon after subsequent exposure to cre-recombinase, expressed either globally or in a tissue-specific manner. Unexpectedly, brother-sister mating of mice heterozygous for the StARD5 floxed allele did not result in any mice homozygous for the floxed allele (expected in ¼ of offspring). Since these mice

have an intact exon 3, we concluded that the mere placement of the loxP sites caused a non-functional allele. Although we had carefully placed the loxP sites in the exon 3 flanking introns so as not to disrupt any known intronic sequence related to splicing, this is probably what occurred. This was unfortunate for 2 reasons. First, this finding indicated that mice with 2 dysfunctional StARD5 alleles were non-viable and thus our physiological studies would be limited to comparing wild-type with StARD5 heterozygous knockout mice. Secondly, rather than being inactivated only after cre-recombinase mediated exon 3 excision, the floxed allele with intact exon 3 was itself inactive. This precluded tissue specific inactivation of the floxed allele, which is necessary for the conditional knockout strategy. Therefore, we were not able to create either global or tissue-specific StARD5 homozygous knockout mice for study.

StARD5 is the fifth member of the START family to be disrupted in mice; the others being StARD12, StARD1, StARD2 (PCTP), and StARD3 (MLN64) (Caron et al., 1998; Caron et al., 1997; Durkin et al., 2005; Kanno et al., 2007b; Kanno et al., 2007c; Kishida et al., 2004). The StARD12 homozygous knockout mice are embryonic lethal around day E10.5 with severe defects in the neural tube, brain, heart, and placenta, as well as alterations in the organization of actin filaments and focal adhesions (Durkin et al., 2005). The StARD12 heterozygous knockout mice were phenotypically normal. StAR (StARD1) was the first START family member to be knocked out, and this knockout mouse provides a model for the human

disease congenital lipoid adrenal hyperplasia (Caron et al., 1997). Both male and female StARD1 homozygous knockout mice have female external genitalia due to a generalized defect in steroid hormone biosynthesis. In addition, knockout mice fail to thrive and die shortly after birth from adrenocortical insufficiency. The StARD2 (PCTP) homozygous knockout mice are viable, but show increased hepatic insulin sensitivity and hepatic esterified cholesterol, and their macrophages after cholesterol loading have decreased cholesterol efflux to ApoA-I and increased apoptosis. In addition, on a lithogenic diet StARD2 knockout mice exhibit impaired excretion of lipids into the bile and increased hepatic free cholesterol-to-phospolipid ratio (Wu et al., 2005; Kanno et al., 2007a; Kanno et al., 2007b; Kanno et al., 2007c; Scapa et al., 2008). Finally, the StARD3 (MLN64) knockout mice are viable but are apparently normal without a recognizable phenotype on chow, high fat, or high cholesterol diets (Kishida et al., 2004).

Since StARD5 homozygous knockout mice were early embryonic lethal, we could only compare adult wild-type and StARD5 heterozygous knockout mice. Careful anatomical and histological examination at autopsy at 12 weeks of age revealed no differences. Measurements of total body and liver weights, plasma and liver lipids, biliary composition, fasting glucose and IPGTT, and macrophage cholesterol efflux to HDL or ApoA-I also showed no differences, except for slightly diminished total body weight at 12 weeks of age in female but not male StARD5 heterozygous knockout mice. This suggests slightly altered metabolism in these

mice, but the finding was not deemed robust enough for follow-up. We have concluded that haploinsufficiency for StARD5 does not compromise a diverse array of metabolic functions.

The ER stress response is activated at all stages of atherosclerotic lesion development (Zhou et al., 2005). It is thought that the ER stress response triggers macrophage apoptosis, which results in further lesion progression. If the ER stress response gene StARD5 is acting early in this process to protect macrophages and restore homeostasis, we hypothesized that reduced StARD5 expression might result in larger atherosclerotic lesions. To explore this idea we evaluated atherosclerosis progression on the LDLR knockout background of wild-type and StARD5 heterozygous knockout mice and found no difference. Either our hypothesis is wrong or our measurement of aortic root cross sectional lesion area is not sensitive or specific enough to pick up a difference. For example, StARD5 haploinsufficiency might have a subtle effect on lesion composition that we might have missed or alternatively affect processes that were not measured such as aspects of lesion stability or regression.

There are several possible explanations for the absence of a clearly observable phenotype in StARD5 heterozygous knockout mice. First, in adult mice the amount of StARD5 might be in excess of what is needed for function and the amount produced under haploinsufficiency may be sufficient for meeting meet organismal needs. Second, functional studies were done with mice fed a chow

diet. It may be that StARD5 heterozygous knockout mice need to be challenged with high fat, high cholesterol, or lithogenic diets to bring out a physiologically relevant phenotype. For example, in StARD2 homozygous knockout mice a lithogenic diet was used to bring out impairment in bile lipid secretions and increases in plasma cholesterol and phospholipids levels (Wu et al., 2005). Third, redundancy is possible and another START gene or a gene of another family might compensate for decreased StARD5 expression. StARD4 and StARD5 have over 30% amino acid identity and, based on initial *in vitro* studies, were both shown capable of promoting intracellular cholesterol transport (Soccio et al., 2002; Soccio and Breslow, 2003). This certainly suggested that the relative lack of either could be compensated for by the other subfamily member. When the StARD4 knockout mice become available, this could be tested by studying StARD5 heterozygous knockout mice on the StARD4 homozygous knockout background. However, at least in the liver, it appears that StARD5 is expressed in Kuppfer cells and StARD4 in parenchymal cells, which makes it difficult to conceive how these 2 intra-cellular proteins could complement each other. Finally, StARD5 may not play a demonstrably significant role in the processes that were examined.

In addition to genetically determined decreased StARD5 expression, we also examined increased expression in transgenic mice. To achieve over expression of StARD5 in reticuloendothelial cells, we used a StARD5 transgene driven by the scavenger receptor A promoter/enhancer. Litter-mates without (wild-type) and with

the transgene were compared for total body and liver weights, plasma and liver lipids, biliary composition, fasting glucose, and macrophage cholesterol efflux to HDL or ApoA-I, and no significant differences were found. Expression of the transgene gave only a ~30% increase in total StARD5 expression, which might not have been large enough to produce a phenotype. Alternatively, for the parameters measured, the amount of StARD5 might not have been rate limiting. We also achieved over-expression of StARD5 using a transgene driven by the apoE promoter/enhancer. These transgenic mice had high levels of StARD5 expression in liver and measurements of total body and liver weights, plasma and liver lipids, and biliary composition were made. Compared to non-transgenic male mice, those expressing StARD5 in the liver had decreased plasma triglyceride levels, as well as decreased gallbladder bile acids, cholesterol, and phospholipid concentration. However, after Rodriguez and colleagues demonstrated that StARD5 is expressed in Kuppfer but not parenchymal cells (these mice express StARD5 driven by the ApoE promoter/enhancer in liver parenchymal cells), we abandoned our studies of these mice because we deemed them unphysiological (Rodriguez-Agudo et al., 2006).

Finally, the transgenic mice in which StARD5 is driven by the scavenger receptor A promoter/enhancer were bred to the LDLR knockout background. Non-transgenic and transgenic mice were compared for atherosclerotic lesion progression and no difference was found. This may have been due to the small

increase in StARD5 expression achieved using this promoter/enhancer and gene. However, the scavenger receptor A promoter/enhancer has been used to drive expression of other transgenes with reasonably high levels of expression achieved (Yan et al., 2007; Zhao et al., 2007). Therefore, it may be necessary to make additional StARD5 scavenger receptor A driven transgenic lines capable of higher expression levels for testing on the LDLR knockout background for effects on atherosclerosis progression.

Future Directions for StARD5

To get a better idea of the crucial but previously unsuspected, role of StARD5 in embryonic development, the precise day of embryonic lethality in StARD5 homozygous knockout mice must be determined. In general, lethality prior to day E3.5 indicates difficulty in fertilization, cleavage, and compaction; between days E3.5 and E6.5 difficulty in implantation and gastrulation; between days E6.5 and E9.5 difficulty in hematopoeisis and cardiovascular development and placental insufficiency; and beyond E9.5 through the perinatal period difficulty in organogenesis. In the case of StARD5 homozygous knockout mice lethality prior to day E9.5 indicates problems either in implantation or organogenesis. We have attempted to procure and genotype day E3.5 embryos (at the blastocyst stage), but have failed thus far we believe due to insufficient starting DNA. As a consequence we need to improve the sensitivity of our analysis by nested PCR or whole genome amplification. However, if this does not work we will have to improve

our harvesting techniques to get more starting DNA. Another approach to inferring the role of StARD5 in embryonic development will be to document when and in what tissues StARD5 expression first occurs. This will be done by timed matings of wild-type mice to procure and whole mount embryos for in situ expression studies at the mRNA and/or protein levels. In addition, the Nat Heintz laboratory at Rockefeller, as part of their GENSAT project, has produced and characterized for brain expression StARD5-GFP-BAC-transgenic mice. These mice have been made available to us, and we intend to use them to assess the timing and location of StARD5 expression by following GFP expression in whole mount embryos of various ages.

Another issue that needs further study is whether or not challenging StARD5 heterozygous knockout mice with different diets might bring out metabolic abnormalities. Thus far we have studied mice consuming a chow diet, which is low in fat (4.5% by weight) and low in cholesterol (0.02%). Future studies might try high fat (up to 60% by weight) and/or high cholesterol (up to 0.5%) diets from weaning to ~12 weeks of age and assessing their consequences for weight gain, plasma and liver lipids, biliary lipid composition, and glucose/insulin homeostasis. There are many precedents for this; for example, recently in studies of StARD2 knockouts, it was necessary to place the mice on lithogenic diets to bring out metabolic abnormalities (Wu et al., 2005).

Future studies should evaluate possible effects of StARD5 on the quality of

atherosclerotic lesions. On the LDLR knockout background, wild-type and StARD5 heterozygous knockout mice showed no difference in atherosclerotic lesion progression as measured by aortic root cross sectional lesion area determined by oil-red-O staining. However, this did not exclude possible effects of StARD5 deficiency on lesion morphology. Tabas and colleagues have shown that on the ApoE knockout background, NPC1 heterozygous knockout mice have normal aortic root cross sectional lesion area but increased lesion cellularity, diminished necrotic core, and less TUNEL-staining of lesional macrophages, suggesting decreased lesional macrophage apoptosois (Feng et al., 2003). In future experiments lesions from LDLR knockout StARD5 heterozygous knockout mice (and controls) should be stained with Masson's trichrome and H&E to look for differences in cellularity, extent of the necrotic core, and thickness of the fibrous cap, as well as TUNEL-staining to assess lesional macrophage apoptosis. In addition to looking for possible StARD5 effects on lesion morphology, it could also be argued that the effects of relative StARD5 deficiency on atherosclerosis might be better observed at later stages of lesion development. In the current study, LDLR knockout wild-type and StARD5 heterozygous knockout mice were weaned at 4 weeks to a semi-synthetic AIN76a diet containing 0.02% cholesterol for 16 week and lesion analysis occurred upon sacrifice at 20 weeks of age. In future experiments it might be preferable to either accelerate lesion formation by increasing dietary cholesterol from 0.02% to 0.5%, or sacrifice mice on the 0.02% cholesterol diet at 32 rather

than 20 weeks of age.

StARD5 is an ER stress response gene and has been hypothesized to act early in free cholesterol loaded macrophages to transport cholesterol out of the ER protecting against apoptosis and restoring homeostasis. This thesis reports studies of bone marrow macrophages derived from wild-type and StARD5 heterozygous knockout mice loaded with tracer amounts of 3H-cholesterol. We found no difference between the genotypes in radiolabeled cholesterol efflux to either ApoAI or HDL over an 8 hour incubation period. Future studies should examine possible effects of StARD5 deficiency or excess in free cholesterol loaded macrophages. Tabas and colleagues have loaded macrophages with free cholesterol by incubation in AcLDL in the presence of an ACAT inhibitor and showed induction of the ER stress response pathway leading to apoptosis (Devries-Seimon et al., 2005; Han et al., 2006). This experiment needs to be done with macrophages from wild-type and StARD5 heterozygous knockout mice to determine whether StARD5 plays an anti-apoptotic role in macrophages. Initial attempts at this experiment following the Tabas protocol have caused sever necrosis rather than apoptosis, possibly due to the use of too high concentrations of either one or both of these reagents (50ug/ml AcLDL, 10ug/ml ACAT inhibitor 58035) or too long an incubation period (14 hours); future titration experiments will be needed to identify the best conditions for this assay. In the future similar *in vitro* studies should be carried out with StARD5 over expressing mice, such as those made with the scavenger receptor A

promoter/enhancer driving StARD5 expression. The transgenic mice we currently have exhibit relatively low level StARD5 transgene expression. Therefore, these studies probably should await the creation of mice with higher transgene expression. It was recently reported that transgenic mice developed using the scavenger receptor A promoter/enhancer exhibit higher expression levels when driving cDNA rather than genomic DNA (Yan et al., 2007; Zhao et al., 2007). Our current strategy involves this promoter driving a genomic construct, but in the future it might be wise to make transgenics with the scavenger receptor A promoter/enhancer driving a StARD5 cDNA construct. Circulating cytokines levels should also be measured in plasma and compared between StARD5 heterozygous knockout and wild-type mice and StARD5 transgenic and wild-type mice. Increased or decreased levels of pro-inflammatory cytokines, such as IL-1b or TNFa, may indicate compromised or enhanced macrophage function in StARD5 deficiency and excess, respectively.

It is possible that the major role of StARD5 is to transport sterol precursors of cholesterol to or within the ER, or preferentially transport newly synthesized cholesterol away from the ER. In this thesis we found wild-type and StARD5 heterozygous knockout mouse macrophages pre-labeled with 3H-cholesterol did not differ in efflux of radiolabeled cholesterol to either ApoAI or HDL. To study whether or not StARD5 transports sterol precursors of cholesterol to or within the ER, or preferentially transport newly synthesized cholesterol away from the ER, we

will do a similar experiment except pre-incubating macrophages with labeled cholesterol precursors, ^{14}C-acetate or ^{14}C-mevalonate. In addition to efflux of newly synthesized radiolabeled cholesterol, the movement of labeled cholesterol from ER to PM and the esterification of labeled cholesterol in the ER by the ACAT reaction will be quantified over time. If StARD5 is involved in the final stages of ER cholesterol synthesis of transporting newly synthesized cholesterol away from the ER as a mechanism for reducing ER stress, decreased expression of StarD5 could lead to an increase in labeled cholesterol synthesis and secretion or movement to the PM. It would also be good to do this experiment under conditions of ER stress where the ability to make StARD5 might be more rate limiting.

We already showed that haploinsufficiency for StARD5 was not sufficient to cause major metabolic derangement and embryonic lethality of homozygous knockouts precluded studying adult mice with a total inability to make StARD5. Future experiments might entail utilizing RNAi to achieve greater than 50% diminution of StARD5 expression in adult mice. We propose either making transgenic mice expressing shRNA for StARD5 in RE cells or administering Ad-StARD5 RNAi to adult mice to knockdown StARD5 between 50 and 90% to examine how this might affect plasma, liver and biliary lipids, glucose/insulin metabolism, and macrophage cholesterol transport.

Finally, protein-protein interactions may be essential for the function of StARD5 and the identification of interacting partners could place StARD5 in a

known cellular pathway. A co-immunoprecipiation assay or a yeast two hybrid should be done to identify potential binding partners.

Future Directions of StARD4 after the Targeted Disruption of StARD4

It is also the goal of our laboratory to understand the physiological role of the cholesterol-regulated, SREBP-regulated StARD4 gene, and one of our main approaches was to make a StARD4 knockout mouse. Since I was the first one in our laboratory to use the recombineering technique to generate conditional knockouts, I designed a conditional knockout strategy for StARD4, very much like for StARD5 (Figure 4.1). This project was then assigned to another student in the laboratory, Joshua Riegelhaupt, who started his work 2 years after me. I spent a lot of time then helping Mr. Rieglhaupt to create the targeting vectors and to trouble-shoot in creating the knockout mouse. A BAC clone encompassing the StARD4 locus was isolated from a mouse C57Bl6 genomic library (BacPac Resources). Our plan was to knockout exon 3 using the Cre-loxP technique. In StARD4 splicing of exons 2and 4 results in a number of pre-termination codons (PTC). A targeting vector was created using the MC1-TK-containing plasmid. A loxP site was introduced into StARD4 intron 2 and an Frt-Pgk-em7-Neo-Frt-loxP cassette placed in StARD4 intron 3. The StARD4 Neo floxed allele was substituted for the endogenous gene by homologous recombination in isogenic mouse embryonic stem (ES) cells. One correctly targeted ES clone was identified by Southern blotting, expanded, and injected into blastocysts. Chimeras were produced, which

upon further breeding gave germ-line transmission. After conversion of the StARD4 Neo floxed allele to a null allele missing exon 3, brother-sister mating of heterozygous knockout mice was undertaken. In the first litter one of eight mice was a StARD4 homozygous knockout, which appears normal and is thriving after 6 weeks of age. This suggests StARD4 homozygous knockout mice are not embryonic lethal. Thus future studies will be able to compare the three genotypes, wild-type, heterozygous knockouts, and homozygous knockouts. We will also create and characterize conditional knockouts with StARD4 deficiency in liver (Alb-Cre) and macrophages (LysM-Cre). In the future StARD4 knockouts will be characterized for the traits measured in the StARD5 experiments enumerated in previous section of this thesis. Since StARD4 is a dietary cholesterol down-regulated gene, we will have to pay particular attention to studying mice on both low and high cholesterol diets and perhaps on treatment with cholesterol-lowering statins as well.

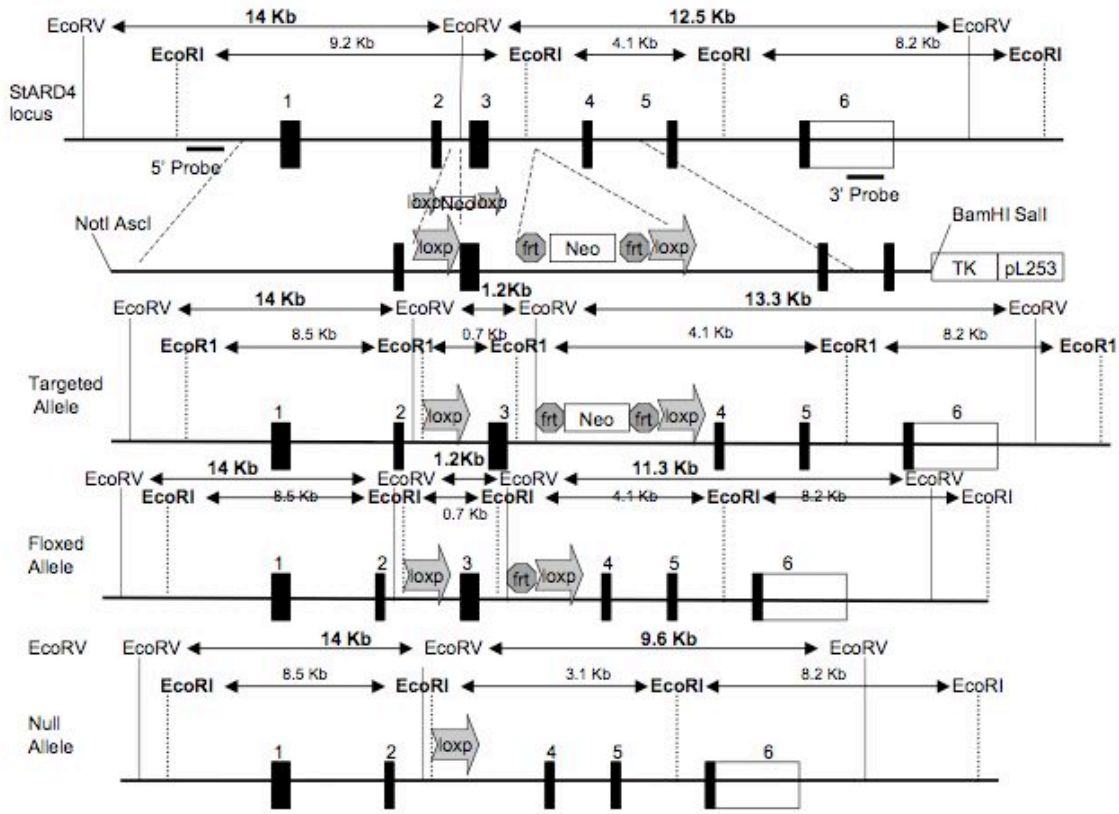

Figure 4.1. **Gene targeting and generation of a conditional knockout (floxed) allele of the StARD4 gene**. A) Targeting strategy to flank exon 3 of StARD4 with loxP sites. The targeting vector was constructed by placing a Neo selectable marker flanked by Frt sites with a loxP site in intron 3. A second loxP site was introduced in intron 2

Discussion of ADAM11

ADAM11 homozygous knockout mice are viable and grow and develop normally. Autopsy at 12 weeks of age did not reveal any gross anatomical or histological abnormalities.

Functional Role of ADAM11 in the Brain

Takahashi and colleagues showed ADAM11 homozygous knockout mice have a defect in the hidden water maze test, impairment in the rotating rod task, and reduced responses to the formalin paw test and acetic acid writhing test. To these abnormalities we now add altered brain wave activity and absence-like seizures. Thus it appears that ADAM11 plays roles in learning, motor coordination, nociception, brain electrical activity, and seizure control.

Since ADAM11 is catalytically inactive, Takahashi and colleagues have proposed it plays an important signaling or structural role at the synaptic junction either by integrin-dependent or integrin-independent mechanisms (Cai et al., 1998; Takahashi et al., 2006a; Takahashi et al., 2006b). In Xenopus, ADAM11 (MDC11a) is expressed in neural crest cells and is thought to be involved in cell-cell or cell-matrix interactions during neural crest cell migration (Cai et al., 1998). Rybnikova and colleagues have proposed that ADAM11 may play a role in any one of the many integrin functions in the adult or developing brain, including neuronal plasticity, neuronal migration, neuronal differentiation, neuritic outgrowth, and synapse formation (Rybnikova et al., 2002). Other groups have hypothesized that because

of strong homology in their integrin binding domains, ADAM11, ADAM22, and ADAM23 may be partially redundant in the brain (Sagane et al., 1998; Sagane et al., 1999).

Unlike the ADAM11 homozygous knockout, ADAM22 and ADAM23 homozygous knockout mice have severe ataxia, convulsions, and perinatal death; both die before the third week post-birth (Mitchell et al., 2001; Sagane et al., 2005). The post-synaptic PM protein ADAM22 through its cytoplasmic tail anchors to the scaffolding protein postsynaptic density-95 (PSD-95), and through its extracellular disintegrin domain serves as a receptor for LGI1 (Fukata et al., 2006). LGI1 is secreted by pre-synaptic neurons and by binding to the disintegrin domain of ADAM22 increases AMPA receptor-mediated post-synaptic transmission. The LGI1-ADAM22 disintegrin domain interaction appears to alter the interaction between the ADAM22 cytoplasmic tail and the scaffold protein PSD-95, which in turn promotes the association of PSD-95 with the post-synaptic AMPA glutamate receptor subtype (Fukata et al., 2006). The amino acid residues in the ADAM22 disintegrin domain that are crucial for LGI1 binding are completely conserved in both ADAM11 and ADAM23. Utilizing an *in vitro* assay, Fukata and colleagues showed both the ADAM22 and ADAM23 disintegrin domains bind LGI1, but did not examine the ADAM11 disintegrin domain (Fukata et al., 2006). Since the ADAM22 cytoplasmic tail is very different from the ADAM11 and ADAM23 cytoplasmic tails, it is unlikely that after receiving the LGI1 signal that the latter interact in the same

way as ADAM22 with PSD-95. Instead, it is more likely that the LGI1 interaction with ADAM11 and ADAM23 is competitive with the LGI1 interaction with ADAM22, and may serve to block the latter, as described for dominant negative interactions. It is also possible that LGI1 interaction with ADAM11 and ADAM23 might modulate entirely different pathways in post-synaptic neurons.

Although ADAM11 function in the brain was not the main goal of this thesis, we did perform a few preliminary studies. Since ADAM11 is highly expressed in hippocampus and amygdala (Rybnikova et al., 2002), we performed a fear conditioning test, but did not find a difference between ADAM11 homozygous knockout and wild-type mice. ADAM11 is also expressed in thalamus and cerebral cortex (Rybnikova et al., 2002), where neuronal defects commonly cause seizures. Therefore, we performed electroencephalography (EEG) on ~20 week old ADAM11 homozygous knockout mice to test for seizure activity. We found the knockout mice had a major change in background brain rhythms, with most brain waves in the 5-6Hz or theta range and no faster beta- or alpha-wave activity observed. ADAM11 knockout mice also exhibited constant cortical discharges and at a rate of 1/hour non-convulsive seizures indicative of absence-like epilepsy. These preliminary studies require further work to determine the natural history of these seizures and to delve more deeply into mechanism. Since this type of work is outside the expertise of our laboratory, we are actively seeking a laboratory with these interests to take over this project.

With regard to mechanisms underlying altered brain electrical activity in ADAM11 homozygous knockout mice, one clue might be the results of our yeast two hybrid study that revealed a strong interaction between the cytoplasmic tail of ADAM11 and 3HAO. 3HAO is in the pathway from tryptophan to the excitotoxin quinolinic acid (QA). It converts the unstable 3-hydroxyanthranilic acid (3-HA) to an unstable intermediate 2-amino-3-carboxymuconic acid semialdehyde (ACMS), which non-enzymatically and spontaneously cyclizes to form QA. Normally, the enzyme αamino-βcarboxymuconate- εsemialdehyde decarboxylase (ACMSD), also known as picolinic carboxylase, diverts the unstable ACMS to a benign catabolite and prevents the accumulation of QA. However, altered activity of either 3HAO or ACMSD can result in QA accumulation. QA is an endogenous agonist of the NMDA glutamate receptor subtype and a potent neurotoxin. Elevated levels of QA have been implicated in inflammatory diseases of the CNS, including AIDS and Lyme disease dementia, Huntington's disease, Alzheimer's disease, and epilepsy (Eastman et al., 1994; Köhler et al., 1988). Schwarcz and colleagues have shown that 3HAO activity is markedly increased in both seizure-prone EL and DBA/2 mice as compared to non-epileptic strains in all brain regions examined, leading them to hypothesize that enhanced production of QA contributes to seizure susceptibility in mice (Eastman et al., 1994; Köhler et al., 1988). More studies are needed to determine whether ADAM11 affects 3HAO activity in neurons and whether the ADAM11 homozygous knockout mice have altered 3HAO activity or altered QA

levels as a possible explanation for their altered brain wave activity and non-convulsive seizures.

Functional Role of ADAM11 in the Liver

ADAM11 is a catalytically inactive member of the A Disintegrin and Metalloprotease (ADAM) family. It is expressed in the liver only in hepatocytes with highest expression near the portal triads at the peripheral parts of hepatic lobules and lowest expression near the central vein at the center of the hepatic lobules (Rybnikova et al., 2002). There are several reasons to suspect that ADAM11 might play an important role in liver metabolism, including that cholesterol feeding increases ADAM11 expression in liver but not other tissues, there is a tissue-specific mRNA splicing mechanism capable of producing a liver isoform of ADAM11 that differs in its cytoplasmic tail from the brain form, and ADAM11 up-regulation in liver by an LXR dependent mechanism is a characteristic shared with many genes involved in reverse cholesterol transport (RCT); a process whereby excess cholesterol is transported from peripheral tissues to the liver, for excretion in bile. ADAM11 is localized to the hepatocyte plasma membrane and depending on whether it is basolateral or cannalicular it is in a position to influence the uptake or excretion, respectively, of cholesterol or cholesterol containing particles. ADAM11 could act as a stand-alone receptor or as a co-receptor. Liver ADAM11 with its distinct cytoplasmic tail could also act as an outside-in signaling molecule.

In general to determine the functional role of ADAM11 in liver, we studied

cohorts of mice, including wild-type, ADAM11 heterozygous knockouts, and ADAM11 homozygous knockouts, and used three different diets: 0% cholesterol, high 0.5% cholesterol; and high 0.5% cholic acid. In general, ADAM11 gene dosage (i.e. 2, 1, and 0 functional copies in wild-type, ADAM11 heterozygous knockout mice, and ADAM11 homozygous knockout mice, respectively) had no effect on liver weight or levels of plasma total, HDL, LDL, and VLDL cholesterol, total free cholesterol, triglycerides, glucose, ALT, blood amino acids, and plant sterols (except for free campesterol levels discussed below). There was also no effect of ADAM11 gene dosage on hepatic cholesterol and triglyceride levels, gallbladder bile composition, glucose tolerance, and the global liver gene expression profile.

ADAM11 induction was observed in the livers of wild-type mice fed the 0.5% cholesterol diet. Consequently, we expected to observe the largest difference in phenotype between wild-type and knockout mice fed this diet. However, the absence of ADAM11 had no effect on any of the parameters measured. While liver function tests (ALT) revealed slight liver toxicity in mice fed the 0.5% cholate diet, there was no difference in toxicity between wild-type and ADAM11 knockout mice. Finally, in addition to its role in RCT and cholesterol homeostasis, LXRs in the liver also modulate glucose homeostasis. However, ADAM11 is apparently not involved since the loss of ADAM11 does not affect fasting glucose levels or impair glucose tolerance.

On a high cholesterol diet, the loss of ADAM11 resulted in a slight, but statistically significant, decrease in free campesterol levels in male mice, and a similar, but not statistically significant, decrease in females. However, there was no alteration in total campesterol levels, or total and free sitosterol and brassicasterol levels. Plant sterols cannot be synthesized endogenously and are thus completely derived from the diet and their absorption is regulated by intestinal ABCG5/8 and NPC1L1 (Sehayek and Breslow, 2005). Phytosterol levels, in particular levels of total campesterol, correlate positively with dietary cholesterol absorption and inversely with markers of whole body cholesterol synthesis, and elevated phytosterol levels may be pro-atherogenic and a risk factor for coronary heart disease (Sehayek and Breslow, 2005). A role for ADAM11 in specifically regulating free campesterol is unlikely, since ADAM11 has not been detected in intestine. In addition, the decrease in free campesterol but not free sitosterol or brassicasterol levels is peculiar because no known physiological process distinguishes them. Also, total campesterol is normal suggesting this is not a major physiological alteration. It is doubtful that isolated low levels of free campesterol indicates a role for ADAM11 in some novel metabolic pathway, rather the observation is probably a false positive. Moreover, the modest size of the difference observed in free campesterol levels leads us to think it is not biologically significant and not worth following up.

The process of RCT is thought to be anti-atherogenic. To examine whether

the putative RCT gene ADAM11 plays a role in atherosclerosis progression, we evaluated aortic cross sectional lesion area in ADAM11 knockout mice on the LDLR knockout background. We found total loss of ADAM11 has no effect on plasma lipids or atherosclerosis. However, there are two potential drawbacks of this study. First, we employed the AIN76a 0.02% cholesterol diet to induce atherosclerosis in these mice. Since the induction of ADAM11 in wild-type mice is highest on a 0.5% cholesterol diet, it is possible that the effect of ADAM11 loss on atherosclerosis could only be observed after a long-term feeding using a high cholesterol diet. Additionally, we only analyzed atherosclerosis on the LDLR knockout background. There may be phenotypic differences between the LDLR and ApoE knockout backgrounds, especially if there is an interaction of the LDLR with ADAM11.

Many members of the ADAM family have been demonstrated to serve as signal transducers, playing a role in the transferring of information between the cell and its extracellular milieu. We performed a microarray of total RNA from mouse livers in order to explore whether the loss of ADAM11 in the liver has an effect on gene expression and gene pathways. While we did identify 17 genes whose expression was greater than two-fold changed, all of these genes were expressed at low or marginal levels in the liver, and none of the genes has a known function related to sterol, triglyceride, or glucose metabolism. Since none of these genes share a known common pathway, we have not further investigated the relationship of these genes with ADAM11.

There are several possible reasons for the lack of a clearly observable, phenotype for liver expressed ADAM11, as studied with the ADAM11 knockout mouse model. First, it is possible that ADAM11 does not play a significant role in the processes that were examined. It is also possible that ADAM11's expression in mouse livers and its regulation by cholesterol and LXRs are vestigial (too low), in which case the loss of ADAM11 would have little or no effect on the liver, plasma or gallbladder bile. Alternatively, compensatory mechanisms may exist. Another gene, possible even another ADAM family member, could compensate for the loss of ADAM11. The extent of the redundancy that exists among ADAM family members remains unclear, but is hypothesized to be significant given that ADAMs often share over 30% sequence similarity. In fact, ADAM11 has over a 50% sequence similarity to its subfamily members ADAM22 and ADAM23, with over 70% similarity among the three different disintegrin domains (Sagane et al., 1998; Sagane et al., 1999). While these two genes, ADAM22 and ADAM23, are highly expressed in the brains of mice, ADAM23 was shown to be expressed at low levels in the liver; ADAM22 has not been found in the liver. If the compensatory mechanism involves increased gene expression, this would likely be detected by the microarray; however, it is also possible that a redundant mechanism alters protein stability, rather than RNA expression. In this case, proteomic studies, such as a two-dimensional difference gel electrophoresis, could be revealing. It is possible that a double knock-out of ADAM11 and its compensatory gene would

result in an observable phenotype. Unfortunately, the ADAM22 knockout dies shortly after birth, and therefore analysis of sterol metabolism and the process of RCT in the double knockout of ADAM11 and ADAM23 is not feasible at this time. However, the eventual creation of a liver-specific conditional knockout of ADAM23, along with our conditional knockout of ADAM11 may allow this study to be performed.

In order to elucidate the function of the two ADAM11 splice forms, we attempted to identify novel binding partners of the two different cytoplasmic tails of ADAM11 by performing a yeast two-hybrid screen. Only one gene, 3HAO (3-hydroxyanthranilic acid 3,4-dioxygenase), was identified in this analysis and was shown to interact with both ADAM11 cytoplasmic tails. 3HAO is an enzyme that plays an important role in the metabolic transformation of tryptophan to nicotinamide in the kynurenine pathway, the main route of metabolism of the essential amino acid tryptophan. 3-HAO has been shown to be widely expressed in numerous tissues including brain, inflammatory cells, lung, stomach, intestine, and epididymis. The gene is also highly expressed in the liver, the major site of the systemic kynurenine pathway metabolism, which is likely related to high uptake and transport capacity of hepatocytes for tryptophan and kynurenine. However, mRNA levels of 3HAO and plasma levels of tryptophan were unaltered in the knockout mice. In addition, the interaction with 3HAO was with both cytoplasmic tails questioning the specificity of the interaction and making it hard to know if this interaction is functional

in brain and/or liver or in neither.

Future Directions for ADAM11 in the brain

Many questions need to be addressed to gain a better understanding of the physiological role of ADAM11 in the brain. To date, due to logistical constraints only three male ADAM11 homozygous knockout mice, aged 20 weeks, have undergone EEG testing. More mice of both genders and a variety of ages need to be studied to determine the natural history of the seizures observed. For example, absence seizures in humans have specific age-related expression patterns, and this information might have pathophysiological significance as well as make the ADAM11 homozygous knockout mouse a more attractive model for a human disease with a similar expression pattern.

It will also be necessary to develop a new antibody to ADAM11, so that we can carefully document the brain regions and cells that express ADAM11 by immunohistochemical staining. This would complement previous RNA in situ hybridization studies by Rybnikova, and allow identification of brain regions and cells that actually express ADAM11 protein, which may not always correspond to ADAM11 mRNA expression. In addition, seizures are often associated with complex seizure-induced histological changes in cerebral cortex, hippocampus and thalamus; so a thorough histological study of brains from knockout mice, beyond H&E stains, should be performed. Many seizure disorders have a derangement or alteration in the number of excitatory and/or inhibitory neurons; therefore all

interneurons in ADAM11 knockout mouse brain sections should be stained and counted. This will require immunohistochemical analysis with antibodies that identify various types of inhibitory neurons, such as antibodies to GABA alpha and beta receptors, neuropeptide Y (NPY), calbindin, calretinin, reelin, Gad, somatostatin, and parvalbumin, and antibodies that identify excitatory neurons, such as antibodies to zinc transporter 3 (znt3) and acetylcholinesterase. Other potentially useful antibodies are to c-Fos, an indirect marker of neuronal activity, iba1, a microglial marker, and GFAP an astrocyte marker. Timm's stain should also be used as it is a zinc detecting histological marker found in mossy fiber projections, which are often altered after seizures. Finally, since seizures can induce neuronal cell death, knockout mouse brains should also be examined for markers of apoptosis.

Since ADAM11 knockout mice exhibit seizures, along with spatial learning impairment and motor coordination problems, the question arises as to whether or not ADAM11 affects synaptic transmission and plasticity? Electrophysiological studies of slices of the hippocampus and cerebellum of ADAM11 knockout mice would be useful in this regard.

We have also established a conditional floxed allele of ADAM11, which allow for engineering mice with cell-specific or tissue-specific loss of ADAM11. Using transgenics that express Cre in various regions or cells of the brain, the region in the brain in which loss of ADAM11 is most essential for the seizure phenotype could

be identified. Currently there are only a few brain cell-specific Cre transgenic lines, but some might be useful, including emx1-Cre, expressed in cerebral cortex and hippocampus, camK2a-Cre, expressed in cortex, amygdale, and hippocampal CA1 neurons, c-kit-Cre, expressed in hippocampal CA1, CA2 and CA3 neurons, anterior dentate gyrus, and the ganglion cell layer of the retina, and grik4-Cre, expressed in hippocampal CA3 neurons. Utilizing these cell- and tissue-specific expressing Cre transgenics to create cell- and tissue-specific ADAM11 knockout mice coupled with careful histological examination would be an essential element in explaining the brain phenotypes in ADAM11 knockout mice.

Future Directions for ADAM11 in the Liver

Is the expression of ADAM11 on the hepatocyte surface polarized? Hepatocytes are polarized with a basolateral side facing the liver sinusoids and the blood, and an apical side facing the bile canaliculi and the bile. ADAM11 expression on the basolateral membrane would suggest it plays a role in cholesterol uptake/efflux from/to the blood; alternatively, ADAM11 expression on the cannalicular membrane suggests a role in biliary lipid efflux. Development of a better antibody is needed to address this question, since my previous attempts with existing antibodies have failed to elucidate endogenous levels of ADAM11 protein expression in the liver.

Which proteins interact with ADAM11? To gain better insight into the function of ADAM11, we need to determine which proteins interact with ADAM11. We have

already reported the interaction of the cytoplasmic tails of ADAM11 with the enzyme 3HAO using yeast two-hybrid strategy. Using another technique, such as GST-fusions, we want to identify other novel cytoplasmic interactions, and using either GST-fusions or yeast two hybrid screens we would also hope to identify novel extracellular interactions, in particular proteins that interact with the disintegrin domain of ADAM11. To fully cover the ADAM11 interacting proteome we will need to use homogenates or prey from liver and brain tissue.

Does the loss of ADAM11 cause changes in protein expression in the liver? The microarrays did detect RNA expression changes in several genes in the livers of ADAM11 knockout mice on a high cholesterol diet, but did not suggest an obvious pathway for study that might be affected by ADAM11. Proteomic studies, such as a two-dimensional difference gel electrophoresis, are needed to determine which proteins are differentially affected in the livers of these knockout mice.

Does the loss of ADAM11 cause changes in plant sterol absorption? Since levels of free campesterol were reduced in the ADAM11 knockout mice on a high cholesterol diet, plasma measurements of the knockout mice should be repeated on a low cholesterol diet. Biliary plant sterols should also be measured under both conditions. Radiolabeled sterol absorption studies are needed to determine whether these mice have altered ability to take up phytosterols.

Although ADAM11 does not appear to affect cholesterol homeostasis or atherosclerotic development in our studies, new techniques by Rader and

colleagues on how to examine the *in vivo* role of genes in the process of RCT could help give us a more direct answer as to whether the LXR-regulated gene ADAM11 plays role in RCT. Rader's techniques involve tracing the movement of cholesterol from 3H-cholesterol–labeled J774 macrophages injected intraperitoneally into plasma, then liver, and ultimately into the bile and feces as free cholesterol or bile acids (Zhang et al., 2003).

Other questions that should be addressed in determining ADAM11's non-neural function as it pertains to its regulation in the liver by cholesterol and LXRs are whether the loss of ADAM11 affects atherosclerosis in the ApoE knockout background. In future experiments it might be preferable to either accelerate lesion formation by increasing dietary cholesterol from 0.02% to 0.5%, or sacrifice mice on the 0.02% cholesterol diet at 32 rather than 20 weeks of age.

Chapter 5: Materials and Methods

Animals and Diets:

All animal protocols were approved by The Rockefeller University Animal Care and Use Committee. All mice were bred and housed at the Rockefeller University Laboratory Animal Research Center in a single humidity- and temperature-controlled room with a 12h dark-light cycle.

Mice: Wild-type C57BL/6 male mice were obtained from The Jackson Laboratory (stock no. 00664). *LDLR–/–* mice on the C57BL/6 background were obtained from The Jackson Laboratory (B6.129S7-Ldlrtm1Her/J, stock no. 002207, henceforth called LDLR–/–). ACTFLPe transgenic mice on the C57BL/6 background were obtained from The Jackson Laboratory (B6.Cg-Tg (ACTFLPe) 9205Dym/J, stock no. 005703, henceforth called Flp). These mice have active flippase expression in all mouse tissues. CMV-Cre transgenic on the C57BL/6 background were obtained from The European Mutant Mouse Arhcive (EMMA) (B6.129P2-Tg(CMV-cre)1Cgn/CgnIbcm, stock no. 01149, henceforth called CMV-Cre) These mice have active Cre recombinase expression in all mouse tissues. Alb-Cre transgenic on the C57BL/6 background were obtained from The Jackson Laboratory (B6.Cg-Tg(Alb-cre)21Mgn/J, stock no. 003574, henceforth called Alb-Cre). These mice have active Cre recombinase expression mainly in hepatocytes. LysM-Cre transgenic on the C57BL/6 background were obtained from Ira Tabas. These mice have active Cre recombinase expression mainly in the

reticuloendothelial system (particularly macrophages). Albino mice on the C57BL/6 background were obtained from The Jackson Laboratory (B6(Cg)-Tyrc-2J/J, stock no. 000058, henceforth called albino).

To assess fertility and fecundity, littermate males (>6 weeks old) were placed in cages with two mature wild-type females for 1 month or more. Littermate females were caged with a wild-type male for a similar period. The number of mice achieving a pregnancy and the number of offspring from each mating set or pregnancy were recorded.

Dietary Studies: For dietary studies involving the ADAM11 knockout mice, 6-week old mice were fed a semi-synthetic modified AIN76a diet containing 10% kcal as fat, added with 0.00% cholesterol (wt/wt) ((Clinton/Cybulsky Rodent Diet), Research Diets D12102N), which was fed to the mice for one week before the start of each experiment. Mice were then split into three groups and then fed either this control 0.00% cholesterol diet or this diet supplemented with either 0.50% cholesterol (wt/wt) (Research Diets D00083101) or 0.50% cholic acid (wt/wt) (Research Diets D07040901) for one week, before sacrifice.

For dietary studies involving scanvenger receptor A-hStARD5 transgenic mice and ApoE-hD5 transgenic mice, 6-week old mice were fed a semisynthetic modified AIN76a diet containing 10%kcal as fat, added with 0.00% cholesterol (Clinton/Cybulsky Rodent Diet), Research Diets D12102N), which was fed to the mice for one week before the start of each experiment. Mice were then split into

two groups and fed either this control 0.00% cholesterol diet or this diet supplemented with 0.50% cholesterol (wt/wt) (Research Diets D00083101) for one week, before sacrifice.

For dietary studies involving StARD5 knockout mice, 4-week old mice were split into two groups and fed either a normal chow diet or a high fat diet containing 60% kcal as fat from lard with 0.03% cholesterol (Research Diets D12492)(these mice are currently still under analysis) . Mice were fed either diet until sacrifice at 12 weeks.

For all atherosclerosis studies, mice were crossed onto the LDLR-/- background. Mice were weaned at 4-weeks and then fed a semisynthetic modified AIN76a diet containing 10% kcal as fat, supplemented with 0.02% cholesterol (Clinton/Cybulsky Rodent Diet), Research Diets D00110804). Mice were fed this diet for 16 weeks prior to sacrifice.

Adenovirus: For adenovirus injections, eight week old male C57Bl/6 animals were anesthetized with ketamine/xylazine and were injected via the retro-orbital plexus with $1x10^9$ pfu of ADAM11 adenovirus(designed by Kara Maxwell and made by Viraquest) in PBS per mouse. Mice were sacrificed after 5, 17, 29, 53, and 101 hours after injection.

Sacrifice of Animals

At the end of all dietary mouse experiments, food was removed from the cage early in the light cycle (9am). Mice were fasted for 6 hours, but with full access

to water. Prior to sedation, blood glucose levels were measured from tail blood using a glucometer (Bayer). For all dietary studies, mice were sedated with ketamine/xylazine and sacrificed. The gallbladder bile was aspirated, and blood was drawn through heart puncture. The animals were exsanguinated with heparinized PBS. Harvested tissues were frozen in liquid nitrogen and stored at -80C or stored in RNAlater (Ambion) according to the manufactuere instructions. The animals were perfused with formalin and the heart was removed by cutting halfway between the aortic root and the brachiocephalic artery. The tissue was frozen in Tissue-Tek OCT compound. The brachiocephalic artery was cut at the point where it branches from the aorta and 1mm distal to its bifurcation into the subclavian and carotid arteries. For all neurologic studies, mice were sedated with Avertin and sacrificed, prior to the removal of the brain.

Creation of Transgenic Mice

To generate transgenic mice overexpressing StARD5 in liver, human StARD5 ORF was PCR amplified. The human sequence was used so that transgene mRNA exprssion could be distinguished from the endogenous mouse genes. This ORF was cloned into the KpnI/Xho1 sites of the pLIV.7, a transgene construct in which liver expression is driven by the human ApoE promoter and enhancer. SacII and SpeI digestion isolated the linear ~6.5kb transgene fragment from the vector. The fragments were purified by ethanol precipitation. Pronuclear injection of the transgene was carried out at The Rockefeller University, potential

founders were screened by PCR using the gene specific primers, and 4 founder mice were generated. These founders were mated with C57Bl/6 animals to generate transgenic and wildtype littermates.

To generate transgenic mice overexpressing StARD5 in macrophages, the full length human StARD5 gene (BAC RP11-770M20) was inserted using techniques by Copeland and into the J900 expression vector, which encodes the scavenger receptor promoter-enhancer A (SREP) [gift by Chris Glass (UCSD, La Jolla, California, USA) and Jeanine D'Armiento (Columbia, NY, NY, USA)]. The translational initiation codon of the full-length human StARD5 gene was ligated downstream of the SREP containing the SmaI site (Table 5.1). The expression cassette was removed by digestion with NotI and SalI, and purified from agarose gels. Pronuclear injection of the transgene cassette was carried out at The Rockefeller University potential founders were screened by PCR using the gene specific primers, and 2 founder mice were generated. These founders were mated with C57Bl/6 animals to generate transgenic and wildtype littermates.

Creation of Knockout Mice

To generate the conditional knockout construct, the procedures from Copeland and knockouts were adopted (http://recombineering.ncifcrf.gov/default.asp). Only freshly prepared BAC DNA (R24-252B21 was used for StARD5, RP- was used for StARD4, RP23-166M9 was used for ADAM11) (BACPAC Resources, http://bacpac.chori.org) was used for

experiments. After the design of StARD4cko, Joshua Riegelhaupt in our lab took over the project. Primer sequences used for constructing the ADAM11, StARD5, and StARD4 conditional knockout vectors are listed in Table 5.1. PCR amplification was performed using the ROCHE Expand High-Fidelity Taq kit according to the manufacturers'instructions. The PCR products were purified using a QIAGEN spin column, digested with the appropriate restriction enzyme (NEB), and purified again with QIAGEN spin columns. The retrieval vector was generated by mixing 3 μL of PCR product 1 (A-B, NotI/HindIII), 3 μL of PCR product 2 (Y-Z, HindIII, BamHI), 2 μL of MC1TK (PL253, NotI/BamHI), 1 μL of 10x ligation buffer, and 1 μL of T4 DNA ligase. The loxP-Neo-loxP targeting vector was generated by mixing 3 μL of PCR product 1 (C-D, NotI/EcoRI), 3 μL of PCR product 2 (E-F, BamHI/SalI), 2 μL of floxed Neo cassette (PL452, EcoRI/BamHI), 1 μL of pSK+ (NotI/SalI), 1.2 μL of 10x ligation buffer, and 1 μL of T4 DNA ligase. The frt-Neo-frt-loxP targeting vector was generated by mixing 3 μL of PCR product 1 (G-H, NotI/EcoRI), 3 μL of PCR product 2 (I-J, BamHI/SalI), 2 μL of floxed Neo cassette (PL451, EcoRI/BamHI), 1 μL of pSK+ (NotI/SalI), 1.2 μL of 10x ligation buffer, and 1 μL of T4 DNA ligase. The ligation mixtures were incubated at 16°C for 2 h, and 0.5 μL was transformed into electro-competent DH10B cells (Invitrogen). In brief summary of the recombineering to generate the conditional knockouts, 1 μL of fresh BAC DNA (100 ng) was electroporated into EL350 cells and selected by chloramphenicol. These cells were then targeted by electroporation with the modified retrieval vector PL253,

which was digested with HindIII to linearize the plasmid, and were selected by ampicillin. These cells were then targeted by electroporation with the modified minitargeting vector (PL452), which was digested with NotI and SalI to excise the targeting cassette, and were selected by ampicillin and kanamycin. Cre expression in the EL350 strain was induced by arabinose-containing medium, leading to the excision of the floxed Neo cassette, and cells were selected by ampicillin and the loss of resistance to kanamycin. These cells were then targeted by electroporation with the modified minitargeting vector (PL451), which was digested with NotI and SalI to excise the targeting cassette, and were selected by ampicillin and kanamycin. All cloning junctions and loxP and Frt site orientations were sequence-verified, using forward and reverse sequencing primers. For gene targeting, 20 μg of NotI-linearized cko-targeting vector DNA was electroporated into ES cells by The Rockefeller University Gene Targeting Facility. To screen for ES clones with homologous recombination, southern probes upstream and downstream of the targeting construct were designed. For ADAM11, three positive ES clones were injected, one of which led to positive chimeras. For StARD5, five positive ES clones were injected, one of which led to positive chimeras. For StARD4, one positive ES clones was injected and has recently led to a putative positive chimera.

Table 5.1. **Primers for Recombineering**

Primers for Creating StARD5cKO

Primer ID	Primer Description	Sequence
		ataagcggccgcaggcgcgccagggcagcagctggcaagc
A	NotI-AscI-StARD5 promoter for	aataag
B	HindIII-StARD5 promoter rev	gtcaagctttatgttttgatgctggaggcaggcc
C	NotI-StARD5 intron2-3 for	ataagcggccgcgtgcgcacttttaacaaagtctgtc
D	EcoRI-BsrGI-StARD5 intron2-3 rev	gtcgaattctgtacaacacagcttgctagaaacga
E	BamHI-StARD5 intron 2-3 for	ataggatccctgtgaggactttgtacctgtttg
F	SalI-StARD5 intron 2-3 rev	gtcgtcgactggagaggaatttgatccaccgag
G	NotI-StARD5 intron3-4 for	ataagcggccgcaggcaggatttctctgtatagcccag
H	EcoRI-EcoRV-StARD5 intron3-4 rev	gtcgaattcgatatcttccctagaacccacacacaagctg
I	BamHI-StARD5 intron 3-4 for	ataggatccctaagttctgcttctcaccctggca
J	SalI-StARD5 intron 3-4 rev	gtcgtcgacgtgtcagcctgtggatttcctagc
Y	HindIII-StARD5 intron 4-5 for	gtcaagcttagatcttcaaggaaagcttggtg
Z	BamHI-SAlI StARD5 intron 4-5 rev	gtcggatccagtcgaccaggggcagatacagaggaatgac

To introduce ~8.5kb BAC into PL253/Retrieval Vector
AB ~530bp
YZ ~320bp
To introduce loxPNeoLoxP (PL452) into StARD5
CD ~250bp
EF ~180bp
To introduce FrtNeoFrtLoxP (PL451) into StARD5
GH ~250bp
IJ ~180bp

Primers for Creating StARD4cKO

Primer ID	Primer Description	Sequence
A	NotI-StARD4 promoter for	ataatgcggccgcttgatctgtacccgagaggt
B	HindIII-StARD4 promoter rev	gcagaagctttgtagtcaggaaaggccagt
C	NotI-StARD4 intron2-3 for	ataagcggccgcgtgtggaatggatgtacaat
D	EcoRI-StARD4 intron2-3 rev	gcgggaattccgtgtctgatatcagtgcaa
E	BamHI-StARD4 intron 2-3 for	ataaggatccagagcgtgtgagtggacagt
F	SalI-StARD4 intron 2-3 rev	gtcagtcgactttcagtagctcagagatcc
G	NotI-StARD4 intron3-4 for	ttatgcggccgccagagatgaatactcagcat
H	EcoRV-StARD4 intron3-4 rev	ccacgatatccaatcttcctgtccaggtca
I	BamHI-StARD4 intron 3-4 for	ttacggatccgtcagcagtctaggaatgag
J	SalI-StARD4 intron 3-4 rev	atctgtcgacaactaggccagagggcaaat
Y	HindIII-StARD4 intron 4-5 for	gcctaagcttcacacccacacatgagtgaa
Z	BamHI StARD4 intron 4-5 rev	acatggatccctcaacattcagaaggaggg

To inroduce ~8.5kb BAC into PL253/Retrieval Vector
AB ~280bp
YZ ~320bp
To introduce loxPNeoLoxP (PL452) into StARD5
CD ~180bp
EF ~360bp
To introduce FrtNeoFrtLoxP (PL451) into StARD5
GH ~380bp
IJ ~300bp

Table 5.1. continued. **Primers for Recombineering**

Primers for Creating ADAM11cKO

Primer ID	Primer Description	Sequence
A	NotI-AscI-Adam11 intron 2-3 for	ataagcggccgcaggcgcgccagccagcagcccagtgctgg
B	HindIII-Adam11-intron2-3 rev	gtcaagcttttctaagccccttcctttgatcc
C	NotI-Adam11 intron 11-12 for	ataagcggccgcgtccccacactgtaccctgccag
D	EcoRI-DraI-Adam11 intron 11-12 rev	gtcgaattctttaaaacattccctgcacagcccaaggt
E	BamHI-Adam11 intron 11-12 for	ataggatccgctctttgcctttctctgcc
F	SalI-Adam11 intron 11-12 rev	gtcgtcgacgaagggagagagtggtcagg
G	NotI-Adam11 intron 18-19 for	ataagcggccgccccttataagtttggcgctgaagag
H	EcoRI-EcoRV-Adam11 intron 18-19rev	gtcgaattcgatatcagaatacactagacactgggcaggc
I	BamHI-Adam11 intron 18-19 for	ataggatccgatctggtggatcgtaacatgggt
J	SalI-Adam11 intron 18-19 rev	gtcgtcgacgtagcccagagctgagctgaggtt
Y	HindIII-Adam11 intron25-26 for	gtcaagcttcaccctgaactcacacatcactc
Z	BamHI-SalI-Adam11 intron 25-26rev	gtcggatccagtcgaccctaactgcaacgttctggagttcctgg
To introduce ~8.5kb BAC into PL253/Retrieval Vector		
AB	~420bp	
YZ	~230bp	
To introduce loxPNeoLoxP (PL452) into ADAM11		
CD	~160bp	
EF	~160bp	
To introduce FrtNeoFrtLoxP (PL451) into ADAM11		
GH	~200bp	
IJ	~250bp	

Primers for Creating Scavenger Receptor A Enhancer and Promoter -hStARD5

Primer ID	Primer Description	Sequence
		attacccgggatggacccggcgctggcagcccagatga
A	SmaI-hStARD5 ATG	
B	ClaI-hSTARD5 intron 1-2 rev	gatcatcgattccacgaagccgtctccgcgacccctt
Y	ClaI-hSTARD5 fownstream for	gatcatcgattgtgttccaaactccatctgcctg
Z	SalI-hStARD5 downstream rev	gatcgtcgactccccagagttccccatgcagacatga
To introduce ~11.5kb BAC into J900 (SR-A)		
AB	~150bp	
YZ	~500bp	

Genotyping Mice

Animal tail tips were digested with proteinase K, and the extracts were ethanol-precipitated for DNA isolation. The primers and sequence for each PCR are included in Table 5.2

Conditions for genotyping LDLR-/-: 5 min 940C; 10 cycles of 20 sec 950C, 30 sec 640C, 1 min 720C; 30 cycles of 20 sec 950C, 30 sec 580C, 1 min 720C; 5 min 720C

Conditions for genotyping Flp: 5 min 940C; 35 cycles of 30 sec 940C, 1 min 580C, 1 min 720C; 5 min 720C

Conditions for genotyping CMV-Cre: 3 min 940C; 12 cycles of 20 sec 940C, 30 sec 640C, 35 sec 720C; 25 cycles of 20 sec 940C, 30 sec 580C, 35 sec 720C; 5 min 720C

Conditions for genotyping Alb-Cre: 5min 940C; 35 cycles of 30 sec 940C, 1 min 510C, 1 min 720C; 5 min 720C

Conditions for genotyping LysM-Cre: 5min 940C; 35 cycles of 1 min 940C, 1 min 600C, 2 min 720C; 5 min 720C

Conditions for genotyping SR-hD5 transgenics: 5min 940C; 35 cycles of 30 sec 940C, 45 sec 600C, 1:15 min 720C; 5 min 720C

Conditions for genotyping ApoE-hD5 transgenics: 5min 940C; 35 cycles of 30 sec 940C, 1 min 600C, 1 min 720C; 5 min 720C

Conditions for genotyping ADAM11 KO (Sagane): 5min 940C; 35 cycles of

30 sec 950C, 45 sec 610C, 1:30 min 720C; 5 min 720C

Conditions for genotyping ADAM11cko: 5min 940C; 35 cycles of 30 sec 940C, 30 sec 600C, 1:30 min 720C; 5 min 720C. For ADAM11cko southern blotting, genomic DNA was digested with either BamHI (5'probe) or EcoRV (3' probe) and probed with genomic DNA upstream or downstream of the targeted genomic sequence.

Conditions for genotyping StARD5cko: 5min 940C; 35 cycles of 30 sec 940C, 45 sec 600C, 1:30 min 720C; 5 min 720C. For StARD5cko southern blotting, genomic DNA was digested with either BsrGI (5'probe) or BamHI (3'probe) and probed with genomic DNA upstream or downstream of the targeted genomic sequence. All probes were labeled using the Decaprime II Kit (Ambion) and 32P-dATP (GE Healthcare)

Table 5.2. **Sequences of Primers used for Genotyping**

Primers for PCR Genotyping

Genotype		Name of Primer	Sequence
LDLR		IMR59	cgcagtgctcctcatctgacttgt
		IMR46	accccaagacgtgctcccaggatga
		IMR14	aggtgagatgacaggagatc
ACTFLPe		oIMR0042	ctaggccacagaattgaaagatct
		oIMR0043	gtaggtggaaattctagcatcatcc
		oIMR1348	cactgatattgtaagtagttt
		oIMR1349	ctagtgcgaagtagtgatcag
LysM-Cre		Cre8	cccagaaatgccagattacg
		Mlys1	ccttgggctgccagaatttctc
		Mlys2	ttacagtcggccaggctgac
CMV-Cre		oIMR0042	ctaggccacagaattgaaagatct
		oIMR0043	gtaggtggaaattctagcatcatcc
		oIMR0567	accagccagctatcaactcg
		oIMR0568	ttacattggtccagccacc
Alb-Cre		oIMR0042	ctaggccacagaattgaaagatct
		oIMR0043	gtaggtggaaattctagcatcatcc
		oIMR1084	gcggtctggcagtaaaaactatc
		oIMR1085	gtgaaacagcattgctgtcactt
ApoEhD5	a	hApoEexon4 for	taggggtccaccccaggag
		pLIV.7 down-rev	gcagatgcgtgaaacttggtgaatc
	b	hApoE-F234for	atggaattttctatggaggccg
		hd5-176rev	gtcccacacctcctctagtgtcc
	c	hD5-Kpn for	gtcgtggtaccatggacccggcgctggcagc
		hD5-Xho rev	gtcgtctcgagttactcatggaattgcttcactgctttctg
SR-hD5	a	SREPfor	gaagtggataaatcagtgctgc
		hD5int1-2rev	acctccttagctgcgaccac
	b	hD5ex2 for	tagccctgggttgctcaaggaaac
		hD5ex3rev	accggtcacattctcatcccact
ADAM11 KO (Sagane)		Adam1227for	cgaaccgtgcctctctctac
		AdamNeo-1952-for	tgaatgaactgcaggacgag
		Adam1772rev	ctggctcctgcatccaaggggg
ADAM11cKO	deletion	Adam11ex18for	gcggtgaatgagtgtgacattg
		Adam11ex19rev	accgtccagcttgtgaaggttag
		Adam11ex11for	ggttgccatggaaacgtgggca
	floxed	Adam11ex18for	gcggtgaatgagtgtgacattg
		Adam11-2ndloxprev	cgaagttatattatgtacctgactg
	Neo	Adam11ex18for	gcggtgaatgagtgtgacattg
		Adam11neorev	accaaagaacggagccggttgg
StARD5cko	deletion	StARD5ex2for	ggaatcaagtcttgagatctcc
		StARD5ex3for	ctgggaatctgactctagca
		StARD5int3-4rev	ctggtaactgccttgaaagcactg
	floxed	StARD5ex3for	ctgggaatctgactctagca
		StARD5-2ndloxprev	cgaagttatattatgtacctgactg
	Neo	StARD5ex3for	ctgggaatctgactctagca
		StARD5neorev	accaaagaacggagccggttgg

Table 5.2. continued. **Primers for Genotyping**

Primers for Southern Blot

Genotype		Name of Primer	Sequence
StARD5cko	Upstream	5' Upstream For	ggttctgcagtgcctggaatgtcc
		5' Upstream Rev	ccaaatggctccatggaaacaaaatac
	Downstrean	3' Downstream For	ggagcgcagtgtactgcctgag
		3' Downstream Rev	gccttcccagagctgtttggagag
ADAM11cko	Upstream	5' Upstream For	agtgttctgcctctgcccaga
		5' Upstream Rev	gccacaggcccaatcttcttcca

Mouse Plasma, Liver, and Gallbladder Analysis

Plasma was immediately separated by centrifugation. Lipoproteins were isolated by sequential ultracentrifugation from 60 μl of plasma at d <1.006 g/ml [very low-density lipoprotein (VLDL)], 1.006 ≤d ≥1.063 g/ml (intermediate-density lipoprotein and LDL), and d >1.063 g/ml (high-density lipoprotein). The cholesterol in each of these fractions and in the total plasma was assayed enzymatically (Roche/Hitachi) and free cholesterol was measured enzymatically (Wako). The level of cholesterol ester was calculated by subtracting the free cholesterol content from the total cholesterol content. The triglycerides in the total plasma were assayed by enzymatic assay (Roche). For plasma plant sterol measurements, cholesterol, campesterol, sitosterol, stigmasterol, and brassicasterol concentrations in plasma and bile were determined by a recently described liquid chromatography tandem mass spectrometry method in Leipzig, Germany. In this thesis, plasma plant sterol "levels" are expressed as the ratio of absolute plasma plant sterol concentration (in μg/dl) to absolute total plasma cholesterol concentration (in mg/dl). Gallbladder bile was isolated and analyzed for cholesterol, phospholipids, and bile acids by

enzymatic assay (Roche, Sigma). Total liver lipids were extracted according to a modified method from Folch. Briefly, snap-frozen liver tissues (~100 mg) were homogenized and extracted twice with chloroform/methanol (v/v = 2:1) solution. The organic layer was dried under nitrogen gas and resolubilized in chloroform containing 2% Triton X-100. This extract was dried again and resuspended and then assayed for TG and TC concentration using commercial kits as described above. 3HAO activity levels were measured as described by Muller (Muller et al., 2007). Briefly, liver homogenate (3ml) containing 0.01M PBS pH7.4, 10uM 3-HA, 100 uM ferrous sulphate and 100uM ascorbic acid was incubated at 37C for 30min in a shaking water bath. After incubate 2ml HCl (3M) was added to each test tube to terminate the reaction. The resulting precipitate was then centrifuged at 4500xg for 10min. An aliquot of the supernatant from each test tube was removed for spectrophotometric analysis at 360nm. An extinction coefficient of 47500 M-1 cm-1 was used to determine the concentration of 2-amino-3-carboxymuconic semialdehyde.

Quantification of Atherosclerosis

To quantify cross-sectional lesion area in the aortic root, formalin-fixed hearts were embedded in OCT. The heart was oriented so that the three valves of the aortic root were in the same plane and 12mm sections were saved onto glass slides. Sections were stained with oil red O. Lesion area was quantified in every fourth section, and the average was reported for five measurements. To quantify

cross-sectional lesion area in the brachiocephalic artery, the Y-shaped piece of brachiocephalic artery was sectioned distally to proximally at 10mm thickness, beginning from the branch point for the subclavian and carotid arteries. Atherosclerotic lesions lumenal to the internal elastic lamina were quantified by oil red O-stained sections at 200, 400, and 600 mm from the branching point of the brachiocephalic into the carotid and subclavian arteries.

Intraperitoneal Glucose Tolerance Test

For the intraperitoneal glucose tolerance test (IPGTT), mice fasted for 6h following the dark (feeding) cycle. After intraperitoneal injection of of glucose (in physiologic saline) (2g/kg of body weight), blood was drawn from the tail vein at 0, 15, 30, 60 and 120min Blood glucose levels were measured from tail blood using a handheld blood glucometer (Bayer). IPGTT were performed on mice 3-4 days prior to sacrifice. Area under curve (AUC) was calculated using the trapezoidal method.

Culturing Mouse Bone Marrow Macrophages

Macrophages were obtained from mice. The macrophages were harvested from bone marrow of the femur of mice. All macrophages were cultured in Dulbecco's modified Eagle's medium supplemented with 10% FBS and recombinant GM-CSF for two weeks.

Cholesterol Efflux from Bone Marrow Macrophage

Bone marrow macrophages were incubated in 1-2 uCi/ml 3H cholesterol in

minimal essential medium (MEM) containing 10% fetal bovine serum overnight in 12-well plates at 37°C and 5% CO2. The next day, cells were enriched with cholesterol by incubation with acetylated LDL(BTI), 50 ug protein/ml, along with 1-2 uCi/ml 3H cholesterol (GE) in minimal essential medium (MEM) containing 10% fetal bovine serum. The medium was removed and the cells were washed with phosphate-buffered saline (PBS) and incubated with serum free MEM with either no acceptor, lipid free ApoA-I (10ug/ml) (BTI), or HDL (50ug/ml) (BTI). Media with these cholesterol acceptors were added for various lengths of time (4, 8, 24hours), the media was removed, centrifuged, and 100ul aliquots were counted. The cells were dissolved in 0.1M NaOH for several hours and 100ul aliquots were counted. The percent efflux of lipid was calculated as cpm in medium divided by the sum of the cpm in the media and in the cells. Cholesterol efflux experiments were performed in triplicate, and the data (% efflux) are expressed as mean ± SEM for 3-4 animals per genotype.

Eliciting and Culturing Mouse Peritoneal Macrophages

Macrophages were obtained from mice. The macrophages were harvested three to four days after intraperitoneal (i.p.) injection of concanavalin A by peritoneal lavage. All macrophages were cultured in Dulbecco's modified Eagle's medium supplemented with 10% FBS, 1% glutamine, and 20% L-cell conditioned medium for 48-72 h, at which point they were typically at ~90% confluency.

Assay of Macrophage Apoptosis

Procedures were adapted from the Tabas laboratory (Columbia University, New York, NY). Peritoneal macrophages were FC loaded by treating cells with 50 ug/ml ac-LDL and 10ug/ml ACAT inhibitor 58035 (Novartis; gift from Tabas lab) in full media for 14-16 hours. Control cells were treated with either the ACAT inhibitor or the ac-LDL. Midstage and late-stage apoptosis in peritoneal macrophages was assayed by annexin V and propidium iodine staining, respectively, with the Vybrant Apoptosis Assay Kit No. 2 (Molecular Probes, Carlsbad, Calif). At the end of incubation, the macrophages were gently washed once with PBS and incubated for 15 minutes at room temperature with 120 μL annexin-binding buffer (25 mmol/L HEPES, 140 mmol/L NaCl, 1 mmol/L EDTA, pH 7.4, 0.1% BSA) containing 10 μL Alexa Fluor 488–conjugated annexin V and 1 μL of 100-μg/mL propidium iodine. The staining mixture was then removed and replaced with 120 μL annexin-binding buffer. The cells were viewed immediately at room temperature with an inverted fluorescent microscope equipped with filters appropriate for fluorescein and rhodamine, and images were obtained with a camera equipped with imaging software. Three fields of cells ({approx}650 cells per field) were photographed for each condition, and the number of annexin V/propidium iodine–positive cells in each field was counted and expressed as a percent of the total number of cells.

Sample Preparation for Gene Expression Analysis

Total RNA was isolated from cultured cells or tissue using TRIzol reagent

(Invitrogen), followed by RNeasy cleanup (Qiagen), according to the manufacturer's instructions. Total RNA was then subjected to RNeasy Cleanup (Qiagen) for microarray and RT-PCR.

Quantitative RT-PCR

For RT-PCR analysis, RNA was treated with Dnase I (Ambion), and 1-5ug was reverse transcribed using Superscript III (Invitrogen) with oligo-DT primers. A 7700 Sequence Detection System (Applied Biosystems) was used with the default thermal cycling profile (95C for 10 min; 40 cycles of 95C 15sec, 60C 1 min; 4C soak). The quencher dye (TAMRA) was the passive reference. The threshold was set in the linear range of normalized fluorescence, and a threshold cycle (Ct) was measured in each well. Each sample was amplified in duplicate for the genes of interest and the housekeeping gene cyclophilin A. Each cDNA values for genes of interest were normalized to the corresponding value for the housekeeping gene cyclophilinA (Table 5.3) and expressed as a ratio, allowing for variability in the initial quantities of mRNA.

Affymetrix Microarrays

Target Preparation and Hybridization—All protocols were conducted as described in the Affymetrix GeneChip Expression Analysis technical manual with the help of Wenxiang Zhang and Connie Zhoa at the Rockefeller Genomics Facility. Briefly, 10ug of total RNA was converted to first strand cDNA using Superscript II reverse transcriptase primed by a poly(T) oligomer that incorporated the T7

promoter. Second strand cDNA synthesis was followed by in vitro transcription for linear amplification of each transcript and incorporation of biotinylated CTP and UTP. The cRNA products were fragmented to 200 nucleotides or less, heated at 99 °C for 5 min, and hybridized for 16 h at 45 °C to mouse MOE 430A or MOE set 430A&B Affymetrix microarrays. The microarrays were then washed at low (6 SSPE) and high (100 mM MES, 0.1 M NaCl) stringency and stained with streptavidin-phycoerythrin. Fluorescence was amplified by adding biotinylated anti-streptavidin and an additional aliquot of streptavidin-phycoerythrin stain. A confocal scanner was used to collect fluorescence signal at 3-m resolution after excitation at 570 nm. The average signal from two sequential scans was calculated for each microarray feature. Initial Data Analysis—Affymetrix Microarray Suite 5.0 was used to quantitate expression levels for targeted genes; default values provided by Affymetrix were applied to all analysis parameters. Border pixels were removed, and the average intensity of pixels within the 75th percentile was computed for each probe. The average of the lowest 2% of probe intensities occurring in each of 16 microarray sectors was set as background and subtracted from all features in that sector. Probe pairs were scored positive or negative for detection of the targeted sequence by comparing signals from the perfect match and mismatch probe features. The number of probe pairs meeting the default discrimination threshold (0.015) was used to assign a call of absent, present, or marginal for each assayed gene, and a p value was calculated to reflect confidence in the detection call. A

weighted mean of probe fluorescence (corrected for nonspecific signal by subtracting the mismatch probe value) was calculated using the one-step Tukey's biweight estimate. This signal value, a relative measure of the expression level, was computed for each assayed gene. Global scaling was applied to allow comparison of gene signals across multiple microarrays; after exclusion of the highest and lowest 2%, the average total chip signal was calculated and used to determine what scaling factor was required to adjust the chip average to an arbitrary target of 150. All signal values from one microarray were then multiplied by the appropriate scaling factor (Genespring version 6.1 (Silicon Genetics Software)).

Table 5.3. **Primers for TaqMan quantitative RT-PCR**

Gene		Sequence
cyclophilin A	forward	GGCCGATGACGAGCCC
	reverse	TGTCTTTGGAACTTTGTCTGCAA
	probe	6FAM-TGGGCCGCGTCTCCTTCGA
StARD5(1)	forward 1	GACGCGTCGGGCTGG
	reverse 1	AACTCCTCAGATGGCCTCCA
	probe 1	6FAM-TGTCGGGAAGGCAATGGAGTTTCAA
StARD5(2)	forward 1	TGGCACCATCAGCTCCAAT
	reverse 1	TCTCACAAAACCGGGCTTTG
	probe 1	6FAM-CCCATGTGGAACATCCATTGTGTCCC
hStARD5	forward 1	TGTGACCGGTTTTGAAATTATCC
human	reverse 1	GCGGAGGGAGTGGAGGTT
	probe 1	6FAM-GCGGAGGGAGTGGAGGTT
StARD4 (1)	forward 1	GAGAGATGGCTGACCCTGAGA
	reverse 1	TCAGACAGTCCTTCCAGTTTGATC
	probe 1	6FAM-CCCGTGGTCACAGATTGGCAGGA
StARD4 (2)	forward 1	TGCCGTGGTTTGCGG
	reverse 1	AGGCAGGAACATGGCTTCTCTA
	probe 1	6FAM-CTCTGCTCCTACCCTGTCAGCTCCATGA
ADAM11 (1)	forward 1	TGCCGGCCACGTCATC
	reverse 1	CCCGGTCAACAGAATGCAA
	probe 1	6FAM-TCCCGCTGTCCTTGTCTCCATTTCATC
ADAM11 (2)	forward 1	TCAAGCCAGTGTCCCCCTAA
	reverse 1	TACAGCGGCCTCCATAGCA
	probe 1	6FAM-AAGCTGGACGGTTACTACTGTGATCATGAGCA

All primers and probes are to mouse genes unless indicated
All probes are labeled at the 5' end with 6'FAM and at the 3' end with TAMRA
Parenthesis indicates an alternative primer and probe for a given gene

Western Blotting

Proteins were isolated from cells or mouse tissues by homogenization in RIPA buffer (50 mM Tris, pH 7.4/150 mM NaCl/1 mM EDTA/0.1% SDS/1% Triton X-100/1% deoxycholate) with complete mini protease inhibitor cocktail (Roche). Crude extracts were centrifuged at 16,000 x g for 10 min to pellet cellular debris and nuclei. Protein concentration was measured by the BCA assay (Pierce), and 5–50 μg of protein (depending on experiment) was electrophoresed for Western blotting. The following dilutions were used: anti-ADAM11a, 1:1,000(gift from Sagane); anti-StARD5(PTG), 1:200; anti-GFP (Clontech), 1:2000, and anti--tubulin (Sigma), 1:10,000; anti-beta actin (Sigma), 1:10,000. For the detection of antibody protein complexes, the SuperSignal West Pico or Femto Kit (Pierce) was used according to the manufacturer's instructions. Band intensities were measured by using IMAGE Pro Plus.

Contextual Fear Conditioning

In collaboration with Erin Norris from the Strickland lab at Rockefeller University, mice were not disturbed for 2 weeks before experimentation to ensure that control animals were nonstressed. All experiments were conducted during the light cycle. Each conditioning chamber was equipped with a speaker, house light, and a video camera. The chamber floors consisted of rods that were connected to a shock generator. Mice were habituated to the behavioral room for 2 hours on the day of training. During habituation to the room, mice were placed individually into

the conditioning chambers to expose them to a different territory. During the training day, mice were placed individually into a conditioning chamber cleaned with an ammonia-based solution for 2 minutes, during which time is considered the "baseline period". Mice were then exposed to three tone-footshock pairings (tone, 20 sec, 85 dB, 3.5 kHz; footshock, 1 sec, 0.6 mA) with an intertrial interval of 60 seconds. Upon completion of training, mice were returned to their home cages and room to be tested 24 hrs later. The training sessions were video recorded in order to analyze the animals'baseline freezing behavior (every 5 seconds) during training. During the testing day, mice were habituated to the behavioral room for 2 hours. Mice were then placed individually into the same chamber (same scent, lighting, etc) as the previous day for a 2 minute period, during which time their behavior was recorded. Freezing behavior, or the complete lack of movement in response to the context, was scored every 5 seconds. After the contextual testing is completed, the shape, floor, and walls of the chamber is altered significantly, and the ammonia fragrance is replaced with an ethanol-based scent. The mice are placed into this novel context for 2 minutes, during which time they will be exposed to the tone (85 dB, 3.5 kHz) for 60 seconds. During this testing period, the mice will be scored every 5 seconds for freezing behavior, first prior to the tone, which ensures that the mice are not freezing to the new context, and during the tone.

Electroencephalographic (EEG) recordings

In collaboration with Dr. Noebels (Baylor, Texas, USA) adult ADAM11-/- and

ADAM11+/+ littermate mice (aged 3-5 months) were implanted for EEG recordings

Yeast Two Hybrid

In collaboration with the Duke YMSG facility, the two cytoplasmic tails of ADAM11 were cloned onto a Gal4 DNA binding domain (BD)(pGBT9).

The sequence that was used:

ADAM11a: GGCGGCACGGGCTGGGGATTTAAAAACATCCGTCGTGG

AAGGTACGACCCGACCCAGCAGGGGGCAGTGTGA

ADAM11b: GGCGGCACGGGCTGGGGATTTAAAAACATCCGTCGTGG

AAGGTCCGGAGGGGCCTAA

These vectors were transformed into yeast containing a library of mouse liver proteins fused to the Gal4 activation domain (AD). Positive interactions were detected by growth on plates with a selectable markers.

StARD5 Complementation Experiments

In collaboration with Steve Sturley (Columbia University, NY, NY), GFP-tagged human StARD5 was cloned into pRS426 and transfected into yeast strains: wildtype, upc2.1, and arv1. Yeast strains were grown in either YEPD (1% yeast extract, 2% bacto-peptone, 2% glucose) or in synthetic minimal media containing 0.67% Yeast Nitrogen Base (Difco) supplemented with the appropriate amino acids and adenine. Yeast transformations were performed using standard procedures. For routine propagation of plasmids, Escherichia coli XL1Blue cells were used and grown in Luria broth medium supplemented with ampicillin (200 μg/ml). Neutral lipid

radiolabeling and TLC analysis was performed using standard conditions.

Data and Statistical Analysis

All data are expressed as mean ± SEM. Statistical analysis was performed using SPSS. Because normality could not be assessed for our small sample sizes and non-normal distributions have been reported in previous larger atherosclerosis studies in mice, the non-parametric Mann-Whitney test was used to test significance. Significance is indicated by an asterisk in the figures/tables.

References

Adams, S.H., Chui, C., Schilbach, S.L., Yu, X.X., Goddard, A.D., Grimaldi, J.C., Lee, J., Dowd, P., Colman, S., and Lewin, D.A. (2001). BFIT, a unique acyl-CoA thioesterase induced in thermogenic brown adipose tissue: cloning, organization of the human gene and assessment of a potential link to obesity. Biochem J 360, 135-142.

Ainola, M., Li, T.F., Mandelin, J., Hukkanen, M., Choi, S.J., Salo, J., and Konttinen, Y.T. (2008). Involvement of ADAM8 in osteoclastogenesis and pathological bone destruction. Ann Rheum Dis.

Al-Fakhri, N., Wilhelm, J., Hahn, M., Heidt, M., Hehrlein, F.W., Endisch, A.M., Hupp, T., Cherian, S.M., Bobryshev, Y.V., Lord, R.S., et al. (2003). Increased expression of disintegrin-metalloproteinases ADAM-15 and ADAM-9 following upregulation of integrins alpha5beta1 and alphavbeta3 in atherosclerosis. J Cell Biochem 89, 808-823.

Alberti, S., Schuster, G., Parini, P., Feltkamp, D., Diczfalusy, U., Rudling, M., Angelin, B., Bjorkhem, I., Pettersson, S., and Gustafsson, J.A. (2001). Hepatic cholesterol metabolism and resistance to dietary cholesterol in LXRbetaeta-deficient mice. J Clin Invest 107, 565-573.

Alpy, F., and Tomasetto, C. (2005). Give lipids a START: the StAR-related lipid transfer (START) domain in mammals. J Cell Sci 118, 2791-2801.

Alpy, F., and Tomasetto, C. (2006). MLN64 and MENTHO, two mediators of endosomal cholesterol transport. Biochem Soc Trans 34, 343-345.

Alpy, F., Wendling, C., Rio, M.C., and Tomasetto, C. (2002). MENTHO, a MLN64 homologue devoid of the START domain. J Biol Chem 277, 50780-50787.

Amour, A., Knight, C.G., English, W.R., Webster, A., Slocombe, P.M., Knäuper, V., Docherty, A.J., Becherer, J.D., Blobel, C.P., and Murphy, G. (2002). The enzymatic activity of ADAM8 and ADAM9 is not regulated by TIMPs. FEBS Lett 524, 154-158.

Anderson, R.N. (2001). Deaths: Leading causes for 1999. National Vital Statistics Reports 49, 1-88.

Arakane, F., Kallen, C.B., Watari, H., Foster, J.A., Sepuri, N.B., Pain, D., Stayrook, S.E., Lewis, M., Gerton, G.L., and Strauss, J.F. (1998a). The mechanism of action of steroidogenic acute regulatory protein (StAR). StAR acts on the outside of mitochondria to stimulate steroidogenesis. J Biol Chem 273, 16339-16345.

Arakane, F., Kallen, C.B., Watari, H., Stayrook, S.E., Lewis, M., and Strauss, J.F. (1998b). Steroidogenic acute regulatory protein (StAR) acts on the outside of mitochondria to stimulate steroidogenesis. Endocr Res 24, 463-468.

Atshaves, B.P., Jefferson, J.R., McIntosh, A.L., Gallegos, A., McCann, B.M., Landrock, K.K., Kier, A.B., and Schroeder, F. (2007a). Effect of sterol carrier protein-2 expression on sphingolipid distribution in plasma membrane lipid rafts/caveolae. Lipids 42, 871-884.

Atshaves, B.P., McIntosh, A.L., Landrock, D., Payne, H.R., Mackie, J.T., Maeda, N., Ball, J., Schroeder, F., and Kier, A.B. (2007b). Effect of SCP-x gene ablation on branched-chain fatty acid metabolism. Am J Physiol Gastrointest Liver Physiol 292, G939-951.

Atshaves, B.P., McIntosh, A.L., Payne, H.R., Gallegos, A.M., Landrock, K., Maeda, N., Kier, A.B., and Schroeder, F. (2007c). SCP-2/SCP-x gene ablation alters lipid raft domains in primary cultured mouse hepatocytes. J Lipid Res 48, 2193-2211.

Back, S.H., Schroder, M., Lee, K., Zhang, K., and Kaufman, R.J. (2005). ER stress signaling by regulated splicing: IRE1/HAC1/XBP1. Methods 35, 395-416.

Baez, J.M., Barbour, S.E., and Cohen, D.E. (2002). Phosphatidylcholine transfer protein promotes apolipoprotein A-I-mediated lipid efflux in Chinese hamster ovary cells. J Biol Chem 277, 6198-6206.

Baez, J.M., Tabas, I., and Cohen, D.E. (2005). Decreased lipid efflux and increased susceptibility to cholesterol-induced apoptosis in macrophages lacking phosphatidylcholine transfer protein. Biochem J 388, 57-63.

Baum, C.L., Reschly, E.J., Gayen, A.K., Groh, M.E., and Schadick, K. (1997). Sterol carrier protein-2 overexpression enhances sterol cycling and inhibits cholesterol ester synthesis and high density lipoprotein cholesterol secretion. J Biol Chem 272, 6490-6498.

Beh, C.T., and Rine, J. (2004). A role for yeast oxysterol-binding protein homologs in endocytosis and in the maintenance of intracellular sterol-lipid distribution. J Cell Sci 117, 2983-2996.

Bengoechea-Alonso, M.T., and Ericsson, J. (2007). SREBP in signal transduction: cholesterol metabolism and beyond. Curr Opin Cell Biol 19, 215-222.

Bièche, I., Tomasetto, C., Régnier, C.H., Moog-Lutz, C., Rio, M.C., and Lidereau, R. (1996). Two distinct amplified regions at 17q11-q21 involved in human primary breast cancer. Cancer Res 56, 3886-3890.

Blobel, C.P. (2005). ADAMs: key components in EGFR signalling and development. Nat Rev Mol Cell Biol 6, 32-43.

Bose, H., Lingappa, V.R., and Miller, W.L. (2002). Rapid regulation of steroidogenesis by mitochondrial protein import. Nature 417, 87-91.

Brewer, J.W., and Diehl, J.A. (2000). PERK mediates cell-cycle exit during the mammalian unfolded protein response. Proc Natl Acad Sci U S A 97, 12625-12630.

Brown, A.J., Sun, L., Feramisco, J.D., Brown, M.S., and Goldstein, J.L. (2002). Cholesterol addition to ER membranes alters conformation of SCAP, the SREBP escort protein that regulates cholesterol metabolism. Mol Cell 10, 237-245.

Brown, M.S., and Goldstein, J.L. (1999). A proteolytic pathway that controls the cholesterol content of membranes, cells, and blood. Proc Natl Acad Sci U S A 96, 11041-11048.

Brügger, B., Sandhoff, R., Wegehingel, S., Gorgas, K., Malsam, J., Helms, J.B., Lehmann, W.D., Nickel, W., and Wieland, F.T. (2000). Evidence for segregation of sphingomyelin and cholesterol during formation of COPI-coated vesicles. J Cell Biol 151, 507-518.

Cai, H., Kratzschmar, J., Alfandari, D., Hunnicutt, G., and Blobel, C.P. (1998). Neural crest-specific and general expression of distinct metalloprotease-disintegrins in early Xenopus laevis development. Dev Biol 204, 508-524.

Cal, S., Freije, J.M., López, J.M., Takada, Y., and López-Otín, C. (2000). ADAM 23/MDC3, a human disintegrin that promotes cell adhesion via interaction with the alphavbeta3 integrin through an RGD-independent mechanism. Mol Biol Cell 11, 1457-1469.

Canault, M., Peiretti, F., Kopp, F., Bonardo, B., Bonzi, M.F., Coudeyre, J.C., Alessi, M.C., Juhan-Vague, I., and Nalbone, G. (2006). The TNF alpha converting enzyme (TACE/ADAM17) is expressed in the atherosclerotic lesions of apolipoprotein E-deficient mice: possible contribution to elevated plasma levels of soluble TNF alpha receptors. Atherosclerosis 187, 82-91.

Canault, M., Peiretti, F., Poggi, M., Mueller, C., Kopp, F., Bonardo, B., Bastelica, D., Nicolay, A., Alessi, M.C., and Nalbone, G. (2008). Progression of atherosclerosis in ApoE-deficient mice that express distinct molecular forms of TNF-alpha. J Pathol 214, 574-583.

Cao, G., Beyer, T.P., Yang, X.P., Schmidt, R.J., Zhang, Y., Bensch, W.R., Kauffman, R.F., Gao, H., Ryan, T.P., Liang, Y., et al. (2002). Phospholipid transfer protein is regulated by liver X receptors in vivo. J Biol Chem 277, 39561-39565.

Caron, K.M., Soo, S.C., and Parker, K.L. (1998). Targeted disruption of StAR provides novel insights into congenital adrenal hyperplasia. Endocr Res 24, 827-834.

Caron, K.M., Soo, S.C., Wetsel, W.C., Stocco, D.M., Clark, B.J., and Parker, K.L. (1997). Targeted disruption of the mouse gene encoding steroidogenic acute regulatory protein provides insights into congenital lipoid adrenal hyperplasia. Proc Natl Acad Sci USA 94, 11540-11545.

Chang, I.Y., Kim, J.H., Hwang, G., Song, P.I., Song, R.J., Kim, J.W., and Yoon, S.P. (2007). Immunohistochemical detection of StarD6 in the rat nervous system. Neuroreport 18, 1615-1619.

Charrier-Hisamuddin, L., Laboisse, C.L., and Merlin, D. (2008). ADAM-15: a metalloprotease that mediates inflammation. Faseb J 22, 641-653.

Charruyer, A., Bell, S.M., Kawano, M., Douangpanya, S., Yen, T.Y., Macher, B.A., Kumagai, K., Hanada, K., Holleran, W.M., and Uchida, Y. (2008). Decreased Ceramide Transport Protein (CERT) Function Alters Sphingomyelin Production following UVB Irradiation. J Biol Chem 283, 16682-16692.

Chen, C., Huang, X., and Sheppard, D. (2006). ADAM33 is not essential for growth and development and does not modulate allergic asthma in mice. Mol Cell Biol 26, 6950-6956.

Cheruku, S.R., Xu, Z., Dutia, R., Lobel, P., and Storch, J. (2006). Mechanism of cholesterol transfer from the Niemann-Pick type C2 protein to model membranes supports a role in lysosomal cholesterol transport. J Biol Chem 281, 31594-31604.

Ching, Y.P., Wong, C.M., Chan, S.F., Leung, T.H., Ng, D.C., Jin, D.Y., and Ng, I.O. (2003). Deleted in liver cancer (DLC) 2 encodes a RhoGAP protein with growth suppressor function and is underexpressed in hepatocellular carcinoma. J Biol Chem 278, 10824-10830.

Cho, C., Bunch, D.O., Faure, J.E., Goulding, E.H., Eddy, E.M., Primakoff, P., and Myles, D.G. (1998). Fertilization defects in sperm from mice lacking fertilin beta. Science 281, 1857-1859.

Clark, B.J., Soo, S.C., Caron, K.M., Ikeda, Y., Parker, K.L., and Stocco, D.M. (1995). Hormonal and developmental regulation of the steroidogenic acute regulatory protein. Mol Endocrinol 9, 1346-1355.

Clark, B.J., and Stocco, D.M. (1995). Expression of the steroidogenic acute regulatory (StAR) protein: a novel LH-induced mitochondrial protein required for the acute regulation of steroidogenesis in mouse Leydig tumor cells. Endocr Res 21, 243-257.

Clark, B.J., Wells, J., King, S.R., and Stocco, D.M. (1994). The purification, cloning, and expression of a novel luteinizing hormone-induced mitochondrial protein in MA-10 mouse Leydig tumor cells. Characterization of the steroidogenic acute regulatory protein (StAR). J Biol Chem 269, 28314-28322.

Cohen, A.W., Hnasko, R., Schubert, W., and Lisanti, M.P. (2004). Role of caveolae and caveolins in health and disease. Physiol Rev 84, 1341-1379.

Collier, F.M., Gregorio-King, C.C., Apostolopoulos, J., Walder, K., and Kirkland, M.A. (2003). ORP3 splice variants and their expression in human tissues and hematopoietic cells. DNA Cell Biol 22, 1-9.

Collins, J.L., Fivush, A.M., Watson, M.A., Galardi, C.M., Lewis, M.C., Moore, L.B., Parks, D.J., Wilson, J.G., Tippin, T.K., Binz, J.G., et al. (2002). Identification of a nonsteroidal liver X receptor agonist through parallel array synthesis of tertiary amines. J Med Chem 45, 1963-1966.

Cornwall, G.A., and Hsia, N. (1997). ADAM7, a member of the ADAM (a disintegrin and metalloprotease) gene family is specifically expressed in the mouse anterior pituitary and epididymis. Endocrinology 138, 4262-4272.

Costet, P., Luo, Y., Wang, N., and Tall, A.R. (2000). Sterol-dependent transactivation of the ABC1 promoter by the liver X receptor/retinoid X receptor. J Biol Chem 275, 28240-28245.

de Brouwer, A.P., Westerman, J., Kleinnijenhuis, A., Bevers, L.E., Roelofsen, B., and Wirtz, K.W. (2002). Clofibrate-induced relocation of phosphatidylcholine transfer protein to mitochondria in endothelial cells. Exp Cell Res 274, 100-111.

Del Mastro, R.G., Turenne, L., Giese, H., Keith, T.P., Van Eerdewegh, P., May, K.J., and Little, R.D. (2007). Mechanistic role of a disease-associated genetic variant within the ADAM33 asthma susceptibility gene. BMC Med Genet 8, 46.

Devries-Seimon, T., Li, Y., Yao, P.M., Stone, E., Wang, Y., Davis, R.J., Flavell, R., and Tabas, I. (2005). Cholesterol-induced macrophage apoptosis requires ER stress pathways and engagement of the type A scavenger receptor. J Cell Biol 171, 61-73.

Dolley, G., Berthier, M.T., Lamarche, B., Després, J.P., Bouchard, C., Pérusse, L., and Vohl, M.C. (2007). Influences of the phosphatidylcholine transfer protein gene variants on the LDL peak particle size. Atherosclerosis.

Dressman, M.A., Baras, A., Malinowski, R., Alvis, L.B., Kwon, I., Walz, T.M., and Polymeropoulos, M.H. (2003). Gene expression profiling detects gene amplification and differentiates tumor types in breast cancer. Cancer Res 63, 2194-2199.

Durand, S., Angeletti, S., and Genti-Raimondi, S. (2004). GTT1/StarD7, a novel phosphatidylcholine transfer protein-like highly expressed in gestational trophoblastic tumour: cloning and characterization. Placenta 25, 37-44.

Durkin, M.E., Avner, M.R., Huh, C.G., Yuan, B.Z., Thorgeirsson, S.S., and Popescu, N.C. (2005). DLC-1, a Rho GTPase-activating protein with tumor suppressor function, is essential for embryonic development. FEBS Lett 579, 1191-1196.

Durkin, M.E., Ullmannova, V., Guan, M., and Popescu, N.C. (2007a). Deleted in liver cancer 3 (DLC-3), a novel Rho GTPase-activating protein, is downregulated in cancer and inhibits tumor cell growth. Oncogene 26, 4580-4589.

Durkin, M.E., Yuan, B.Z., Zhou, X., Zimonjic, D.B., Lowy, D.R., Thorgeirsson, S.S., and Popescu, N.C. (2007b). DLC-1:a Rho GTPase-activating protein and tumour suppressor. J Cell Mol Med 11, 1185-1207.

Eastman, C.L., Urbańska, E.M., Chapman, A.G., and Schwarcz, R. (1994). Differential expression of the astrocytic enzymes 3-hydroxyanthranilic acid oxygenase, kynurenine aminotransferase and glutamine synthetase in seizure-prone and non-epileptic mice. Epilepsy Res 18, 185-194.

Eberlé, D., Hegarty, B., Bossard, P., Ferré, P., and Foufelle, F. (2004). SREBP transcription factors: master regulators of lipid homeostasis. Biochimie 86, 839-848.

Ebisuno, S., Isohashi, F., Nakanishi, Y., and Sakamoto, Y. (1988). Acetyl-CoA hydrolase: relation between activity and cholesterol metabolism in rat. Am J Physiol 255, R724-730.

Edwards, P.A., Kast, H.R., and Anisfeld, A.M. (2002). BAREing it all: the adoption of LXR and FXR and their roles in lipid homeostasis. J Lipid Res 43, 2-12.

Espenshade, P.J., and Hughes, A.L. (2007). Regulation of sterol synthesis in eukaryotes. Annu Rev Genet 41, 401-427.

Evans, J.P., Schultz, R.M., and Kopf, G.S. (1997). Characterization of the binding of recombinant mouse sperm fertilin alpha subunit to mouse eggs: evidence for function as a cell adhesion molecule in sperm-egg binding. Dev Biol 187, 94-106.

Fairn, G.D., and McMaster, C.R. (2008). Emerging roles of the oxysterol-binding protein family in metabolism, transport, and signaling. Cell Mol Life Sci 65, 228-236.

Feng, B., Zhang, D., Kuriakose, G., Devlin, C.M., Kockx, M., and Tabas, I. (2003). Niemann-Pick C heterozygosity confers resistance to lesional necrosis and macrophage apoptosis in murine atherosclerosis. Proc Natl Acad Sci USA 100, 10423-10428.

Feng, B., and Tabas, I. (2002). ABCA1-mediated cholesterol efflux is defective in free cholesterol-loaded macrophages. Mechanism involves enhanced ABCA1 degradation in a process requiring full NPC1 activity. J Biol Chem 277, 43271-43280.

Feng, B., Yao, P.M., Li, Y., Devlin, C.M., Zhang, D., Harding, H.P., Sweeney, M., Rong, J.X., Kuriakose, G., Fisher, E.A., et al. (2003). The endoplasmic reticulum is the site of cholesterol-induced cytotoxicity in macrophages. Nat Cell Biol 5, 781-792.

Fourie, A.M., Coles, F., Moreno, V., and Karlsson, L. (2003). Catalytic activity of ADAM8, ADAM15, and MDC-L (ADAM28) on synthetic peptide substrates and in ectodomain cleavage of CD23. J Biol Chem 278, 30469-30477.

Frank, P.G., Lee, H., Park, D.S., Tandon, N.N., Scherer, P.E., and Lisanti, M.P. (2004). Genetic ablation of caveolin-1 confers protection against atherosclerosis. Arterioscler Thromb Vasc Biol 24, 98-105.

Frank, P.G., Pedraza, A., Cohen, D.E., and Lisanti, M.P. (2001). Adenovirus-mediated expression of caveolin-1 in mouse liver increases plasma high-density lipoprotein levels. Biochemistry 40, 10892-10900.

Friedland, N., Liou, H.L., Lobel, P., and Stock, A.M. (2003). Structure of a cholesterol-binding protein deficient in Niemann-Pick type C2 disease. Proc Natl Acad Sci USA 100, 2512-2517.

Fu, X., Menke, J.G., Chen, Y., Zhou, G., MacNaul, K.L., Wright, S.D., Sparrow, C.P., and Lund, E.G. (2001). 27-hydroxycholesterol is an endogenous ligand for liver X receptor in cholesterol-loaded cells. J Biol Chem 276, 38378-38387.

Fuchs, M., Hafer, A., Münch, C., Kannenberg, F., Teichmann, S., Scheibner, J., Stange, E.F., and Seedorf, U. (2001). Disruption of the sterol carrier protein 2 gene in mice impairs biliary lipid and hepatic cholesterol metabolism. J Biol Chem 276, 48058-48065.

Fukata, Y., Adesnik, H., Iwanaga, T., Bredt, D.S., Nicoll, R.A., and Fukata, M. (2006). Epilepsy-related ligand/receptor complex LGI1 and ADAM22 regulate synaptic transmission. Science 313, 1792-1795.

Gallegos, A.M., Atshaves, B.P., Storey, S.M., McIntosh, A.L., Petrescu, A.D., and Schroeder, F. (2001). Sterol carrier protein-2 expression alters plasma membrane lipid distribution and cholesterol dynamics. Biochemistry 40, 6493-6506.

Giussani, P., Colleoni, T., Brioschi, L., Bassi, R., Hanada, K., Tettamanti, G., Riboni, L., and Viani, P. (2008). Ceramide traffic in C6 glioma cells: evidence for CERT-dependent and independent transport from ER to the Golgi apparatus. Biochim Biophys Acta 1781, 40-51.

Gomes, C., Oh, S.D., Kim, J.W., Chun, S.Y., Lee, K., Kwon, H.B., and Soh, J. (2005). Expression of the putative sterol binding protein Stard6 gene is male germ cell specific. Biol Reprod 72, 651-658.

Guan, M., Tripathi, V., Zhou, X., and Popescu, N.C. (2008). Adenovirus-mediated restoration of expression of the tumor suppressor gene DLC1 inhibits the proliferation and tumorigenicity of aggressive, androgen-independent human prostate cancer cell lines: prospects for gene therapy. Cancer Gene Ther 15, 371-381.

Guo, L.T., Shelton, G.D., Wewer, U.M., and Engvall, E. (2005). ADAM12 overexpression does not improve outcome in mice with laminin alpha2-deficient muscular dystrophy. Neuromuscul Disord 15, 786-789.

Halama, N., Grauling-Halama, S.A., and Jäger, D. (2006). Identification and characterization of the human StARD9 gene in the LGMD2A-region on chromosome 15q15 by in silico methods. Int J Mol Med 18, 653-656.

Han, S., Liang, C.P., DeVries-Seimon, T., Ranalletta, M., Welch, C.L., Collins-Fletcher, K., Accili, D., Tabas, I., and Tall, A.R. (2006). Macrophage insulin receptor deficiency increases ER stress-induced apoptosis and necrotic core formation in advanced atherosclerotic lesions. Cell Metab 3, 257-266.

Hanada, K., Kumagai, K., Tomishige, N., and Kawano, M. (2007). CERT and intracellular trafficking of ceramide. Biochim Biophys Acta 1771, 644-653.

Hanada, K., Kumagai, K., Yasuda, S., Miura, Y., Kawano, M., Fukasawa, M., and Nishijima, M. (2003). Molecular machinery for non-vesicular trafficking of ceramide. Nature 426, 803-809.

Hartmann, D., de Strooper, B., Serneels, L., Craessaerts, K., Herreman, A., Annaert, W., Umans, L., Lübke, T., Lena Illert, A., von Figura, K., et al. (2002). The disintegrin/metalloprotease ADAM 10 is essential for Notch signalling but not for alpha-secretase activity in fibroblasts. Hum Mol Genet 11, 2615-2624.

Hatch, G.M., Gu, Y., Xu, F.Y., Cizeau, J., Neumann, S., Park, J.S., Loewen, S., and Mowat, M.R. (2008). StARD13(Dlc-2) RhoGap Mediates Ceramide Activation of Phosphatidylglycerolphosphate Synthase and Drug Response in Chinese Hamster Ovary Cells. Mol Biol Cell 19, 1083-1092.

Hauet, T., Yao, Z.X., Bose, H.S., Wall, C.T., Han, Z., Li, W., Hales, D.B., Miller, W.L., Culty, M., and Papadopoulos, V. (2005). Peripheral-type benzodiazepine receptor-mediated action of steroidogenic acute regulatory protein on cholesterol entry into leydig cell mitochondria. Mol Endocrinol 19, 540-554.

Haze, K., Yoshida, H., Yanagi, H., Yura, T., and Mori, K. (1999). Mammalian transcription factor ATF6 is synthesized as a transmembrane protein and activated by proteolysis in response to endoplasmic reticulum stress. Mol Biol Cell 10, 3787-3799.

Herren, B., Raines, E.W., and Ross, R. (1997). Expression of a disintegrin-like protein in cultured human vascular cells and in vivo. Faseb J 11, 173-180.

Hirao, T., Nanba, D., Tanaka, M., Ishiguro, H., Kinugasa, Y., Doki, Y., Yano, M., Matsuura, N., Monden, M., and Higashiyama, S. (2006). Overexpression of ADAM9 enhances growth factor-mediated recycling of E-cadherin in human colon cancer cell line HT29 cells. Exp Cell Res 312, 331-339.

Holdt, L.M., Thiery, J., Breslow, J.L., and Teupser, D. (2008). Increased ADAM17 mRNA expression and activity is associated with atherosclerosis resistance in LDL-receptor deficient mice. Arterioscler Thromb Vasc Biol 28, 1097-1103.

Holgate, S.T., Yang, Y., Haitchi, H.M., Powell, R.M., Holloway, J.W., Yoshisue, H., Pang, Y.Y., Cakebread, J., and Davies, D.E. (2006). The genetics of asthma: ADAM33 as an example of a susceptibility gene. Proceedings of the American Thoracic Society 3, 440-443.

Hölttä-Vuori, M., Alpy, F., Tanhuanpää, K., Jokitalo, E., Mutka, A.L., and Ikonen, E. (2005). MLN64 is involved in actin-mediated dynamics of late endocytic organelles. Mol Biol Cell 16, 3873-3886.

Homma, Y., and Emori, Y. (1995). A dual functional signal mediator showing RhoGAP and phospholipase C-delta stimulating activities. Embo J 14, 286-291.

Horiuchi, K., Weskamp, G., Lum, L., Hammes, H.P., Cai, H., Brodie, T.A., Ludwig, T., Chiusaroli, R., Baron, R., Preissner, K.T., et al. (2003). Potential role for ADAM15 in pathological neovascularization in mice. Mol Cell Biol 23, 5614-5624.

Horton, J.D., Goldstein, J.L., and Brown, M.S. (2002). SREBPs: activators of the complete program of cholesterol and fatty acid synthesis in the liver. J Clin Invest 109, 1125-1131.

Horton, J.D., Shimomura, I., Brown, M.S., Hammer, R.E., Goldstein, J.L., and Shimano, H. (1998). Activation of cholesterol synthesis in preference to fatty acid synthesis in liver and adipose tissue of transgenic mice overproducing sterol regulatory element-binding protein-2. J Clin Invest 101, 2331-2339.

Howard, L., Maciewicz, R.A., and Blobel, C.P. (2000). Cloning and characterization of ADAM28: evidence for autocatalytic pro-domain removal and for cell surface localization of mature ADAM28. Biochem J 348 Pt 1, 21-27.

Hu, X., Li, S., Wu, J., Xia, C., and Lala, D.S. (2003). Liver X receptors interact with corepressors to regulate gene expression. Mol Endocrinol 17, 1019-1026.

Hyman, E., Kauraniemi, P., Hautaniemi, S., Wolf, M., Mousses, S., Rozenblum, E., Ringnér, M., Sauter, G., Monni, O., Elkahloun, A., et al. (2002). Impact of DNA amplification on gene expression patterns in breast cancer. Cancer Res 62, 6240-6245.

Hynynen, R., Laitinen, S., Käkelä, R., Tanhuanpää, K., Lusa, S., Ehnholm, C., Somerharju, P., Ikonen, E., and Olkkonen, V.M. (2005). Overexpression of OSBP-related protein 2 (ORP2) induces changes in cellular cholesterol metabolism and enhances endocytosis. Biochem J 390, 273-283.

Ikonen, E. (2006). Mechanisms for cellular cholesterol transport: defects and human disease. Physiol Rev 86, 1237-1261.

Ikonen, E. (2008). Cellular cholesterol trafficking and compartmentalization. Nat Rev Mol Cell Biol 9, 125-138.

Isohashi, F., Nakanishi, Y., and Sakamoto, Y. (1983a). Effects of nucleotides on a cold labile acetyl-CoA hydrolase from the supernatant fraction of rat liver. Biochemistry 22, 584-590.

Isohashi, F., Nakanishi, Y., and Sakamoto, Y. (1983b). Factors affecting the cold inactivation of an acetyl-coenzyme-A hydrolase purified from the supernatant fraction of rat liver. Eur J Biochem 134, 447-452.

Johansson, M., Bocher, V., Lehto, M., Chinetti, G., Kuismanen, E., Ehnholm, C., Staels, B., and Olkkonen, V.M. (2003). The two variants of oxysterol binding protein-related protein-1 display different tissue expression patterns, have different intracellular localization, and are functionally distinct. Mol Biol Cell 14, 903-915.

Joseph, S.B., Bradley, M.N., Castrillo, A., Bruhn, K.W., Mak, P.A., Pei, L., Hogenesch, J., O'Connell R, M., Cheng, G., Saez, E., et al. (2004). LXR-dependent gene expression is important for macrophage survival and the innate immune response. Cell 119, 299-309.

Käkelä, R., Tanhuanpää, K., Laitinen, S., Somerharju, P., and Olkkonen, V.M. (2005). Overexpression of OSBP-related protein 2 (ORP2) in CHO cells induces alterations of phospholipid species composition. Biochem Cell Biol 83, 677-683.

Kanno, K., Wu, M., Scapa, E., Roderick, S., and Cohen, D. (2007a). Structure and function of phosphatidylcholine transfer protein (PC-TP)/StarD2. Biochimica et Biophysica Acta (BBA) - Molecular and Cell Biology of Lipids 1771, 654-662.

Kanno, K., Wu, M.K., Agate, D.S., Fanelli, B.J., Wagle, N., Scapa, E.F., Ukomadu, C., and Cohen, D.E. (2007b). Interacting proteins dictate function of the minimal START domain phosphatidylcholine transfer protein/StarD2. J Biol Chem 282, 30728-30736.

Katoh, M., and Katoh, M. (2004). Characterization of human ARHGAP10 gene in silico. Int J Oncol 25, 1201-1206.

Kaufman, R.J., Scheuner, D., Schroder, M., Shen, X., Lee, K., Liu, C.Y., and Arnold, S.M. (2002). The unfolded protein response in nutrient sensing and differentiation. Nat Rev Mol Cell Biol 3, 411-421.

Kauraniemi, P., Bärlund, M., Monni, O., and Kallioniemi, A. (2001). New amplified and highly expressed genes discovered in the ERBB2 amplicon in breast cancer by cDNA microarrays. Cancer Res 61, 8235-8240.

Kawai, K., Kiyota, M., Seike, J., Deki, Y., and Yagisawa, H. (2007). START-GAP3/DLC3 is a GAP for RhoA and Cdc42 and is localized in focal adhesions regulating cell morphology. Biochem Biophys Res Commun 364, 783-789.

Kawai, K., Yamaga, M., Iwamae, Y., Kiyota, M., Kamata, H., Hirata, H., Homma, Y., and Yagisawa, H. (2004). A PLCdelta1-binding protein, p122RhoGAP, is localized in focal adhesions. Biochem Soc Trans 32, 1107-1109.

Kelly, K., Hutchinson, G., Nebenius-Oosthuizen, D., Smith, A.J., Bartsch, J.W., Horiuchi, K., Rittger, A., Manova, K., Docherty, A.J., and Blobel, C.P. (2005). Metalloprotease-disintegrin ADAM8: expression analysis and targeted deletion in mice. Dev Dyn 232, 221-231.

Kim, C.A., and Bowie, J.U. (2003). SAM domains: uniform structure, diversity of function. Trends Biochem Sci 28, 625-628.

Kim, E., Nishimura, H., and Baba, T. (2003a). Differential localization of ADAM1a and ADAM1b in the endoplasmic reticulum of testicular germ cells and on the surface of epididymal sperm. Biochem Biophys Res Commun 304, 313-319.

Kim, E., Yamashita, M., Nakanishi, T., Park, K.E., Kimura, M., Kashiwabara, S., and Baba, T. (2006). Mouse sperm lacking ADAM1b/ADAM2 fertilin can fuse with the egg plasma membrane and effect fertilization. J Biol Chem 281, 5634-5639.

Kim, T.Y., Jong, H.S., Song, S.H., Dimtchev, A., Jeong, S.J., Lee, J.W., Kim, T.Y., Kim, N.K., Jung, M., and Bang, Y.J. (2003b). Transcriptional silencing of the DLC-1 tumor suppressor gene by epigenetic mechanism in gastric cancer cells. Oncogene 22, 3943-3951.

King, N.E., Zimmermann, N., Pope, S.M., Fulkerson, P.C., Nikolaidis, N.M., Mishra, A., Witte, D.P., and Rothenberg, M.E. (2004). Expression and regulation of a disintegrin and metalloproteinase (ADAM) 8 in experimental asthma. Am J Respir Cell Mol Biol 31, 257-265.

Kishida, T. (2004). Targeted Mutation of the MLN64 START Domain Causes Only Modest Alterations in Cellular Sterol Metabolism. Journal of Biological Chemistry 279, 19276-19285.

Ko, D.C., Binkley, J., Sidow, A., and Scott, M.P. (2003). The integrity of a cholesterol-binding pocket in Niemann-Pick C2 protein is necessary to control lysosome cholesterol levels. Proc Natl Acad Sci USA 100, 2518-2525.

Köhler, C., Eriksson, L.G., Flood, P.R., Hardie, J.A., Okuno, E., and Schwarcz, R. (1988). Quinolinic acid metabolism in the rat brain. Immunohistochemical identification of 3-hydroxyanthranilic acid oxygenase and quinolinic acid phosphoribosyltransferase in the hippocampal region. J Neurosci 8, 975-987.

Korn, B.S., Shimomura, I., Bashmakov, Y., Hammer, R.E., Horton, J.D., Goldstein, J.L., and Brown, M.S. (1998). Blunted feedback suppression of SREBP processing by dietary cholesterol in transgenic mice expressing sterol-resistant SCAP(D443N). J Clin Invest 102, 2050-2060.

Kudo, N., Kumagai, K., Tomishige, N., Yamaji, T., Wakatsuki, S., Nishijima, M., Hanada, K., and Kato, R. (2008). Structural basis for specific lipid recognition by CERT responsible for nonvesicular trafficking of ceramide. Proc Natl Acad Sci USA 105, 488-493.

Kumagai, K., Yasuda, S., Okemoto, K., Nishijima, M., Kobayashi, S., and Hanada, K. (2005). CERT mediates intermembrane transfer of various molecular species of ceramides. J Biol Chem 280, 6488-6495.

Kurisaki, T., Masuda, A., Sudo, K., Sakagami, J., Higashiyama, S., Matsuda, Y., Nagabukuro, A., Tsuji, A., Nabeshima, Y., Asano, M., et al. (2003). Phenotypic analysis of Meltrin alpha (ADAM12)-deficient mice: involvement of Meltrin alpha in adipogenesis and myogenesis. Mol Cell Biol 23, 55-61.

Kurohara, K., Komatsu, K., Kurisaki, T., Masuda, A., Irie, N., Asano, M., Sudo, K., Nabeshima, Y., Iwakura, Y., and Sehara-Fujisawa, A. (2004). Essential roles of Meltrin beta (ADAM19) in heart development. Dev Biol 267, 14-28.

Laitinen, S., Lehto, M., Lehtonen, S., Hyvärinen, K., Heino, S., Lehtonen, E., Ehnholm, C., Ikonen, E., and Olkkonen, V.M. (2002). ORP2, a homolog of oxysterol binding protein, regulates cellular cholesterol metabolism. J Lipid Res 43, 245-255.

Lala, D.S., Syka, P.M., Lazarchik, S.B., Mangelsdorf, D.J., Parker, K.L., and Heyman, R.A. (1997). Activation of the orphan nuclear receptor steroidogenic factor 1 by oxysterols. Proc Natl Acad Sci U S A 94, 4895-4900.

Lehto, M., Hynynen, R., Karjalainen, K., Kuismanen, E., Hyvärinen, K., and Olkkonen, V.M. (2005). Targeting of OSBP-related protein 3 (ORP3) to endoplasmic reticulum and plasma membrane is controlled by multiple determinants. Exp Cell Res 310, 445-462.

Lehto, M., Mäyränpää, M.I., Pellinen, T., Ihalmo, P., Lehtonen, S., Kovanen, P.T., Groop, P.H., Ivaska, J., and Olkkonen, V.M. (2008). The R-Ras interaction partner ORP3 regulates cell adhesion. J Cell Sci 121, 695-705.

Lessmann, E., Ngo, M., Leitges, M., Minguet, S., Ridgway, N.D., and Huber, M. (2007). Oxysterol-binding protein-related protein (ORP) 9 is a PDK-2 substrate and regulates Akt phosphorylation. Cell Signal 19, 384-392.

Leung, T.H., Ching, Y.P., Yam, J.W., Wong, C.M., Yau, T.O., Jin, D.Y., and Ng, I.O. (2005). Deleted in liver cancer 2 (DLC2) suppresses cell transformation by means of inhibition of RhoA activity. Proc Natl Acad Sci USA 102, 15207-15212.

Levine, T.P., and Munro, S. (2002). Targeting of Golgi-specific pleckstrin homology domains involves both PtdIns 4-kinase-dependent and -independent components. Curr Biol 12, 695-704.

Levy, E., Spahis, S., Sinnett, D., Peretti, N., Maupas-Schwalm, F., Delvin, E., Lambert, M., and Lavoie, M.A. (2007). Intestinal cholesterol transport proteins: an update and beyond. Curr Opin Lipidol 18, 310-318.

Li, X.A., Everson, W.V., and Smart, E.J. (2005). Caveolae, lipid rafts, and vascular disease. Trends Cardiovasc Med 15, 92-96.

Liang, G., Yang, J., Horton, J.D., Hammer, R.E., Goldstein, J.L., and Brown, M.S. (2002). Diminished hepatic response to fasting/refeeding and liver X receptor agonists in mice with selective deficiency of sterol regulatory element-binding protein-1c. J Biol Chem 277, 9520-9528.

Lin, D., Sugawara, T., Strauss, J.F., Clark, B.J., Stocco, D.M., Saenger, P., Rogol, A., and Miller, W.L. (1995). Role of steroidogenic acute regulatory protein in adrenal and gonadal steroidogenesis. Science 267, 1828-1831.

Liscum, L., and Munn, N.J. (1999). Intracellular cholesterol transport. Biochim Biophys Acta 1438, 19-37.

Liscum, L., and Sturley, S.L. (2004). Intracellular trafficking of Niemann-Pick C proteins 1 and 2: obligate components of subcellular lipid transport. Biochim Biophys Acta 1685, 22-27.

Liu, P., Rudick, M., and Anderson, R.G. (2002). Multiple functions of caveolin-1. J Biol Chem 277, 41295-41298.

Liu, P., Jenkins, N.A., and Copeland, N.G. (2003). A highly efficient recombineering-based method for generating conditional knockout mutations. Genome Res 13, 476-484.

Loewen, C.J., Roy, A., and Levine, T.P. (2003). A conserved ER targeting motif in three families of lipid binding proteins and in Opi1p binds VAP. Embo J 22, 2025-2035.

Luo, Y., Liang, C.P., and Tall, A.R. (2001). The orphan nuclear receptor LRH-1 potentiates the sterol-mediated induction of the human CETP gene by liver X receptor. J Biol Chem 276, 24767-24773.

Luo, Y., and Tall, A.R. (2000). Sterol upregulation of human CETP expression in vitro and in transgenic mice by an LXR element. J Clin Invest 105, 513-520.

Malerød, L., Juvet, L.K., Hanssen-Bauer, A., Eskild, W., and Berg, T. (2002). Oxysterol-activated LXRalphalpha/RXR induces hSR-BI-promoter activity in hepatoma cells and preadipocytes. Biochem Biophys Res Commun 299, 916-923.

Malhotra, J.D., and Kaufman, R.J. (2007). The endoplasmic reticulum and the unfolded protein response. Semin Cell Dev Biol 18, 716-731.

Masaki, M., Kurisaki, T., Shirakawa, K., and Sehara-Fujisawa, A. (2005). Role of meltrin {alpha} (ADAM12) in obesity induced by high- fat diet. Endocrinology 146, 1752-1763.

Matsunaga, T., Isohashi, F., Nakanishi, Y., and Sakamoto, Y. (1985). Physiological changes in the activities of extramitochondrial acetyl-CoA hydrolase in the liver of rats under various metabolic conditions. Eur J Biochem 152, 331-336.

Matsuno, O., Miyazaki, E., Nureki, S., Ueno, T., Kumamoto, T., and Higuchi, Y. (2006). Role of ADAM8 in experimental asthma. Immunol Lett 102, 67-73.

Matsuura, F., Wang, N., Chen, W., Jiang, X.C., and Tall, A.R. (2006). HDL from CETP-deficient subjects shows enhanced ability to promote cholesterol efflux from macrophages in an apoE- and ABCG1-dependent pathway. J Clin Invest 116, 1435-1442.

Maxfield, F.R., and Menon, A.K. (2006). Intracellular sterol transport and distribution. Curr Opin Cell Biol 18, 379-385.

Maxfield, F.R., and Wustner, D. (2002). Intracellular cholesterol transport. J Clin Invest 110, 891-898.

Maxwell, K.N., Soccio, R.E., Duncan, E.M., Sehayek, E., and Breslow, J.L. (2003). Novel putative SREBP and LXR target genes identified by microarray analysis in liver of cholesterol-fed mice. J Lipid Res 44, 2109-2119.

Miller, W.L. (2007a). Mechanism of StAR's regulation of mitochondrial cholesterol import. Mol Cell Endocrinol 265-266, 46-50.

Miller, W.L. (2007b). StAR search--what we know about how the steroidogenic acute regulatory protein mediates mitochondrial cholesterol import. Mol Endocrinol 21, 589-601.

Miller, W.L. (2007c). Steroidogenic acute regulatory protein (StAR), a novel mitochondrial cholesterol transporter. Biochim Biophys Acta 1771, 663-676.

Miller, W.L., and Strauss, J.F. (1999). Molecular pathology and mechanism of action of the steroidogenic acute regulatory protein, StAR. J Steroid Biochem Mol Biol 69, 131-141.

Mitchell, K.J., Pinson, K.I., Kelly, O.G., Brennan, J., Zupicich, J., Scherz, P., Leighton, P.A., Goodrich, L.V., Lu, X., Avery, B.J., et al. (2001). Functional analysis of secreted and transmembrane proteins critical to mouse development. Nat Genet 28, 241-249.

Mochizuki, S., and Okada, Y. (2007). ADAMs in cancer cell proliferation and progression. Cancer Sci 98, 621-628.

Mochizuki, S., Shimoda, M., Shiomi, T., Fujii, Y., and Okada, Y. (2004). ADAM28 is activated by MMP-7 (matrilysin-1) and cleaves insulin-like growth factor binding protein-3. Biochem Biophys Res Commun 315, 79-84.

Moncecchi, D., Murphy, E.J., Prows, D.R., and Schroeder, F. (1996). Sterol carrier protein-2 expression in mouse L-cell fibroblasts alters cholesterol uptake. Biochim Biophys Acta 1302, 110-116.

Moon, S.Y., and Zheng, Y. (2003). Rho GTPase-activating proteins in cell regulation. Trends Cell Biol 13, 13-22.

Müller, A.C., Dairam, A., Limson, J.L., and Daya, S. (2007). Mechanisms by which acyclovir reduces the oxidative neurotoxicity and biosynthesis of quinolinic acid. Life Sci 80, 918-925.

Murase, S., Cho, C., White, J.M., and Horwitz, A.F. (2008). ADAM2 promotes migration of neuroblasts in the rostral migratory stream to the olfactory bulb. Eur J Neurosci 27, 1585-1595.

Nagao, K., Takahashi, K., Hanada, K., Kioka, N., Matsuo, M., and Ueda, K. (2007). Enhanced apoA-I-dependent cholesterol efflux by ABCA1 from sphingomyelin-deficient Chinese hamster ovary cells. J Biol Chem 282, 14868-14874.

Nagaraja, G.M., and Kandpal, R.P. (2004). Chromosome 13q12 encoded Rho GTPase activating protein suppresses growth of breast carcinoma cells, and yeast two-hybrid screen shows its interaction with several proteins. Biochem Biophys Res Commun 313, 654-665.

Nakanishi, Y., Isohashi, F., Matsunaga, T., and Sakamoto, Y. (1985). Oxidative inactivation of an extramitochondrial acetyl-CoA hydrolase by autoxidation of L-ascorbic acid. Eur J Biochem 152, 337-342.

Ng, D.C., Chan, S.F., Kok, K.H., Yam, J.W., Ching, Y.P., Ng, I.O., and Jin, D.Y. (2006). Mitochondrial targeting of growth suppressor protein DLC2 through the START domain. FEBS Lett 580, 191-198.

Ng, I.O., Liang, Z.D., Cao, L., and Lee, T.K. (2000). DLC-1 is deleted in primary hepatocellular carcinoma and exerts inhibitory effects on the proliferation of hepatoma cell lines with deleted DLC-1. Cancer Res 60, 6581-6584.

Nishimura, H., Kim, E., Fujimori, T., Kashiwabara, S., Kuroiwa, A., Matsuda, Y., and Baba, T. (2002). The ADAM1a and ADAM1b genes, instead of the ADAM1 (fertilin alpha) gene, are localized on mouse chromosome 5. Gene 291, 67-76.

Nishimura, H., Kim, E., Nakanishi, T., and Baba, T. (2004). Possible function of the ADAM1a/ADAM2 Fertilin complex in the appearance of ADAM3 on the sperm surface. J Biol Chem 279, 34957-34962.

Nishimura, H., Myles, D.G., and Primakoff, P. (2007). Identification of an ADAM2-ADAM3 complex on the surface of mouse testicular germ cells and cauda epididymal sperm. J Biol Chem 282, 17900-17907.

Oh, J., Woo, J.M., Choi, E., Kim, T., Cho, B.N., Park, Z.Y., Kim, Y.C., Kim, D.H., and Cho, C. (2005). Molecular, biochemical, and cellular characterization of epididymal ADAMs, ADAM7 and ADAM28. Biochem Biophys Res Commun 331, 1374-1383.

Olayioye, M.A., Hoffmann, P., Pomorski, T., Armes, J., Simpson, R.J., Kemp, B.E., Lindeman, G.J., and Visvader, J.E. (2004). The phosphoprotein StarD10 is overexpressed in breast cancer and cooperates with ErbB receptors in cellular transformation. Cancer Res 64, 3538-3544.

Olayioye, M.A., Vehring, S., Müller, P., Herrmann, A., Schiller, J., Thiele, C., Lindeman, G.J., Visvader, J.E., and Pomorski, T. (2005). StarD10, a START domain protein overexpressed in breast cancer, functions as a phospholipid transfer protein. J Biol Chem 280, 27436-27442.

Patel, S.C., Suresh, S., Kumar, U., Hu, C.Y., Cooney, A., Blanchette-Mackie, E.J., Neufeld, E.B., Patel, R.C., Brady, R.O., Patel, Y.C., et al. (1999). Localization of Niemann-Pick C1 protein in astrocytes: implications for neuronal degeneration in Niemann- Pick type C disease. Proc Natl Acad Sci USA 96, 1657-1662.

Peet, D.J., Turley, S.D., Ma, W., Janowski, B.A., Lobaccaro, J.M., Hammer, R.E., and Mangelsdorf, D.J. (1998). Cholesterol and bile acid metabolism are impaired in mice lacking the nuclear oxysterol receptor LXR alpha. Cell 93, 693-704.

Perry, R.J., and Ridgway, N.D. (2005). Molecular mechanisms and regulation of ceramide transport. Biochim Biophys Acta 1734, 220-234.

Perry, R.J., and Ridgway, N.D. (2006). Oxysterol-binding protein and vesicle-associated membrane protein-associated protein are required for sterol-dependent activation of the ceramide transport protein. Mol Biol Cell 17, 2604-2616.

Peschon, J.J., Slack, J.L., Reddy, P., Stocking, K.L., Sunnarborg, S.W., Lee, D.C., Russell, W.E., Castner, B.J., Johnson, R.S., Fitzner, J.N., et al. (1998). An essential role for ectodomain shedding in mammalian development. Science 282, 1281-1284.

Plaumann, M., Seitz, S., Frege, R., Estevez-Schwarz, L., and Scherneck, S. (2003). Analysis of DLC-1 expression in human breast cancer. J Cancer Res Clin Oncol 129, 349-354.

Pollack, J.R., Sørlie, T., Perou, C.M., Rees, C.A., Jeffrey, S.S., Lonning, P.E., Tibshirani, R., Botstein, D., Børresen-Dale, A.L., and Brown, P.O. (2002). Microarray analysis reveals a major direct role of DNA copy number alteration in the transcriptional program of human breast tumors. Proc Natl Acad Sci USA 99, 12963-12968.

Ponting, C.P., and Aravind, L. (1999). START: a lipid-binding domain in StAR, HD-ZIP and signalling proteins. Trends Biochem Sci 24, 130-132.

Prinz, W. (2002). Cholesterol trafficking in the secretory and endocytic systems. Semin Cell Dev Biol 13, 197-203.

Prinz, W.A. (2007). Non-vesicular sterol transport in cells. Prog Lipid Res 46, 297-314.

Rao, R.P., Yuan, C., Allegood, J.C., Rawat, S.S., Edwards, M.B., Wang, X., Merrill, A.H., Acharya, U., and Acharya, J.K. (2007). Ceramide transfer protein function is essential for normal oxidative stress response and lifespan. Proc Natl Acad Sci USA 104, 11364-11369.

Raya, A., Revert, F., Navarro, S., and Saus, J. (1999). Characterization of a novel type of serine/threonine kinase that specifically phosphorylates the human goodpasture antigen. J Biol Chem 274, 12642-12649.

Raya, A., Revert-Ros, F., Martinez-Martinez, P., Navarro, S., Rosello, E., Vieites, B., Granero, F., Forteza, J., and Saus, J. (2000). Goodpasture antigen-binding protein, the kinase that phosphorylates the goodpasture antigen, is an alternatively spliced variant implicated in autoimmune pathogenesis. J Biol Chem 275, 40392-40399.

Razani, B., Combs, T.P., Wang, X.B., Frank, P.G., Park, D.S., Russell, R.G., Li, M., Tang, B., Jelicks, L.A., Scherer, P.E., et al. (2002). Caveolin-1-deficient mice are lean, resistant to diet-induced obesity, and show hypertriglyceridemia with adipocyte abnormalities. J Biol Chem 277, 8635-8647.

Ren, S., Hylemon, P., Marques, D., Hall, E., Redford, K., Gil, G., and Pandak, W.M. (2004a). Effect of increasing the expression of cholesterol transporters (StAR, MLN64, and SCP-2) on bile acid synthesis. J Lipid Res 45, 2123-2131.

Ren, S., Hylemon, P.B., Marques, D., Gurley, E., Bodhan, P., Hall, E., Redford, K., Gil, G., and Pandak, W.M. (2004b). Overexpression of cholesterol transporter StAR increases in vivo rates of bile acid synthesis in the rat and mouse. Hepatology 40, 910-917.

Repa, J.J., Berge, K.E., Pomajzl, C., Richardson, J.A., Hobbs, H., and Mangelsdorf, D.J. (2002). Regulation of ATP-binding cassette sterol transporters ABCG5 and ABCG8 by the liver X receptors alpha and beta. J Biol Chem 277, 18793-18800.

Repa, J.J., and Mangelsdorf, D.J. (2002). The liver X receptor gene team: potential new players in atherosclerosis. Nat Med 8, 1243-1248.

Roderick, S.L., Chan, W.W., Agate, D.S., Olsen, L.R., Vetting, M.W., Rajashankar, K.R., and Cohen, D.E. (2002). Structure of human phosphatidylcholine transfer protein in complex with its ligand. Nat Struct Biol 9, 507-511.

Rodriguez-Agudo, D., Ren, S., Hylemon, P.B., Montañez, R., Redford, K., Natarajan, R., Medina, M.A., Gil, G., and Pandak, W.M. (2006). Localization of StarD5 cholesterol binding protein. J Lipid Res 47, 1168-1175.

Rodriguez-Agudo, D., Ren, S., Hylemon, P.B., Redford, K., Natarajan, R., Del Castillo, A., Gil, G., and Pandak, W.M. (2005). Human StarD5, a cytosolic StAR-related lipid binding protein. J Lipid Res.

Rodriguez-Agudo, D., Ren, S., Wong, E., Marques, D., Redford, K., Gil, G., Hylemon, P., and Pandak, W.M. (2008). Intracellular cholesterol transporter StarD4 binds free cholesterol and increases cholesteryl ester formation. J Lipid Res 49, 1409-1419.

Romanowski, M.J., Soccio, R.E., Breslow, J.L., and Burley, S.K. (2002). Crystal structure of the Mus musculus cholesterol-regulated START protein 4 (StarD4) containing a StAR-related lipid transfer domain. Proc Natl Acad Sci USA 99, 6949-6954.

Rose, S. (1998). Gastrointestinal and Hepatobiliary Pathophysiology.

Roux, A., Cuvelier, D., Nassoy, P., Prost, J., Bassereau, P., and Goud, B. (2005). Role of curvature and phase transition in lipid sorting and fission of membrane tubules. Embo J 24, 1537-1545.

Rybnikova, E., Kärkkäinen, I., Pelto-Huikko, M., and Huovila, A.P. (2002). Developmental regulation and neuronal expression of the cellular disintegrin ADAM11 gene in mouse nervous system. Neuroscience 112, 921-934.

Sagane, K., Hayakawa, K., Kai, J., Hirohashi, T., Takahashi, E., Miyamoto, N., Ino, M., Oki, T., Yamazaki, K., and Nagasu, T. (2005). Ataxia and peripheral nerve hypomyelination in ADAM22-deficient mice. BMC neuroscience 6, 33.

Sagane, K., Ohya, Y., Hasegawa, Y., and Tanaka, I. (1998). Metalloproteinase-like, disintegrin-like, cysteinee-rich proteins MDC2 and MDC3: novel human cellular disintegrins highly expressed in the brain. Biochem J 334 (Pt 1), 93-98.

Sagane, K., Yamazaki, K., Mizui, Y., and Tanaka, I. (1999). Cloning and chromosomal mapping of mouse ADAM11, ADAM22 and ADAM23. Gene 236, 79-86.

Saito, S., Matsui, H., Kawano, M., Kumagai, K., Tomishige, N., Hanada, K., Echigo, S., Tamura, S., and Kobayashi, T. (2008). Protein phosphatase 2Cepsilon is an endoplasmic reticulum integral membrane protein that dephosphorylates the ceramide transport protein CERT to enhance its association with organelle membranes. J Biol Chem 283, 6584-6593.

Sano, O., Kobayashi, A., Nagao, K., Kumagai, K., Kioka, N., Hanada, K., Ueda, K., and Matsuo, M. (2007). Sphingomyelin-dependence of cholesterol efflux mediated by ABCG1. J Lipid Res 48, 2377-2384.

Scapa, E., Pocai, A., Wu, M., Gutierrez-Juarez, R., Glenz, L., Kanno, K., Li, H., Biddinger, S., Jelicks, L.A., Rossetti, L., et al. (2008). Regulation of energy substrate utilization and hepatic insulin sensitivity by phosphatidylcholine transfer protein/StarD2. Faseb J.

Schoonjans, K., Brendel, C., Mangelsdorf, D., and Auwerx, J. (2000). Sterols and gene expression: control of affluence. Biochim Biophys Acta 1529, 114-125.

Schroder, M., and Kaufman, R.J. (2005). ER stress and the unfolded protein response. Mutat Res 569, 29-63.

Schroeder, F., Atshaves, B.P., McIntosh, A.L., Gallegos, A.M., Storey, S.M., Parr, R.D., Jefferson, J.R., Ball, J.M., and Kier, A.B. (2007). Sterol carrier protein-2: new roles in regulating lipid rafts and signaling. Biochim Biophys Acta 1771, 700-718.

Schroeder, F., Gallegos, A.M., Atshaves, B.P., Storey, S.M., McIntosh, A.L., Petrescu, A.D., Huang, H., Starodub, O., Chao, H., Yang, H., et al. (2001). Recent advances in membrane microdomains: rafts, caveolae, and intracellular cholesterol trafficking. Exp Biol Med (Maywood) 226, 873-890.

Schultz, J.R., Tu, H., Luk, A., Repa, J.J., Medina, J.C., Li, L., Schwendner, S., Wang, S., Thoolen, M., Mangelsdorf, D.J., et al. (2000). Role of LXRs in control of lipogenesis. Genes Dev 14, 2831-2838.

Seals, D.F., and Courtneidge, S.A. (2003). The ADAMs family of metalloproteases: multidomain proteins with multiple functions. Genes Dev 17, 7-30.

Seedorf, U., Ellinghaus, P., and Roch Nofer, J. (2000). Sterol carrier protein-2. Biochim Biophys Acta 1486, 45-54.

Seedorf, U., Raabe, M., Ellinghaus, P., Kannenberg, F., Fobker, M., Engel, T., Denis, S., Wouters, F., Wirtz, K.W., Wanders, R.J., et al. (1998). Defective peroxisomal catabolism of branched fatty acyl coenzyme A in mice lacking the sterol carrier protein-2/sterol carrier protein-x gene function. Genes Dev 12, 1189-1201.

Sehayek, E., and Breslow, J.L. (2005). Plasma plant sterol levels: another coronary heart disease risk factor? Arterioscler Thromb Vasc Biol 25, 5-6.

Sekimata, M., Kabuyama, Y., Emori, Y., and Homma, Y. (1999). Morphological changes and detachment of adherent cells induced by p122, a GTPase-activating protein for Rho. J Biol Chem 274, 17757-17762.

Shamsadin, R., Adham, I.M., Nayernia, K., Heinlein, U.A., Oberwinkler, H., and Engel, W. (1999). Male mice deficient for germ-cell cyritestin are infertile. Biol Reprod 61, 1445-1451.

Shen, X., Zhang, K., and Kaufman, R.J. (2004). The unfolded protein response--a stress signaling pathway of the endoplasmic reticulum. J Chem Neuroanat 28, 79-92.

Shimano, H., Horton, J.D., Hammer, R.E., Shimomura, I., Brown, M.S., and Goldstein, J.L. (1996). Overproduction of cholesterol and fatty acids causes massive liver enlargement in transgenic mice expressing truncated SREBP-1a. J Clin Invest 98, 1575-1584.

Shimano, H., Horton, J.D., Shimomura, I., Hammer, R.E., Brown, M.S., and Goldstein, J.L. (1997a). Isoform 1c of sterol regulatory element binding protein is less active than isoform 1a in livers of transgenic mice and in cultured cells. J Clin Invest 99, 846-854.

Shimano, H., Shimomura, I., Hammer, R.E., Herz, J., Goldstein, J.L., Brown, M.S., and Horton, J.D. (1997b). Elevated levels of SREBP-2 and cholesterol synthesis in livers of mice homozygous for a targeted disruption of the SREBP-1 gene. J Clin Invest 100, 2115-2124.

Shimoda, M., Hashimoto, G., Mochizuki, S., Ikeda, E., Nagai, N., Ishida, S., and Okada, Y. (2007). Binding of ADAM28 to P-selectin glycoprotein ligand-1 enhances P-selectin-mediated leukocyte adhesion to endothelial cells. J Biol Chem 282, 25864-25874.

Silver, D.L., and Tall, A.R. (2001). The cellular biology of scavenger receptor class B type I. Curr Opin Lipidol 12, 497-504.

Simons, K., and Ikonen, E. (2000). How cells handle cholesterol. Science 290, 1721-1726.

Sleat, D.E., Wiseman, J.A., El-Banna, M., Price, S.M., Verot, L., Shen, M.M., Tint, G.S., Vanier, M.T., Walkley, S.U., and Lobel, P. (2004). Genetic evidence for nonredundant functional cooperativity between NPC1 and NPC2 in lipid transport. Proc Natl Acad Sci USA 101, 5886-5891.

Smart, E.J., Ying, Y., Donzell, W.C., and Anderson, R.G. (1996). A role for caveolin in transport of cholesterol from endoplasmic reticulum to plasma membrane. J Biol Chem 271, 29427-29435.

Soccio, R.E., Adams, R.M., Maxwell, K.N., and Breslow, J.L. (2005). Differential gene regulation of StarD4 and StarD5 cholesterol transfer proteins. Activation of StarD4 by sterol regulatory element-binding protein-2 and StarD5 by endoplasmic reticulum stress. J Biol Chem 280, 19410-19418.

Soccio, R.E., Adams, R.M., Romanowski, M.J., Sehayek, E., Burley, S.K., and Breslow, J.L. (2002). The cholesterol-regulated StarD4 gene encodes a StAR-related lipid transfer protein with two closely related homologues, StarD5 and StarD6. Proc Natl Acad Sci USA 99, 6943-6948.

Soccio, R.E., and Breslow, J.L. (2003). StAR-related lipid transfer (START) proteins: mediators of intracellular lipid metabolism. J Biol Chem 278, 22183-22186.

Soccio, R.E., and Breslow, J.L. (2004). Intracellular cholesterol transport. Arterioscler Thromb Vasc Biol 24, 1150-1160.

Sriburi, R., Jackowski, S., Mori, K., and Brewer, J.W. (2004). XBP1: a link between the unfolded protein response, lipid biosynthesis, and biogenesis of the endoplasmic reticulum. J Cell Biol 167, 35-41.

Sriraman, V., Eichenlaub-Ritter, U., Bartsch, J.W., Rittger, A., Mulders, S.M., and Richards, J.S. (2008). Regulated expression of ADAM8 (a disintegrin and metalloprotease domain 8) in the mouse ovary: evidence for a regulatory role of luteinizing hormone, progesterone receptor, and epidermal growth factor-like growth factors. Biol Reprod 78, 1038-1048.

Steffensen, K.R., and Gustafsson, J.A. (2004). Putative metabolic effects of the liver X receptor (LXR). Diabetes 53 Suppl 1, S36-42.

Stein, K.K., Go, J.C., Primakoff, P., and Myles, D.G. (2005). Defects in secretory pathway trafficking during sperm development in Adam2 knockout mice. Biol Reprod 73, 1032-1038.

Stocco, D.M. (2001). StAR protein and the regulation of steroid hormone biosynthesis. Annu Rev Physiol 63, 193-213.

Stocco, D.M. (2002). Clinical disorders associated with abnormal cholesterol transport: mutations in the steroidogenic acute regulatory protein. Mol Cell Endocrinol 191, 19-25.

Strauss, J.F., Liu, P., Christenson, L.K., and Watari, H. (2002). Sterols and intracellular vesicular trafficking: lessons from the study of NPC1. Steroids 67, 947-951.

Suematsu, N., and Isohashi, F. (2006). Molecular cloning and functional expression of human cytosolic acetyl-CoA hydrolase. Acta Biochim Pol 53, 553-561.

Suematsu, N., Okamoto, K., Shibata, K., Nakanishi, Y., and Isohashi, F. (2001). Molecular cloning and functional expression of rat liver cytosolic acetyl-CoA hydrolase. Eur J Biochem 268, 2700-2709.

Sugawara, T., Holt, J.A., Driscoll, D., Strauss, J.F., Lin, D., Miller, W.L., Patterson, D., Clancy, K.P., Hart, I.M., and Clark, B.J. (1995). Human steroidogenic acute regulatory protein: functional activity in COS-1 cells, tissue-specific expression, and mapping of the structural gene to 8p11.2 and a pseudogene to chromosome 13. Proc Natl Acad Sci USA 92, 4778-4782.

Tabas, I. (2002a). Cholesterol in health and disease. J Clin Invest 110, 583-590.

Tabas, I. (2002b). Consequences of cellular cholesterol accumulation: basic concepts and physiological implications. J Clin Invest 110, 905-911.

Takahashi, E., Sagane, K., Nagasu, T., and Kuromitsu, J. (2006a). Altered nociceptive response in ADAM11-deficient mice. Brain Res 1097, 39-42.

Takahashi, E., Sagane, K., Oki, T., Yamazaki, K., Nagasu, T., and Kuromitsu, J. (2006b). Deficits in spatial learning and motor coordination in ADAM11-deficient mice. BMC neuroscience 7, 19.

Tellier, E., Canault, M., Poggi, M., Bonardo, B., Nicolay, A., Alessi, M.C., Nalbone, G., and Peiretti, F. (2008). HDLs activate ADAM17-dependent shedding. J Cell Physiol 214, 687-693.

Teramoto, A., Tsukuda, K., Yano, M., Toyooka, S., Dote, H., Doihara, H., and Shimizu, N. (2004). Less frequent promoter hypermethylation of DLC-1 gene in primary breast cancers. Oncol Rep 12, 141-144.

Thompson, J.D., Higgins, D.G., and Gibson, T.J. (1994). CLUSTAL W: improving the sensitivity of progressive multiple sequence alignment through sequence weighting, position-specific gap penalties and weight matrix choice. Nucleic Acids Res 22, 4673-4680.

Tichauer, J.E., Morales, M.G., Amigo, L., Galdames, L., Klein, A., Quinones, V., Ferrada, C., Alvarez, A.R., Rio, M.C., Miquel, J.F., et al. (2007). Overexpression of the cholesterol-binding protein MLN64 induces liver damage in the mouse. World J Gastroenterol 13, 3071-3079.

Tomasetto, C., Régnier, C., Moog-Lutz, C., Mattei, M.G., Chenard, M.P., Lidereau, R., Basset, P., and Rio, M.C. (1995). Identification of four novel human genes amplified and overexpressed in breast carcinoma and localized to the q11-q21.3 region of chromosome 17. Genomics 28, 367-376.

Tontonoz, P., and Mangelsdorf, D.J. (2003). Liver X receptor signaling pathways in cardiovascular disease. Mol Endocrinol 17, 985-993.

Tóth, B., Balla, A., Ma, H., Knight, Z.A., Shokat, K.M., and Balla, T. (2006). Phosphatidylinositol 4-kinase IIIbeta regulates the transport of ceramide between the endoplasmic reticulum and Golgi. J Biol Chem 281, 36369-36377.

Tsujishita, Y. (2003). Structural genomics of lipid signaling domains. Oncol Res 13, 421-428.

Tsujishita, Y., and Hurley, J.H. (2000). Structure and lipid transport mechanism of a StAR-related domain. Nat Struct Biol 7, 408-414.

Tuckey, R.C., Headlam, M.J., Bose, H.S., and Miller, W.L. (2002). Transfer of cholesterol between phospholipid vesicles mediated by the steroidogenic acute regulatory protein (StAR). J Biol Chem 277, 47123-47128.

Turtoi, A., Brown, I., Oskamp, D., and Schneeweiss, F.H. (2008). Early gene expression in human lymphocytes after gamma-irradiation-a genetic pattern with potential for biodosimetry. Int J Radiat Biol 84, 375-387.

Uittenbogaard, A., and Smart, E.J. (2000). Palmitoylation of caveolin-1 is required for cholesterol binding, chaperone complex formation, and rapid transport of cholesterol to caveolae. J Biol Chem 275, 25595-25599.

Uittenbogaard, A., Ying, Y., and Smart, E.J. (1998). Characterization of a cytosolic heat-shock protein-caveolin chaperone complex. Involvement in cholesterol trafficking. J Biol Chem 273, 6525-6532.

Valkovskaya, N., Kayed, H., Felix, K., Hartmann, D., Giese, N.A., Osinsky, S.P., Friess, H., and Kleeff, J. (2007). ADAM8 expression is associated with increased invasiveness and reduced patient survival in pancreatic cancer. J Cell Mol Med 11, 1162-1174.

Van Eerdewegh, P., Little, R.D., Dupuis, J., Del Mastro, R.G., Falls, K., Simon, J., Torrey, D., Pandit, S., McKenny, J., Braunschweiger, K., et al. (2002). Association of the ADAM33 gene with asthma and bronchial hyperresponsiveness. Nature 418, 426-430.

van Helvoort, A., de Brouwer, A., Ottenhoff, R., Brouwers, J.F., Wijnholds, J., Beijnen, J.H., Rijneveld, A., van der Poll, T., van der Valk, M.A., Majoor, D., et al. (1999). Mice without phosphatidylcholine transfer protein have no defects in the secretion of phosphatidylcholine into bile or into lung airspaces. Proc Natl Acad Sci USA 96, 11501-11506.

Venkateswaran, A., Laffitte, B.A., Joseph, S.B., Mak, P.A., Wilpitz, D.C., Edwards, P.A., and Tontonoz, P. (2000). Control of cellular cholesterol efflux by the nuclear oxysterol receptor LXR alpha. Proc Natl Acad Sci U S A 97, 12097-12102.

Wang, C., JeBailey, L., and Ridgway, N.D. (2002). Oxysterol-binding-protein (OSBP)-related protein 4 binds 25-hydroxycholesterol and interacts with vimentin intermediate filaments. Biochem J 361, 461-472.

Wang, W.J., Baez, J.M., Maurer, R., Dansky, H.M., and Cohen, D.E. (2006). Homozygous disruption of Pctp modulates atherosclerosis in apolipoprotein E-deficient mice. J Lipid Res 47, 2400-2407.

Watari, H., Arakane, F., Moog-Lutz, C., Kallen, C.B., Tomasetto, C., Gerton, G.L., Rio, M.C., Baker, M.E., and Strauss, J.F. (1997). MLN64 contains a domain with homology to the steroidogenic acute regulatory protein (StAR) that stimulates steroidogenesis. Proc Natl Acad Sci U S A 94, 8462-8467.

Watari, H., Blanchette-Mackie, E.J., Dwyer, N.K., Glick, J.M., Patel, S., Neufeld, E.B., Brady, R.O., Pentchev, P.G., and Strauss, J.F. (1999). Niemann-Pick C1 protein: obligatory roles for N-terminal domains and lysosomal targeting in cholesterol mobilization. Proc Natl Acad Sci USA 96, 805-810.

Welch, C.L., Sun, Y., Arey, B.J., Lemaitre, V., Sharma, N., Ishibashi, M., Sayers, S., Li, R., Gorelik, A., Pleskac, N., et al. (2007). Spontaneous atherothrombosis and medial degradation in Apoe-/-, Npc1-/- mice. Circulation 116, 2444-2452.

Weskamp, G., Cai, H., Brodie, T.A., Higashyama, S., Manova, K., Ludwig, T., and Blobel, C.P. (2002). Mice lacking the metalloprotease-disintegrin MDC9 (ADAM9) have no evident major abnormalities during development or adult life. Mol Cell Biol 22, 1537-1544.

West, L.A., Horvat, R.D., Roess, D.A., Barisas, B.G., Juengel, J.L., and Niswender, G.D. (2001). Steroidogenic acute regulatory protein and peripheral-type benzodiazepine receptor associate at the mitochondrial membrane. Endocrinology 142, 502-505.

Wirtz, K.W. (1991). Phospholipid transfer proteins. Annu Rev Biochem 60, 73-99.

Wójcicka, G., Jamroz-Wiśniewska, A., Horoszewicz, K., and Bełtowski, J. (2007). Liver X receptors (LXRs). Part I: structure, function, regulation of activity, and role in lipid metabolism. Postępy higieny i medycyny doświadczalnej (Online) 61, 736-759.

Wong, C.M., Lee, J.M., Ching, Y.P., Jin, D.Y., and Ng, I.O. (2003). Genetic and epigenetic alterations of DLC-1 gene in hepatocellular carcinoma. Cancer Res 63, 7646-7651.

Wu, M.K., and Cohen, D.E. (2005a). Altered hepatic cholesterol metabolism compensates for disruption of phosphatidylcholine transfer protein in mice. Am J Physiol Gastrointest Liver Physiol 289, G456-461.

Wu, M.K., and Cohen, D.E. (2005b). Phosphatidylcholine transfer protein regulates size and hepatic uptake of high-density lipoproteins. Am J Physiol Gastrointest Liver Physiol 289, G1067-1074.

Wu, M.K., Hyogo, H., Yadav, S.K., Novikoff, P.M., and Cohen, D.E. (2005). Impaired response of biliary lipid secretion to a lithogenic diet in phosphatidylcholine transfer protein-deficient mice. J Lipid Res 46, 422-431.

Wyles, J.P., and Ridgway, N.D. (2004). VAMP-associated protein-A regulates partitioning of oxysterol-binding protein-related protein-9 between the endoplasmic reticulum and Golgi apparatus. Exp Cell Res 297, 533-547.

Yamada, S., Yamaguchi, T., Hosoda, A., Iwawaki, T., and Kohno, K. (2006). Regulation of human STARD4 gene expression under endoplasmic reticulum stress. Biochem Biophys Res Commun 343, 1079-1085.

Yamaga, M., Kawai, K., Kiyota, M., Homma, Y., and Yagisawa, H. (2007). Recruitment and activation of phospholipase C (PLC)-delta(1) in lipid rafts by muscarinic stimulation of PC12 cells: Contribution of p122RhoGAP/DLC1, a tumor-suppressing PLCdelta(1) binding protein. Adv Enzyme Regul.

Yamaga, M., Sekimata, M., Fujii, M., Kawai, K., Kamata, H., Hirata, H., Homma, Y., and Yagisawa, H. (2004). A PLCdelta1-binding protein, p122/RhoGAP, is localized in caveolin-enriched membrane domains and regulates caveolin internalization. Genes Cells 9, 25-37.

Yan, D., Jauhiainen, M., Hildebrand, R.B., Willems van Dijk, K., Van Berkel, T.J., Ehnholm, C., Van Eck, M., and Olkkonen, V.M. (2007a). Expression of human OSBP-related protein 1L in macrophages enhances atherosclerotic lesion development in LDL receptor-deficient mice. Arterioscler Thromb Vasc Biol 27, 1618-1624.

Yan, D., Lehto, M., Rasilainen, L., Metso, J., Ehnholm, C., Ylä-Herttuala, S., Jauhiainen, M., and Olkkonen, V.M. (2007b). Oxysterol binding protein induces upregulation of SREBP-1c and enhances hepatic lipogenesis. Arterioscler Thromb Vasc Biol 27, 1108-1114.

Yan, D., Mäyränpää, M.I., Wong, J., Perttilä, J., Lehto, M., Jauhiainen, M., Kovanen, P.T., Ehnholm, C., Brown, A.J., and Olkkonen, V.M. (2008). OSBP-related protein 8 (ORP8) suppresses ABCA1 expression and cholesterol efflux from macrophages. J Biol Chem 283, 332-340.

Yan, D., and Olkkonen, V.M. (2008). Characteristics of oxysterol binding proteins. Int Rev Cytol 265, 253-285.

Yang, P., Baker, K.A., and Hagg, T. (2005). A disintegrin and metalloprotease 21 (ADAM21) is associated with neurogenesis and axonal growth in developing and adult rodent CNS. J Comp Neurol 490, 163-179.

Yang, P., Baker, K.A., and Hagg, T. (2006). The ADAMs family: coordinators of nervous system development, plasticity and repair. Prog Neurobiol 79, 73-94.

Yang, T., Espenshade, P.J., Wright, M.E., Yabe, D., Gong, Y., Aebersold, R., Goldstein, J.L., and Brown, M.S. (2002). Crucial step in cholesterol homeostasis: sterols promote binding of SCAP to INSIG-1, a membrane protein that facilitates retention of SREBPs in ER. Cell 110, 489-500.

Yokozeki, T., Wakatsuki, S., Hatsuzawa, K., Black, R.A., Wada, I., and Sehara-Fujisawa, A. (2007). Meltrin beta (ADAM19) mediates ectodomain shedding of Neuregulin beta1 in the Golgi apparatus: fluorescence correlation spectroscopic observation of the dynamics of ectodomain shedding in living cells. Genes Cells 12, 329-343.

Yu, L., York, J., Von Bergmann, K., Lutjohann, D., Cohen, J.C., and Hobbs, H.H. (2003). Stimulation of cholesterol excretion by the liver X receptor agonist requires ATP-binding cassette transporters G5 and G8. J Biol Chem 278, 15565-15570.

Yuan, B.Z., Durkin, M.E., and Popescu, N.C. (2003a). Promoter hypermethylation of DLC-1, a candidate tumor suppressor gene, in several common human cancers. Cancer Genet Cytogenet 140, 113-117.

Yuan, B.Z., Jefferson, A.M., Baldwin, K.T., Thorgeirsson, S.S., Popescu, N.C., and Reynolds, S.H. (2004). DLC-1 operates as a tumor suppressor gene in human non-small cell lung carcinomas. Oncogene 23, 1405-1411.

Yuan, B.Z., Miller, M.J., Keck, C.L., Zimonjic, D.B., Thorgeirsson, S.S., and Popescu, N.C. (1998). Cloning, characterization, and chromosomal localization of a gene frequently deleted in human liver cancer (DLC-1) homologous to rat RhoGAP. Cancer Res 58, 2196-2199.

Yuan, B.Z., Zhou, X., Durkin, M.E., Zimonjic, D.B., Gumundsdottir, K., Eyfjord, J.E., Thorgeirsson, S.S., and Popescu, N.C. (2003b). DLC-1 gene inhibits human breast cancer cell growth and in vivo tumorigenicity. Oncogene 22, 445-450.

Zhang, J.R., Coleman, T., Langmade, S.J., Scherrer, D.E., Lane, L., Lanier, M.H., Feng, C., Sands, M.S., Schaffer, J.E., Semenkovich, C.F., et al. (2008). Niemann-Pick C1 protects against atherosclerosis in mice via regulation of macrophage intracellular cholesterol trafficking. J Clin Invest 118, 2281-2290.

Zhang, K., and Kaufman, R.J. (2006). The unfolded protein response: a stress signaling pathway critical for health and disease. Neurology 66, S102-109.

Zhang, M., Liu, P., Dwyer, N.K., Christenson, L.K., Fujimoto, T., Martinez, F., Comly, M., Hanover, J.A., Blanchette-Mackie, E.J., and Strauss, J.F. (2002). MLN64 mediates mobilization of lysosomal cholesterol to steroidogenic mitochondria. J Biol Chem 277, 33300-33310.

Zhang, Y., Repa, J.J., Gauthier, K., and Mangelsdorf, D.J. (2001). Regulation of lipoprotein lipase by the oxysterol receptors, LXRalphalpha and LXRbetaeta. J Biol Chem 276, 43018-43024.

Zhang, Y., Zanotti, I., Reilly, M.P., Glick, J.M., Rothblat, G.H., and Rader, D.J. (2003). Overexpression of apolipoprotein A-I promotes reverse transport of cholesterol from macrophages to feces in vivo. Circulation 108, 661-663.

Zhao, B., Song, J., Chow, W.N., St Clair, R.W., Rudel, L.L., and Ghosh, S. (2007). Macrophage-specific transgenic expression of cholesteryl ester hydrolase significantly reduces atherosclerosis and lesion necrosis in Ldlr mice. J Clin Invest 117, 2983-2992.

Zheng, S.L., Mychaleckyj, J.C., Hawkins, G.A., Isaacs, S.D., Wiley, K.E., Turner, A., Chang, B.L., von Kap-Herr, C., Carpten, J.D., Pettenati, M., et al. (2003). Evaluation of DLC1 as a prostate cancer susceptibility gene: mutation screen and association study. Mutat Res 528, 45-53.

Zhou, H.M., Weskamp, G., Chesneau, V., Sahin, U., Vortkamp, A., Horiuchi, K., Chiusaroli, R., Hahn, R., Wilkes, D., Fisher, P., et al. (2004a). Essential role for ADAM19 in cardiovascular morphogenesis. Mol Cell Biol 24, 96-104.

Zhou, J., Lhoták, S., Hilditch, B.A., and Austin, R.C. (2005). Activation of the unfolded protein response occurs at all stages of atherosclerotic lesion development in apolipoprotein E-deficient mice. Circulation 111, 1814-1821.

Zhou, X., Thorgeirsson, S.S., and Popescu, N.C. (2004b). Restoration of DLC-1 gene expression induces apoptosis and inhibits both cell growth and tumorigenicity in human hepatocellular carcinoma cells. Oncogene 23, 1308-1313.

Zhu, P., Sang, Y., Xu, H., Zhao, J., Xu, R., Sun, Y., Xu, T., Wang, X., Chen, L., Feng, H., et al. (2005). ADAM22 plays an important role in cell adhesion and spreading with the assistance of 14-3-3. Biochem Biophys Res Commun 331, 938-946.